AFWL-TR-83-97

(2)

AFWL-TR-
83-97

AD-A134820

SOIL CHARACTERIZATION AND EVALUATION AT WHITE SANDS MISSILE RANGE, NEW MEXICO

Edward L. Miller
Robert J. Majka

October 1983

Final Report

Approved for public release; distribution unlimited.

DTIC
ELECTE
NOV 1 8 1983
S
B

AIR FORCE WEAPONS LABORATORY
Air Force Systems Commmand
Kirtland Air Force Base, NM 87117

DTIC FILE COPY

83 11 18 065

This final report was prepared by the Air Force Weapons Laboratory, Kirtland Air Force Base, New Mexico, under Job Order 672A0850. Major Robert J. Majka (NTED) was the Laboratory Project Officer-in-Charge.

When Government drawings, specifications, or other data are used for any purpose other than in connection with a definitely Government-related procurement, the United States Government incurs no responsibility or any obligation whatsoever. The fact that the Government may have formulated or in any way supplied the said drawings, specifications, or other data, is not to be regarded by implication, or otherwise in any manner construed, as licensing the holder, or any other person or corporation; or as conveying any rights or permission to manufacture, use, or sell any patented invention that may in any way be related thereto.

This report has been authored by employees of the United States Government. Accordingly, the United States Government retains a nonexclusive, royalty-free license to publish or reproduce the material contained herein, or allow others to do so, for the United States Government purposes.

This report has been reviewed by the Public Affairs Office and is releasable to the National Technical Information Services (NTIS). At NTIS, it will be available to the general public, including foreign nations.

If your address has changed, if you wish to be removed from our mailing list, or if your organization no longer employs the addressee, please notify AFWL/NTED, Kirtland AFB, NM 87117 to help us maintain a current mailing list.

This technical report has been reviewed and is approved for publication.

Robert J. Majka

ROBERT J. MAJKA
Major, USAF
Project Officer

FOR THE COMMANDER

T. D. McCarson

TILLMAN D. MCCARSON
Lt Colonel, USAF
Chief, Technology Branch

JOHN W. STORM
Colonel, USAF
Chief, Civil Engineering Research Div

DO NOT RETURN COPIES OF THIS REPORT UNLESS CONTRACTUAL OBLIGATIONS OR NOTICE ON A SPECIFIC DOCUMENT REQUIRES THAT IT BE RETURNED.

UNCLASSIFIED

SECURITY CLASSIFICATION OF THIS PAGE (When Data Entered)

REPORT DOCUMENTATION PAGE	READ INSTRUCTIONS BEFORE COMPLETING FORM
1. REPORT NUMBER: AFWL-TR-83-97	2. GOVT ACCESSION NO.: A134820
3. RECIPIENT'S CATALOG NUMBER:	
4. TITLE (and Subtitle): SOIL CHARACTERIZATION AND EVALUATION AT WHITE SANDS MISSILE RANGE, NEW MEXICO	5. TYPE OF REPORT & PERIOD COVERED: Final Report
	6. PERFORMING ORG. REPORT NUMBER:
7. AUTHOR(s): Edward L. Miller, Robert J. Majka	8. CONTRACT OR GRANT NUMBER(s):
9. PERFORMING ORGANIZATION NAME AND ADDRESS: Air Force Weapons Laboratory (NTED), Kirtland Air Force Base, NM 87117	10. PROGRAM ELEMENT, PROJECT, TASK AREA & WORK UNIT NUMBERS: 64312F/672A0850
11. CONTROLLING OFFICE NAME AND ADDRESS: Air Force Weapons Laboratory (NTED), Kirtland Air Force Base, NM 87117	12. REPORT DATE: October 1983
	13. NUMBER OF PAGES: 204
14. MONITORING AGENCY NAME & ADDRESS (if different from Controlling Office)	15. SECURITY CLASS. (of this report): Unclassified
	15a. DECLASSIFICATION DOWNGRADING SCHEDULE:

16. DISTRIBUTION STATEMENT (of this Report)

Approved for public release; distribution unlimited.

17. DISTRIBUTION STATEMENT (of the abstract entered in Block 20, if different from Report)

18. SUPPLEMENTARY NOTES

This report was submitted to the College of Engineering, University of New Mexico to fulfill degree requirements.

19. KEY WORDS (Continue on reverse side if necessary and identify by block number)

Soil Characterization	Grain Size Distribution	Seismic Velocity
White Sands Missile Range	Mill Race	Soil Stress
Soil Chemistry	Misty Castle Series	Atomic Absorbance Test
Triaxial Compression Test	Pre-DIRECT COURSE	
Unconfined Compression	DIRECT COURSE	

20. ABSTRACT (Continue on reverse side if necessary and identify by block number)

A complete site characterization of the subsoil conditions down to 10 meters (32 feet) was conducted at White Sands Missile Range, New Mexico. This included testing 54 borehole samples and 6 trench bulk samples for grain-size distribution Atterberg Limits, natural and hygroscopic moisture contents, and specific gravities. Trench bulk samples were also tested for Standard Proctor maximum dry densities and optimum water contents, unconfined compressive strengths, and tri-axially-confined compressive strengths. Additional tests were performed in the

(Over)

DD FORM 1 JAN 73 1473 EDITION OF 1 NOV 65 IS OBSOLETE

UNCLASSIFIED

SECURITY CLASSIFICATION OF THIS PAGE (When Data Entered)

20. ABSTRACT (Continued).

field to include downhole nuclear density gauge measurements, standard penetration tests, and seismic refraction surveys. Atomic Absorbance tests and X-ray diffraction tests were conducted in the laboratory to determine concentrations and nature of calcium and magnesium in the soil. Correlations between strength values and cementation of soil particles was established as well as correlations between strength properties and seismic refraction measurements.

ACKNOWLEDGEMENTS

This project was directly supported by the Air Force Weapons Laboratory (AFWL) personnel and funds. The authors wish to express their appreciation to the AFWL staff, particularly Mr Eric Rinehart and secretaries Lori, Eva, Eleanor, and Lynn; to Mr Dave Bedsun (CERF) who provided equipment and technical expertise in all field tests performed; to Professor John B. Carney, Jr. for his supervision and assistance in the completion of this project; and to the wives, Kathy and OK Sun, who endured the late nights of study and separations during site visits to White Sands Missile Range.

Laboratory research was conducted in the soils and sanitation laboratories at the University of New Mexico. Professor Bruce Thompson and Ron Methany provided valuable assistance in the field of soil chemistry and X-ray diffraction tests.

In addition, the authors wish to thank MSgt John E. Miller (ret) for his outstanding technical assistance in the soils laboratory and support in the field of chemistry.

Accession For
NTIS GRA&I ☑
DTIC TAB ☐
Unannounced ☐
Justification
By
Distribution/
Availability Codes
Dist | Avail and/or Special
A-1

TABLE OF CONTENTS

Section		Page
I	INTRODUCTION	1
II	FACT-FINDING SURVEY	2
	1. Library Search	2
	2. Site Survey	2
III	PRELIMINARY SUBSOIL EXPLORATION	4
	1. Borehole Samples	4
	2. Standard Penetration Test	4
	3. Downhole Nuclear Density Gauge	4
	4. Testing Procedures	5
	A. Sample Preparation	5
	B. Grain-Size Distribution	5
	C. Specific Gravity	6
	D. Consistency Limits	6
	E. Soil Classification	7
IV	DETAILED SUBSOIL EXPLORATION	8
	1. Trench Bulk Samples	8
	A. Field Sampling	8
	B. Testing Procedures	8
	2. Seismic Survey	8
	3. Standard Proctor Test	8
	4. Unconfined Compression Test	9
	5. Triaxial Compression Test	9
V	TESTING RESULTS	11
VI	DISCUSSION OF RESULTS	34
VII	CONCLUSIONS	36
VIII	EFFECTS OF CALICHE ON STATIC STRENGTH PROPERTIES	37
IX	SUBSURFACE SEISMIC INVESTIGATIONS	59
	Appendix A: Grain-Size Distribution Curves	140
	Appendix B: Unconfined Compression Tests on Soil Samples Air-Dried From Various Initial Water Contents	165

(Table of Contents Continued)

Appendix C:	Unconfined Compression Tests on Soil Samples at Various Water Contents	170
Appendix D:	Triaxial Compression Tests on Air-Dried Soil Samples	175
Appendix E:	Triaxial Compression Tests on Soil Samples at Various Water Contents	182
Appendix F:	Site Plan, White Sands Missile Range Survey Area	195
REFERENCES		197

LIST OF FIGURES

Figure		Page
1	Photograph - Soil Particles; T-1 (4-5 feet).	50
2	Photograph - Soil Particles; T-1 (8.5-9.5 feet).	51
3	Photograph - Soil Particles; T-1 (12-13 feet).	52
4	Photograph - Soil Particles; T-2 (4-5 feet).	53
5	Photograph - Soil Particles; T-2 (8.5-9.5 feet).	54
6	Photograph - Soil Particles; T-2 (12-13 feet).	55
7	Determining Depths h_a, h_b, and h_p.	62
8	Seismic - Time Versus Distance.	63
9	Seismic - V_2 Plot.	64
10	Seismic Calculations.	65
11	Irregular Underlying Surfaces.	67

TABLES

Table		Page
1	Field Identification of Soil	12
2	Standard Penetration Test Correlations	16
3	In-Situ Densities	18
4	Grain-Size Distribution	20
5	Particle Size Percentages	26
6	Soil Samples Identification Data	27
7	Soil Classification	29
8	Compaction Data	30
9	Unconfined Compression Data	31
10	Triaxial Compression Data	32
11	Calcrete Formation	38
12	Seismic Velocities of Subsurface Calcrete	39
13	Interpretation of Penetration Resistance	40
14	Moh's Hardness Scale	40
15	Amount of Soil Used in Samples	42
16	Atomic Absorbance Results-Standards	46
17	Atomic Absorbance Results-Samples	47
18	Concentrations in Samples	48
19	Actual Concentrations - Soil	49
20	Seismic Velocities of Various Types of Caliche	60
21	Typical Seismic Velocities for Soils and Rock	60
22	Seismic Results - Velocities	66

SECTION I

INTRODUCTION

The United States Air Force, and on a local level the Air Force Weapons Laboratory (AFWL) at Kirtland AFB, have on-going programs for research and testing of various weapons effects. Specifically, AFWL is interested in the response of strategic structures, in and around various soils, to airblast and ground shock loadings.

The material characteristics needed for effective design and evaluation of weapon systems and effects in this context are: material index properties; grain-size distribution; specific weight; poisson's ratio; deformation versus strength properties; compressibilities; and failure envelopes. Additionally, the dynamic characteristics of soil as a function of impulse loads would be beneficial in correlating the effects of initial shock loadings.

The purpose of this study is to investigate and evaluate the subsoil conditions in and around the Mill Race site located at White Sands Missile Range (WSMR), New Mexico. The intent is to characterize the subsoil to a depth of 10 meters (approximately 33 feet) within an area of 2.59 kilometers square (1 square mile) with Mill Race site at the center. Due to time, equipment, and cost considerations, it was impractical to investigate all parameters required, within the confines of this project. As a result, an effort was made to provide as many of the parameters as feasible, which includes material index properties, grain-size distribution, specific gravities, densities, and deformation versus strength properties.

Due to the scope, this project was undertaken by two Air Force graduate students. To provide separate areas of research, each student worked on an additional investigative area. These topics are covered under separate sections within this report. They include subsurface seismic investigations and the effects of caliche on static strength parameters.

SECTION II

FACT-FINDING SURVEY

1. LIBRARY SEARCH

Prior to visiting the WSMR site, technical reports, geologic index maps, topographic maps, and physiographic publications were reviewed. This literature provided information which assisted in selection of the actual site. Topography and geology of the region indicated the portion of the range under consideration to be primarily alluvial plains and playas. Possible igneous or metamorphic rock outcrops could be present due to early volcanic activity in the surrounding mountain region. Due to past wet periods followed by the present semi-arid climatic conditions, much of the area was formed by discre periods of deposition. As a result, the subsoil tends to be a layered s of alluvial and other sedimentary deposits. Average particle sizes to b expected are generally silt-size to sand, since the larger sizes were dep sited closer to the alluvial fans and mountain areas. Actual thicknesses alluvial layers could vary from several meters to hundreds of meters, depending on their nature of deposition. High winds are prevalent in th and also affect the layer thicknesses and composition. The leaching of a cementation by calcium carbonate is also prevalent in this area. Actual cementation can vary from individually coated particles to thick sheets of caliche. The natural water table is located 60-90 meters (200-300 feet) below ground.

Topography of the area is indicated as relatively flat. Due to the presence of old playas and erosion channels, elevations tend to vary over small areas. Swales are common and may reach depths of 3-8 meters (9-24 feet). The area is extremely dry with some periods of sudden storms. Vegetation is sparse and mostly cactus and yucca trees. The actual Mill Race site is level and has been brought back to grade (after the initial MILL RACE test) by the addition of backfill and ejecta (material thrown from the crater after blast).

With this knowledge of local site conditions, and several reports on isolated seismic/borehole investigations, a preliminary decision was made to use the Mill Race site as the center of the area to be characterized. This matched plans for future projects as well as the key concern of having relatively level terrain in test regions.

2. SITE SURVEY

Several visits were made to the site prior to performing any field testing or sampling. The initial visit included a walk-through of the entire area under consideration. Possible areas of conflict were identified, such as deep swales and existing structures, which could interfere with testing operations. Based on existing road patterns and general topography, the actual area of 2.59 kilometers square was adjusted to lie with its western edge along Route 13 (primary compacted dirt road). This placed GZ-3 (MILL RACE site) near the center, slightly southeast.

The next series of visits were used to survey the area and locate intended boreholes. A geodetic survey marker (Defense Mapping Agency Survey Brass Plate/Douquette RM 1/DNA 10/1978), located on Douquette Mound, and magnetic North were used to initially set in an iron pipe (IP-1) which formed the northwestern corner of the site. Three additional iron pipes (IP-2, IP-3, and IP-4) were located from Douquette Mound and IP-1, along the eastern edge of

Route 13 in a straight line (180° backsights). Based on Douquette Mound and the 4 iron pipes, boreholes were located. Each borehole was located using triangulation with the set markers as well as with each other. Temporary stakes were then set. Initial selection of borehole locations was predicated on an even distribution over the entire site; however, cost limitations reduced the actual number of boreholes to five. Selection of locations therefore became critical. The site was divided into four quadrants. One borehole was approximately centered in each quadrant, with the fifth hole located between the two western quadrants. This configuration provided the maximum area exposure. Minor adjustments in locations were made based on previous soil investigations within the site. This spacing was also intended to provide information on locating trenches and seismic runs during the final exploration phase. A site plan depicting all locations is provided in Appendix F.

SECTION III

PRELIMINARY SUBSOIL EXPLORATION

1. BOREHOLE SAMPLES

Civil Engineering Research Facility (CERF) personnel and equipment assisted in the borehole sampling. A truck-mounted auger (Central Mine Equipment-Model No. 75) was used to drill the boreholes. A split-spoon sampler (Dimensions: Overall Length 2'8"; Inside Diameter 1-3/8"; Outside Diameter 2"; Area Ratio = 111.6%) was used to take the samples every .6-.8 meter (2-2.5 feet) down to a depth of 4.9 meters (16 feet), then every 1.5 meters (5 feet) down to a final depth of approximately 10 meters (32 feet). As samples were retrieved, they were identified and placed in plastic bags. A balance and measuring tins were not available at the site, and the downhole water content measuring device (Downhole Density Gauge Probe-Model No. 1351) was not operating. The plastic bags were used in an attempt to preserve natural water content until a laboratory determination could be made. Field identification of samples is recorded in Section V, Table 1.

2. STANDARD PENETRATION TEST

During the sampling within boreholes, the Standard Penetration Test was accomplished and at each depth a sample was taken. A standard 63.5 kilogram (140 pounds) weight was dropped at a height of 76 centimeters (30 inches) to provide an energy of 480 Joules (N-M) per blow. The weight was used to drive the sampler to the top of each depth in consideration, then the number of blows was recorded to drive the sampler the next 30.5 centimeters (12 inches). Two marks were made on the support rods each time to assist in determining the required penetration. The borehole was cleaned by raising the auger and spinning the soil off. The auger was then reinserted and the sampler was inserted in the hollow stem of the auger.

Table 2, Section V lists relative densities of the in-situ material in relation to number of blows. Relative density is determined by the ratio of (maximum void ratio less natural void ratio) over (maximum void ratio less minimum void ratio). Terzaghi and Peck provided a simple correlation of relative densities versus number of blows, based on numerous tests on sands. These correlations were used in developing Table 2. Additionally, the number of blows was related to approximate values for the angle of internal friction "ϕ", taken from a chart developed by Terzaghi and Peck. It is noted that the relationships developed by Terzaghi and Peck applied to sands. The soil at WSMR is primarily sand with varying amounts of gravel and fines. Varying degrees of cementation are also present, which will tend to increase the number of blows.

3. DOWNHOLE NUCLEAR DENSITY GAUGE

Personnel were checked out on the downhole nuclear density gauge (Model 504/Serial No. 50/Standard Serial No. 107) by WSMR Radioactive Safety members. A hole approximately 10.2 centimeters (4 inches) was drilled vertically into the ground near each borehole. A section of 6.4 cm (2.5 inches) diameter plastic pipe was then inserted into each hole to a depth of 6.7 meters (22 feet). Sand was then poured around the pipe to hold the pipe in the center of the hole. Also, the sand provided a standard medium for the nuclear particles to travel through between the pipe and the soil to be measured.

Six Standard counts (readings) for the equipment were taken. The nuclear density gauge was then placed over the mouth of a pipe section and its probe lowered slowly down the hole. Two counts (readings) were taken approximately every .61 meter (2.0 feet) until the probe could no longer be lowered (due to crimping of plastic pipe). This procedure was repeated for each pipe section.

The following method was then used to estimate in-situ densities for the soil. The average of the two readings at each depth was divided by the average of the six standard counts. The result was a count ratio number. A standard chart, provided with the equipment, was then used to relate the count ratio number to in-situ density. Results of this test are given in Section V, Table 3.

4. TESTING PROCEDURES

A. SAMPLE PREPARATION

Fifty-four samples taken from the five borings (depths down to 9.8 meters) were analyzed. Due to the nature of this material, small amounts were available for analysis at each depth; approximately 300-800 grams.

A small portion of each sample was used to obtain hygroscopic moisture and approximate values of natural moisture content (some loss of water in bag). See Table 6, Section V. Each sample was then airdried for 24 hours and ground by mortar and rubber pestal to separate individual particles. The samples were then passed through a Number 10 sieve (2.0 mm). The amount retained on the Number 10 sieve was used for a coarse-sieve analysis. The amount passing the Number 10 sieve was divided for additional tests. Eighty grams was used for the hydrometer and fine sieve analysis. Thirty grams was used for the specific gravity test. The remainder of the minus Number 10 sieve material was used for consistency limits (Atterberg Limits) tests.

The 80 gram sample was mixed with five grams of sodium-metahexaphosphate and approximately 300 ml of distilled water and let set for 24 hours. The sodium-metahexaphosphate acted as a dispersing agent to further separate individual fine particles.

B. GRAIN-SIZE DISTRIBUTION

The coarse sieve, hydrometer test, and fine sieve analysis were performed using standard techniques. The only problem encountered was flocculation during hydrometer analysis of certain samples. This could be a result of non-dispersion or lack of specific particle sizes. Grain-size distribution data was obtained for each sample and is summarized in Table 4, Section V. Representative grain-size distribution curves were also prepared, to show the range of size distributions over various depths within each borehole. These are found in Appendix A. Table 5, Section V depicts the amounts of gravel, sand, silt, and clay-size particles over different depth ranges within each borehole.

C. SPECIFIC GRAVITY

The Standard test was performed on the oven-dried material less than Number 10 sieve-size (2.0 mm), for each sample. The specific gravity of solids was determined by the following equation:

$$Gs = \frac{\text{(Weight Dry Soil) X Gw}}{\text{(Weight Dry Soil)+(Weight Pycnometer+Water)-(Weight Pycnometer+Soil+water)}}$$

In this equation Gs is the specific gravity of solids (equal to unit weight of solids over unit weight of water) and Gw is the specific gravity of water. Results of this test are found in Table 6, Section V.

D. CONSISTENCY LIMITS

The minus Number 40 sieve-size (.42 mm) material was used for the consistency, or Atterberg Limits, tests. The technique developed by Casagrande was used for the Liquid Limit Test, employing a standard brass cup mounted on a firm base plate.

Water was added to each sample until a clay-like texture was achieved. A portion of the sample was then placed into the bottom of the cup, using a spatula, and levelled to a height of approximately 8 mm. A groove was cut into the sample with the following approximate dimensions: 11 mm at top of groove and 2 mm at bottom. The cup was then raised and dropped on the base plate, using a crank-handle, at a height of 1 cm. The number of blows were counted to just close the bottom of the groove about 1.3 cm (.5 inch). Five trials were run at increasing water contents. The number of blows versus water content was plotted and the "best-fit" straight line drawn through the points. The Liquid Limit (W_L) was that water content corresponding to 25 blows on the straight line. For those soils with a very small amount of material available, only one W_L test was run. The W_L for the soil was then estimated using the following equation:

$$W_L = W\left(\frac{N}{25}\right)^{.121}$$

where N is the number of blows and W is the water content for the sample.

Three balls of soil were set aside after the initial wetting. These balls were then used to perform the Plastic Limit Test. Each ball was worked between the fingers, then rolled on a ground glass plate to form a thread. The water content was taken for each thread when it just crumbled at .32 cm (1/8 inch). The Plastic Limit (W_p) was taken as the average of the three water contents.

The plastic range, or Plasticity Index, of each sample was found by subtracting the Plastic Limit from the Liquid Limit. A tabulation of the consistency limits is found in Table 6, Section V.

E. SOIL CLASSIFICATION

The soil at each depth (each borehole) was classified in accordance with the Unified Soil Classification System. This method is used by the military and appears to be the most widely accepted procedure. It takes into account grain-size distribution, uniformity and curvature coefficients, and consistency limits. Results are found in Section V, Table 7.

SECTION IV

DETAILED SUBSOIL EXPLORATION

1. TRENCH BULK SAMPLES

A. FIELD SAMPLING

Based on the type of soil found in each borehole, location of the borehole, and general terrain, trenches were located to provide bulk samples most representative of all soil types in the area. Again, due to cost limitations, only two trenches could be excavated. This made selection of their locations extremely critical. Final locations were selected to provide one area of relatively fine sandy silt with known caliche layers, and a second area of coarser gravelly sand with little cementation.

Douquette Mound, the iron pipes, and temporary boreholes were used in conjunction with triangulation to locate trenches 1 and 2. Trench 1 is located in the north central region of the area, between borings 2 and 3. Trench 2 is located in the south central region (slightly west), between borings 1 and 5. See Appendix F.

A backhoe was used to excavate both trenches. Excavations were made down to 1.2-1.5 meters (4-5 feet), 2.6-2.9 meters (8.5-9.5 feet), and 3.7-4.0 meters (12-13 feet). Further depths were prohibited due to backhoe limitations. At each depth, bulk samples of approximately 91 kilograms (200 pounds) were hand-excavated and placed in containers. Small samples from each container were taken for natural water content determinations. Trench 1 had a loose sandy silt down to 1.2 meters (4 feet); then caliche down to 4.0 meters (13 feet). Below 4.0 meters (13 feet), the caliche appeared to continue. Trench 2 had a loose sandy silt down to .6 meters (2 feet); then caliche down to 2.4 meters (8 feet); then lightly cemented gravelly sand (with rocks up to 10 cm (4 inches) diameter down to 3.0 meters (10 feet); then loose, gravelly sand down to 4.0 meters (13 feet). Below 4.0 meters (13 feet), the loose, gravelly sand appeared to continue.

B. TESTING PROCEDURES

Classification tests were accomplished on the six samples (2 trenches with 3 depths each) in a procedure similar to Section III-4. These tests included the coarse-sieve analysis, hydrometer and fine-sieve analysis, specific gravity test, consistency limits, natural moisture content, and hygroscopic moisture content. Results can be found in Section V, Tables 4-7.

2. SEISMIC SURVEY

This subject is covered separately in Section IX, Subsurface Seismic Investigations.

3. STANDARD PROCTOR TEST

The standard proctor test was performed on all trench samples to provide data on maximum dry density versus optimum moisture contents. Material passing the Number 4 sieve (4.76 mm) was used. Equipment included a 10.2 cm (4 inch)

mold with an inner volume of .0009 m^3 (.033 $feet^3$) and a 2.5 kilogram (5.5 pounds) hammer (weight). Each sample was compacted in 3 layers at 25 blows per layer, with a 30.5 cm (12 inches) drop of the weight. Each sample was compacted at increasing water contents until the total weight dropped off. Values of dry density versus water content were plotted and a smooth curve drawn through the points. The peak of the curve was taken as the maximum dry density and optimum moisture content. Results of these tests are found in Section V, Table 8.

4. UNCONFINED COMPRESSION TEST

Samples from each trench depth (except Trench 2, Depths 2.6-2.9 meters and 3.7-4.0 meters) were compacted into cylinders 7.12 cm (2.802 inches) high and with a 3.56 cm (1.402 inches) diameter. Soil from Trench 2, Depths 2.6-2.9 meters and 3.7-4.0 meters could not be molded into cylinders due to the high sand content. The cylinders were compacted in 5 layers at 13 blows per layer. A .33 Kilogram (.72 pounds) hammer was used at a drop height of 38.1 cm (15 inches).

Cylinders were made at approximately 2 percent less than optimum moisture content, optimum moisture content, and optimum moisture content plus 2 percent. Additionally, a separate cylinder at each moisture content was prepared then allowed to dry for 72 hours. The intent was to see how well these cylinders set up when allowed to dry from various moisture contents. Increases in peak failure stress under these conditions are discussed in Section VIII, Effects of Caliche on Static Strength Properties.

Each cylinder was tested on a standard compression machine (Wykeham Farrance Eng. LTD, England, Capacity 10 Tons/WFE 42 Speed Gear Box) with zero confining pressure. A vertical force was applied at a (gear speed) rate of .65 mm per minute until failure was indicated by a drop in axial force accompanied with high strain changes. Typical shear failures could be obtained in all cylinders except those which had been allowed to dry. These cylinders achieved much higher peak stresses at low strains, then tended to rupture violently once peak stress was reached. Tabulated results of this test are found in Section V, Table 9.

5. TRIAXIAL COMPRESSION TEST

Samples from each trench were compacted in cylinders similar to those used in the unconfined compression test. All samples (Unconfined and Triaxial) were compacted at the same time to achieve similar water contents (Wopt - 2%; Wopt; Wopt + 2%), then sealed with aluminum foil and hot wax to preserve moisture until testing. These samples were then tested on the same Wykeham Farrance Eng. LTD compression equipment. A plastic cell containing water surrounded the soil sample during testing. Pressurizing the water (by expanding a rubber membrane in an outer cell) created an all-around confining pressure on the sample. Three different confining pressures were used (51.7 KN/m^2 (7.5psi); 86.2 KN/m^2 (12.5 psi); 120.7 KN/m^2 (17.5psi)). A vertical force (in addition to the confining pressure) was then applied at a (gear speed) rate of .65 mm per minute until failure occurred.

Additional samples from each trench were tested in triaxial compression, using air-dried soil. The method used to make cylinder samples was as follows: Attached rubber membrane to base plate (over porous stone) with 2 O-rings; assembled 3-piece metal collar around rubber membrane and stretched top of

membrane over top of collar; added soil in 5 layers and rodded each layer 30 times; leveled top of soil and added a top porous stone; added plastic head over porous stone; unfolded top of membrane over porous stone and plastic head and attached 2 O-rings (above collar); hooked up vacuum to base plate and closed all valves; turned vacuum on for a few seconds at 34.5 KN/m^2 (5psi) then closed valve on base plate before turning vacuum off; unhooked vacuum and removed collar; released the vacuum pressure inside the membrane, after the confining pressure had been applied. These samples were then tested by a step application of 3 different confining pressures. An all-around confining pressure of 51.7 KN/m^2 (7.5psi) was applied, then the vertical stress was increased until failure was imminent (small stress changes with large strain changes). The compression machine was turned off and the confining pressure increased to 86.2 KN/m^2 (12.5psi). The compression machine was then turned on and the axial stress increased until failure was imminent, then the stress was removed. This was repeated one more time at a confining pressure of 120.7 KN/m^2 (17.5psi); however, the sample was allowed to fail for this final step.

Results of all triaxial tests are found in Table 10, Section V, and include the peak deviator stress at failure versus percent strain, the failure modulus "E_f", and the initial tangent modulus "E_{IT}".

SECTION V

TESTING RESULTS

Results of each classification and strength test are presented in tabulated form in this section. Any accompanying graphs can be found in separate appendices.

TABLE 1

FIELD IDENTIFICATION OF SOIL

Borehole	Depth Meters (Feet)	Description
B-1	.31-.61(1-2)	Light brown; sandy silt; less than 1 percent gravel; crumbles easily in fingers.
	1.1-1.4(3.5-4.5)	Light brown; silty sand with minor cementation; 3-5 percent gravel; some difficulty in breaking clumps with fingers.
	1.8-2.1(6-7)	Light brown; fine sand with some silt; less than 1 percent gravel but larger size (up to 1 inch); crumbles easily in fingers.
	2.6-2.9(8.5-9.5)	Dark brown; gravelly sand with some fines; few large cobbles up to 3 inches; courser material.
	3.4-3.7(11-12)	Brownish gray; sandy gravel with sizes up to 2 inches.
	4.1-4.4(13.5-14.5)	Similar to 3.4-3.7 meters depth.
	4.9-5.2(16-17)	Similar to 3.4-3.7 meters depth.
	5.6-5.9(18.5-19.5)	Similar to 3.4-3.7 meters depth.
	6.4-6.7(21-22)	Dark brown; course sand with fines; clumps are disc-shaped; heavy cementation; clumps cannot be broken with fingers.
	7.9-8.2(26-27)	Dark brown; fine silty sand with some gravel; clumps are disc-shaped; moderate cementation; clumps break in fingers with some difficulty.
	9.4-9.8(31-32)	Similar to 7.9-8.2 meters depth.
B-2	.31-.61(1-2)	Light tan to grayish brown; fine sandy silt.
	1.1-1.4(3.5-4.5)	Similar to .31-.61 meter depth.
	1.8-2.1(6-7)	Similar to .31-.61 meter depth but with light cementation.
	2.6-2.9(8.5-9.5)	Slightly darker tan; sandy silt; clumps are disc-shaped; clumps break easily in fingers.
	3.4-3.7(11-12)	Similar to 1.8-2.1 meters depth; some clumps which break easily in fingers.

TABLE 1 (continued)

Borehole	Depth Meters (Feet)	Description
B-2 (cont'd)	4.1-4.4(13.5-14.5)	Similar to 3.4-3.7 meters depth but has disc-shaped clumps which break easily in hand.
	4.9-5.2(16-17)	Light tan; sandy silt with some gravel; moderate cememtation; clumps break in fingers with some difficulty.
	6.4-6.7(21-22)	Similar to 4.9-5.2 meters depth.
	7.6-7.9(25-26)	Dark brown; fine silty sand; clumps break easily in fingers.
	7.9-8.2(26-27)	Dark brown with light tan mottled tone; fine sand with some gravel and silt; heavy cementation; clumps are disc-shaped; clumps cannot be broken with fingers.
	9.4-9.8(31-32)	Similar to 7.6-7.9 meters depth.
B-3	.31-.61(1-2)	Light brown; sandy silt with less than 1 percent gravel.
	1.1-1.4(3.5-4.5)	Light tan; fine silty sand with less than 1 percent gravel; some pieces up to 2 inches size.
	1.8-2.1(6-7)	Similar to 1.1-1.4 meters depth.
	2.6-2.9(8.5-9.5)	Similar to 1.1-1.4 meters depth but with light cementation.
	3.4-3.7(11-12)	Dark tan; silty sand; moderate cementation; clumps break in fingers with some difficulty.
	4.1-4.4(13.5-14.5)	Similar to 3.4-3.7 meters depth.
	4.6-4.9(15-16)	Light brown; loose layer of silty sand.
	4.9-5.2(16-17)	Similar to 3.4-3.7 meters depth.
	6.4-6.7(21-22)	Similar to 3.4-3.7 meters depth.
	7.6-7.9(25-26)	Similar to 4.6-4.9 meters depth.
	7.9-8.2(26-27)	Light brown; silty sand with some gravel; material courser and has some granite pieces; some gravel up to 2 inches size.
	9.4-9.8(31-32)	Similar to 7.9-8.2 meters depth but has disc-shaped clumps which break in fingers with some difficulty; moderate cementation.

TABLE 1 (continued)

Borehole	Depth Meters (Feet)	Description
B-4	.31-.61(1-2)	Light brown; sandy silt.
	1.1-1.4(3.5-4.5)	Reddish brown; silty sand with some gravel; light cementation; clumps are disc-shaped; clumps break easily in fingers.
	1.8-2.1(6-7)	Tan; course sand with some fines; 3-5 percent gravel; some cobbles up to 2 inches.
	2.6-2.9(8.5-9.5)	Similar to 1.8-2.1 meters depth but slightly higher gravel content.
	3.4-3.7(11-12)	Similar to 2.6-2.9 meters depth.
	4.1-4.4(13.5-14.5)	Similar to 2.6-2.9 meters depth.
	4.9-5.2(16-17)	Dark reddish brown; silty sand with some gravel; moderate cementation; clumps break in fingers with some difficulty.
	6.4-6.7(21-22)	Light brown; silty sand with some gravel; moderate cementation; clumps are disc-shaped; clumps break in fingers with some difficulty.
	7.9-8.2(26-27)	Similar to 6.4-6.7 meters depth.
	9.4-9.8(31-32)	Reddish brown to light tan mottled tone; silty sand; heavy cementation; clumps are disc-shaped; clumps cannot be broken in fingers.
B-5	.31-.61(1-2)	Light brown; sandy silt; less than 1 percent gravel.
	1.1-1.4(3.5-4.5)	Light tan to white; fine powder silt to clay size; light cementation.
	1.8-2.1(6-7)	Similar to .31-.61 meter depth but with light cementation; clumps break easily in fingers.
	2.6-2.9(8.5-9.5)	Light brown; slightly courser sand with silt and some gravel up to 2 inches size; moderate cementation; clumps break in fingers with some difficulty.
	3.4-3.7(11-12)	Similar to 2.6-2.9 meters depth.

TABLE 1 (continued)

Borehole	Depth Meters (Feet)	Description
B-5 (cont'd)	4.1-4.4(13.5-14.5)	Similar to 1.1-1.4 meters depth but with moderate cementation.
	4.9-5.2(16-17)	Similar to 4.1-4.4 meters depth.
	6.4-6.7(21-22)	Similar to 2.6-2.9 meters depth.
	7.9-8.2(26-27)	Reddish brown; silty sand with some gravel up to 3 inches size; heavy cementation; clumps are disc-shaped; clumps cannot be broken with fingers.
	9.4-9.8(31-32)	Similar to 2.6-2.9 meters depth.

TABLE 2

STANDARD PENETRATION TEST INTERPRETATIONS

Borehole	Depth Meters (Feet)	Blows/Foot (N)	Relative Density Dr (percent)	Condition	Angle of Internal Friction ϕ (Degrees
B-1	.31-.61(1-2)	15	40-60	Med. Dense	31.5
	1.1-1.4(3.5-4.5)	54	80-100	Very Dense	42.0
	1.8-2.1(6-7)	25	40-60	Med. Dense	34.5
	2.6-2.9(8.5-9.5)	31	60-80	Dense	36.3
	3.4-3.7(11-12)	66	80-100	Very Dense	43.7
	4.1-4.4(13.5-14.5)	46	60-80	Dense	40.4
	4.9-5.2(16-17)	52	80-100	Very Dense	41.6
	5.6-5.9(18.5-19.5)	29	40-60	Med. Dense	35.8
	6.4-6.7(21-22)	53	80-100	Very Dense	41.8
	7.9-8.2(26-27)	29	40-60	Med. Dense	35.8
	9.4-9.8(31-32)	48	60-80	Dense	40.9
B-2	.31-.61(1-2)	23	40-60	Med. Dense	33.9
	1.1-1.4(3.5-4.5)	39	60-80	Dense	38.6
	1.8-2.1(6-7)	47	60-80	Dense	40.6
	2.6-2.9(8.5-9.5)	33	60-80	Dense	36.6
	3.4-3.7(11-12)	43	60-80	Dense	39.5
	4.1-4.4(13.5-14.5)	87	80-100	Very Dense	44.0
	4.9-5.2(16-17)	91	80-100	Very Dense	44.0
	6.4-6.7(21-22)	51	8-100	Very Dense	41.2
	7.9-8.2(26-27)	70	80-100	Very Dense	44.0
	9.4-9.8(31-32)	32	60-80	Dense	36.5
B3	.31-.61(1-2)	12	40-60	Med. Dense	30.5
	1.1-1.4(3.5-4.5)	27	40-60	Med. Dense	35.2
	1.8-2.1(6-7)	31	60-80	Dense	36.3
	2.6-2.9(8.5-9.5)	63	80-100	Very Dense	43.1
	3.4-3.7(11-12)	92	80-100	Very Dense	44.0
	4.1-4.4(13.5-14.5)	76	80-100	Very Dense	44.0
	4.9-5.2(16-17)	85	80-100	Very Dense	44.0
	6.4-6.7(21-22)	45	60-80	Dense	40.1
	7.9-8.2(26-27)	52	80-100	Very Dense	41.6
	9.4-9.8(31-32)	53	80-100	Very Dense	41.8
B-4	.31-.61(1-2)	37	60-80	Dense	38.1
	1.1-1.4(3.5-4.5)	44	60-80	Dense	39.9
	1.8-2.1(6-7)	49	60-80	Dense	41.0
	2.6-2.9(8.5-9.5)	24	40-60	Med. Dense	34.1
	3.4-3.7(11-12)	28	40-60	Med. Dense	35.5
	4.1-4.4(13.5-14.5)	34	60-80	Dense	36.8
	4.9-5.2(16-17)	42	60-80	Dense	39.2
	6.4-6.7(21-22)	42	60-80	Dense	39.2
	7.9-8.2(26-27)	27	40-60	Med. Dense	35.2
	9.4-9.8(31-32)	111	80-100	Very Dense	44.0

TABLE 2 (continued)

Borehole	Depth Meters (Feet)	Blows/Feet (N)	Relative Density Dr (percent)	Condition	Angle of Internal Friction (ϕ) Degrees
B-5	.31-.61(1-2)	18	40-60	Med. Dense	32.5
	1.1-1.4(3.5-4.5)	49	60-80	Dense	41.0
	1.8-2.1(6-7)	50	60-80	Dense	41.1
	2.6-2.9(8.5-9.5)	81	80-100	Very Dense	44.0
	3.4-3.7(11-12)	40	60-80	Dense	38.8
	4.1-4.4(13.5-14.5)	74	80-100	Very Dense	44.0
	4.9-5.2(16-17)	66	80-100	Very Dense	43.7
	6.4-6.7(21-22)	35	60-80	Dense	37.2
	7.9-8.2(26-27)	66	80-100	Very Dense	43.7
	9.4-9.8(31-32)	48	60-80	Dense	40.9

TABLE 3
IN-SITU DENSITIES

Borehole	Depth Meters (Feet)	In-Situ Density Kg/m^3 (pcf)
B-1	.31 (1.0)	1,617.9 (101.0)
	.91 (3.0)	1,734.8 (108.3)
	1.52 (5.0)	1,758.8 (109.8)
	2.13 (7.0)	1,798.9 (112.3)
	2.74 (9.0)	1,746.0 (109.0)
	3.35 (11.0)	1,830.9 (114.3)
	3.96 (13.0)	1,734.8 (108.3)
	4.57 (15.0)	1,802.1 (112.5)
B-2	.31 (1.0)	1,566.7 (97.8)
	.91 (3.0)	1,689.9 (105.5)
	1.52 (5.0)	1,665.9 (104.0)
	2.13 (7.0)	1,638.7 (102.3)
	2.74 (9.0)	1,826.1 (114.0)
	3.35 (11.0)	1,689.9 (105.5)
	3.96 (13.0)	1,786.1 (111.5)
	4.27 (14.0)	1,814.9 (113.3)
B-3	.31 (1.0)	1,874.2 (117.0)
	.91 (3.0)	1,617.9 (101.0)
	1.52 (5.0)	1,726.8 (107.8)
	2.13 (7.0)	1,830.9 (114.3)
	2.74 (9.0)	1,738.0 (108.5)
	3.35 (11.0)	1,770.0 (110.5)
B-4	.31 (1.0)	1,638.7 (102.3)
	.91 (3.0)	1,630.7 (101.8)
	1.52 (5.0)	1,702.8 (106.3)
	2.13 (7.0)	1,722.0 (107.5)
	2.74 (9.0)	1,850.1 (115.5)
	3.35 (11.0)	1,806.9 (112.8)
	3.96 (13.0)	1,887.0 (117.8)
	4.57 (15.0)	1,814.9 (113.3)
	5.18 (17.0)	1,890.2 (118.0)
	5.49 (18.0)	1,879.0 (117.3)

TABLE 3 (continued)

B-5	.31 (1.0)	1,606.7 (100.3)
	.91 (3.0)	1,590.6 (99.3)
	1.52 (5.0)	1,670.7 (104.3)
	2.13 (7.0)	1,734.8 (108.3)
	2.74 (9.0)	1,770.0 (110.5)
	3.35 (11.0)	1,673.9 (104.5)
	3.96 (13.0)	1,694.8 (105.8)
	4.57 (15.0)	1,654.7 (103.3)
	5.18 (17.0)	1,649.9 (103.0)

TABLE 4

GRAIN-SIZE DISTRIBUTION

B1 % PASSING

	GRAVEL				SAND								SILT SIZE			CLAY SIZE	
					COARSE		MEDIUM		FINE								
DEPTH	1.5"	1.0"	3/4"	3/8"	#4	#10	#20	#40	#60	#100	#140	#200	.05	.01	.005	.002	.001
1'-2'	100	100	100	99.5	98.2	95.2	87.1	77.1	69.9	60.0	53.0	44.7	38.0	26.5	23.5	15.5	12.0
3.5'-4.5'	100	100	100	97.4	91.4	79.4	76.4	73.4	69.6	56.0	47.4	33.4	33.0	23.5	20.0	16.0	12.1
6'-7'	100	100	100	95.3	92.4	85.7	75.0	65.7	57.4	48.0	42.7	36.2	36.0	13.0	1.3	0	0
8.5'-9.5'	100	94.3	94.3	89.6	79.0	62.7	51.2	42.0	35.3	30.0	26.4	26.0	25.5	10.0	0	0	0
11'-12'	100	100	92.8	73.9	58.4	44.7	32.4	23.2	17.9	17.0	16.0	15.0	13.0	9.5	7.0	5.7	5.7
13.5'-14.5'	100	100	98.2	91.2	83.6	67.6	46.2	31.4	24.0	19.1	15.9	14.5	12.7	8.5	6.5	6.0	5.5
16'-17'	100	100	98.1	87.7	80.2	67.0	47.3	29.4	20.9	16.5	13.2	12.5	11.0	7.0	5.6	0	0
18.5'-19.5'	100	100	100	96.4	91.5	70.2	38.7	19.1	12.3	9.5	7.3	7.0	7.0	3.9	2.5	0	0
21'-22'	100	100	100	100	99.7	94.9	85.6	78.5	75.0	71.5	68.8	63.2	58.0	41.4	33.5	19.0	3.8
26'-27'	100	100	94.0	93.2	91.6	81.1	76.8	71.5	66.7	60.0	55.7	48.1	46.0	32.5	28.5	22.0	17.8
31'-32'	100	100	100	100	99.0	92.3	87.6	80.3	74.6	63.0	54.7	42.5	38.5	30.5	27.0	21.9	17.2

TABLE 4

GRAIN-SIZE DISTRIBUTION

B2 % PASSING

	GRAVEL				SAND								SILT SIZE			CLAY SIZE	
					COARSE		MEDIUM		FINE								
DEPTH	1.5"	1.0"	3/4"	3/8"	#4	#10	#20	#40	#60	#100	#140	#200	.05	.01	.005	.002	.001
1'-2'	100	100	100	100	99.8	97.4	93.5	87.2	80.6	69.5	61.6	50.1	46.0	27.9	3.3	2.2	2.0
3.5'-4.5'	100	100	100	100	99.9	97.0	93.4	89.3	84.8	76.5	70.7	60.3	59.0	13.0	2.0	1.9	1.8
6'-7'	100	100	100	100	99.3	94.3	91.8	88.0	84.2	76.0	70.7	62.0	58.0	18.5	3.3	2.1	2.0
8.5'-9.5'	100	100	100	100	99.8	95.7	91.6	83.7	76.4	64.5	57.5	48.4	47.5	41.0	21.5	3.5	0
11'-12'	100	100	100	100	99.1	89.4	87.9	84.2	80.0	72.0	66.7	58.6	57.0	25.5	2.0	0	0
13.5'-14.5'	100	100	100	100	99.4	89.8	85.6	80.3	75.1	65.5	58.7	50.4	48.5	11.0	1.8	0	0
16'-17'	100	100	100	100	98.6	90.3	84.5	78.4	72.9	62.0	55.9	48.6	41.0	9.0	1.0	0	0
21'-22'	100	100	100	98.7	96.6	85.6	79.7	73.9	68.8	60.5	54.7	52.0	46.0	23.5	5.5	0	0
25'-26'	100	100	100	100	99.6	95.0	89.1	80.8	73.3	61.5	53.5	42.0	35.5	17.0	3.2	2.8	2.6
26'-27'	100	100	100	98.7	96.1	75.2	70.9	64.8	59.1	51.5	45.1	45.0	42.0	39.0	17.0	0	0
31'-32'	100	100	100	97.2	93.2	83.5	68.6	56.1	48.2	40.0	33.9	26.7	20.5	14.5	12.1	6.0	1.0

TABLE 4

GRAIN-SIZE DISTRIBUTION

B3 % PASSING

	GRAVEL				SAND								SILT SIZE			CLAY SIZE	
					COARSE		MEDIUM		FINE								
DEPTH	1.5"	1.0"	3/4"	3/8"	#4	#10	#20	#40	#60	#100	#140	#200	.05	.01	.005	.002	.001
1'-2'	100	100	100	99.2	98.6	93.9	84.1	73.8	66.4	55.0	47.2	38.2	31.0	22.3	17.3	13.0	7.7
3.5'-4.5'	100	100	100	99.4	97.1	90.3	77.6	66.2	58.4	48.5	41.5	33.7	31.5	13.5	1.3	0	0
6'-7'	100	100	100	99.3	96.5	90.3	78.7	69.2	61.9	52.0	45.5	36.8	32.5	8.0	1.3	0	0
8.5'-9.5'	100	100	100	100	99.8	98.1	95.0	90.3	85.1	74.0	66.2	55.8	52.5	41.5	1.3	0	0
11'-12'	100	100	100	100	99.1	96.2	92.5	87.7	82.2	71.0	63.1	52.2	50.0	43.3	1.3	0	0
13.5'-14.5'	100	100	100	100	99.8	98.5	96.6	93.7	88.9	76.0	68.0	56.1	51.5	20.0	0.7	0	0
15'-16'	100	100	100	100	99.6	97.1	92.9	86.3	79.3	66.0	58.0	45.9	44.9	22.0	4.0	0	0
16'-17'	100	100	100	100	98.8	95.8	90.0	84.1	78.0	66.0	58.5	51.3	47.0	23.0	0	0	0
21'-22'	100	100	94.1	92.4	91.6	88.0	81.2	75.7	70.0	60.5	54.5	47.6	44.5	7.0	0	0	0
25'-26'	100	100	100	100	99.7	96.6	93.0	87.1	79.6	65.0	56.1	44.9	39.5	6.0	0	0	0
26'-27'	100	100	96.6	89.4	84.9	79.0	72.0	65.7	58.9	47.5	40.2	30.6	28.0	4.0	0	0	0
31'-32'	100	100	100	98.3	96.7	91.7	86.2	80.7	75.5	68.5	64.1	57.8	54.2	41.0	29.2	0	0

TABLE 4

GRAIN-SIZE DISTRIBUTION

B4 % PASSING

	GRAVEL				SAND								SILT SIZE			CLAY SIZE	
					COARSE		MEDIUM		FINE								
DEPTH	1.5"	1.0"	3/4"	3/8"	#4	#10	#20	#40	#60	#100	#140	#200	.05	.01	.005	.002	.001
1'-2'	100	100	100	100	99.9	99.4	95.6	87.8	79.7	62.5	53.1	42.9	37.5	27.0	22.0	12.3	1.0
3.5'-4.5'	100	100	100	98.7	97.1	92.5	81.1	72.0	65.9	56.5	50.4	42.3	35.0	23.5	20.0	16.5	14.7
6'-7'	100	100	100	97.5	94.2	86.9	75.3	67.1	61.7	52.5	47.2	38.2	35.5	28.2	25.0	21.5	19.6
8.5'-9.5'	100	92.2	92.2	84.3	75.1	59.4	39.9	27.4	21.0	20.0	19.0	18.0	15.5	12.0	10.0	9.0	8.1
11'-12'	100	100	100	89.5	76.0	56.4	35.7	24.5	19.2	18.0	17.5	17.0	15.0	10.5	8.0	7.0	7.6
13.5'-14.5'	100	100	96.1	84.2	73.3	67.8	49.5	34.7	27.3	22.5	20.0	18.0	10.0	7.5	5.7	3.5	2.5
16'-17'	100	100	96.6	94.4	92.5	89.2	83.9	78.7	74.9	67.5	63.0	52.9	46.0	29.5	24.0	17.0	12.8
21'-22'	100	100	100	100	99.9	96.7	90.6	84.9	79.2	64.5	54.8	48.8	41.0	32.5	28.2	14.5	3.4
26'-27'	100	100	100	100	99.5	98.8	97.6	94.9	89.8	75.5	66.8	51.6	47.0	36.0	3.3	2.5	2.0
31'-32'	100	100	100	100	99.9	96.7	95.0	93.3	88.3	71.0	60.6	48.6	44.5	30.0	3.9	3.6	3.3

TABLE 4

GRAIN-SIZE DISTRIBUTION

B5 % PASSING

	GRAVEL				SAND								SILT SIZE			CLAY SIZE	
					COARSE		MEDIUM		FINE								
DEPTH	1.5"	1.0"	3/4"	3/8"	#4	#10	#20	#40	#60	#100	#140	#200	.05	.01	.005	.002	.001
1'-2'	100	100	100	99.3	97.0	93.8	88.7	82.0	75.2	60.5	50.7	38.8	33.5	25.0	20.5	15.5	12.2
3.5'-4.5'	100	100	100	100	99.9	99.5	98.8	96.6	92.9	77.5	67.7	51.2	48.0	6.0	0	0	0
6'-7'	100	100	100	99.5	96.8	95.2	92.9	90.3	86.5	69.0	58.3	38.1	34.0	7.0	0	0	0
8.5'-9.5'	100	100	96.4	94.6	91.9	86.9	77.0	69.7	65.5	59.0	55.1	47.1	45.5	16.0	4.5	0	0
11'-12'	100	100	100	100	99.5	97.1	92.5	88.0	83.7	79.0	76.2	61.6	51.0	16.0	0	0	0
13.5'-14.5'	100	100	100	99.4	99.3	98.6	96.5	93.1	88.3	77.0	69.5	57.1	53.0	12.0	3.4	0	0
16'-17'	100	100	100	99.3	99.0	96.8	92.2	88.1	82.7	70.0	62.7	46.9	42.0	4.4	3.4	0	0
21'-22'	100	96.0	92.6	89.7	86.4	79.3	68.9	58.5	50.5	43.0	38.5	28.2	26.5	5.0	3.2	0	0
26'-27'	100	100	100	98.9	98.4	97.2	94.0	90.4	86.2	71.0	61.4	47.9	41.5	30.5	2.0	0	0
31'-32'	100	100	96.4	92.3	91.3	86.7	73.5	62.9	56.8	47.5	41.7	34.3	30.5	21.0	16.5	12	8.9

TABLE 4

GRAIN-SIZE DISTRIBUTION

T-1 (% PASSING)

	GRAVEL				SAND								SILT SIZE			CLAY SIZE	
					COARSE		MEDIUM		FINE								
DEPTH	1.5"	1.0"	3/4"	3/8"	#4	#10	#20	#40	#60	#100	#140	#200	.05	.01	.005	.002	.001
4'-5'	100	100	100	100	99.7	98.0	92.1	83.9	76.7	66.0	58.2	50.0	46.4	40.8	37.8	30.0	25.0
8.5'-9.5'	100	100	100	99.8	99.5	98.6	94.0	85.1	76.5	63.7	54.7	47.0	46.8	37.4	33.9	28.3	18.5
12'-13'	100	100	100	98.7	98.5	97.3	95.1	89.7	84.5	73.7	67.6	60.3	59.4	55.7	52.0	38.2	34.4

T-2 (% PASSING)

	GRAVEL				SAND								SILT SIZE			CLAY SIZE	
					COARSE		MEDIUM		FINE								
DEPTH	1.5"	1.0"	3/4"	3/8"	#4	#10	#20	#40	#60	#100	#140	#200	.05	.01	.005	.002	.001
4'-5'	100	100	100	99.2	98.1	93.9	87.1	80.1	72.3	59.0	50.3	40.8	37.1	22.2	6.0	5.2	5.2
8.5-9.5	100	100	98.0	91.2	88.4	81.2	63.3	49.2	39.4	30.5	24.7	19.3	17.4	6.2	5.1	5.1	5.1
12'-13'	100	96.2	93.2	88.9	85.0	73.6	60.4	49.9	43.0	34.2	28.2	21.5	18.0	12.8	4.0	3.8	3.8

TABLE 5

PARTICLE SIZE PERCENTAGES

		RANGE					
Borehole	Depth Meters (Feet)	Gravel %	Course Sand %	Medium Sand %	Fine Sand %	Silt Size %	Clay Size %
B-1	0-1.5(0-5)	2-9	18-21	17-18	15-23	17-29	15-16
	1.5-3.0(5-10)	8-21	27-37	12-18	4-12	26-36	0
	3.0-6.1(10-20)	9-42	35-72	6-13	2-5	7-13	0-6
	6.1-7.3(20-24)	0-1	21-22	7-8	8-9	44-45	11-20
	7.3-9.8((24-32)	1-9	12-20	11-17	12-31	21-26	21-22
B-2	0-7.0(0-23)	0-4	10-23	12-20	8-20	44-60	0-4
	7.0-9.8(23-32)	1-7	18-37	13-20	13-20	20-45	0-7
B-3	0-2.4(0-8)	1-4	24-31	17-19	15-17	25-37	0-13
	2.4-4.6(8-15)	0-1	6-12	16-18	18-20	52-56	0
	4.6-8.5(15-28)	1-15	13-20	15-24	12-20	30-52	0
	8.5-9.8(28-32)	3-4	15-17	12-13	10-11	57-58	0
B-4	0-2.4(0-8)	0-6	13-27	14-25	14-20	16-31	12-22
	2.4-4.6(8-15)	24-27	38-52	7-12	1-5	9-15	3-9
	4.6-7.0(15-23)	0-8	13-15	11-21	14-21	29-36	14-17
	7.0-9.8(23-32)	0-1	4-7	19-22	22-24	45-49	2-4
B-5	0-.9(0-3)	2-4	14-16	21-22	21-22	23-24	15-16
	.9-3.0(3-10)	0-8	3-22	10-21	11-31	38-51	0
	3.0-4.6(10-15)	0-1	6-12	9-16	17-20	57-62	0
	4.6-9.8(15-32)	1-9	8-38	15-20	14-23	22-48	0-12
Trench 1	0-3.0(0-10)	0-1	13-14	10-13	7-9	8-13	28-30
	3.0-4.6(10-15)	1-2	7-8	10-11	7-8	7-8	38-39
Trench 2	0-1.8(0-6)	0-1	13-14	13-14	9-10	31-32	5-6
	1.8-4.6(6-15)	8-11	23-32	8-9	5-7	12-14	3-5

TABLE 6

SOIL SAMPLES IDENTIFICATION DATA

Boring	Depth Meters (Feet)	W_N (%)	W_{HYGR} %	Gs	W_L (%)	W_p (%)	I_p
B-1	.31-.61(1-2)	4.06	1.95	2.65	24	10	14
	1.1-1.4(3.5-4.5)	4.12	1.97	2.63	21	14	7
	1.8-2.1(6-7)	7.41	4.87	2.63	24	17	7
	2.6-2.9(8.5-9.5)	3.67	2.13	2.68	22	15	7
	3.4-3.7(11-12)	1.61	.99	2.67	15	14	1
	4.1-4.4(13.5-14.5)	1.95	1.06	2.67	15	14	1
	4.9-5.2(16-17)	1.68	.87	2.66	16	15	1
	5.6-5.9(18.5-19.5)	1.58	.75	2.65	16	15	1
	6.4-6.7(21-22)	6.89	2.68	2.66	29	12	17
	7.9-8.2(26-27)	6.65	2.29	2.67	20	14	6
	9.4-9.8(31-32)	7.50	2.57	2.61	22	16	6
B-2	.31-.61(1-2)	5.64	5.56	2.69	26	13	13
	1.1-1.4(3.5-4.5)	11.67	9.25	2.65	31	22	9
	1.8-2.1(6-7)	9.61	7.14	2.69	26	19	7
	2.6-2.9(8.5-9.5)	7.00	3.44	2.67	21	10	11
	3.4-3.7(11-12)	15.10	11.30	2.81	32	21	11
	4.1-4.4(13.5-14.5)	12.16	10.28	2.75	32	23	9
	4.9-5.2(16-17)	11.38	8.14	2.80	33	28	5
	6.4-6.7(21-22)	9.77	6.38	2.75	31	22	9
	7.6-7.9(25-26)	7.24	3.48	2.70	24	16	8
	7.9-8.2(26-27)	13.23	6.16	2.74	27	19	8
	9.4-9.8(31-32)	4.88	2.02	2.67	23	18	5
B-3	.31-.61(1-2)	3.63	2.01	2.62	22	15	7
	1.1-1.4(3.5-4.5)	5.58	4.35	2.69	23	18	5
	1.8-2.1(6-7)	4.95	3.27	2.70	21	19	2
	2.6-2.9(8.5-9.5)	9.78	6.79	2.70	28	19	9
	3.4-3.7(11-12)	8.19	4.61	2.69	27	20	7
	4.1-4.4(13.5-14.5)	13.23	10.66	2.72	32	26	6
	4.6-4.9(15-16)	10.79	8.28	2.70	31	25	6
	4.9-5.2(16-17)	10.64	7.52	2.72	31	25	6
	6.4-6.7(21-22)	10.38	8.01	2.77	32	23	9
	7.6-7.9(25-26)	7.17	4.95	2.72	25	20	5
	7.9-8.2(26-27)	4.96	3.49	2.73	22	18	4
	9.4-9.8(31-32)	7.51	3.03	2.68	24	20	4

TABLE 6
(continued)
SOIL SAMPLES IDENTIFICATION DATA

Boring	Depth Meters (Feet)	W_N (%)	W_{HYGR} %	Gs	W_L (%)	W_p (%)	I_p
B-4	.31-.61(1-2)	3.51	2.56	2.61	19	16	3
	1.1-2.4(3.5-4.5)	4.72	2.23	2.64	24	13	11
	1.8-2.1(6-7)	3.86	1.41	2.65	22	14	8
	2.6-2.9(8.5-9.5)	1.89	.95	2.67	19	16	3
	3.4-3.7(11-12)	1.69	.75	2.64	18	14	4
	4.1-4.4(13.5-14.5)	1.47	.79	2.65	16	15	1
	4.9-5.2(16-17)	6.84	2.24	2.64	26	14	12
	6.4-6.7(21-22)	6.34	3.13	2.69	22	12	10
	7.9-8.2(26-27)	11.58	6.18	2.73	29	25	4
	9.4-9.8(31-32)	11.34	6.17	2.73	31	22	9
B-5	.31-.61(1-2)	3.85	1.72	2.61	21	12	9
	1.1-1.4(3.5-4.5)	14.69	12.19	2.62	34	34	0
	1.8-2.1(6-7)	9.52	6.82	2.76	29	29	0
	2.6-2.9(8.5-9.5)	8.03	5.46	2.73	25	25	0
	3.4-3.7(11-12)	10.73	6.52	2.77	27	18	9
	4.1-4.4(13.5-14.5)	14.37	12.56	2.73	31	26	5
	4.9-5.2(16-17)	13.87	10.68	2.75	36	24	12
	6.4-6.7(21-22)	10.50	5.84	2.74	28	19	9
	7.9-8.2(26-27)	10.35	5.67	2.72	24	16	8
	9.4-9.8(31-32)	5.11	1.80	2.65	22	13	9
Trench 1	1.2-1.5(4-5)	4.10	1.60	2.64	29	23	7
	2.6-2.9(8.5-9.5)	3.75	1.10	2.64	23	14	9
	3.7-4.0(12-13)	3.80	1.20	2.65	26	17	9
Trench 2	1.2-1.5(4-5)	8.50	6.30	2.73	27	20	7
	2.6-2.9(8.5-9.5)	7.25	5.10	2.74	27	24	3
	3.7-4.0(12-13)	4.50	2.60	2.73	23	19	4

TABLE 7. SOIL CLASSIFICATION

Borehole	Depth Meters (Feet)	% Passing #200	% Passing #4	W_L (%)	I_p	Cu (AVE)	Cz (AVE)	USCS Class.
B-1	0-1.5(0-5)	33-45	91-98	21-24	7-14	246	6	SC
	1.5-3.0(5-10)	26-36	79-93	22-24	7-8	92	9	SM-SC
	3.0-6.1(10-20)	7-15	58-92	15-16	0-1	47	5	*SM
	6.1-7.3(20-24)	63-64	99-100	29-30	17-18	41	.2	CL
	7.3-9.8(24-32)	42-48	91-99	20-22	6-7	380	1	SM-SC
B-2	0-7.0(0-23)	50-62	96-100	21-33	5-13	11	.2	CL
	7.0-9.8(23-32)	26-45	93-100	23-27	5-8	60	2	SC
B-3	0-2.4(0-8)	33-38	96-99	21-23	2-7	30	1	SM-SC
	2.4-4.6(8-15)	52-56	99-100	27-32	6-9	13	.2	CL
	4.6-8.5(15-28)	30-50	84-100	22-32	4-9	13	.5	SM-SC
	8.5-9.8(28-32)	57-58	96-97	24-25	4-5	21	.1	CL
B-4	0-2.4(0-8)	38-43	94-100	19-24	3-11	350	10	SC
	2.4-4.6(8-15)	17-18	73-76	16-19	1-4	250	15	*SM
	4.6-7.0(15-23)	50-53	92-100	22-26	10-12	45	.2	CL
	7.0-9.8(23-32)	48-50	99-100	29-31	4-9	16	.1	SC
B-5	0-.9(0-3)	38-39	97-98	21-22	9-10	25	1	SC
	.9-3.0(3-10)	38-50	91-100	25-34	0-1	12	.5	*SM
	3.0-4.6 (10-15)	57-62	99-100	27-31	5-9	8	.3	CL
	4.6-9.8(15-32)	28-48	86-99	22-36	8-12	20	2	SC
Trench 1	0-3.0(0-10)	47-50	99-100	23-29	7-9	1300	.4	SC
	3.0-4.6(10-15)	60-61	98-99	26-27	9-10	250	.1	CL
Trench 2	0-1.8(0-6)	40-41	98-99	27-28	7-8	23	.3	SM-SC
	1.8-4.6(6-15)	19-22	85-89	23-27	3-4	75	2	*SM

*These layers were very sandy and difficult to perform the Plastic Limit Test on. Their designation as a silty sand and the low Plasticity Index (0-4) confirm this condition.

TABLE 8

COMPACTION DATA

TRENCH	Depth Meters (Feet)	W_N (%)	W_{HYGR} (%)	W_{OPT} (%)	γ_{dmax} Kg/m^3 (pcf)
T-1	1.2-1.5(4-5)	4.10	1.60	13.80	1,898 (118.5)
	2.6-2.9(8.5-9.5)	3.75	1.10	11.10	2,010 (125.5)
	3.7-4.0(12-13)	3.80	1.20	12.90	1,858 (116.0)
T-2	1.2-1.5(4-5)	8.50	6.30	15.10	1,658 (103.5)
	2.6-2.9(8.5-9.5)	7.25	5.10	13.40	1,863 (116.3)
	3.7-4.0(12-13)	4.50	2.60	11.10	1.996 (124.6)

*Values of W_{OPT} and γ_{dmax} were obtained by the Standard Proctor Test, using material passing the Number 4 Sieve (4.76 mm).

TABLE 9

UNCONFINED COMPRESSION DATA

Trench	Depth Meters (Feet)	W_{INT} (%)	W_{FINAL} (%)	W_{HYGR} (%)	σ_f Kn/M^2(psi)	ϵ_f (%)	E_f Kn/m^2(psi) (X1000)	E_{3T_2} Kn/m^2(psi) (X1000)
T-1	1.2-1.5(4-5)	9.6	9.6	1.6	398 (58)	1.4	28 (4)	36 (5)
		9.6	1.6	1.6	1485 (215)	.9	165 (24)	330 (48)
		13.0	13.0	1.6	621 (90)	1.5	41 (6)	154 (22)
		13.0	1.6	1.6	3020 (438)	1.2	252 (37)	303 (44)
		14.9	14.9	1.6	360 (52)	2.2	16 (2)	42 (6)
		14.9	1.7	1.6	5205 (755)	1.3	400 (58)	588 (85)
T-1	2.6-2.9(8.5-9.5)	8.1	8.1	1.1	547 (79)	1.1	50 (7)	50 (7)
		8.1	1.1	1.1	3302 (479)	.7	472 (68)	588 (85)
		10.8	10.8	1.1	290 (42)	3.8	8 (1)	100 (15)
		10.8	1.1	1.1	5520 (801)	1.4	394 (57)	500 (73)
		12.6	12.6	1.1	174 (25)	14.0	1.2 (.2)	11 (2)
		12.6	1.2	1.1	4350 (631)	2.0	218 (32)	215 (31)
T-1	3.7-4.0(12-13)	10.6	10.6	1.2	498 (72)	6.5	8 (1)	42 (6)
		10.6	1.2	1.2	8240 (1195)	1.2	687 (100)	952 (138)
		12.5	12.5	1.2	216 (31)	18.6	1.2 (.2)	13 (2)
		12.5	1.3	1.2	4925 (714)	1.7	290 (42)	313 (45)
		14.7	14.7	1.2	96 (14)	14.3	.7 (.1)	11 (2)
		14.7	1.1	1.2	5110 (741)	1.2	426 (62)	625 (91)
T-2	1.2-1.5(4-5)	13.4	13.4	6.3	309 (45)	1.7	18 (3)	20 (3)
		13.4	6.1	6.3	7090 (1028)	1.2	591 (86)	870 (126)
		15.4	15.4	6.3	295 (43)	3.3	9 (1)	11 (2)
		15.4	6.1	6.3	8265 (1199)	1.1	751 (109)	1000 (145)
		17.0	17.0	6.3	143 (21)	6.7	2.1 (.3)	2.8 (.4)
		17.0	6.0	6.3	5360 (777)	1.6	335 (49)	400 (58)

*The cylinder (sample) was allowed to dry for 72 hours for those specimens above which show final water content less than initial water content. The bottom two sample depths for Trench 2 (2.6-2.9 and 3.7-4.0 meters) were not tested in unconfined compression, since they could not be molded (soil was too sandy).

TABLE 10. TRIAXIAL COMPRESSION DATA

Trench	Depth Meters (Feet)	W (%)	γ_d Kg/m^3(pcf)	σ_c KN/m^2(psi)	σ_f KN/m^2(psi)	ϵ_f (%)	E_f KN/m^2(psi) (X1000)	E_{IT_2} KN/m^2(psi) (X1000)
T-1	1.2-1.5(4-5)	1.6	1297 (81)	51.7 (7.5)	147 (21)	5.5	2.7 (.4)	10 (2)
		1.6	1297 (81)	86.2 (12.5)	248 (36)	8.6	2.9 (.4)	-
		1.6	1297 (81)	120.7 (17.5)	331 (48)	12.0	2.8 (.4)	-
		9.6	1650 (103)	51.7 (7.5)	600 (87)	1.2	50 (7)	100 (15)
		9.6	1666 (104)	86.2 (12.5)	713 (103)	1.8	40 (6)	100 (15)
		9.6	1602 (100)	120.7 (17.5)	695 (101)	2.9	24 (3)	91 (13)
		13.0	1842 (115)	51.7 (7.5)	664 (96)	1.5	44 (6)	133 (19)
		13.0	1778 (111)	86.2 (12.5)	560 (81)	5.3	11 (2)	133 (19)
		13.0	1826 (114)	120.7 (17.5)	701 (102)	6.0	12 (2)	80 (12)
		14.9	1874 (117)	51.7 (7.5)	519 (75)	5.7	9 (1)	67 (10)
		14.9	1874 (117)	86.2 (12.5)	522 (76)	6.8	8 (1)	100 (15)
		14.9	1874 (117)	120.7 (17.5)	537 (78)	8.9	6 (.9)	91 (13)
T-1	2.6-2.9(8.5-9.5)	1.0	1509 (94)	51.7 (7.5)	131 (19)	5.2	2.5 (.4)	11 (2)
		1.0	1509 (94)	86.2 (12.5)	320 (46)	8.6	3.7 (.5)	-
		1.0	1509 (94)	120.7 (17.5)	429 (62)	11.4	3.8 (.6)	-
		8.1	1794 (112)	51.7 (7.5)	601 (87)	.9	67 (10)	133 (19)
		8.1	1794 (112)	86.2 (12.5)	599 (87)	2.5	24 (3)	133 (19)
		8.1	1778 (111)	120.7 (17.5)	601 (87)	4.3	14 (2)	111 (16)
		10.8	2002 (125)	51.7 (7.5)	385 (56)	11.8	3.3 (.5)	100 (15)
		10.8	2002 (125)	86.2 (12.5)	432 (63)	12.1	3.6 (.5)	100 (15)
		10.8	1986 (124)	120.7 (17.5)	467 (68)	11.8	4.0 (.6)	100 (15)
		12.6	1922 (120)	51.7 (7.5)	197 (29)	13.2	1.5 (.2)	63 (9)
		12.6	1922 (120)	86.2 (12.5)	180 (26)	13.9	1.3 (.2)	63 (9)
		12.6	1938 (121)	120.7 (17.5)	235 (34)	14.5	1.6 (.2)	63 (9)
T-1	3.7-4.0(12-13)	1.3	1394 (87)	51.7 (7.5)	164 (24)	5.2	3.1 (.4)	14 (2)
		1.3	1394 (87)	86.2 (12.5)	293 (42)	9.1	3.2 (.5)	-
		1.3	1394 (87)	120.7 (17.5)	398 (58)	13.5	2.9 (.4)	-
		10.6	1922 (120)	51.7 (7.5)	475 (69)	9.3	5.1 (.7)	133 (19)

TABLE 10. TRIAXIAL COMPRESSION DATA (continued)

Trench	Depth Meters (Feet)	W (%)	γ_d Kg/m^3(pcf)	σ_c KN/m^2(psi)	σ_f KN/m^2(psi)	ε_f (%)	E_f KN/m^2(psi) (X1000)	E_{IT} KN/m^2(psi) (X1000)
T-1	(3.7-4.0(12-13)	10.6	1906 (119)	86.2 (12.5)	542 (79)	10.5	5.2 (.8)	167 (24)
		10.6	1938 (121)	120.7 (17.5)	543 (79)	11.5	4.7 (.7)	167 (24)
		12.5	1922 (120)	51.7 (7.5)	286 (41)	13.3	2.2 (.3)	80 (12)
		12.5	1922 (120)	86.2 (12.5)	283 (41)	17.7	1.6 (.2)	80 (12)
		12.5	1938 (121)	120.7 (17.5)	323 (47)	14.2	2.3 (.3)	80 (12)
		14.7	1906 (119)	51.7 (7.5)	178 (26)	13.4	1.3 (.2)	60 (9)
		14.7	1890 (118)	86.2 (12.5)	174 (25)	11.9	1.5 (.2)	60 (9)
		14.7	1906 (119)	120.7 (17.5)	147 (21)	8.5	1.7 (.2)	40 (6)
T-2	1.2-2.5(4-5)	6.3	1538 (96)	51.7 (7.5)	182 (26)	4.3	4.2 (.6)	40 (6)
		6.3	1538 (96)	86.2 (12.5)	342 (50)	7.1	4.8 (.7)	-
		6.3	1538 (96)	120.7 (17.5)	465 (67)	10.1	4.6 (.7)	-
		13.4	1810 (113)	51.7 (7.5)	508 (74)	2.3	22 (3)	100 (15)
		13.4	1810 (113)	86.2 (12.5)	568 (82)	2.9	20 (3)	133 (19)
		13.4	1810 (113)	120.7 (17.5)	675 (98)	3.8	18 (3)	100 (15)
		15.4	1826 (114)	51.7 (7.5)	420 (61)	4.5	9.3 (1)	143 (21)
		15.4	1842 (115)	86.2 (12.5)	517 (75)	5.6	9.2 (1)	143 (21)
		15.4	1842 (115)	120.7 (17.5)	660 (96)	5.8	11 (2)	143 (21)
		17.0	1810 (113)	51.7 (7.5)	346 (50)	9.0	3.8 (.6)	100 (15)
		17.0	1794 (112)	86.2 (12.5)	368 (53)	6.5	5.7 (.8)	100 (15)
		17.0	1810 (113)	120.7 (17.5)	500 (73)	9.3	5.4 (.8)	100 (15)
T-2	2.6-2.9(8.5-9.5)	5.1	1586 (99)	51.7 (7.5)	270 (39)	6.7	4.0 (.6)	50 (7)
		5.1	1586 (99)	86.2 (12.5)	385 (56)	9.1	4.2 (.6)	-
		5.1	1586 (99)	120.7 (17.5)	485 (70)	11 3	4.3 (.6)	-
T-2	3.7-4.0(12-13)	2.6	1698 (106)	51.7 (7.5)	173 (25)	4.5	3.8 (.6)	71 (10)
		2.6	1698 (106)	86.2 (12.5)	316 (46)	7.3	4.3 (.6)	-
		2.6	1698 (106)	120.7 (17.5)	438 (64)	9.8	4.5 (.7)	-

*Trench 2 (Depths 2.6-2.9 and 3.7-4.0 meters) could not be molded due to high sand content; therefore, the only data shown is for air-dried compacted samples.

SECTION VI

DISCUSSION OF RESULTS

Initial field investigation of soil, as depicted in Table 1, indicated that the entire area of White Sands Missile Range in this survey consists primarily of sandy soil with varying degrees of fines. This type soil is typical in alluvial plains. Further laboratory testing and classification of the soil samples agreed with these initial findings. Four specific categories of soil are evident throughout the area. These are clayey sand (SC), silty sand (SM), silty sand to clayey sand (SM-SC), and low plasticity clay (CL). Using MILLRACE GZ-3 as the center of the area, the southern half appears to consist of a top layer of clayey sand ranging from 1-3 meters (3-10 feet) thick, with the thicker layers lying west of GZ-3. The clayey sand is underlain by a layer of silty sand ranging from 1.5-4.6 meters (5-15 feet) thick. This is followed by a layer of clay 2.1-2.7 meters (7-9 feet) thick, underlain by clayey sand. The northern half of the site consists of similar layers; however, the clay layer appears to be closer to the surface. In the western section of the North half, clay is seen about 4.6 meters (15 feet) below the ground surface. East of Douquette Mound clay is at the ground surface and reaches thicknesses of 7 meters (23 feet).

Particle size distribution varies over wide areas, as well as depths. The finer soils are located much deeper in the southern half of the site, while the northern half has the finer soil at relatively shallow depths. It is of interest to note that a comparison of Tables 5 and 7 shows a very small percentage of clay-size particles in the borehole depths classified as CL. This phenomena can best be explained by the results of the hydrometer test. These particular soils (CL) contained large amounts of cementing agents in either powder or clump form which created a non-dispersion of particles during the hydrometer test. This was evidenced by visible flocculation within the solutions. As a result, Table 5 clearly shows that these soils have the highest content of silt-size particles. If dispersion had been effective, the silt-size "clumps" would have separated, causing an increase in the clay-size particles.

All of the soils investigated are well graded based on their coefficient of curvature and uniformity. Additionally, natural and hygroscopic moisture contents tend to be very low and nearly equivalent. Liquid limits and plasticity indexes are low, with a slightly higher plastic range in the clay areas. Specific gravities varied from 2.61 to 2.81. The higher specific gravities appeared to correlate with areas of obvious cementation, in most cases. This is expected since calcite has a specific gravity of about 2.72.

Standard penetration test results indicated the in-s' . soil to be dense to very dense over the entire site, to the full 10 meter (32 feet) depth. A few areas of medium density and pockets of loose gravelly sand were found sporadically throughout the site. This tends to corroborate the existence of caliche in this area. N-values were very high for certain layers (greater than 50) and reached 90-111 in some cases. Caliche will be looked at further in Section VIII of this report. Specific in-situ densities taken with the downhole nuclear density gauge ranged from 1567-1890 Kg/m^3 (98-118 pcf), with

the higher densities at lower depths as would be expected. Maximum dry densities, as determined from the Standard Proctor Test, ranged from 1658-2010 Kg/m^3 (104-125 pcf) at depths down to 4 meters (15 feet). The higher values were found in the soils containing larger amounts of clay-size particles or gravelly sand. Soils with higher amounts of silt-size particles to fine sand tended to have lower maximum dry densities.

Unconfined compression tests were run solely on soils with high silt and clay-size percentages due to mold limitations, while triaxial tests included soils with higher gravel and coarse sand contents. Young's Modulus at failure tends to be higher at shallower depths and lower water contents (about 2-3% below optimum). Additionally, the modulus is higher in the soils with high percentages of clay-size particles. Peak failure stresses for both confined and unconfined conditions also follow this pattern, while strains tend to increase with increasing water content (above optimum). The highest failure stresses were found in the soils containing larger amounts of fines. For these soils, peak failure stresses ranged from 400-700 KN/m^2 (59-100 psi) if a high clay-size content was evident. If a high silt content was evident, peak failure stresses ranged from 500-675 KN/m^2 (73-98 psi). Lower failure stress values were evidenced at higher water contents for both cases. See Tables 9 and 10.

Two additional tests were accomplished. First, specimens were compacted at various water contents matching those used in the unconfined compression test. These cylinders were then allowed to air dry for 72 hours at which time they reached hygroscopic moisture contents. As time passed, they became stronger as evidenced by feel and sight. The cylinders were then tested in unconfined compression. Failure stress increases, from this wetting/drying condition, ranged from 400-5300 percent. Peak failure stresses tended to increase more with increasing initial water content, increasing depth, and a higher silt fraction (vice clay).

The second additional test performed was triaxial compression on samples compacted from air-dry soil. In this case, the water contents were also hygroscopic, however particle cementation was not allowed. Peak failure stresses decreased significantly from values found in the other (wet sample) triaxial tests, and tended to be highest in the coarser soils (up to 485 KN/m^2).

SECTION VII

CONCLUSIONS

The previous field and laboratory test results lead to the following conclusions:

(1) The site at WSMR, characterized by this project, consists primarily of sandy soil with traces of gravel throughout the region. Heavier gravel contents are found in the southern region. The sand has varying degrees of fines and has been deposited in alternating layers of SM, SM-SC, and SC, with some thick layers of low plasticity clay.

(2) The in-situ soil is dense to very dense over most of this region and shows strong evidence of caliche.

(3) Peak failure stresses of soil samples tested for this site vary over a large range, up to 700 KN/m^2 (7.2 tons per square foot) in a wet condition. The actual in-situ strength is most likely higher, since the natural moisture contents tend to be near the hygroscopic moisture contents and the in-situ densities are high. The tests indicated that failure stresses increased significantly for compacted samples which were first wet, then allowed to dry. Past geological conditions indicate that actual wetting/drying periods did occur.

(4) The items evaluated in regard to analysis of weapon systems effects included material index properties, grain-size distribution, specific gravities, and deformation versus strength properties. Results are found in Tables 1-10 and Appendices A-F. Additional information on caliche and seismic refraction is available in Sections VIII and IX.

(5) This report primarily evaluated static properties of the subsoil. Detailed testing of dynamic properties should also be conducted to provide better correlations with the dynamic effects of weapon blasts. Some recommended test are seismic surveys which determine both shear and compressive waves, the dynamic odometer which uses impulse loads, and the cylindrical in-situ test (Reference 1) which uses high explosive shock impulses in the field.

SECTION VIII

EFFECTS OF CALICHE ON STATIC STRENGTH PROPERTIES

1. INTRODUCTION

Numerous tests and reports by the Air Force Weapons Laboratory, as well as the Civil Engineering Research Facility, have indicated the presence of cemented soils known as "caliche" within the boundaries of White Sands Missile Range (WSMR), New Mexico. Due to the nature of this range (test site), each report has attempted to characterize the type of cementation and its possible effects on soil properties. None of the reports located, however, indicated any actual laboratory tests having been performed.

The purpose of this section of the project is to delineate the nature of caliche which may be expected in this region and to correlate this with various soil properties and strength parameters. Prior to discussing actual tests performed, a look at the current state-of-the-art is in order.

2. STATE-OF-THE-ART

Much research on caliche has been accomplished in South and Southwestern Africa by the National Institute for Road Research. This research has been documented in many articles through the years by F. Netterberg, who has gained expertise in this field. Many names are used to describe "cemented soil" throughout the world, to include: caliche, surface limestone, hardpan, kankar, *jigilin*, and duracrust. F. Netterberg uses the name "calcrete," which was coined by Lamplugh (1902) and originates from the two Latin words, "calx," meaning lime, and "crescere," meaning grow (or lime grown together). This appears appropriate, since calcrete is essentially created from lime substances (e.g., calcium) which grow within the soil itself by the formation of crystals.

The main chemical composition of calcrete is calcium and silicate with smaller amounts of magnesim, alumina, and iron in the forms CaO, SiO_2, MgO, Al_2O_3, and Fe_2O_2. Calcium is generally found as a carbonate (or calcite), $CaCO_3$, while magnesium is always present in the form of dolomite. These two compounds are generally found to be the cementing agents in calcrete, with calcium carbonate being the primary agent. Magnesium is found in much smaller amounts, primarily due to wetter initial periods, and tends to increase with distance from the rock source. Calcium carbonate is generally present as fine-grained material adhering to detrital quartz grains and traversed by silica and course calcite veins.

Calcrete is formed in stages, where hardness increases over each stage. Initially, carbonate is precipitated from soil or ground water acting over (or from) a calcium and magnesium-producing source (certain rocks release these chemicals upon weathering). Calcrete is, therefore, a pedogenic material which is formed by near-surface cementation or replacement of a host soil during the precipitation and evaporation process. The stages of formation are represented in Table 11.

Table 11

CALCRETE FORMATION

(Initial) Sand or Gravel with Silt or Clay with carbonate-coated grains	(Initial) Heavy Clay-size concentrations
(Stage 1) Calcified Sand or Gravel	(Stage 1) Powder Calcrete
(Stage 2) Nodular Calcrete	
(Stage 3) Honeycomb Calcrete	
(Stage 4) Hardpan Calcrete	
(Stage 5) Boulder Calcrete	

Powder calcrete is a fine, loose, powder consisting of calcium carbonate with few visible soil particles and little or no nodular development. It has a large silt or clay-size faction in it. Calcified sand, or gravel, is generally loose material weakly cemented by calcium carbonate and has a higher sand or gravel content. Nodular calcrete is discreet, usually intact, very soft to very hard concentrations of carbonate-cemented soil, with the maximum diameter of nodules less than 6.35 cm (2.5 inches). Honeycomb calcrete is continuously honeycombed with voids up to 2.54 cm (1 inch) diameter filled with basic soil. Hardpan calcrete is a firm to very hard sheetlike layer underlain by looser material, where the layer is generally less than 45.7 cm (18 inches) thick. The material underneath is not cemented, most likely due to the hardpan layer becoming impermeable (stops further leaching) or a decrease in rainfall which would decrease the leaching depth. Hardpan can occur as sheet, tufaceous (porous), shattered, bedded (layered), or conglomeratic (cemented river gravels). Boulder calcrete is weathered hardpan (forms boulder-like pieces).

The formation of calcrete is relatively simple. Calcium carbonate is released from some source, such as river water, alluvial run-off, or weathering of underlying bedrock. The calcium carbonate, which is in solution in water, is then leached down to lower layers of the subsoil due to increased rainfall, increased permeability of top soil layers, or a decrease in temperature (causes decrease in evaporation). As the calcite settles out of solution, it adheres to and grows on surrounding soil particles. Evaporation of soil or ground water increases this growth process. Greater thicknesses of calcrete are found in semiarid regions where annual rainfall is less than 550 mm (21.7 inches) and there is a fluctuating but steadily dropping water table. The distribution and thickness of calcrete are dependent on the five factors responsible for soil formation. These are climate, topography, parent material, biological factors, and time. Geology is also important and is a

subfactor of parent material. As previously stated, the primary climatic condition necessary is a mean annual rainfall less than 550 mm. If higher temperatures prevail, then a higher amount of rainfall is required to form calcrete, up to 625 mm (24.6 inches). The depth of calcrete formation increases with increased rainfall, due to increased leaching. Topographically, calcrete is normally found in flatter regions or in depressions, where moisture can accumulate, weather underlying soil, release calcium and magnesium, and evaporate in-situ. This is particularly true in alluvial plains. Drainage beds can also be excellent locations for calcrete, providing all other conditions are met. As far as parent material is a concern, calcrete is most likely to form over calcareous rocks, such as limestone, dolomite, calcareous shales, mudstones, and basalt which release calcium and magnesium on weathering. It may also be found over granite or sandstone if drainage conditions are favorable. For a given climate, calcrete formation is slower in a less permeable soil. Essentially, biological factors concern vegetation. Calcretes tend to be associated with the presence of bush and grass cover. Specifically, certain types of calciphilic plants are evident in calcrete areas. Some of these are gabbabos, saliebos, and vaalbos. Plants of the Acacia reficiens genus (woody, leguminous plants of warm regions with pinnate leaves or leaves reduced to phyllodes-branches resemble foliage leaves and white or yellow flower clusters) can also be found in calcrete regions. Although not calciphilous, acacia plants indicate the presence of shallow water which can indicate calcrete in a semiarid region. The last factor for calcrete formation is time. Time tends to increase the developmental stage and hardness of calcrete formed.

Based on the factors which form calcrete, there are several ways available to detect calcrete formations. Some of these are seismic surveys, aerial photography analysis, infrared imagery, and probing. Seismic analysis entails the measurement of seismic wave velocities in the subsoil and is covered in detail in Section IX of this report. Essentially, the various forms of calcrete have seismic velocities as listed in Table 12.

Table 12

SEISMIC VELOCITIES OF SUBSURFACE CALCRETE

Type Calcrete	Velocity m/sec (feet/sec)
Calcified Sand	450-1200 (1476-3937)
Powder Calcrete	400-1000 (1312-3280)
Nodular Calcrete	600-900 (1968-2952)
Honeycomb Calcrete	900-1200 (2952-3937)
Hardpan Calcrete	1200-4500 (3937-14,763)
Boulder Calcrete	Erratic

Items, such as topography, drainage, vegetation, parent material, and basic geology, can be inferred from aerial photo interpretation and infrared imagery. Probing involves the hammering of a metal probe (2-inch diameter pipe with top 10 inches solid and bottom 12 inches hollow with rod or probe at bottom that is 3/8 inch in diameter and 84 inches long) into the ground until refusal or concerned depth is reached. Penetration resistance is taken as an indicator of the relative strength of the calcrete and is related to type of calcrete as seen in Table 13.

Table 13

INTERPRETATION OF PENETRATION RESISTANCE

Penetration Resistance	Color of Soil	Calcrete Type
Low	White (sandy)	Calcified Sand
Low to Fair	White	Powder Calcrete
Fair to High	White or Pale Pink	Tufaceous Hardpan
High	White or Pale Pink	Loose, Hard Nodular Calcrete or Stiff Hardpan
Refusal	White or Pale Pink	Hard to Very Hard Boulder Calcrete or Sheet Hardpan

Other properties of calcrete include: crushing strength, plasticity index, particle-size distribution and grading. Crushing strength tends to increase with time and fineness of particles. In the field, strength is taken as a function of Mohs' Hardness Scale. Mohs' hardness values typically found in calcrete are powder and calcified sand (0-1), nodular calcrete (1-5), honeycomb calcrete (2-5.5), hardpan (1.5-6), and boulder calcrete (3-5). Mohs' scale for hardness is relative as depicted in Table 14.

Table 14

MOHS' HARDNESS SCALE

Type Mineral	Relative Hardness Value
Talc (Magnesium Silicate)	1
Gypsum (Calcium Sulphate)	2
Calcite (Calcium Carbonate)	3
Fluorite (Calcium Fluoride)	4
Apatite (Calcium Phosphate)	5
Orthoclase (Potassic Feldspar)	6
Quartz	8
Fused Alumina	12
Diamond	15

Plasticity index may be a poor indicator of calcrete quality due to the unreliability of obtaining the index, and a high plasticity index may be found while pure calcium carbonate is non-plastic (with high liquid limit about 30 percent). Even so, the plasticity index is often used as an indicator where it tends to be higher if the calcrete was formed in clays rather than sands and generally increases with depth. The plasticity index tends to fall in the following ranges: calcified sand (0-150), powder (3-15), nodular (0-20), honeycomb (0-20), hardpan (0-3), and boulder (0-3). Reddish to brownish color may indicate a lower plasticity index in calcrete as well as a courser faction in particle-size. Grey to white colors would indicate the opposite. In general, calcretes tend to be poorly graded with a high silt or clay-size faction. Calcified sand and powder calcrete tend to have in-situ densities from a loose condition to medium dense. Nodular calcrete is loose, while honeycomb, hardpan, and boulder calcrete are dense to very dense.

Another observation about calcrete is that it tends to cement or "self-stabilize" when subjected to alternate wetting and drying periods. Additionally, flocculation is frequently encountered during hydrometer analysis. Flocculation can be prevented by the addition of 20 ml of a 36 gm/liter solution of tetra sodium pyrophosphate, as a dispersing agent.

3. TESTING PROCEDURES

A. LIBRARY SEARCH

This portion, entitled "Library Search," is included to explain why caliche, or calcrete, was suspected in the 2.59 kilometers squared (1 square mile) area of concern at WSMR. Section II.1 of this report stated that the area was primarily an alluvial basin with possibilities of underlying igneous rock, such as granite or basalt. The region is also semiarid which has past periods of alternating wet/dry seasons and currently has a very low annual rainfall. The actual water table is very deep (about 60-90 meters below ground). Average particle sizes are silt-size to sand. Topography is relatively flat with the existence of old lake playas and erosion channels. Vegetation is primarily bush and grass (cactus and yucca trees). Additionally, the field standard penetration test indicated very high N-values (medium to very dense), which was also indicated by the downhole nuclear density gauge results. Actual particle-size distribution found through laboratory testing showed areas with high silt or clay-size content along with a high percentage of sand. Liquid limits and plasticity indexes ranged from 15-36 and 0-18. The color of samples taken from boreholes and trenches ranged from greyish white to reddish brown.

All of the previous findings are indicators of the presence of caliche, as evidenced by current state-of-the-art research. Several reports by different agencies have also indicated the presence of caliche in the form of calcium sulphates (gypsum) or calcium carbonates; however, detailed analysis was not performed in the region of concern at WSMR. One report, "HAVE HOST Cylindrical In-Situ (CIST) Data Analysis and Material Model Report," specifically found that caliche tended to form more in the regions of sands with fines than in clean sands.

Based on this evidence and the fact that the two trenches represented

three different soil types (High Clay-Fraction, High Silt-Fraction, Relatively Clean Gravelly Sand), it was decided to test for actual content of calcium and magnesium, type of chemical formation (carbonate, sulphate, or silicate), and various strength properties.

B. PREPARATION OF SAMPLES

Literature on soil chemistry indicated numerous tests for carbonate concentrations, most of which dealt with a very slow process of titration. In lieu of this, it was decided to perform the much quicker Atomic Absorbance (AA) test. Preparation of samples was fairly standard in all the various tests. First, about 9 kg (20 pounds) of soil from each trench depth (two trenches at three depths each) was air-dried, then riffle-split three times to obtain approximately 1 kg (2.2 pounds) of sample. This material was ground in a morter and rubber pestal, then passed through a number 10 sieve (2.0 mm). The material passing the number 10 sieve was quartered four times to obtain a representative sample of about 200 grams. This material was then passed through a number 40 sieve (.42 mm).

The next step was to prepare a reagent which would release the Ca++ and Mg++ elements from the soil samples. The best reagent appeared to be diluted hydrochloric acid. "A Textbook of Soil Chemical Analysis" recommended using a 4-molar hydrochloric acid (4M HCL) solution. The solution was, therefore, made by adding 140 ml of concentrated HCL to 260 ml of distilled water to form 400 ml of solution. Four hundred milliliters were deemed adequate (vice 1 liter) for the number of samples to be tested (need about 30 ml of solution per sample). The amount of soil to be used in the test varies according to expected $CaCO_3$ concentration in the minus number 40 material. Table 15 shows the amounts to be used.

Table 15

AMOUNT OF SOIL USED IN SAMPLES

Amount of Soil Used (grams)	Percent $CACO_3$
20	0-5
10	5-10
5	10-20
2	20-50
1	50

Five grams of soil were used, since a concentration of 10-20 percent $CaCO_3$ was expected in most samples. Thirty milliliters of 4M HCL were placed in each of 24 plastic flasks. Five grams of soil from each depth were added to a flask (four samples taken from each of six depths). The flasks were agitated for approximately 15 minutes in a mechanical shaker. The solution was then filtered through coarse filter paper into test tubes. The result was a clear, yellow liquid. This yielded soil concentrations of about 167 gm/liter.

During the actual AA test, this dilution ratio was found to be outside

the range of standards, therefore, each flask was further diluted. An approximation of the dilution factor was made by testing the standards first. The final dilution factors used were 1:400 (1 ml solution to 399 ml distilled water) for the calcium readings and 1:10 for the magnesium readings. It was noted that the actual concentrations would then be determined by multiplying the dilution factor (400 or 10) times the concentration found in the AA test.

C. PREPARATION OF STANDARDS

The two references by Perkin-Elmer Corporation provided information on preparation of standards. The standards are required in order to calibrate the AA equipment. Theoretically, atomic absorption operates in accordance with Beer's Law where concentration is proportional to absorbance. In reality, this relationship deviates (not linear) due to such causes as stray light present or non-homogeneous temperature and space in the absorbing cell. A plot is, therefore, made of known concentrations versus absorbance for the standards. This plot is then used with the actual samples to correlate absorbance versus concentration.

Selection of number and concentration of standards appear to be complex and vary appreciably with expected concentraions in the soil samples. Personnel with experience in this field were consulted, and it was decided to use nine standards for Ca++ and six standards for Mg++. See Table 16. The magnesium standards were prepared by first weighing out 3-4 grams of Mg++ ribbon and placing this into a flask. Concentrated HCL was poured into the flask to wash off the oxidation residue from the ribbon surfaces. This process was complete when the color turned from shiny metallic to a dull appearance. Distilled water was then added to stop the reaction. The liquid was then poured out and acetone used to dry the ribbon. The ribbon was then air-dried, and 1 gram was placed in a clean flask. Next, 40 ml of (1 + 1) HCL solution (1 volume HCL to 1 volume distilled water) was made. This solution was added 5 ml at a time until all of the Mg++ ribbon (1 gram) was dissolved--called Solution 1. A separate solution, called Solution 2, was then made of (1/100 v/v) HCL solution, by adding 10 ml concentrated HCL to 1000 ml distilled water. It is noted here that the acid should always be added to the water, not vice versa, in order to avoid a violent reaction. Solution 1 was then poured into a 1000 ml flask; Solution 2 was used to rinse the remaining Solution 1 into the flask, and then enough of Solution 2 was added to the 1000 ml flask to make 1 liter. This final solution was called the Stock Solution for Mg++ and was at a concentration of 1 g (Mg++)/liter of solution (or 1 mg per ml).

The standards for Mg++ were then prepared by adding various amounts of the stock solution to different amounts of distilled water to obtain diluted solutions of different concentrations. For example, 2 ml of stock solution were pipetted into a flask containing 48 ml of distilled water. This created a solution of 2 mg (Mg++) per 50 ml solution, or a concentration of 40 mg (Mg++) per liter.

The calcium stock and standards were prepared in a similar manner; however, calcium was used in a powder form vice metal to avoid a violent reaction upon addition of the HCL.

D. ATOMIC ABSORBANCE TEST

Atomic Absorbance (AA) tests are predicated on the basis that all elements have a specific number of electrons surrounding their nuclei. The atoms tend to be in a ground or stable state normally. The addition of light energy to the atoms will create an excited or unstable state as the energy is absorbed while outer electrons become unstable. The atom will immediately try to return to its stable stable, whereby, light energy will be released. As the number of atoms in the light path increases, the amount of light (of specific wavelength) absorbed also increases. By measuring the amount of light absorbed at a specific wavelength, the amount of analyte (element in vapor) can be determined. Results of the AA tests are found in Tables 16-17.

The five basic components of the AA machine are a light source, absorption cell, manochromator, detector to measure light intensity and amplify the signal, and a display to show the readings. The type of machine used for this project was a Perkin-Elmer 560 Atomic Absorbance Spectrophotometer. A special light source is used as well. This consists of a Hollow Cathode Lamp specific to a particular element (e.g., Ca++ and Mg++). Basically, the lamp emits a spectrum of light (of specific element origin) which passes through the absorption cell (flame) containing the sample vapor and is focused through a manochromator for light dispersion. The dispersed, isolated specific wavelength for the element goes to the detector which produces an electric current. The current is then processed by instrument electronics and the amount of light attenuation or element absorbance is displayed. The function of the flame is to convert the sample aerosol (created from sample solution) into an atomic vapor which can absorb light from the primary source (cathode lamp). The flame source can be either an air-acetylene mixture or a nitrous oxide-acetylene mixture. Air-acetylene was used due to the highly volatile nature of nitrous oxide-acetylene mixtures. One possible source of error can come from the sample element not being totally absorbed by the flame. For instance, magnesium absorption is interferred by the presence of silicon or aluminum. This can be eliminated by using a nitrous oxide-acetylene flame or by adding .1-1.0 percent lanthanum to the solution.

E. CALCULATION OF CONCENTRATIONS

A standard computer program provided by another graduate student (Tucker Green) was used with the Apple Computer to plot the standards and determine the various sample element concentrations. The concentrations of Ca++ and Mg++ in each sample are then adjusted by the dilution factors (400 for Ca++ and 10 for Mg++). See Table 18. The actual percentage of Ca++ or Mg++ in the soil is then calculated by dividing the adjusted concentrations by the original concentration of soil solution (167 g/liter), then multiplying this by the percent of minus number 40 material (.42 mm in the soil). See Table 19.

F. X-RAY DIFFRACTION

X-ray diffraction analysis was performed on the samples (by Ron Methany) from Trenches 1 and 2 in order to determine the nature of calcium and magnesium present, as well as any obvious trace elements. This process uses the spectrometric powder technique, where x-ray diffraction traces are made on mounted

samples. Material passing the number 40 sieve (.42 mm) was used to correlate findings with the Atomic Absorbance tests.

The results of the test indicated large amounts of calcium present in the form of carbonate, as well as silicons. Minor trace elements of potassium, iron, alumina, and magnesium were also evident. For the most part, the magnesium could not be detected, due to extremely low content.

Photographs of the samples under spectrometric analysis are found in Section VIII-4, Figures 1-6.

G. UNCONFINED/TRIAXIAL COMPRESSION TESTS

Detailed procedures on these tests are found in Section IV of this report. In addition to performing standard tests, samples were wet then dried in order to look at some of the cementation effects.

4. TESTING RESULTS

Results of the atomic absorbance and x-ray diffraction tests are given in this section in Tables 16-19 and Figures 1-6. Results of the unconfined and triaxial tests are found in Section V, Tables 9-10.

TABLE 16
ATOMIC ABSORBANCE RESULTS - STANDARDS

Element	Concentration (mg/liter)	3 Readings	3 Standard Deviations
Ca^{++}	3	.015/.015/.016	.0004/.0005/.0006
"	5	.022/.021/.022	.0011/.0006/.0004
"	7	.032/.033/.033	.0010/.0007/.0005
"	10	.038/.039/.039	.0010/.0009/.0009
"	20	.063/.066/.067	.0011/.0021/.0027
"	30	.106/.102/.109	.0036/.0024/.0009
"	40	.141/.142/.142	.0025/.0018/.0049
"	50	.196/.195/.199	.0041/.0040/.0033
"	60	.236/.243/.238	.0026/.0025/.0087
Mg^{++}	10	.378/.372/.373	.0041/.0035/.0057
"	20	.618/.612/.605	.0041/.0047/.0051
"	30	.759/.763/.758	.0057/.0044/.0054
"	40	.846/.844/.844	.0094/.0035/.0049
"	50	.903/.900/.904	.0029/.0037/.0054
"	60	.952/.949/.956	.0062/.0031/.0054

TABLE 17
ATOMIC ABSORBANCE RESULTS - SAMPLES

Element	Trench	Depth Meters (Feet)	3 Readings	3 Standard Deviations
Ca^{++}	T-1	1.2-1.5 (4-5)	.108/.107/.103	.0024/.0024/.0041
		1.2-1.5 (4-5)	.097/.091/.092	.0041/.0045/.0039
		2.6-2.9 (8.5-9.5)	.148/.145/.148	.0053/.0039/.0043
		2.6-2.9 (8.5-9.5)	.164/.161./163	.0024/.0049/.0051
		3.7-4.0 (12.13)	.251/.248/.249	.0085/.0113/.0091
		3.7-4.0 (12-13)	.255/.251/.257	.0043/.0073/.0088
Ca^{++}	T-2	1.2-1.5 (4-5)	.056/.050/.053	.0020/.0016/.0022
		1.2-1.5 (4-5)	.055/.055/.055	.0024/.0024/.0020
		2.6-2.9 (8.5-9.5)	.052/.055/.051	.0012/.0014/.0015
		2.6-2.9 (8.5-9.5)	.051/.046/.049	.0017/.0016/.0017
		3.7-4.0 (12-13)	.112/.112/.109	.0027/.0026/.0029
		3.7-4.0 (12-13)	.107/.104/.108	.0019/.0030/.0032
Mg^{++}	T-1	1.2-1.5 (4-5)	.571/.573/.575	.0101/.0049/.0066
		1.2-1.5 (4-5)	.523/.539/.532	.0053/.0047/.0046
		2.6-2.9 (8.5-9.5)	.534/.530/.529	.0083/.0031/.0080
		2.6-2.9 (8.5-9.5)	.571/.574/.558	.0045/.0037/.0065
		3.7-4.0 (12-13)	.610/.608/.610	.0105/.0050/.0052
		3.7-4.0 (12-13)	.628/.631/.623	.0055/.0050/.0055
Mg^{++}	T-2	1.2-1.5 (4-5)	.611/.613/.611	.0033/.0034/.0046
		1.2-1.5 (4-5)	.599/.602/.605	.0072/.0041/.0069
		2.6-2.9 (8.5-9.5)	.596/.595/.591	.0069/.0035/.0032
		2.6-2.9 (8.5-9.5)	.568/.564/.560	.0051/.0040/.0023
		3.7-4.0 (12-13)	.545/.535/.539	.0042/.0089/.0040
		3.7-4.0 (12-13)	.523/.525/.524	.0029/.0063/.0032

TABLE 18
CONCENTRATIONS IN SAMPLES

Element	Trench	Depth Meters (Feet)	Concentration (mg/liter)	Dilution Factor	Adjusted Concen. (mg/liter)
Ca^{++}	T-1	1.2-1.5 (4-5)	28.3	400	11,320
		1.2-1.5 (4-5)	24.8	400	9,920
		2.6-2.9 (8.5-9.5)	39.5	400	15,800
		2.6-2.9 (8.5-9.5)	44.0	400	17,600
		3.7-4.0 (12-13)	67.9	400	27,160
		3.7-4.0 (12-13)	69.3	400	27,720
Ca^{++}	T-2	1.2-1.5 (4-5)	13.9	400	5,560
		1.2-1.5 (4-5)	14.5	400	5,800
		2.6-2.9 (8.5-9.5)	13.4	400	5,360
		2.6-2.9 (8.5-9.5)	12.9	400	5,160
		3.7-4.0 (12-13)	29.7	400	11,880
		3.7-4.0 (12-13)	28.3	400	11,320
Mg^{++}	T-1	1.2-1.5 (4-5)	20.2	10	202
		1.2-1.5 (4-5)	17.5	10	175
		2.6-2.9 (8.5-9.5)	17.5	10	175
		2.6-2.9 (8.5-9.5)	19.9	10	199
		3.7-4.0 (12-13)	22.6	10	226
		3.7-4.0 (12-13)	23.9	10	239
Mg^{++}	T-2	1.2-1.5 (4-5)	22.8	10	228
		1.2-1.5 (4-5)	22.1	10	221
		2.6-2.9 (8.5-9.5)	21.6	10	216
		2.6-2.9 (8.5-9.5)	19.6	10	196
		3.7-4.0 (12-13)	18.1	10	181
		3.7-4.0 (12-13)	17.1	10	171

TABLE 19
ACTUAL CONCENTRATIONS - SOIL

Element	Trench	Depth Meters (Feet)	Concentration (%)	-No. 40 (%)	Concen. in Soil (%)
Ca^{++}	T-1	1.2-1.5 (4-5) 2.6-2.9 (8.5-9.5) 3.7-4.0 (12-13)	6.0-6.8 9.5-10.6 16.3-16.6	83.9 85.1 89.7	5.0-5.7 8.1-9.0 14.6-14.9
Ca^{++}	T-2	1.2-1.5 (4-5) 2.6-2.9 (8.5-9.5) 3.7-4.0 (12-13)	3.3-3.5 3.1-3.2 6.8-7.1	80.1 49.2 49.9	2.6-2.8 1.5-1.6 3.4-3.5
Mg^{++}	T-1	1.2-1.5 (4-5) 2.6-2.9 (8.5-9.5) 3.7-4.0 (12-13)	.11-.12 .11-.12 .14	83.9 85.1 89.7	.09-.10 .09-.10 .13
Mg^{++}	T-2	1.2-1.5 (4-5) 2.6-2.9 (8.5-9.5) 3.7-4.0 (12-13)	.13-.14 .12-.13 .10-.11	80.1 49.2 49.9	.10-.11 .06 .05

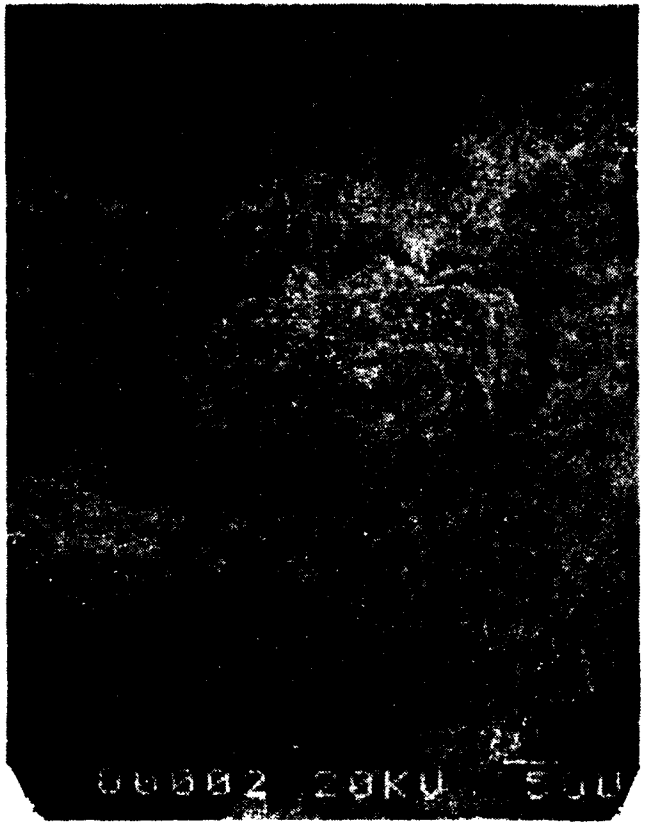

Figure 1. Trench 1 (4-5 feet)

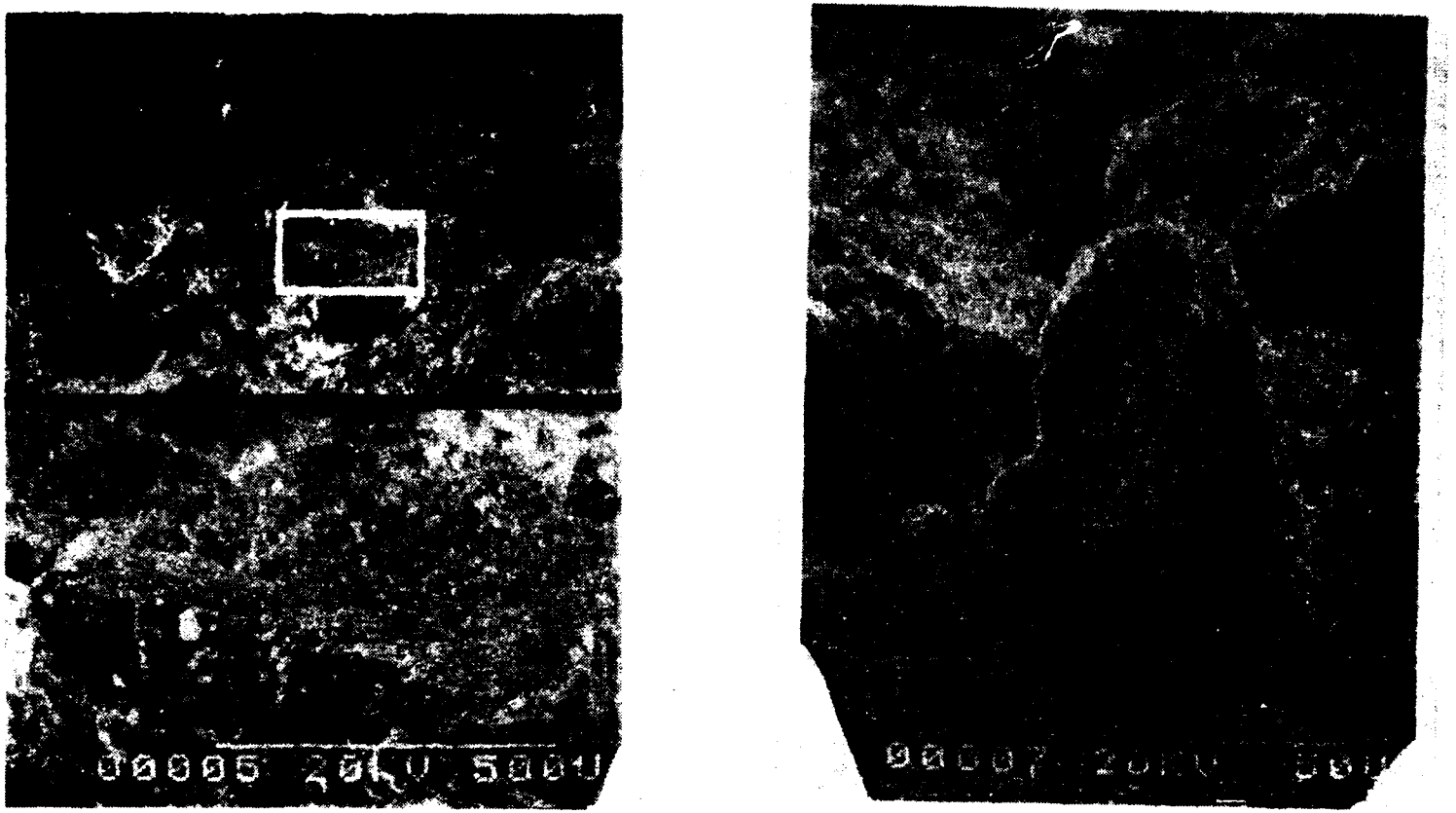

Figure 2. Trench 1 (8.5-9.5 feet)

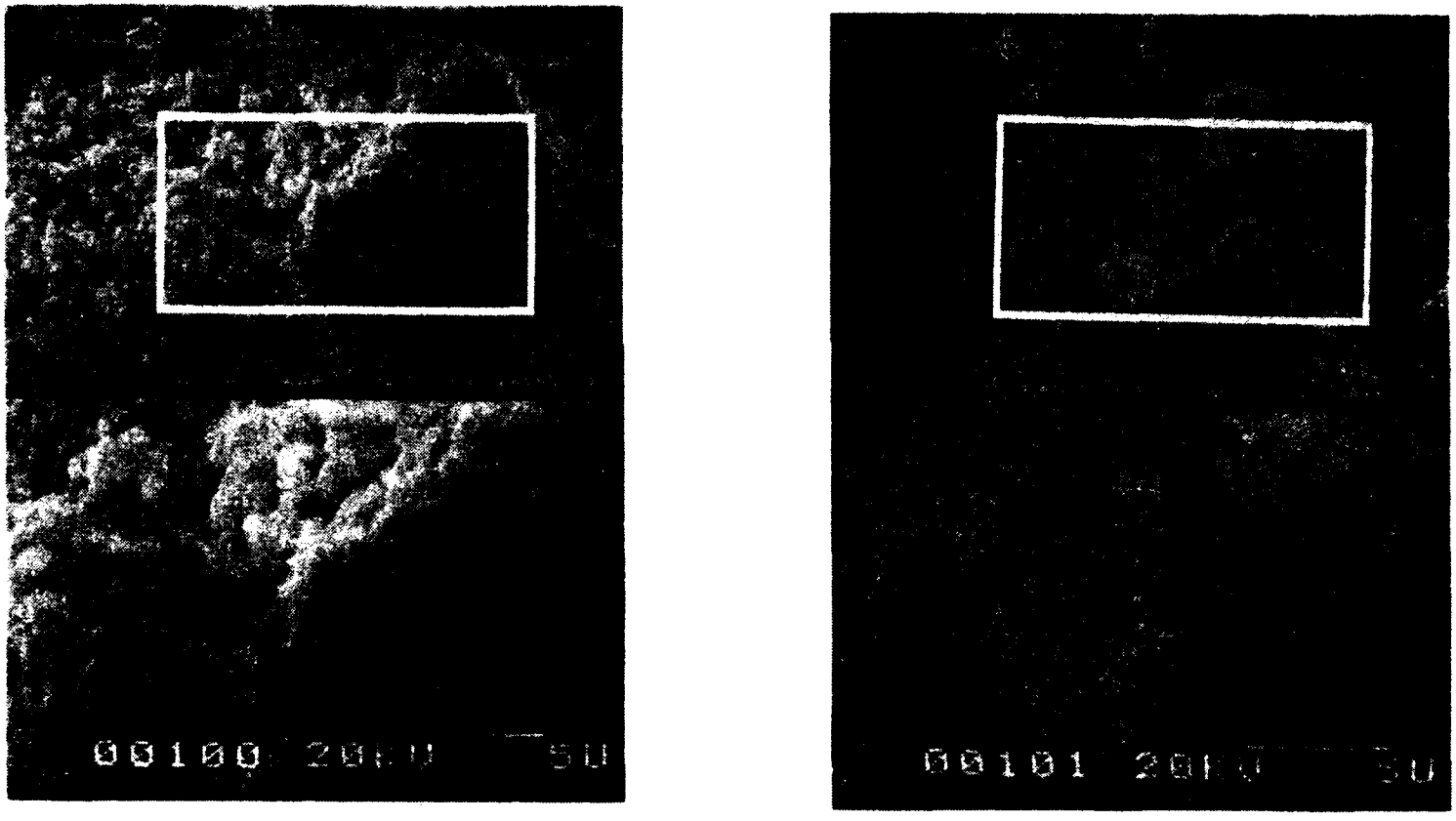

Figure 3. Trench 1 (12-13 feet)

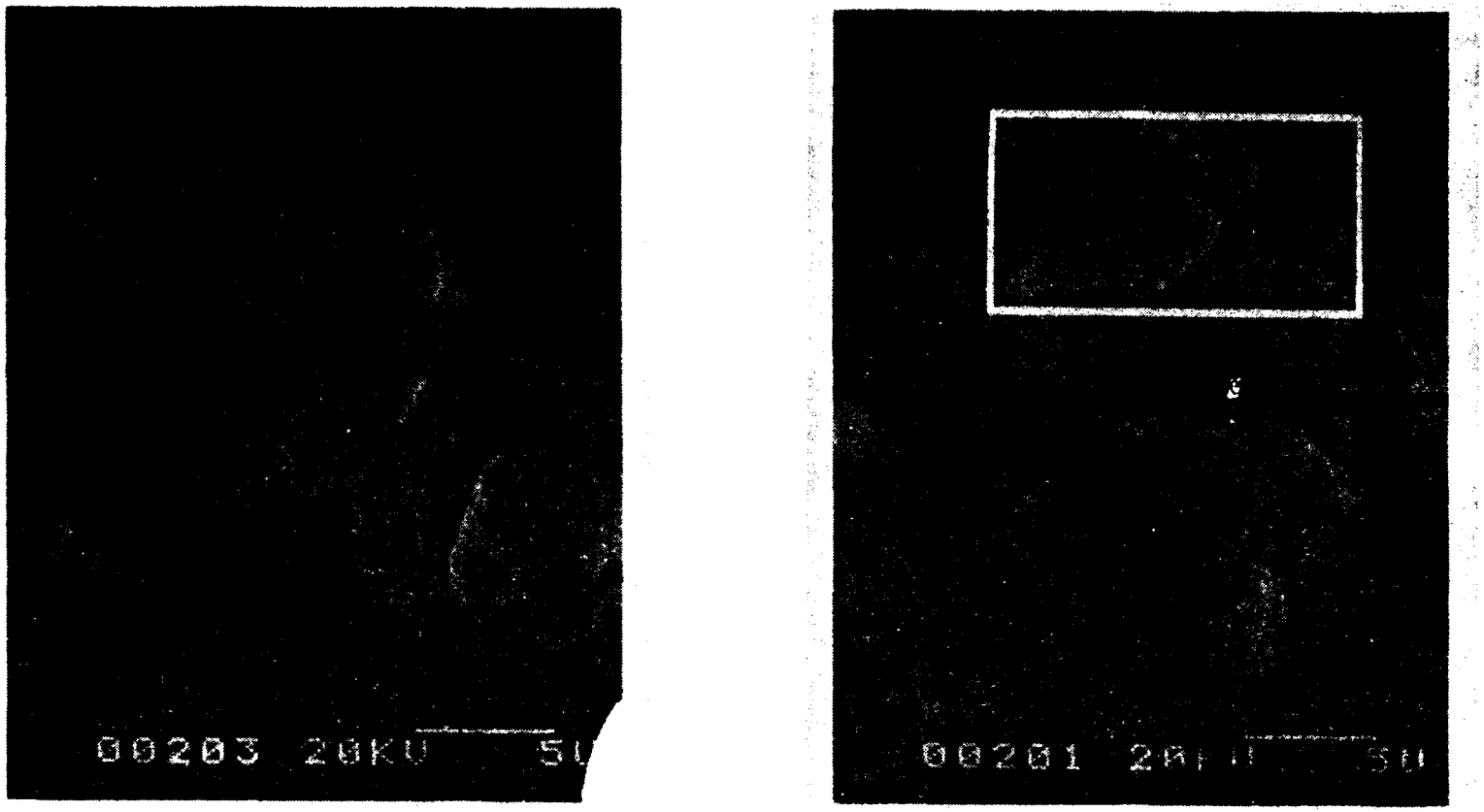

Figure 4. Trench 2 (4-5 feet)

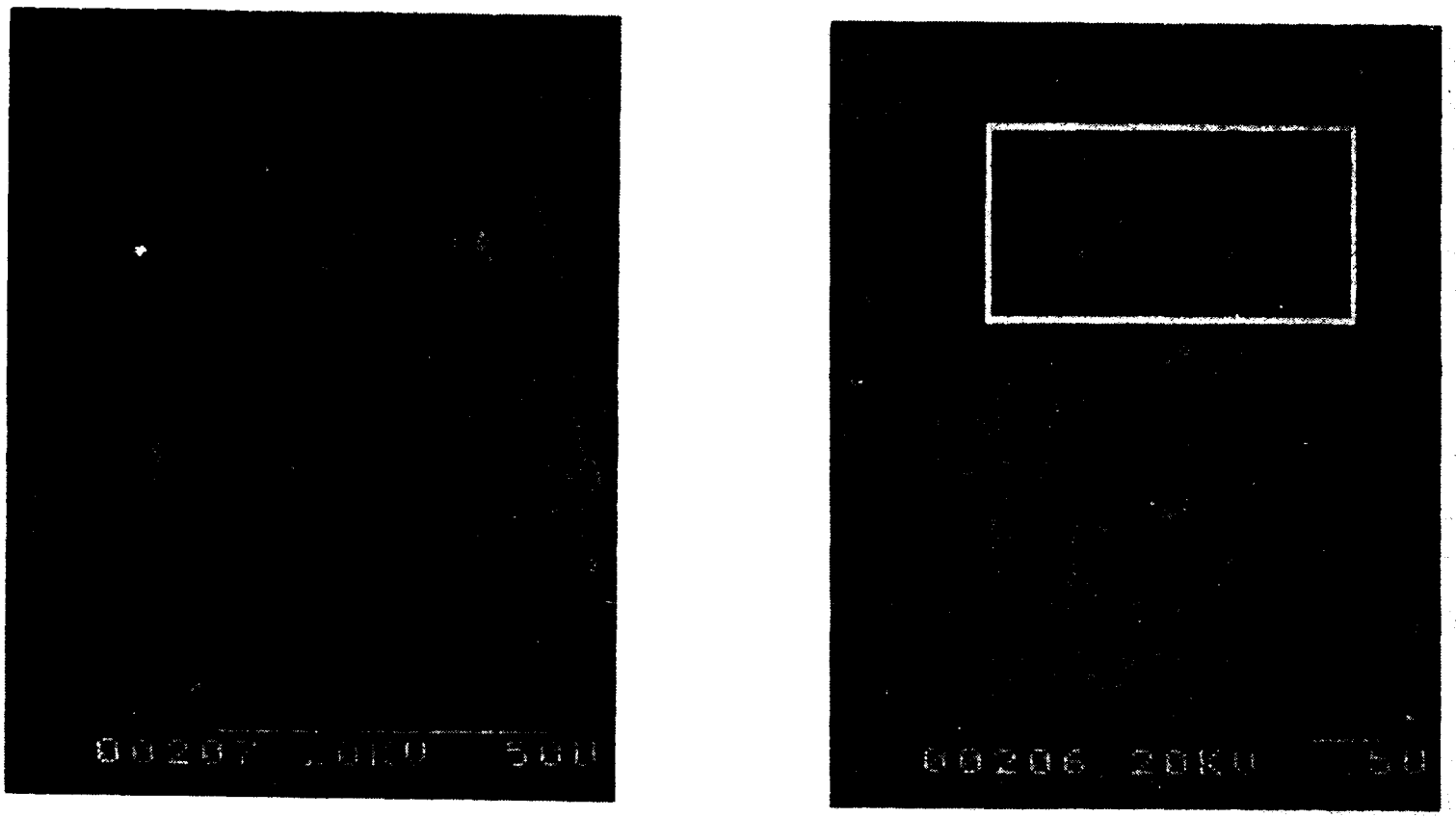

Figure 5. Trench 2 (8.5-9.5 feet)

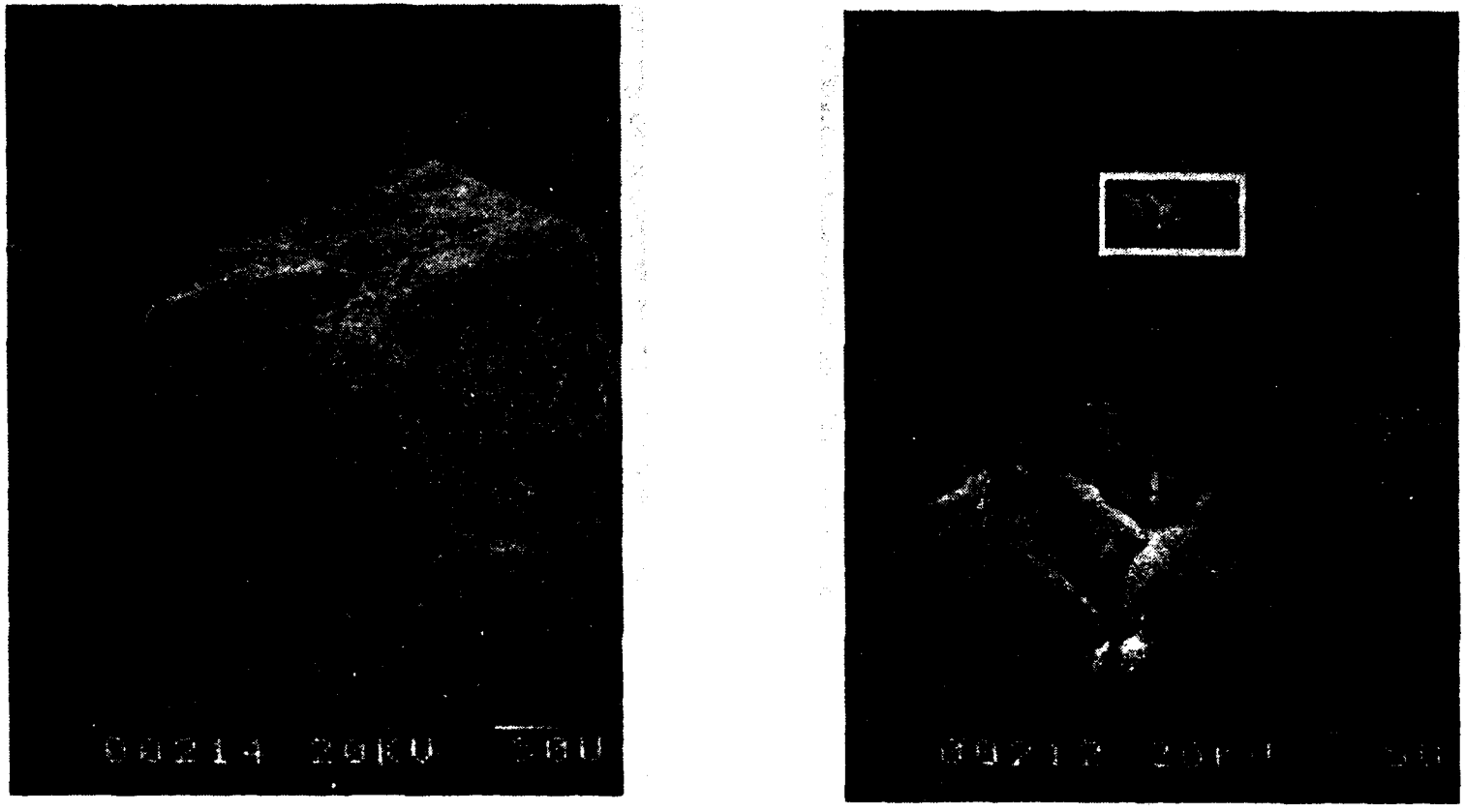

Figure 6. Trench 2 (12-13 feet)

5. DISCUSSION OF RESULTS

Climatic, geological, topographic, biological, and other physiographic conditions in the survey area were found to be ideal conditions for the formation of caliche. This included such conditions as acacia vegetation, flat land, runoff area (alluvial basin), semiarid region with past wet/dry seasons, falling water table, sandy soil with fines, evidence of past volcanic activity (igneous parent rock). This was further corroborated by extremely high N-values (up to 111 blows/foot) obtained in the Standard Penetration Test, as well as physical conditions of the soil observed during laboratory and field testing. This included grain-size distribution (sandy silt to sandy clay primarily), color (white to reddish brown), nature of split-spoon samples (hard disc-shaped clumps), and consistency limits (low plasticity index with a liquid limit about that of portland cement-30 percent).

The atomic absorbance test results, Tables 16-19, show high concentrations of calcium in Trench 1, which increases with depth (ranging from 5-15 percent). Calcium is also present in Trench 2, but in lesser amounts (ranging from 1.5-3.5 percent). Magnesium is present in very small amounts, .09-.13 percent in Trench 1 and .05-.11 percent in Trench 2. The x-ray diffraction test showed the calcium to be in carbonate form, as expected. Photographs of the samples, Figures 1-6, clearly show the calcium carbonate crystals clinging to quartz and other particles. The increasing content of calcium carbonate with depth is also very apparent, as well as the higher content in Trench 1.

One of the primary tests performed to see the effects of cementation was the unconfined compression test. Cylinders were compacted at various water contents and tested. Additional cylinders were compacted at similar water contents, but allowed to dry for 72 hours. This time period was found to be the optimum drying time to return the soil to its original hygroscopic moisture contents, specific gravities, liquid limits, and plasticity indexes. Although the top two sample layers are labeled SC and the bottom layer is labeled CL, both soils contain about the same amounts of sand and gravel with a slight increase of the coarse sand in the top two layers and a slight increase of clay-size particles in the bottom layer. These slight differences make a hairline distinction based on the Unified Soil Classification System. For all practical purposes, the disturbed samples are considered identical. With this in mind, the results of the tests can be compared.

The unconfined compression test results indicated that failure stresses increased significantly during the cementation process. Although these stress increases are to be expected for nearly any compacted soil as it dries, the increases obtained for these soils were abnormally high, 300-5300 percent increase. The cylinders essentially set up similar to small concrete cylinders. Another observation, in reviewing Tables 9-10, is that for a given soil (Trench 1-Three Depths) the peak failure stress increase varied directly with the amount of cementing agent and amount of initial water content in the soil. It is also noted that the peak failure stress increased more in soil comprised primarily of silty sand than it did in soil comprised primarily of clayey sand. The silty sand had higher water contents, but less cementing agent. This of course brings out the possibility of particle size and water content being equally, if not more, important than the actual amount of cementing agent present. Additional tests would have to be performed to corroborate this hypothesis.

Strains at failure were reduced by 20-92 percent during the cementation process. Higher reductions in strain were associated with increasing cementing agent and water content. Although the silty sand samples had high reductions in strain, no exact correlations can be made based on particle size, since similar or greater strain reductions were achieved in the clayey sand soils.

Comparing peak failure stresses for the wet samples alone in the unconfined and triaxial compression tests, the results indicate that for a given soil (e.g., Trench 1-Three Depths) the failure stress tends to decrease with increasing water content and cementing agent. This is an important concept in caliche in that it shows a very real problem with wetting effects on this type soil. This problem is discussed in the conclusions of this section.

One final observation is that there was a greater presence of calcium carbonate in the sands which contained greater amounts of fines, especially sands with a large amount of clay-size particles. This, of course, could be due to different degrees of carbonate source present in the specific areas, but the close proximity of the trenches tends to negate this reasoning. It is more likely that the higher concentrations of calcium carbonate are found in sands with greater amounts of fines due to the nature of calcite formation. Essentially, the calcium carbonate in solution has to leach through the soil layers slow enough to be able to adhere to the particles during evaporation (drying). Coarser soils would tend to drain the water too rapidly. Another possible explanation is the process of calcite growth. Crystallization of the calcium carbonate will occur more rapidly if particles are more closely spaced so that voids can be filled and the crystals can build on each other.

6. CONCLUSIONS

Several conclusions are evident in this study of caliche at White Sands Missile Range.

(1) Climate, topography, parent material, biological factors, and time directly influence the formation of caliche. Each of these factors must be favorable to provide a source of calcium carbonate, water, proper soil gradation for leaching and adhesion, and evaporation. White Sands Missile Range meets these requirements and has an abundance of caliche within its subsoil.

(2) Higher N-values for the Standard Penetration Test are obtained in layers of caliche due to the cementation of particles and corresponding increase in densities (filling of voids with crystals).

(3) Flocculation is common in caliche during the hydrometer analysis, due to the cementation of the silt and clay-size particles. This was evident during the numerous hydrometer tests conducted on the borehole and trench samples. Additional tests for the minus 200 sieve-size faction (.074 mm) should be conducted in the areas of heavy cementation of fine material. Flocculation possibly can be prevented during these tests by the addition of 20 ml of a 36 gm/liter solution of tetrasodium pyrophosphate, as suggested by F. Netterberg.

(4) Magnesium content can be difficult to obtain by the AA method

if silicon or aluminum is present in the sample. This is normally prevented by using a nitrous oxide-acetylene flame or adding .1-1.0% lanthanum to the solution. Neither was done in the AA tests run for this project; however, the low concentrations of Mg^{++} are deemed correct due to the low concentrations of silicon and alumina in the samples. The X-ray diffraction tests corroborated the low concentration of magnesium.

(5) The amount of calcium carbonate increases with depth due to leaching and increases with the presence of fines in the sand. This is due to a lower permeability increasing the calcium carbonate content during evaporation and the rapid formation of crystals in the smaller voids. It is also due to the increased surface area available for adhesion, with the fines filling voids.

(6) Time is an important factor in the strength of caliche. For laboratory cylinders, 72 hours was found to be optimum in returning the soil at any initial moisture content to its hygroscopic moisture content. Hygroscopic moisture content was selected in order to correlate results with the compacted air-dry samples. Additional tests should be conducted allowing the cylinders to dry at various time intervals, then testing them in unconfined compression. This could be used to develop a chart relating strength increase to initial moisture content and drying time (or final moisture content). Correlations could then be made of anticipated field strengths based on known wetting/drying periods and amounts of calcium carbonate.

(7) Strength increases significantly during the cementation process. The magnitude of increases in strength varies directly with the amount of calcium carbonate and initial water content in the soil. Although increases in peak failure stress were found to be greater in sands containing high silt factions than in sands containing high clay factions, more tests must be conducted to validate this hypothesis.

(8) Strains at failure are reduced by 20-92 percent during the cementation process. The two key factors affecting this reduction are increasing calcium carbonate and initial water content, which increase the magnitude of strain reduction. Particle size does not appear to greatly affect the reduction, as compared to these two factors.

(9) An important phenomena occurs in caliche soils upon wetting. The cementation tends to break down and the soil loses much of its shear strength. The strength decreases more rapidly with increasing calcium carbonate concentration and water content. This effect is probably due to the calcium carbonate crystals returning to solution with the addition of water. If the soil once again is allowed to dry, the crystals will reform. There was some evidence that the soil tended to increase more in strength after successive wetting/drying periods. This should be researched through further testing to see if there is an optimum number of successive wettings for strength increase. This information could also be used to correlate strength properties with soils in the field based on past wetting/drying periods.

(10) The AA test is a relatively simple method of obtaining concentrations of calcium or magnesium in the soil; however, it is limited. The test does not tell the nature of the compounds. The X-ray diffraction test should be used in conjunction with the AA test in order to determine whether the compound is a carbonate, silicate, or sulphate. Additionally, X-ray diffraction can determine tract elements if these are of concern.

SECTION IX

SUBSURFACE SEISMIC INVESTIGATION

1. INTRODUCTION

During the summer of 1982 a total of twelve seismic refraction surveys were conducted at the Mill Race test site, White Sands Missile Range, New Mexico. The purpose of these surveys was to establish the depths to various soil layers and to determine subsurface seismic velocities. The seismic surveys are part of a site characterization survey for the Air Force Weapons Laboratory (AFWL), Kirtland AFB. The depth of investigation, established by AFWL, was approximately 10 meters (32 feet).

In the investigation area five boreholes were drilled and two trenches were excavated. The trenches were used to obtain bulk samples of soil for laboratory testing as described in Section III, paragraph 4, and Section IV. At each of these locations a seismic survey was conducted. Five additional survey points were chosen. The location of these five points was based on preliminary soil data obtained during the boring operation and trench excavation process. Appendix F shows the location and direction of each seismic line.

Data from the borings indicated an irregular interface between underlying soil layers. Time versus distance plots based on data from the seismic surveys confirmed this. The method chosen to determine the depth of interface and the subsurface seismic velocities, is contained in a September 1975 Technical Note by Hideo Masuda, "Practical Method of Seismic Refraction Analysis for Engineering Study." Excerpts from this study were made into class notes for CE 461, Soil Engineering for Highways and Airfields.

Results from the seismic surveys in conjunction with data from the laboratory tests will be used in this report to identify the type of soil present and its strength parameters. AFWL weapons effects personnel will also use this data to predict soil response during future tests.

2. STATE OF THE ART

Of major concern at the Mill Race test site was the location of caliche layers. Depending on its thickness, strength and density, caliche can adversely affect the anticipated results of weapons simulating tests. Energy waves generated through the soil by the blast can be deflected in random directions rather than in predicted directions. Waves can be suppressed or magnified depending on the properties of the caliche.

Shallow seismic refraction surveys have found increasing application in materials surveying and other work around the world. The shallow refraction method has been successfully applied to caliche identification in South West Africa. This method is best suited to determine rippability, consistency and, as used in this report, a supplement for drilling. Hard layers of caliche are usually underlined by a finer powder caliche. This material has a lower seismic velocity and is not detected by the seismic refraction method. The surveys in Africa produced varying results on seismic velocities in caliche. Table 20 lists velocities for different types of caliche.

TABLE 20. SESIMIC VELOCITIES OF VARIOUS TYPES OF CALICHE

MATERIAL TYPE	SEISMIC VELOCITY (m/s)
Hardpan Caliche	1200 - 4500
Honeycomb Caliche	900 - 1200
Nodular Caliche	600 - 900
Powder Caliche	400 - 1000
Calcified Sand	450 - 1200

Caliche is also found by a study of its relation to topography. Hardpan caliche often occurs on rises of cemented alluvial or pan terraces. Caliche with the lowest Plasticity Index will normally be found on rises or slopes. The hardness of a caliche usually increases with the distance of the terrace from the feature. Gaps of non-calcified material may exist between terraces. In areas where granite is present, such as in the north section of WSMR where Mill Race is located, caliche is usually associated with basic igneous rock such as dolerite or basalt or other lime-rich rocks.

3. TESTING PROCEDURES

A. Library Search

Prior to visiting the Mill Race site several technical reports pertaining to the site and to the south west part of the United States in general were reviewed. These reports contain data from seismic tests conducted at WSMR and at sites with similar soil deposits.

Reference 10, Geological Influences on Nuclear Weapons Effects in Western Alluvial Valleys, pages 46 to 49 and 73 - 74, provides data and information for the southwest part of the United States in general. The following typical seismic velocities for soil and rock were provided in this report.

TABLE 21. TYPICAL SEISMIC VELOCITES FOR SOILS AND ROCK

MATERIAL	SEISMIC VELOCITY (m/s)
Loose and dry soil	180 - 1000
Coarse and compact soils	900 - 2600
Cemented soils	900 - 4300
Limestone	2100 - 6400
Igneous Rock	3000 - 6700

Strength and inertial properties of the site material are the parameters that establish the nature, intensity, and velocity of advance of the ground motion generated by a nuclear event. Usually in soils and rocks the higher the density the higher the velocity because the denser material is more resistant to deformation. Boundaries (caliche layers) at which material properties change abruptly can drastically alter the nature of the motion by creating new waves such as strong surface waves. Cementation can increase density by as much as 20 percent and can double seismic velocities. Caliche does have some good properties for weapons testing. Caliche cemented alluvium produces a more competent medium for cratering which results in reduced ejecta. However, massive cementation also influences the size of the ejecta particles. Loose, minimally cemented alluvium will generate ejecta particles no larger than in-situ size material. With caliche present the size of the ejecta particles increases dramatically.

Ground motion, one of the properties measured during the Mill Race event, is strongly influenced by the properties of the material through which it propagates. The reaction of the material governs both the magnitude of the motion at a particular point and the attenuation of effects with depth and range. Depending upon the soil present at a test site, ground disturbances may arrive at a point of interest prior to the arrival of the airblast. These early disturbances result from air-induced energy propagating ahead of the airblast wave in the surface layer or from energy which has been refracted into a soil layer that is faster than the one you are testing. The location of dense fast layers of soil or very loose layers are of special interest to weapons effects personnel as they can alter anticipated experiment results.

A second report that was reviewed was reference 2, a summary of the Geologic Characterization of the Mill Race Site, WSMR. This report was prepared by the New Mexico Engineernig Research Institute as part of the site selection process for Mill Race. Four potential ground zero sites were investigated. Fifteen seismic refraction lines were run during this investigation. Only one, line 13, was run at the site where the Mill Race event was conducted. Data from this line showed a seismic velocity of 822 meters per second (2697 fps) for soil down to a depth of 60 meters (198 feet). The spacing of the geophones did not allow for more precise measurements at shallower depths. Each line was approximately 640 meters (2110 feet). One half of the line was made up of 12 geophones spaced 15 meters (50 feet) apart. The other half had geophones spaced 34 meters (110 feet) apart. The seismic velocities obtained during the site selection process agrees with the results obtained during our survey, which are presented in paragraph 4 of this section of the report.

A third report reviewed was reference 3, Soil Sampling and Downhole Seismic Surveys at the Pre-Direct Course and Direct Course Sites, WSMR. The Direct Course Site is located in the north central section of our 2.59 kilometer square area. The Pre-Direct Course area is located between our bore holes one and four. Seismic velocities for the first two meters of soil averaged 550 meter per second and for the next seven meters they averaged from 780-1155 meters per second. Borings in the area showed a silty sand down to one meter, caliche from one to three meters, gravelly sand from three to five meters and alternating layers of similar material down to 18 meters.

B. Seismic Field Test

Twelve seismic refraction surveys were conducted at the Mill Race Site. At each location two 36 meter (120 foot) seismic lines were run. Therefore the total line length at each location was 72 meters (240 feet). Each line was reversed (shots recorded on both ends). This is required by Hideo Masuda in his Technical Note mentioned in the introduction to this section. The geophones used were Walker Hall-Sears type Z-3 with a natural frequency of 4.5 hertz. The geophones were recorded by an SIE RS-44, 24 channel seismic amplifier. Each geophone was placed five feet apart. Energy was supplied by striking an alluminum plate on the ground with a 16 pound hammer .

The seismic amplifier was located in a camper on the back of a pickup truck. Two lines from this unit, each with 12 geophones, were run along the ground. The aluminum plate was placed five feet from the end of the line. Next to the plate, another geophone was placed. This geophone sent a signal to the recorder that the plate had been struck. Two readings were taken at each end of the 36 metyer (120 foot) line. The north 36 meter side of the line was always

run first. After it was completed the geophone lines were moved to the south 36 meter section and the same process was repeated.

Several problems were encountered with military aircraft practicing over the site and with drilling operations at the Pre-Direct Course Site. The amplifier and geophones are very sensitive to noise. Three sets of readings produced unreliable results. These were at locations B-1 south, B-3 south and B-5 south. Time versus distance plots for soil with irregular interfaces produce lines with varying slopes. Plots for the three locations in question produced lines that were even more irregular. The data from these runs could not be used in this survey.

C. Calculations

The following data sheet and graphs, Figures 8, 9 and 10 are representative of the calculations for all twelve sites. The calculations for the remaining 11 sites are contained in Appendix IX-A of this section. All calculations are as shown in Hideo Masuda's Technical Note, referenced in the introduction to this section and as taught in CE 461, Soil engineering for Highways and Airfields. They are the basic equations used to determine velocities and depths to interface for irregular surfaces.

The first step in determining velocity and depth is to plot time versus distance (See Figure 8). These data are taken directly from the printed readout of the seismic amplifier. The time that the energy source takes to go from the metal plate (point p) to each geophone (point A) is T_{ap} or on the reverse run T_{bp}. The time the energy source takes to go from the plate to the last geophone (total travel time) is T_{ab}. This value is averaged if the time varies between the first run and the reverse seismic run. T_{ap} and T_{bp} are then plotted versus time. A best fit line is drawn between these points. The slope of these two lines is the seismic velocity of the second layer, V_2. V_2 values are then averaged (See Figure 9). V_1 values are determined by taking the slope of the first sloping line of Figure 8. These values are also averaged. The ratio of V_1 to V_2 is used to determine as shown in Figure 10. In Figure 10, t_{ap} and t_{bp} are the times corresponding to the intercept of the two V_2 lines in Figure 9 with the vertical axes. These two times are used to calculate h_a, the depth to the underlying irregular surface under point A, h_b the depth from point B to the irregular surface and h_p the depth to the irregular surface under the remaining geophones. The depths h_a and h_b and h_p are measured perpendicular to the irregular surface as shown in Figure 7.

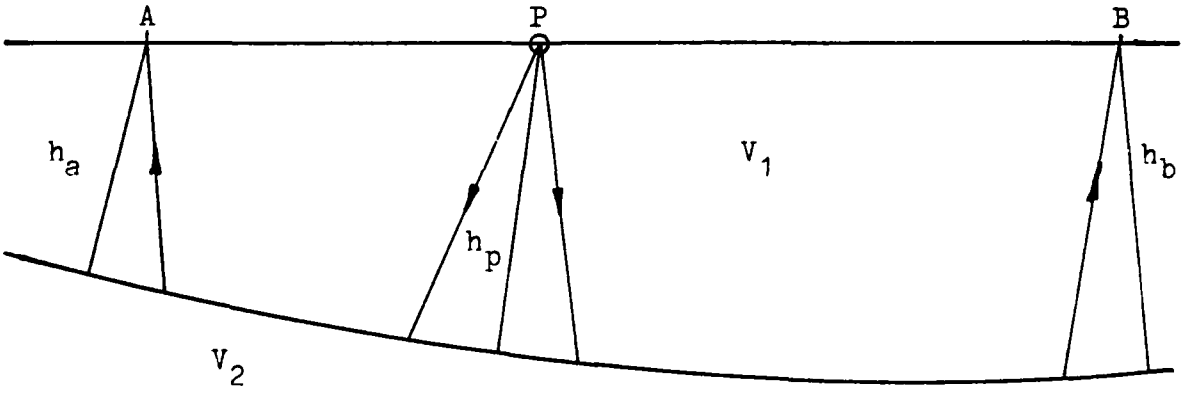

Figure 7. Determining depth h_a, h_b and h_p

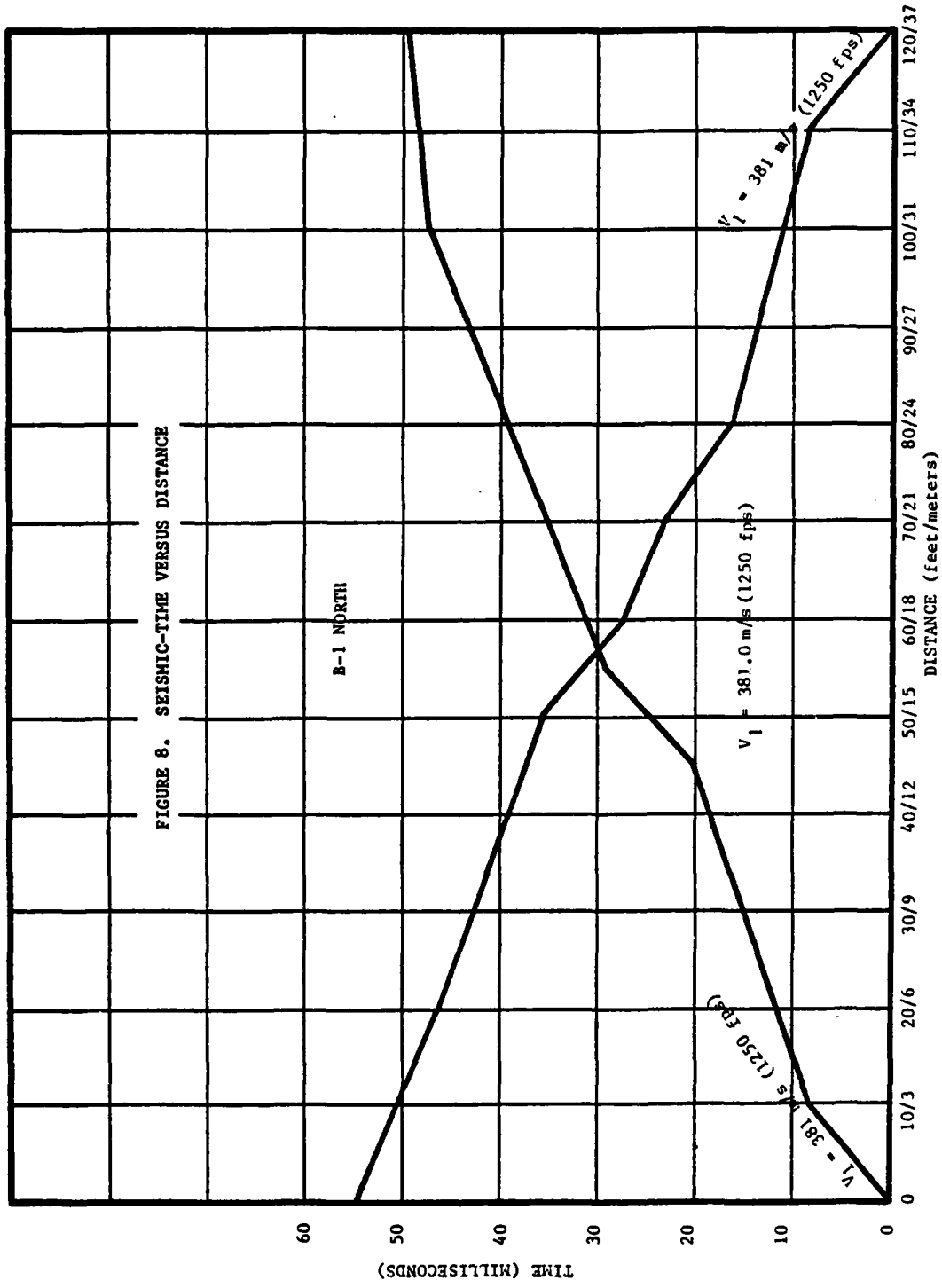

FIGURE 8. SEISMIC-TIME VERSUS DISTANCE

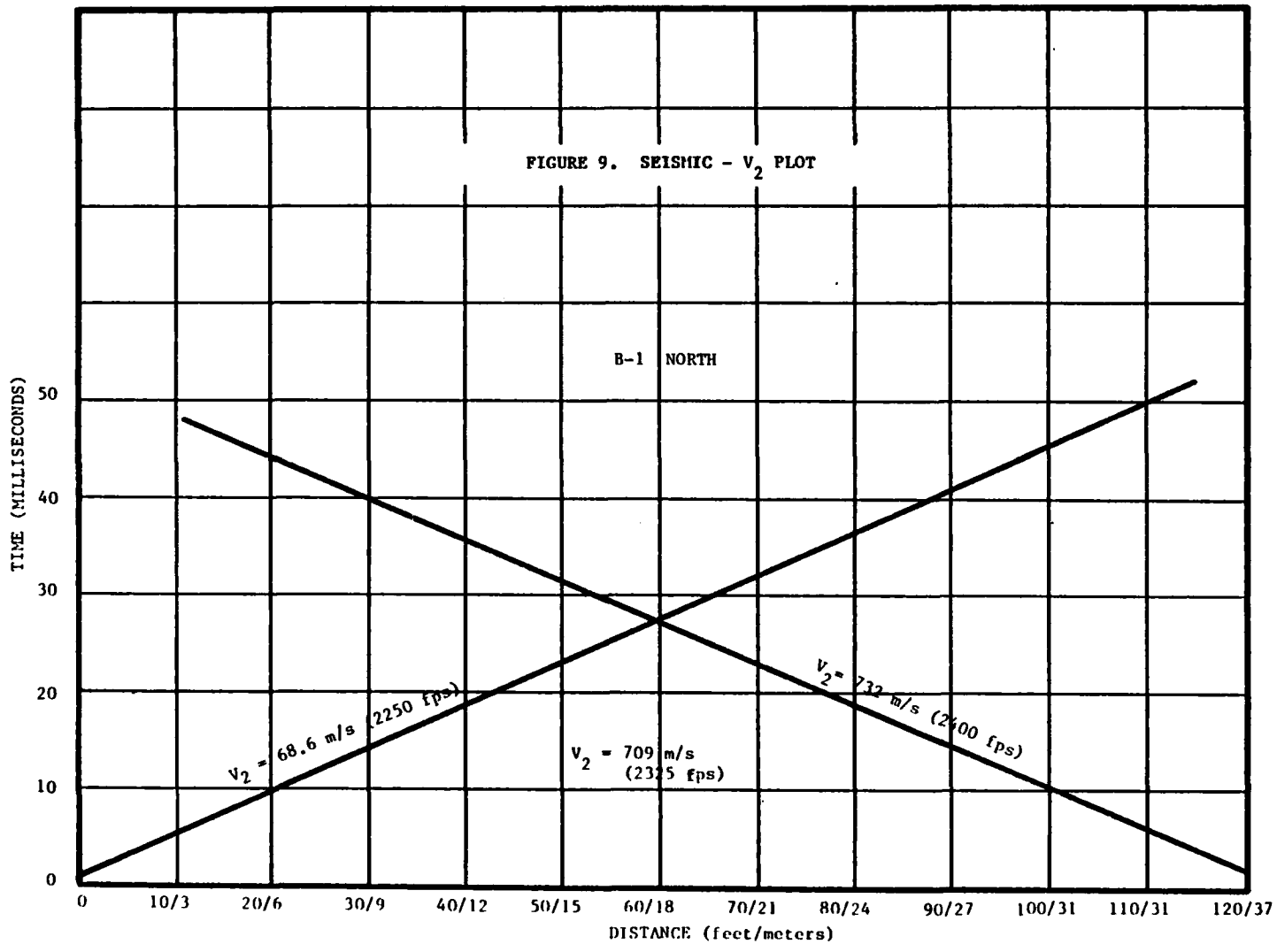

FIGURE 9. SEISMIC - V_2 PLOT

	1	2	3	4	5	6	7	8	9	10	11	12	13
X — A	0	10	20	30	40	50	60	70	80	90	100	110	120
X — B	120	110	100	90	80	70	60	50	40	30	20	10	0
T_{AP}	0	8.0	11.5	14.9	17.9	25	31.5	35.5	39.5	43.5	47.0	48.0	44.0
T_{BP}	54.9	51.2	46.4	42.0	38.5	35.5	26.9	23.0	15.8	12.5	11.1	8.0	0
$(T_{AP} + T_{BP} - T_{AB})$		7.25	5.95	4.95	4.45	8.55	6.45	6.55	3.35	4.05	6.15	4.05	
T'_{AP}		4.38	8.53	12.43	15.68	20.73	28.28	32.23	37.83	41.48	43.93	45.98	
T'_{BP}		47.58	43.43	39.53	36.28	31.23	23.68	19.73	14.13	10.48	8.03	5.98	
h_p	ft m	5.37 1.63	4.41 1.34	3.67 1.12	3.30 1.01	6.30 1.93	4.78 1.46	4.85 1.48	2.48 0.76	3.00 .92	4.56 1.39	3.00 .92	

$V_1 = \frac{10}{.008} = 1250$ fps (381 mps)

$V_1 = \frac{10}{.008} = 1250$ fps (381 mps)

$\overline{V}_1 = 1250$ fps (381 mps)

$V_2 = \frac{56-20}{.025-.010} = 2250$ fps (685.8 mps)

$V_2 = \frac{56-20}{.025-.010} = 2400$ fps (731.5 mps)

$\overline{V}_2 = 2325$ fps (708.7 mps)

$\text{SIN}\ \alpha\ c = \frac{\overline{V}_1}{V_2} = .5376$

$\alpha\ c = 32.5^{o}$

$t'_{AP} = .0003$

$t'_{BP} = .0015$

$h_p = \frac{\overline{V}_1}{2\text{COS}\alpha c}\ (T_{AP} + T_{BP} - T_{AB})$

$h_A = \frac{\overline{V}_1\ t'_{AP}}{\text{COS}\alpha c} = .50$ ft (.15 m)

$H_B = \frac{\overline{V}_1\ t'_{BP}}{\text{COS}\alpha c} = 2.2$ ft (0.68 m)

FIGURE 10. B-1 NORTH SEISMIC CALCULATIONS

4. RESULTS

TABLE 22
SEISMIC RESULTS

Location	Velocity (m/s)	
	Layer 1	Layer 2
B-1 (north)	381	709
B-2 (north)	469	1086
B-2 (south)	530	827
B-3 (north)	415	882
B-4 (north)	360	842
B-4 (south)	397	937
B-5 (north)	386	981
T-1 (north)	411	942
T-1 (south)	343	871
Pt.-A (north)	463	976
Pt.-A (north)	523	938
Pt.-B (north)	394	837
Pt.-B (south)	425	871
Pt.-C (north)	381	892
Pt.-C (south)	442	868
Pt.-D (north)	404	1025
Pt.-D (south)	391	1057
Pt.-E (north)	457	793
Pt.-E (south)	381	805
Pt.-F (north)	383	881
Pt.-F (south)	460	938

Figures 11A through F, show the underlying irregular surfaces for each seismic location. In theory archs should be struck off at each h_A, h_B and h_P depth. A french curve was used in these figures for aesthetic reasons only.

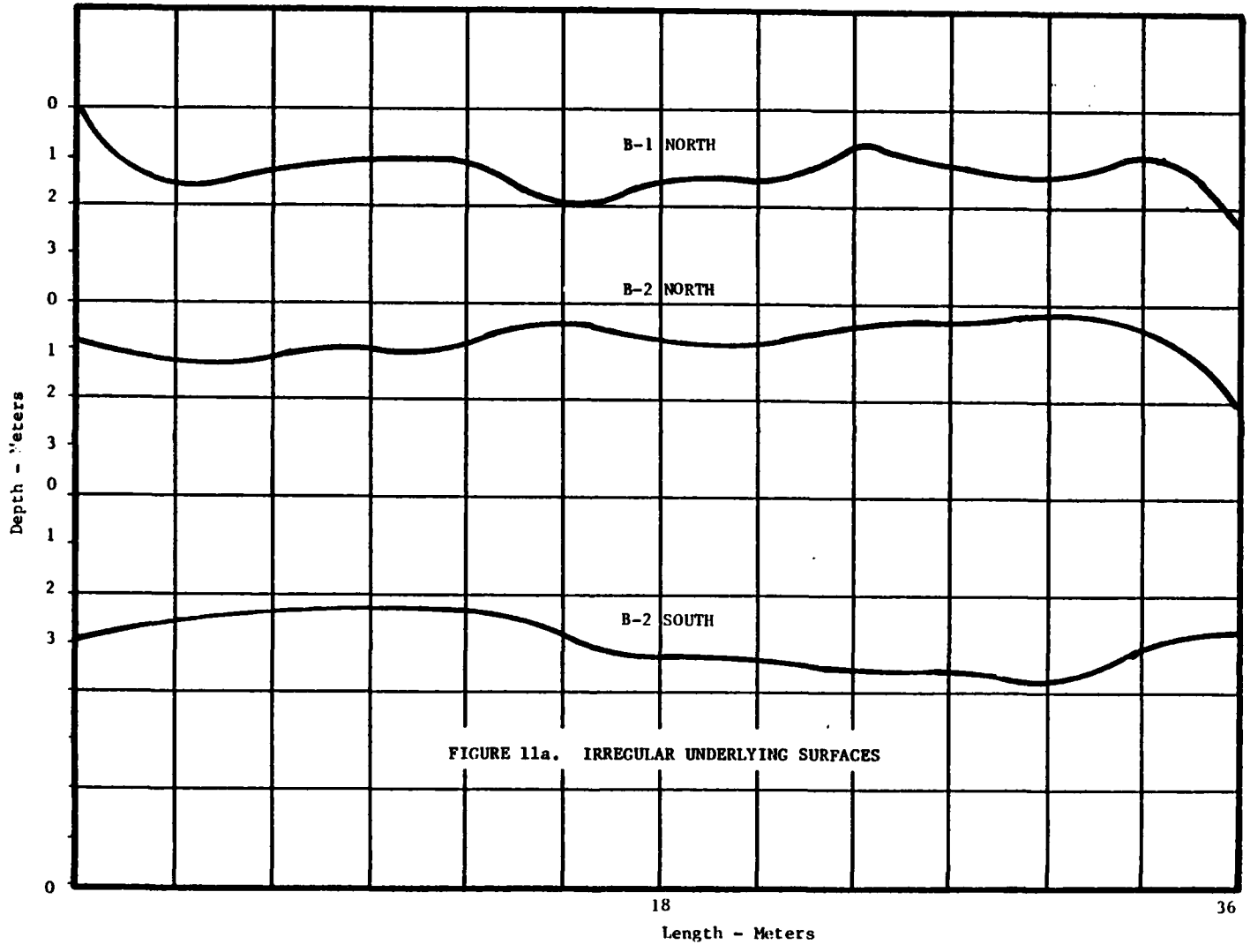

FIGURE 11a. IRREGULAR UNDERLYING SURFACES

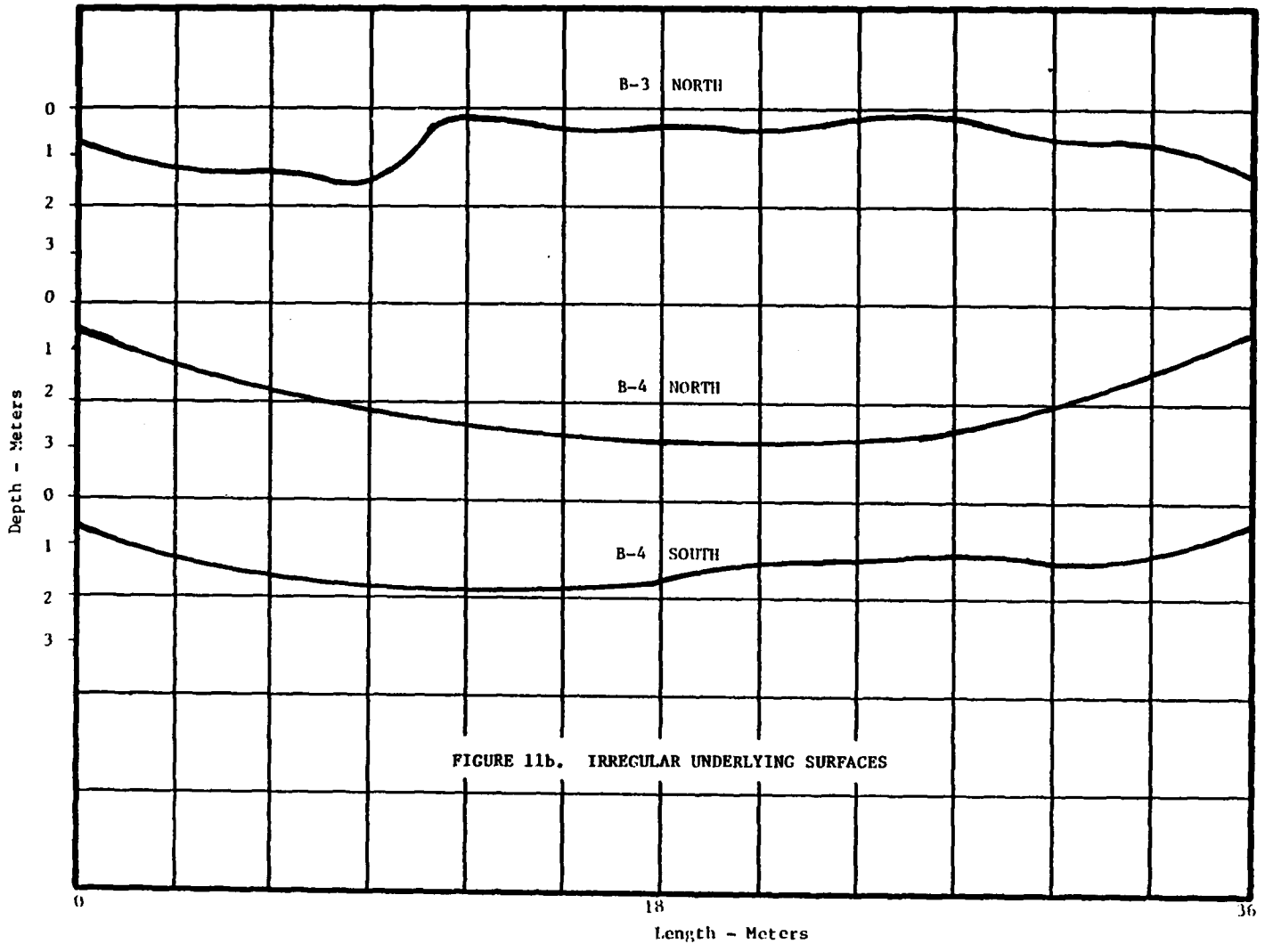

FIGURE 11b. IRREGULAR UNDERLYING SURFACES

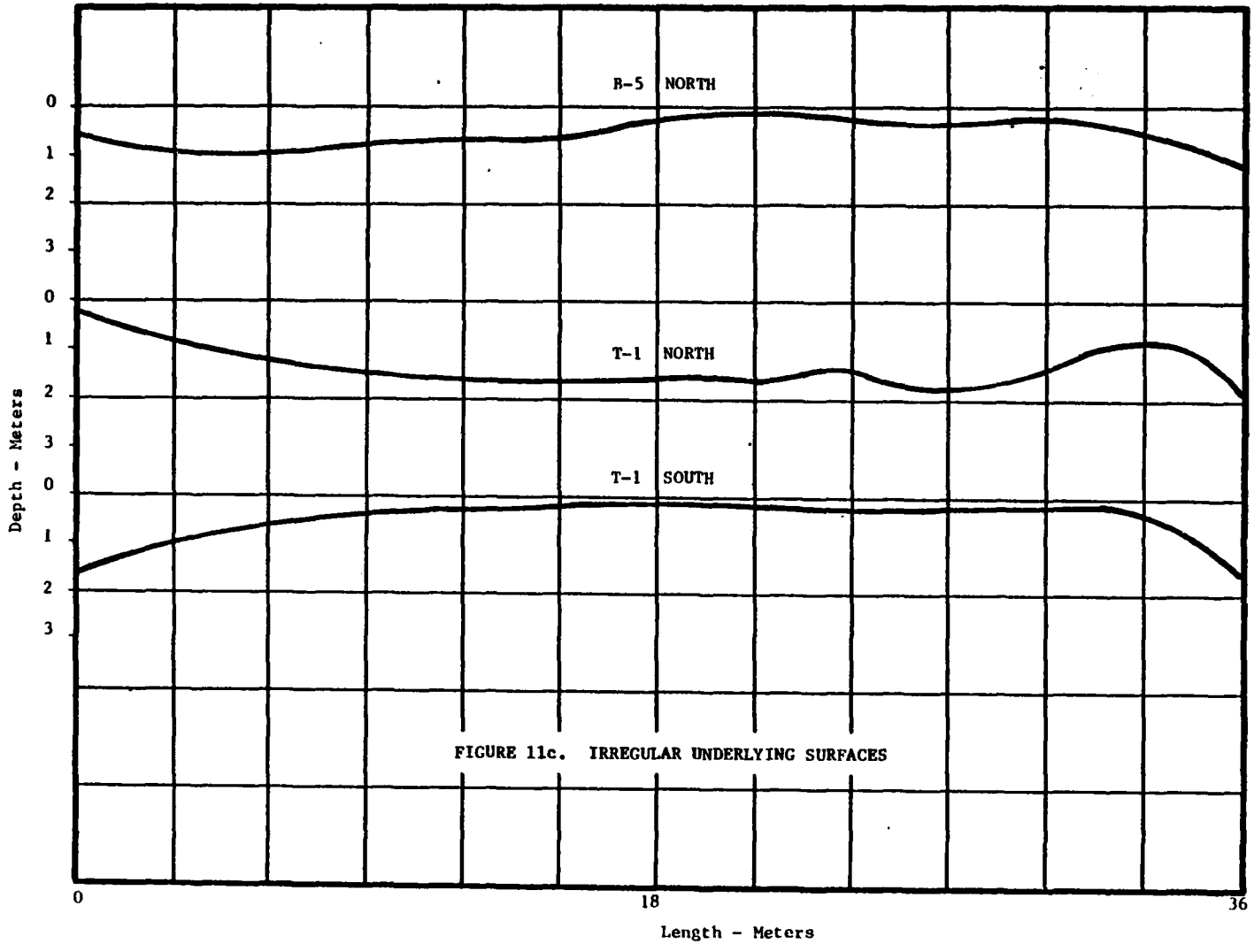

FIGURE 11c. IRREGULAR UNDERLYING SURFACES

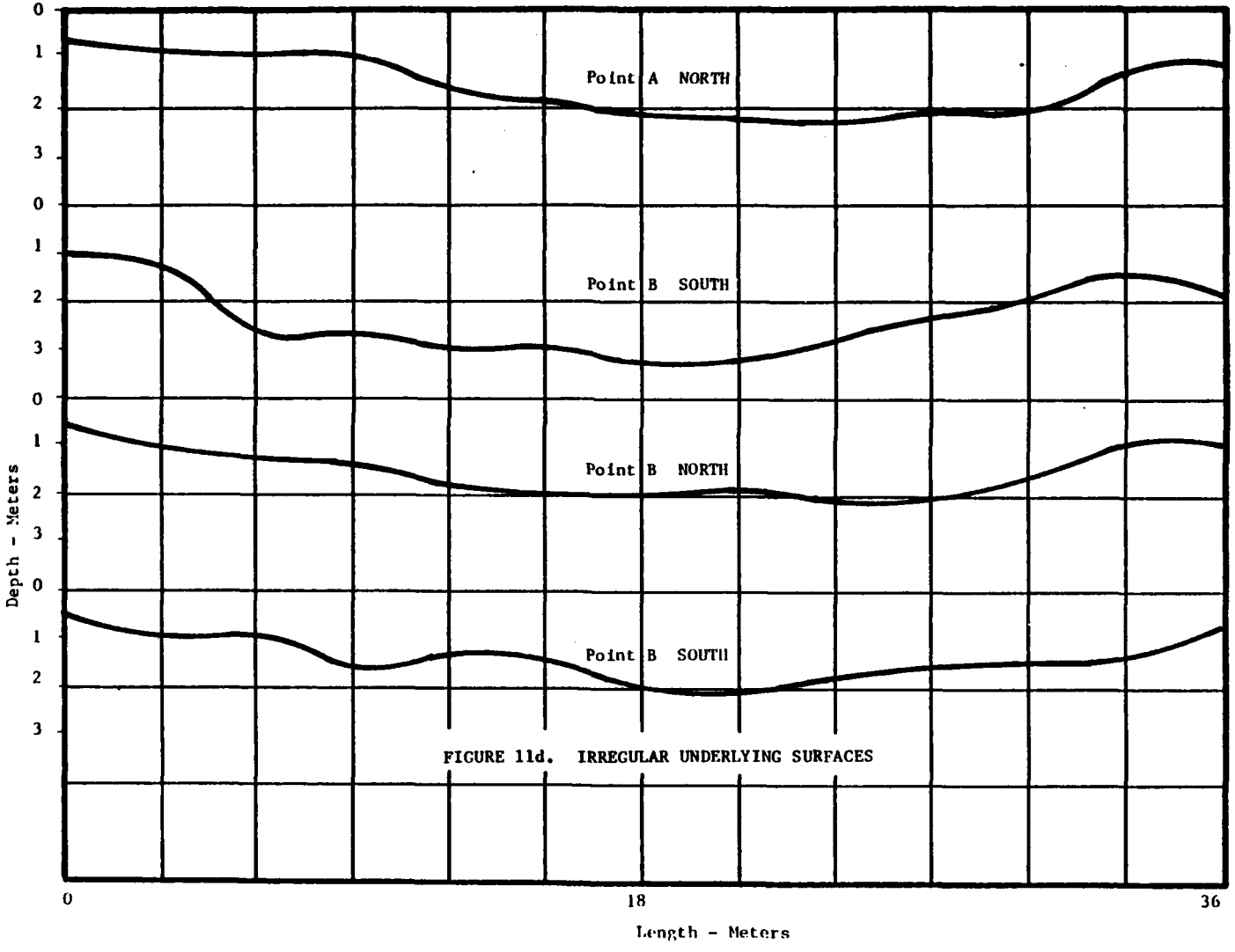

FIGURE 11d. IRREGULAR UNDERLYING SURFACES

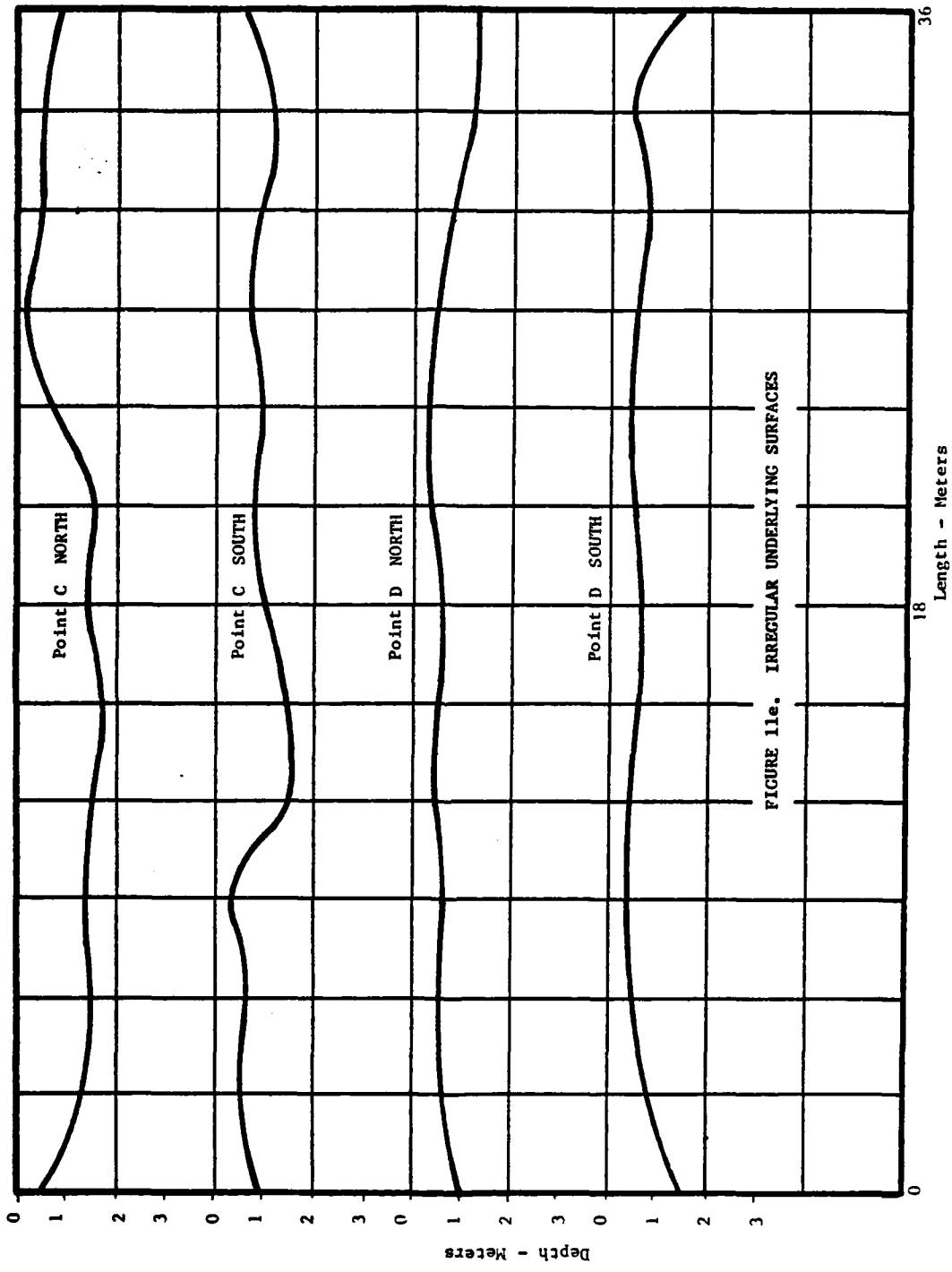

FIGURE 11e. IRREGULAR UNDERLYING SURFACES

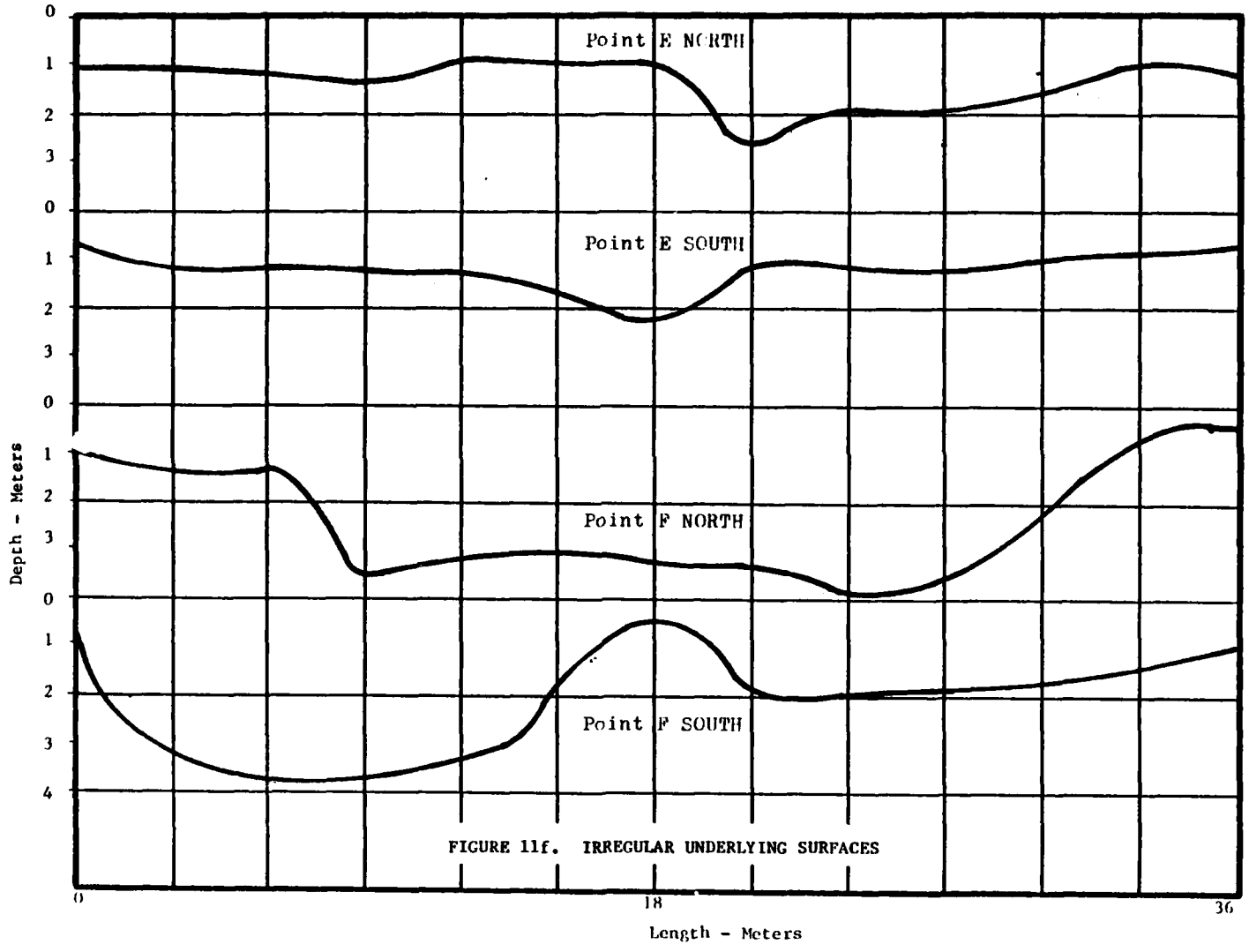

FIGURE 11f. IRREGULAR UNDERLYING SURFACES

5. DISCUSSION OF RESULTS

Seismic velocities for the first layer of soil varied from 343 meters per second (1125 fps) to 530 meters per second (1740 fps) as shown in Table 22, with an average of 420 meters per second (1380 fps). This compares to 550 meters per second determined during the Pre-Direct Course Site survey. Surface soil at each seismic site varied from a low density silty sandy material to a very loose silty sandy material. A significant amount of organic material, from plants and animals, was also present in the first layer. During the seismic survey and seven days prior to it, no rainfall was recorded at the site. Table 21 provides typical seismic velocities for various types of soil and rock. Layer 1 at the Mill Race Area is typical of the loose and dry soil in Table 21 with a velocity range of 180-1000 meters per second.

Seismic velocities for layer two varied from 709 meters per second (2330 fps) to 1086 meters per second (3560 fps) as shown in Table 22, with an average of 905 meter per second (2970 fps). This compares to 780-1155 meters per second found during the Pre-Direct Course survey. According to Table 21 for typical seismic velocities, layer two falls into one of two groups, coarse and compact soils with a velocity of 900-2600 meters per second or cemented soils, 900-4300 meters per second. Table 20, that presents velocities for various types of caliche, has three categories that our soil could fit into: honeycomb caliche, 900-1200 meters per second; powder caliche, 400-1000 meters per second; and calcified sand, 450-1200 meters per second. All three types of soil have been identified in the reports discussed in the library search portion of this section, as being present in the Mill Race Test Area. Our own soil classification, Table 7, identifies most of the soil in the Mill Race Area as silty sand or clayey sand. Blow counts from Table 2, averaged 20 blows per foot for the first 1.4 meters (4.5 feet) and over 50 flows per foot down to 9.8 meters (32 feet). 20 blows per foot is indicative of medium dense material and 50 blows per foot indicates very dense material.

During the trench excavation a white to very light pink layer of soil was observed to begin at a depth of 1 meter. Its texture, color, density (in this layer the back hoe experienced difficulty in excavating the material) identified this soil as caliche. Section VIII of this report identifies the chemical composition of the soils that were tested. This section also confirms the presence of cabonates which is essential in the formation of caliche.

Eight miles to the east of the site are the Oscura Mountains. Large drainage patterns can be observed starting at the base of the mountains and heading toward the Mill Race Site. The irregular surface pattern of the second soil layer identified was caused in part by runoff in the test area. Much of the surface soil is with some organic material. Over time it has filled in the low lying areas and left this irregular subsurface layer. Arroyos are also present in the area. The boring at location four shows a sizeable amount of gravel. The seismic line for this location produced a concave surface for the second seismic layer. This same result can be seen in several plots of Figure 11A to F.

6. CONCLUSIONS

Previous seismic surveys conducted in the Mill Race Test Area produced velocities up to 550 meters per second for the first layer of soil and from 780 to 1155 meters per second for the second layer of soil, down to a depth of 15 meters.

(1) Typical velocities for the first soil layer compared to previous seismic surveys. Velocities up to 530 meters per second were obtained during this survey.

(2) Typical velocities for the second soil layer also compared with previous seismic surveys. Velocities between 709 and 1086 meters per second were obtained.

(3) Equations for an irregular surface from CE 461, Soil Engineering for Highways and Air Fields based on a September 1975 Technical Note by Hideo Masuda, are valid for reducing data obtained at the Mill Race test site.

(4) The seismic survey produced an accurate picture of the underlying irregular surface.

(5) The seismic survey also confirmed the results of the laboratory tests, both chemical composition and standard classification tests.

(6) Velocities for the second layer are indicative of typical velocities for caliche.

APPENDIX IX A

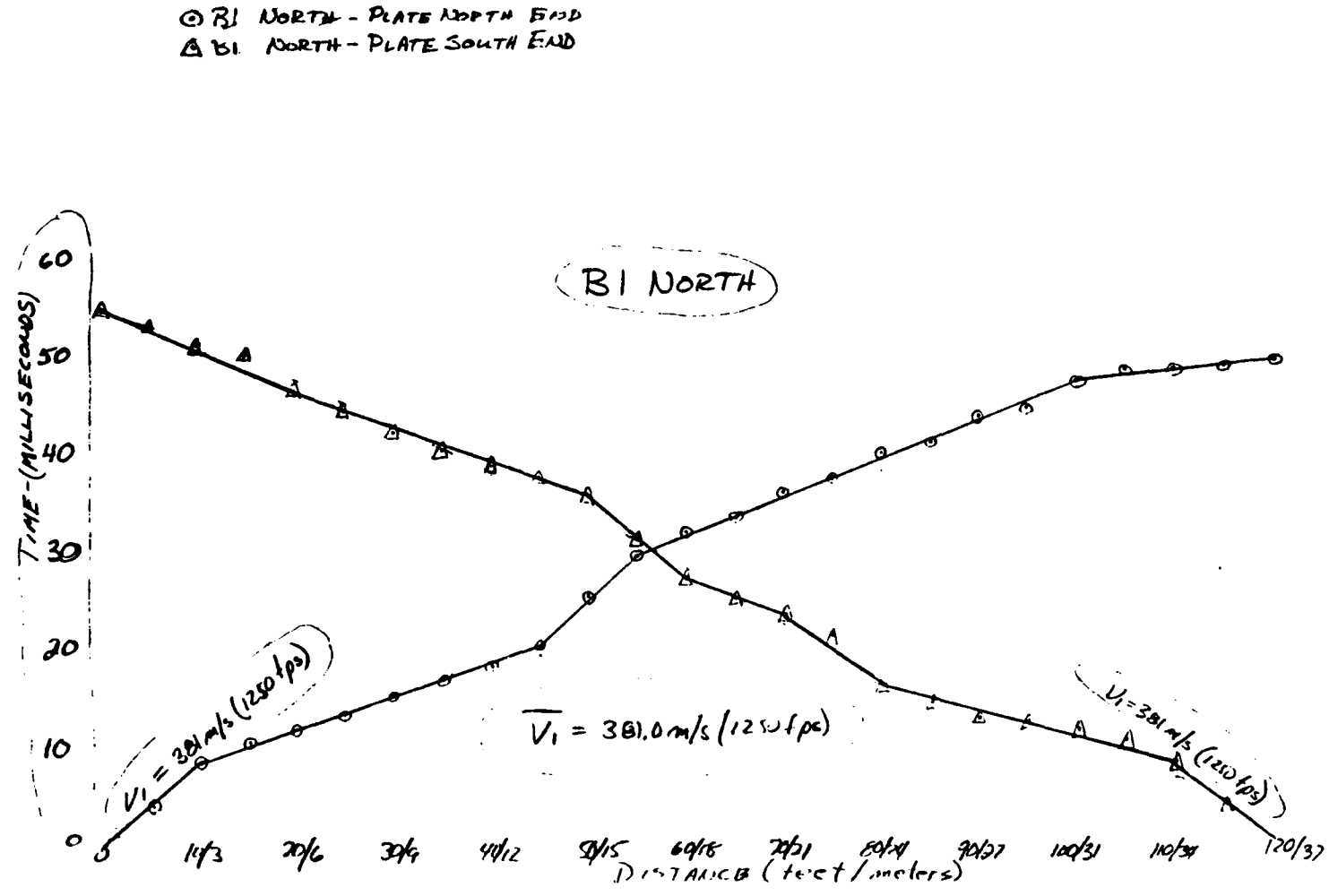
⊙ B1 NORTH - PLATE NORTH END
△ B1 NORTH - PLATE SOUTH END
B1 NORTH
TIME-(MILLISECONDS)
60
50
40
30
20
10
0
V_1 = 381 m/s (1250 fps)
$\overline{V_1}$ = 381.0 m/s (1250 fps)
V_1 = 381 m/s (1250 fps)
14/3
20/6
30/9
40/12
50/15
60/18
70/21
80/24
90/27
100/31
110/34
120/37
DISTANCE (feet/meters)

Figure 9

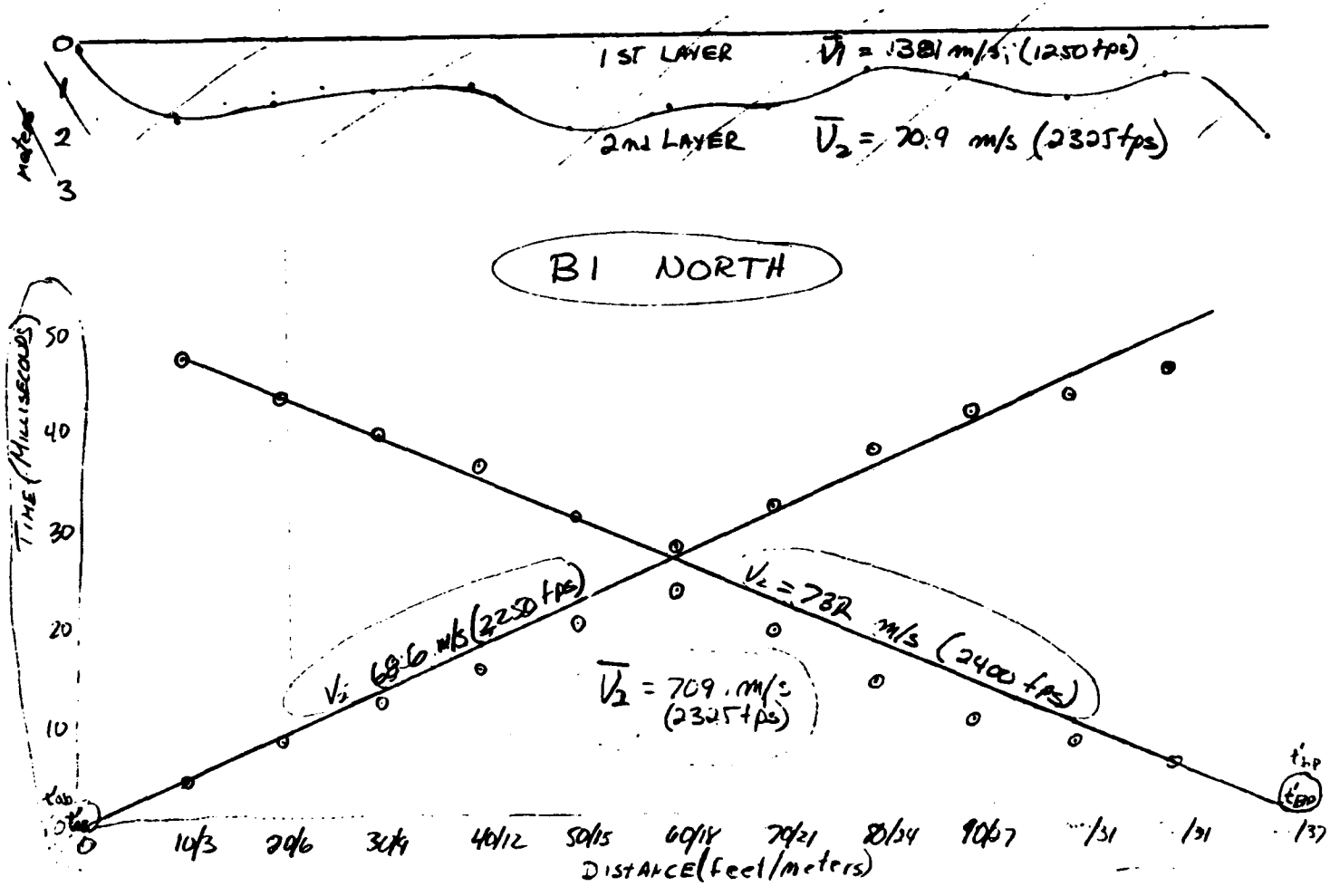

1 ST LAYER
$\bar{V}_1$ = 381 m/s (1250 fps)
2nd LAYER
$\bar{V}_2$ = 70.9 m/s (2325 fps)
meters
0
1
2
3
B1 NORTH
TIME (MILLISECONDS)
50
40
30
20
10
V_1 68.6 m/s (2250 fps)
V_2 = 732 m/s (2400 fps)
$\bar{V}_2$ = 709 m/s (2325 fps)
0
10/3
20/6
30/9
40/12
50/15
60/18
70/21
80/24
90/27
/31
/31
/37
DISTANCE (feet/meters)

Figure 10

	1	2	3	4	5	6	7	8	9	10	11	12	13
X → A	0	10	20	30	40	50	60	70	80	90	100	110	120
X ← B	120	110	100	90	80	70	60	50	40	30	20	10	0
T_{AP}	0	8.0	11.5	14.9	17.9	25	31.5	35.5	37.5	43.5	[illegible]	48.0	[illegible]
T_{BP}	[illegible]	51.2	[illegible]	[illegible]	38.[illegible]	35.5	[illegible]	[illegible]	[illegible]	[illegible]	[illegible]	6.0	0
$[T_{AP}+T_{BP}-T_{AB}]$		[illegible]	[illegible]	4.95	4.45	3.55	[illegible]	[illegible]	3.35	4.05	[illegible]	[illegible]	
T'_{AP}		[illegible]	[illegible]	12.43	15.62	[illegible]	[illegible]	[illegible]	[illegible]	[illegible]	[illegible]	45.98	
T'_{BP}		47.58	[illegible]	39.53	36.28	31.23	[illegible]	[illegible]	[illegible]	[illegible]	[illegible]	5.93	
h_P	ft/m	5.37/1.63	4.41/1.34	3.67/1.12	3.30/1.01	6.30/1.93	4.78/1.46	4.85/1.48	2.48/0.76	3.00/.92	4.56/1.39	3.00/.92	

$V_1 = \frac{10}{.008} = 1250\,fps\ (381\,mps)$

$V_1 = \frac{10}{.008} = 1250\,fps\ (381\,mps)$

$\overline{V}_1 = 1250\,fps\ (381\,mps)$

$V_2 = \frac{56-20}{.025-.009} = 2250\,fps\ (685.8\,mps)$

$V_2 = \frac{56-20}{.025-.010} = 2400\,fps\ (731.5\,mps)$

$\overline{V}_2 = 2375\,fps\ (708.7\,mps)$

$\sin\alpha_c = \frac{\overline{V}_1}{\overline{V}_2} = .5376$

$\alpha_c = 32.5°$

$t'_{AP} = .0003$

$t'_{BP} = .0015$

$h_A = \frac{\overline{V}_1\, t'_{AP}}{\cos\alpha_c} = .50\,ft\ (.15\,m)$

$h_B = \frac{\overline{V}_1\, t'_{BP}}{\cos\alpha_c} = 2.24\,ft\ (0.6\,m)$

$h_P = \frac{\overline{V}_1}{2\cos\alpha_c}\left[T_{AP}+T_{BP}-T_{AB}\right]$

$\overline{T}_{AB} = [illegible]$

B-1 North

Figure 11

⊙ B2 NORTH - PLATE NORTH END

△ B2 NORTH - PLATE SOUTH END

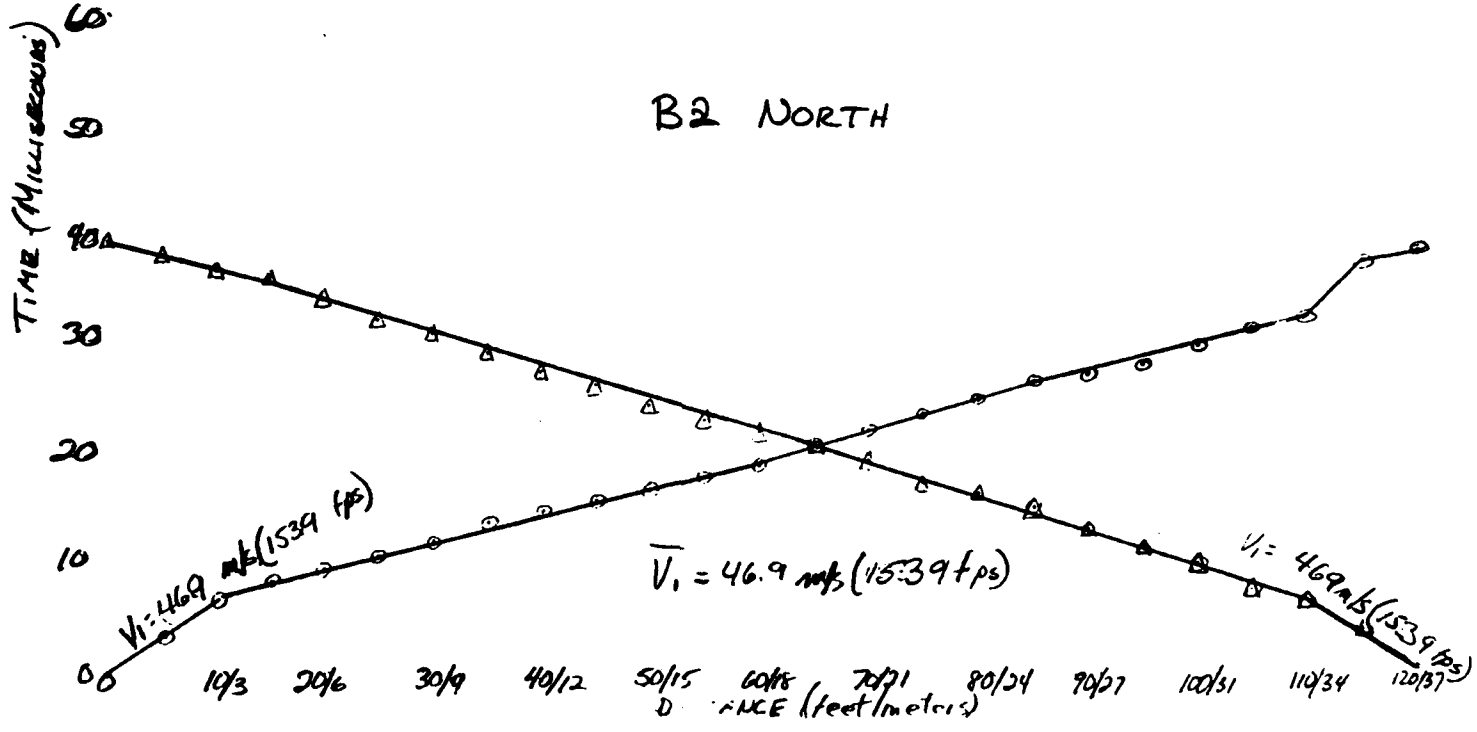

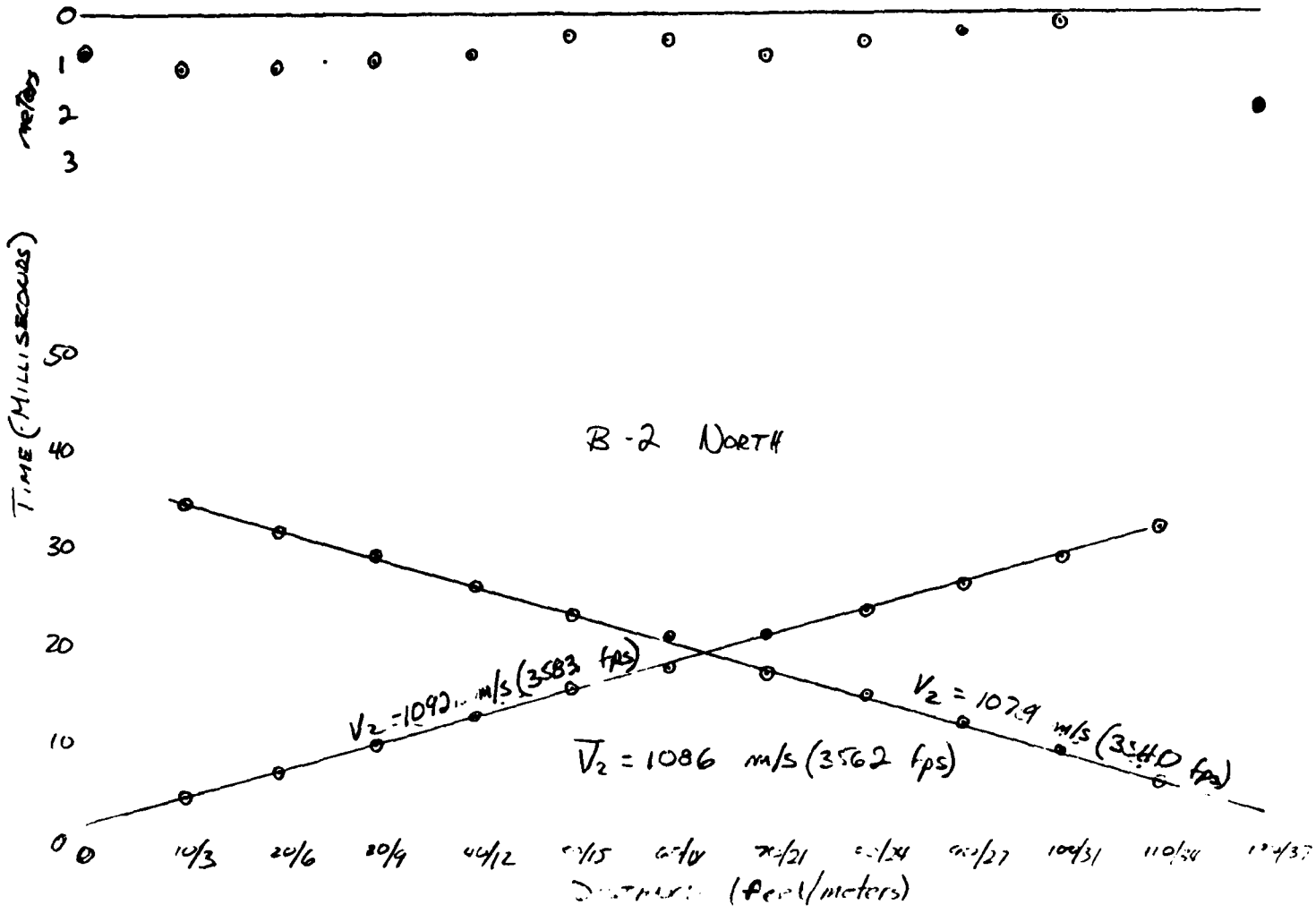

B-2 NORTH
TIME (MILLISECONDS)
meters
0
1
2
3
50
40
30
20
10
0
10/3
20/6
30/9
40/12
100/31
110/34
V_2 = 1092 m/s (3583 fps)
V_2 = 1079 m/s (3540 fps)
$\bar{V}_2$ = 1086 m/s (3562 fps)
(feet/meters)

E-2 Board

	1	2	3	4	5	6	7	8	9	10	11	12	13
X → A	0	10	20	30	40	50	60	70	80	90	100	110	120
X ← B	120	110	100	90	80	70	60	50	40	30	20	10	0
T_{AP}		[illegible]	9.1	11.A	[illegible]	[illegible]	[illegible]	[illegible]	[illegible]	[illegible]	[illegible]	[illegible]	[illegible]
T_{BP}	39.5	[illegible]	[illegible]	[illegible]	[illegible]	[illegible]	[illegible]	[illegible]	16.1	[illegible]	[illegible]	[illegible]	[illegible]
$[T_{AP}+T_{BP}-T_{AB}]$		1.2	1.1	2.A	3.0	1.6	.9	3.0	1.9	1.0	0.4	[illegible]	
T'_{AP}		[illegible]	7.05	7.9	13.0	15.7	[illegible]	21.5	[illegible]	[illegible]	29.3	[illegible]	
T'_{BP}		[illegible]	21.9	29.1	[illegible]	33.3	[illegible]	17.5	15.15	12.5	9.7	[illegible]	
h_p	ft / m	3.17 / 1.1	3.15 / 1.1	3.2 / .99	2.6 / .8	1.4 / .4	1.6 / .5	2.6 / .8	1.6 / .5	.8 / .3	.3 / .1	0 / 0	

$V_1 = \frac{10}{.0065} = 1538.5$ fps

$V_1 = \frac{10}{.0065} = 1538.5$ fps

$\bar{V}_1 = 1538.5$ fps (468.9 m/s)

$V_2 = \frac{52-12}{.017-.005} = 35833$ fps (1092.2 m/s)

$V_2 = \frac{41-2}{.015-.005} = 3539.8$ fps (1078.9 m/s)

$\bar{V}_2 = 3561.6$ fps (1085.6 m/s)

$\sin \alpha_c = \frac{\bar{V}_1}{\bar{V}_2} = .4320$

$\alpha_c = 25.593°$

$t'_{AP} = .0015$

$t'_{BP} = .0036$

$h_A = \frac{\bar{V}_1 t_{AP}}{\cos \alpha_c} = 2.6$ ft (.8 m)

$h_B = \frac{\bar{V}_1 t_{BP}}{\cos \alpha_c} = 6.1$ ft (1.9 m)

$h_p = \frac{\bar{V}_1}{2 \cos \alpha_c} [T_{AP} + T_{BP} - T_{AB}] =$

$\bar{T}_{AB} = 39.0$

⊙ B2 - South - Plate North End
△ B2 South - Plate South End

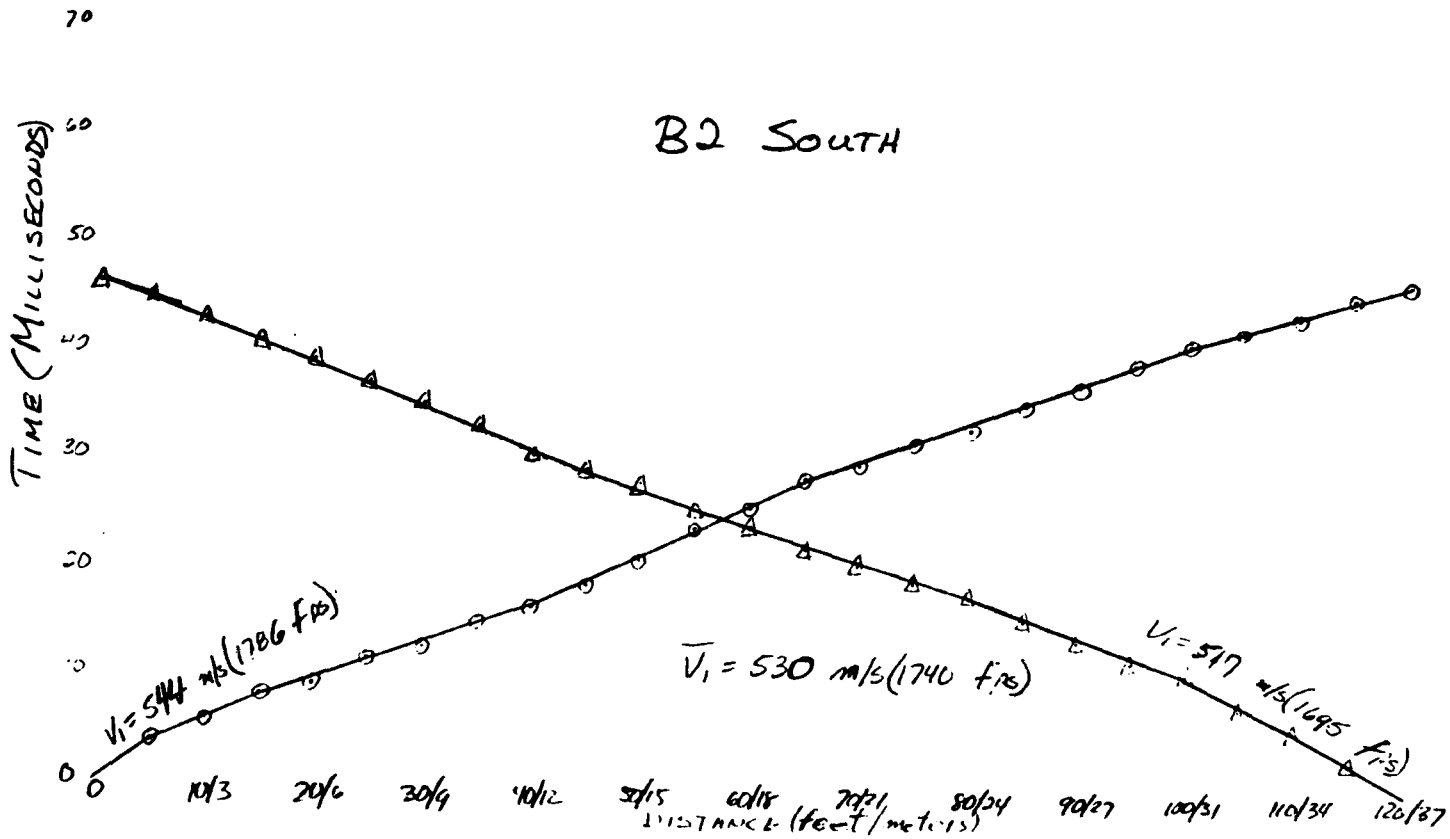

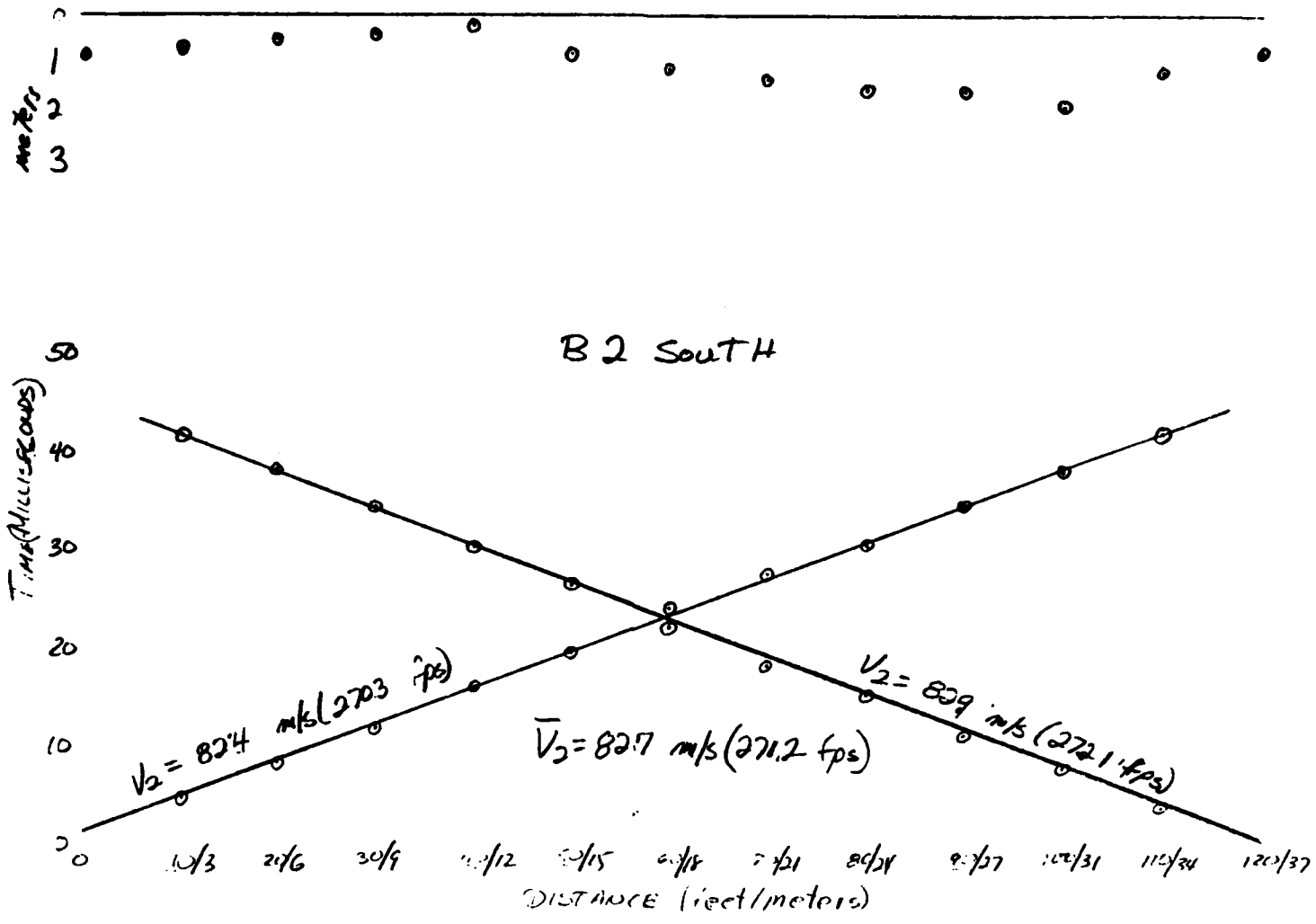
B 2 SOUTH
0
1
2
3
meters
50
40
30
20
10
0
TIME (Milliseconds)
V_2 = 824 m/s (2703 fps)
V_2 = 809 m/s (2721 fps)
$\bar{V}_2$ = 827 m/s (2712 fps)
10/3
20/6
30/9
40/12
50/15
60/18
70/21
80/24
90/27
100/31
110/34
120/37
DISTANCE (feet/meters)

	1	2	3	4	5	6	7	8	9	10	11	12	13
X → A	0	10	20	30	40	50	60	70	80	90	100	110	120
X ← B	120	110	100	90	80	70	60	50	40	30	20	10	0
T_{AP}		5.6	9.0			30.9			33.6				
T_{BP}						28.0	31.9		17.3	13.8			
$[T_{AP}+T_{BP}-T_{AB}]$		1.9	1.4	1.0	0.5				4.3	4.4			
T'_{AP}		4.65	2.3	12.0					27.9	34.9			
T'_{BP}						26.3			15.6	11.6			
h_p ft / m		2.16 / 0.66	1.59 / 0.48	1.14 / 0.35	.57 / 0.17	2.72 / 0.83	3.52 / 1.07	4.31 / 1.31	4.88 / 1.49	4.99 / 1.52	6.13 / 1.87	3.86 / 1.18	

$V_1 = \frac{10}{.0056} = 1785.7 fps (544.3 m/s)$

$V_1 = \frac{10}{.0059} = 1694.9 fps (516.6 m/s)$

$\bar{V}_1 = 1740.3 fps (530.4 m/s)$

$V_2 = \frac{50-10}{.0147-.0111} = 2700.7 fps (803.8 m/s)$

$V_2 = \frac{50-10}{.0147-.0110} = 2721.1 fps (809.1 m/s)$

$\bar{V}_2 = 2711.9 fps (826.5 m/s)$

$\sin \alpha_c = \frac{\bar{V}_1}{\bar{V}_2} = .6417$

$\alpha_c = 39.92°$

$t'_{AP} = 0.0012$

$t'_{BP} = 0.0011$

$h_A = \frac{\bar{V}_1 t_{AP}}{\cos \alpha_c} = \underset{0.83 m}{2.72 ft}$

$h_B = \frac{\bar{V}_1 t_{BP}}{\cos \alpha_c} = \underset{0.76 m}{2.50 ft}$

$h_p = \frac{\bar{V}_1}{2 \cos \alpha_c} [T_{AP} + T_{BP} - T_{AB}] =$

$\bar{T}_{AB} = 46.5$

NORTH — POINT B-3 - NORTH 120 FEET — SOUTH

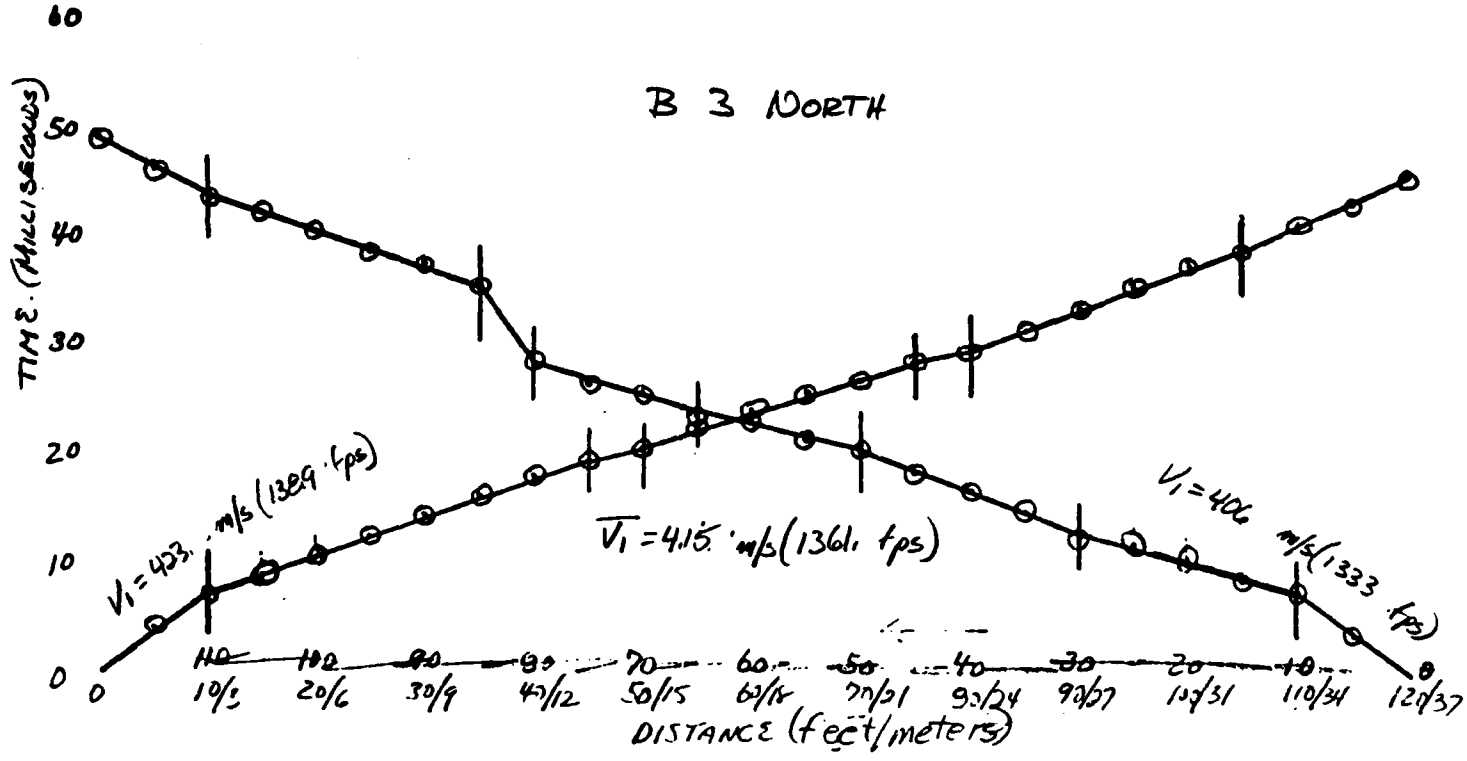

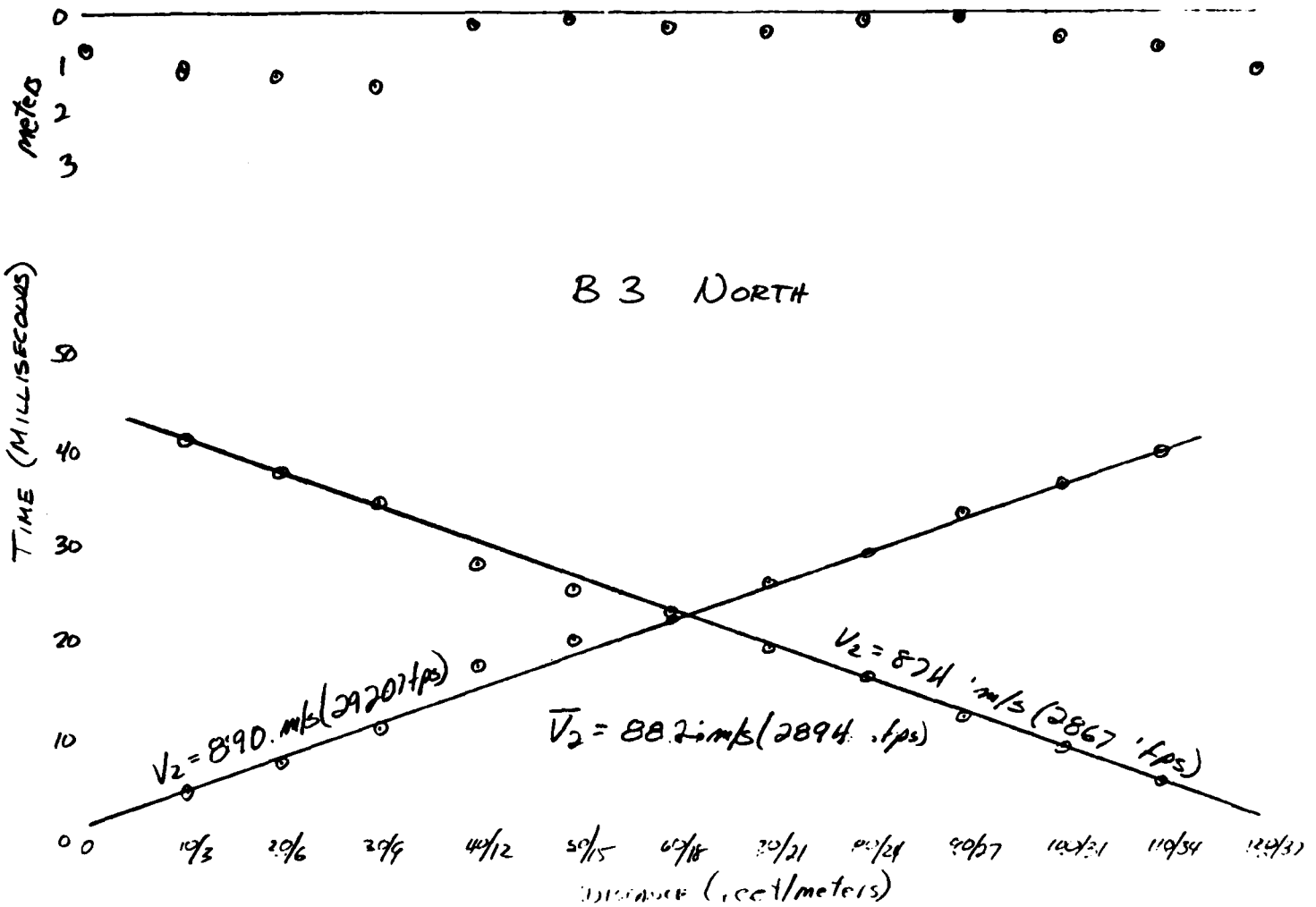
B 3 NORTH
TIME (MILLISECONDS)
meters
0
1
2
3
50
40
30
20
10
0
10/3
20/6
30/9
40/12
50/15
60/18
70/21
80/24
90/27
100/31
110/34
120/37
V2 = 890. m/s (29207 fps)
V2 = 874 m/s (2867 fps)
V̄2 = 88.2 m/s (2894 fps)
DISTANCE (feet/meters)

B-3 NORTH

	1	2	3	4	5	6	7	8	9	10	11	12	13
X → A	0	10	20	30	40	50	60	70	80	90	100	110	120
X ← B	120	110	100	90	80	70	60	50	40	30	20	10	0
T_{AP}	0	7.2	10.6	14.5	18.1	20.6	24.0	27.0	29.5	33.5	37.5	41.[illegible]	[illegible]
$T_{B.P}$	49.2	43.5	40.5	37.[illegible]	[illegible]	[illegible]	23.0	20.[illegible]	16.7	12.[illegible]	10.5	7.5	0
$[T_{AP}+T_{BP}-T_{AB}]$		4.9	5.3	6.3	0.8	0.5	1.2	1.7	0.6	0.3	2.2	2.9	
T'_{AP}		4.75	7.95	11.35	17.7	24.35	23.4	26.15	29.2	33.35	36.4	39.75	
T'_{BP}		41.05	37.[illegible]	34.45	28.1	25.45	22.4	19.65	16.6	12.4[illegible]	9.4	[illegible]	
h_P	ft / m	3.77 / 1.15	4.09 / 1.25	4.86 / 1.48	.62 / 0.19	0.39 / .12	.93 / .28	1.31 / .40	.46 / .14	.23 / .07	1.70 / .52	2.23 / .68	

$V_1 = \frac{10}{.0072} = 1388.9\,fps\ (423.3\,m/s)$

$V_1 = \frac{10}{.0075} = 1333.3\,fps\ (406.40\,m/s)$

$\bar{V}_1 = 1361.1\,fps\ (414.9\,m/s)$

$V_2 = \frac{50-10}{.0187-.005} = 2919.7\,fps\ (889.9\,m/s)$

$V_2 = \frac{50-10}{.02-.00605} = 2867.4\,fps\ (873.9\,m/s)$

$\bar{V}_2 = 2893.6\,fps\ (881.6\,m/s)$

$\sin\alpha_c = \frac{\bar{V}_1}{\bar{V}_2} = .4704$

$\alpha_c = 28.059$

$t'_{AP} = .0014$

$t'_{BP} = .0025$

$h_A = \frac{\bar{V}_1\, t_{AP}}{\cos\alpha_c} = 2.16\,ft$ 0.66 m

$h_B = \frac{\bar{V}_1\, t_{BP}}{\cos\alpha_c} = 3.86\,ft$ 1.18 m

$h_P = \frac{\bar{V}_1}{2\cos\alpha_c}\left[T_{AP}+T_{BP}-T_{AB}\right] =$

$\bar{T}_{AB} = 45.8$

POINT B-4 - NORTH 120 FEET

NORTH — SOUTH

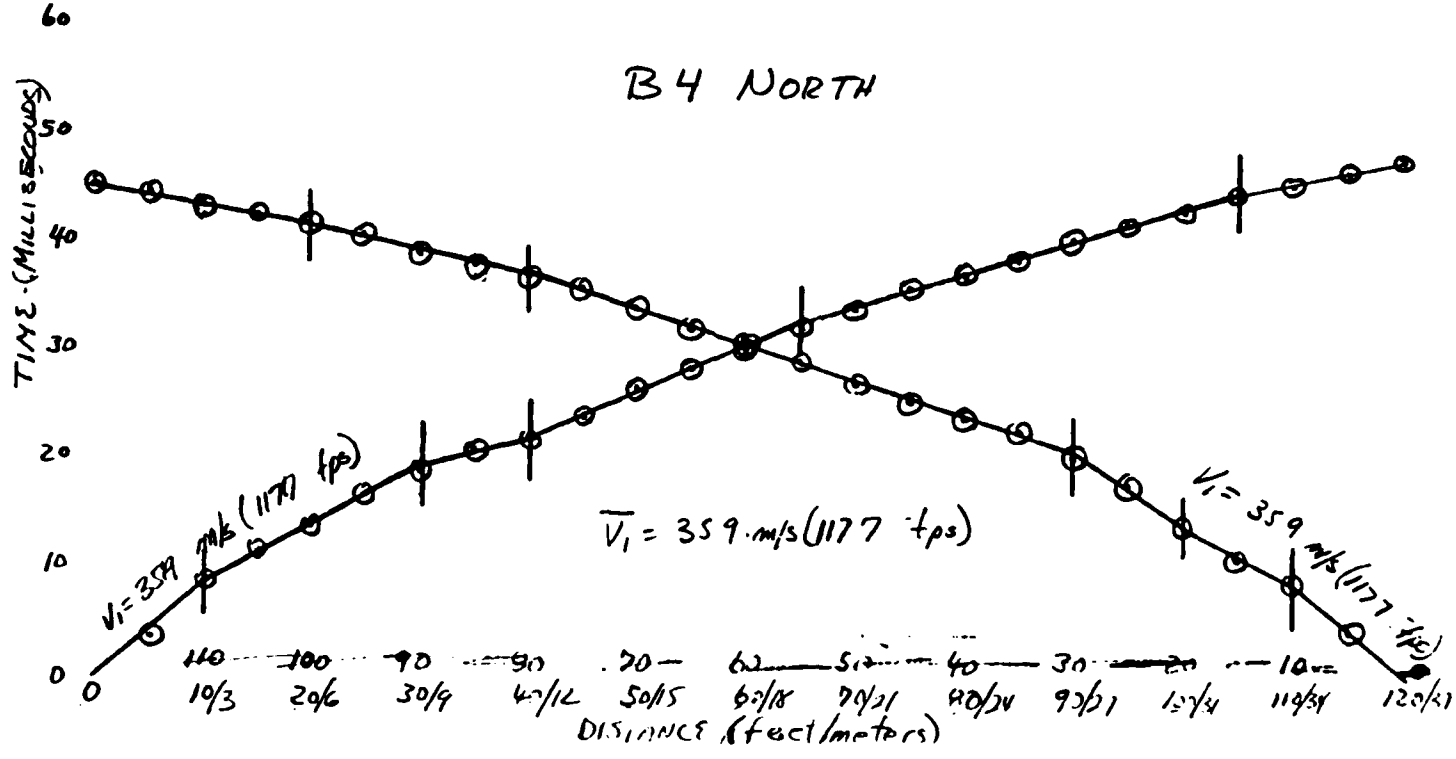

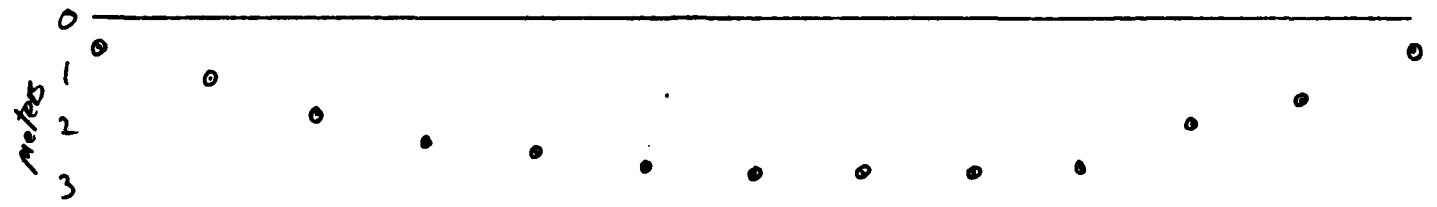
0
1
2
3
meters

B 4 NORTH

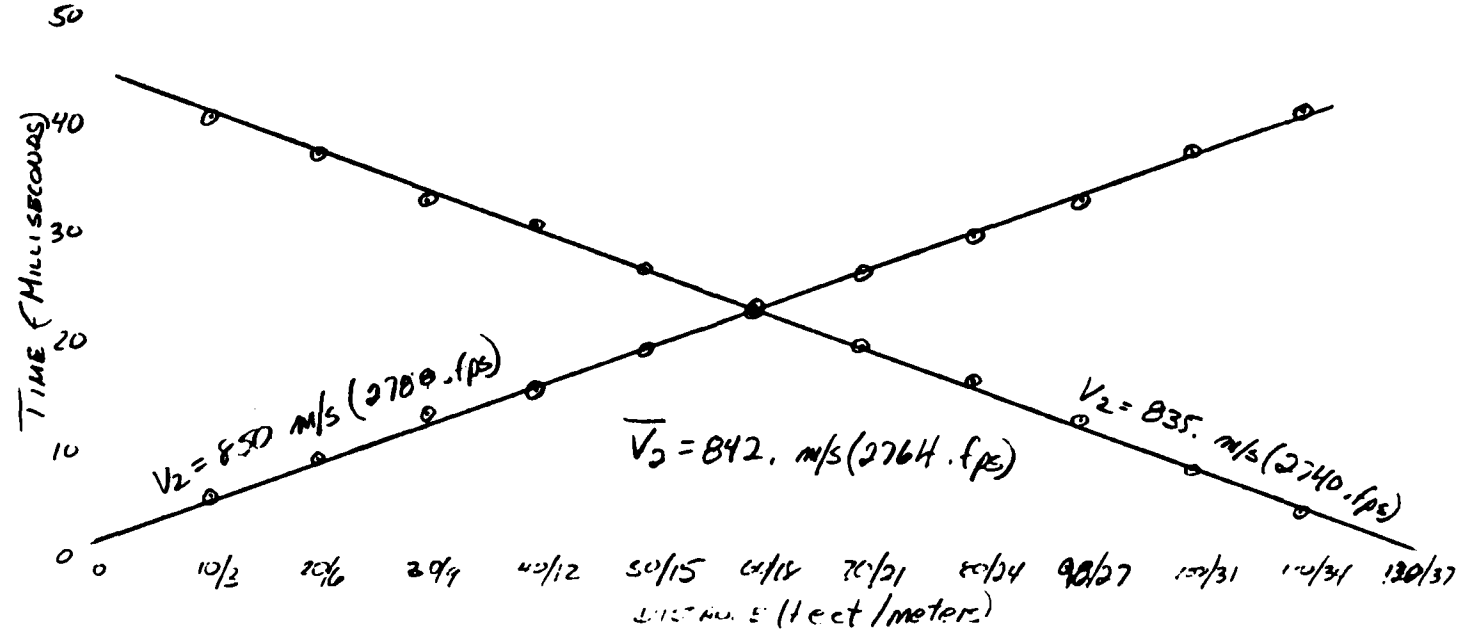
50
40
30
20
10
0
TIME (Milliseconds)
V_2 = 850 m/s (2788. fps)
$\overline{V_2}$ = 842. m/s (2764. fps)
V_2 = 835. m/s (2740. fps)
0
10/3
20/6
30/9
40/12
50/15
60/18
70/21
80/24
90/27
100/31
110/34
120/37
Distance (feet/meters)

	1	2	3	4	5	6	7	8	9	10	11	12	13
X → A	0	10	20	30	40	50	60	70	80	90	100	110	120
X ← B	120	110	100	90	80	70	60	50	40	30	20	10	0
T_{AP}	0	[illegible]	13.6	18.9	21.6	26.2	30.5	[illegible]	36.3	[illegible]	[illegible]	[illegible]	[illegible]
T_{BP}	[illegible]	[illegible]	[illegible]	[illegible]	36.3	33.6	30.0	26.3	23.5	[illegible]	[illegible]	[illegible]	0
$[T_{AP}+T_{BP}-T_{AB}]$		5.4	9.0	11.4	12.3	13.7	14.4	14.2	14.2	13.9	9.9	[illegible]	
T'_{AP}		5.8	9.1	13.2	15.45	19.35	23.3	[illegible]	29.7	[illegible]	[illegible]	[illegible]	
T'_{BP}		40.3	37.0	32.9	30.65	[illegible]	[illegible]	[illegible]	16.4	13.[illegible]	[illegible]	4.8	
h_p	ft / m	3.51 / 1.07	5.85 / 1.78	7.41 / 2.26	8.00 / 2.44	8.91 / 2.72	9.36 / 2.85	9.23 / 2.81	9.23 / 2.81	9.09 / 2.75	6.44 / 1.96	4.81 / 1.47	

$V_1 = \frac{10}{.0085} = 1176.5\,fps\ (358.6\,m/s$

$V_1 = \frac{10}{.0084} = 1176.5\,fps\ (358.6\,m/s)$

$\bar{V}_1 = 1176.5\,fps\ (358.6\,m/s)$

$V_2 = \frac{50-10}{.01935-.005} = 2787.5\,fps\ (849.6\,m/s)$

$V_2 = \frac{50-10}{.0197-.0051} = 2739.7\,fps\ (835.1\,m/s)$

$\bar{V}_2 = 2763.6\,fps\ (842.4\,m/s)$

$\sin\alpha_c = \frac{\bar{V}_1}{\bar{V}_2} = .4257$

$\alpha_c = 25.196°$

$t'_{AP} = .0014$

$t'_{BP} = .0013$

$h_A = \frac{\bar{V}_1\, t_{AP}}{\cos\alpha_c} = 1.82\,ft$ $.55\,m$

$h_B = \frac{\bar{V}_1\, t_{BP}}{\cos\alpha_c} = 1.69\,ft$ $.52\,m$

$h_p = \frac{\bar{V}_1}{2\cos\alpha_c}\left[T_{AP}+T_{BP}+T_{AB}\right] =$

$\bar{T}_{AB} = 46.1$

NORTH — POINT B-4 - SOUTH 120 FEET — SOUTH

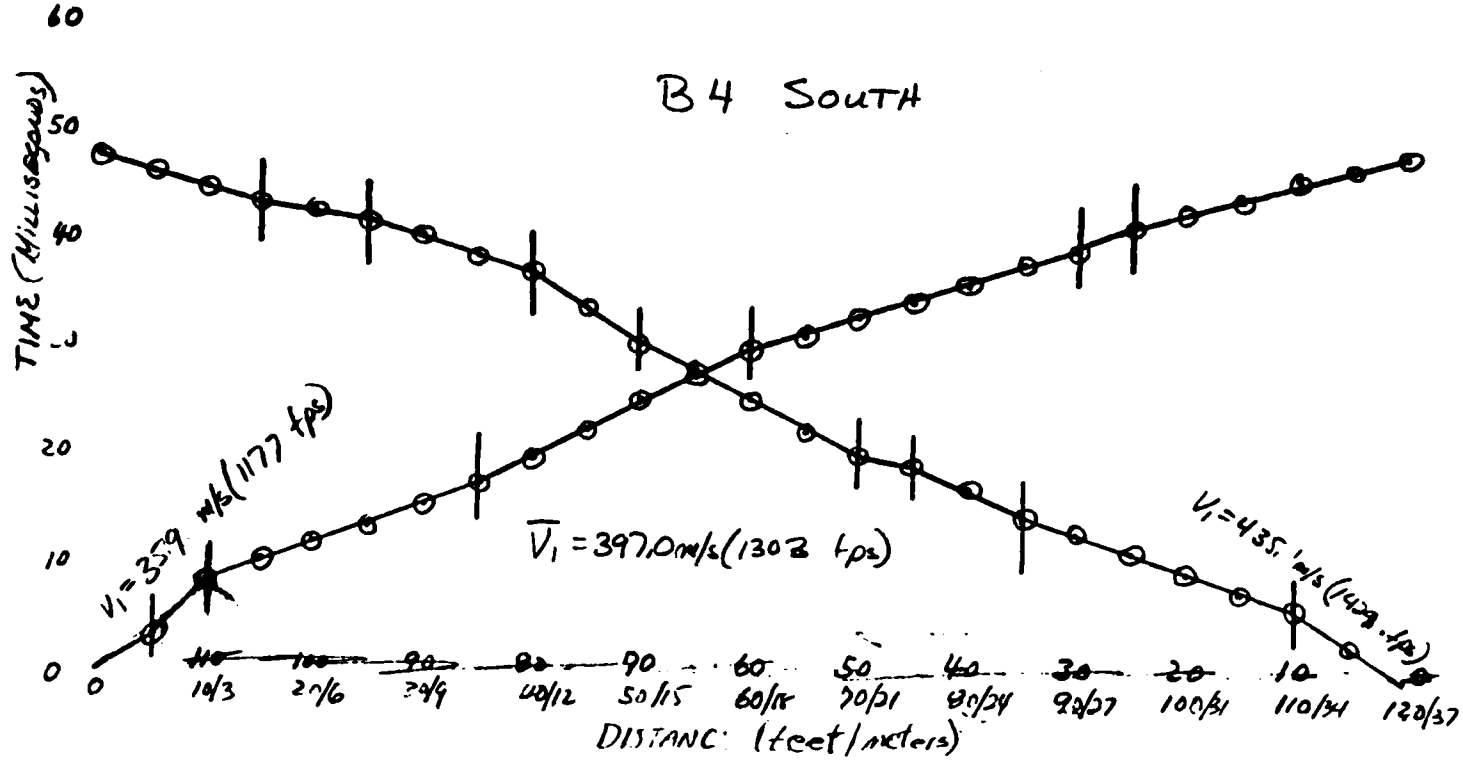

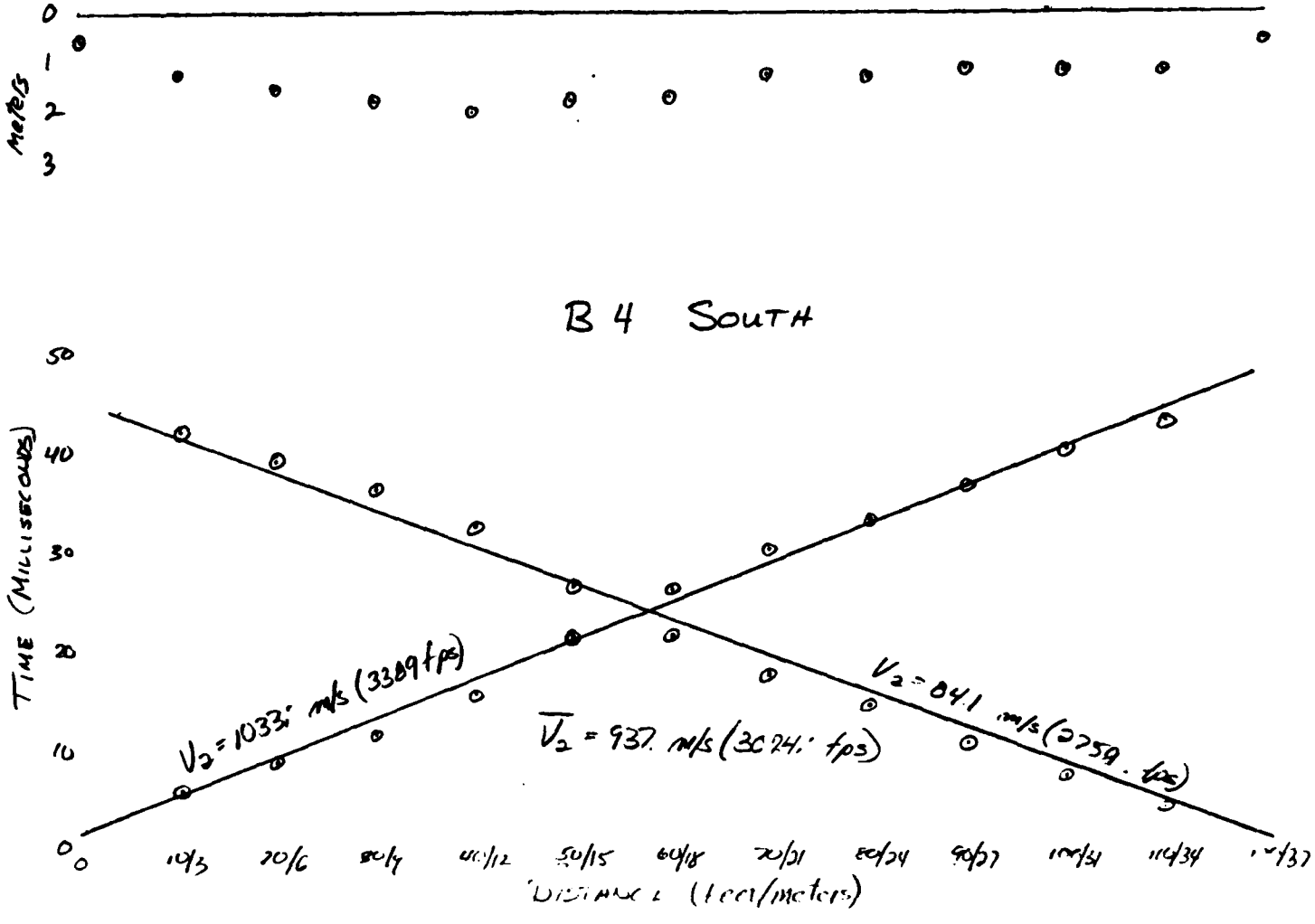
0
1
2
3
METERS
B 4 SOUTH
50
40
30
20
10
0
TIME (MILLISECONDS)
V_2 = 1033 m/s (3389 fps)
$\overline{V_2}$ = 937 m/s (3024 fps)
V_2 = 841 m/s (2759 fps)
0
10/3
20/6
30/9
40/12
50/15
60/18
70/21
80/24
90/27
100/30
110/34
120/37
DISTANCE (feet/meters)

B4 SOUTH

	1	2	3	4	5	6	7	8	9	10	11	12	13
X → A	0	10	20	30	40	50	60	70	80	90	100	110	120
X ← B	120	110	100	90	80	70	60	50	40	30	20	10	0
T_{AP}	0	8.5	[illegible]	[illegible]	[illegible]	[illegible]	[illegible]	[illegible]	[illegible]	39.5	[illegible]	46.2	48.0
T_{BP}	47.6	44.9	42.5	40.2	37.0	30.5	[illegible]	20.5	17.5	13.5	10.0	7.0	0
$[T_{AP}+T_{BP}-T_{AB}]$		5.6	6.9	8.0	9.2	3.2	7.7	5.1	5.9	5.2	5.2	5.4	
T'_{AP}		[illegible]	8.75	11.4	15.4	21.4	[illegible]	30.15	33.25	36.9	40.4	43.5	
T'_{BP}		47.1	[illegible]	36.2	30.4	26.4	21.65	[illegible]	14.5	[illegible]	[illegible]	11.3	
h_p	ft/m	4.03/1.23	4.96/1.51	5.75/1.75	6.62/2.02	5.40/1.80	5.54/1.69	4.10/1.25	4.24/1.29	3.74/1.14	3.74/1.14	3.88/1.18	

$V_1 = \frac{10}{.0085} = 1176.5\,fps\ (358.6\,m/s)$

$V_1 = \frac{10}{.007} = 1428.6\,fps\ (435.4\,m/s)$

$\bar{V}_1 = 1302.6\,fps\ (397.0\,m/s)$

$V_2 = \frac{50-10}{.021-.0092} = 3389.8\,fps\ (1033.2\,m/s)$

$V_2 = \frac{50-10}{.0195-.003} = 2758.6\,fps\ (840.8\,m/s)$

$\bar{V}_2 = 3074.2\,fps\ (937.0\,m/s)$

$\sin \alpha_c = \frac{\bar{V}_1}{\bar{V}_2} = .4237$

$\alpha_c = 25.070°$

$t'_{AP} = .0013$

$t'_{BP} = .0012$

$h_A = \frac{\bar{V}_1\, t_{AP}}{\cos \alpha_c} = 1.87\,ft$ $.57\,m$

$h_B = \frac{\bar{V}_1\, t_{BP}}{\cos \alpha_c} = 1.73\,ft$ $.53\,m$

$h_p = \frac{\bar{V}_1}{2\cos \alpha_c}\,[T_{AP}+T_{BP}-T_{AB}] =$

$\bar{T}_{AB} = 47.8$

⊙ B5 NORTH - PLATE NORTH END
△ B5 NORTH - PLATE SOUTH END

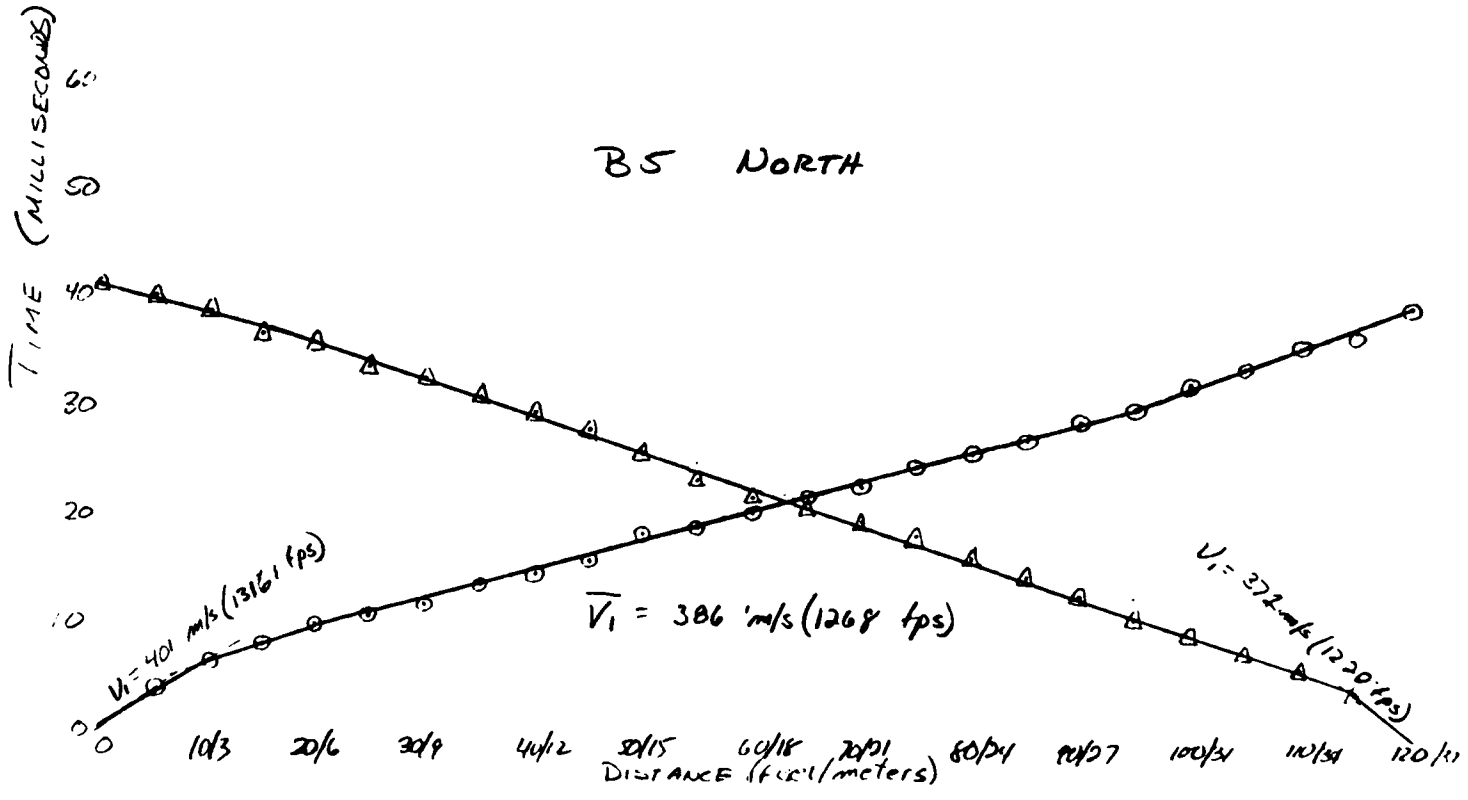

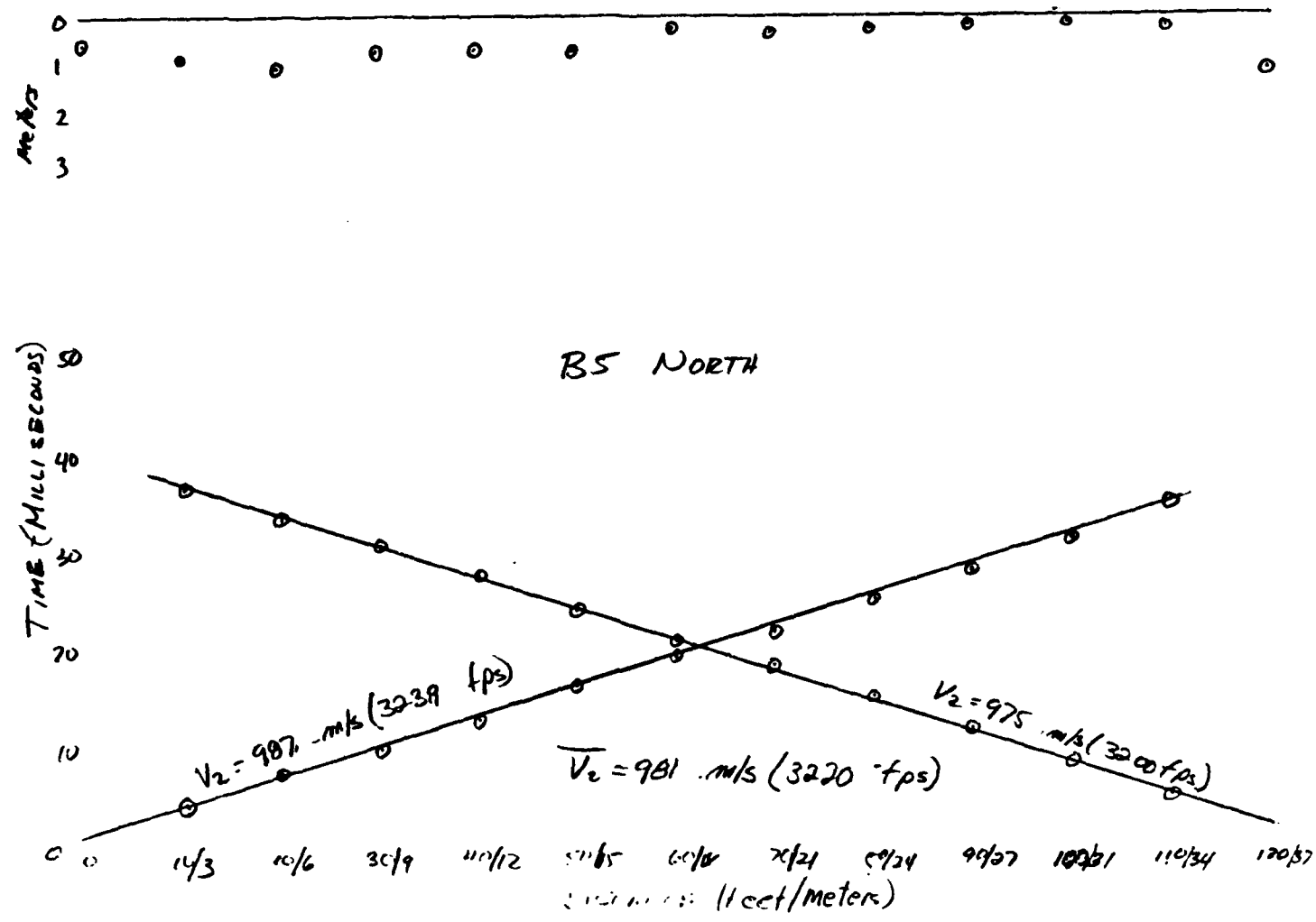
0
1
2
3
B5 NORTH
TIME (MILLISECONDS)
50
40
30
20
10
0
$V_2 = 987$ m/s (3239 fps)
$V_2 = 975$ m/s (3200 fps)
$\overline{V_2} = 981$ m/s (3220 fps)
14/3
30/9
120/37
(Feet/Meters)

R 5 Data

	1	2	3	4	5	6	7	8	9	10	11	12	13
X → A	0	10	20	30	40	50	60	70	80	90	100	110	120
X ← B	120	110	100	90	80	70	60	50	40	30	20	10	0
T_{AP}	0	6.5	7.9	11.9	16.3	19.5	22.1	24.4	25.9	28.2	30.5	32.3	34.0
T_{BP}	34.0	32.5	30.9	29.5	27.5	25.9	24.4	22.8	21.2	19.2	16.5	13.2	9.5
$[T_{AP}+T_{BP}-T_{AB}]$		4.1	4.18	3.4	3.3	3.4	1.2	1.7	1.1	0.9	0.7	1.0	
T'_{AP}		4.145	7.75	10.2	13.2	16.8	19.7	22.1	25.4	28.5	31.9	35.3	
T'_{BP}		36.55	33.5	30.8	27.9	24.2	21.3	18.9	15.7	12.5	9.0	5.7	
h_p	1.1 m	2.63 / .86	3.31 / 1.01	3.39 / .72	2.78 / .69	2.31 / .72	1.83 / .25	1.17 / .36	.76 / .23	.62 / .19	.48 / .15	.69 / .21	

$V_1 = \frac{5}{.0038} = 1315.8$ fps (401.1 m/s)

$V_1 = \frac{5}{.0041} = 1219.5$ fps (371.7 m/s)

$\bar{V}_1 = 1267.7$ fps (386.4 m/s)

$V_2 = \frac{50-10}{.0160-.0044s} = 3238.9$ fps (987.2 m/s)

$V_2 = \frac{50-10}{.0183-.0052} = 3200.8$ fps (975.6 m/s)

$\bar{V}_2 = 3219.5$ fps (981.2 m/s)

$\sin \alpha_c = \frac{\bar{V}_1}{\bar{V}_2} = .3938$

$\alpha_c = 23.189°$

$t'_{AP} = .0013$

$t'_{BP} = .0026$

$h_A = \frac{\bar{V}_1 t_{AP}}{\cos \alpha_c} = 1.79$ ft (.55 m)

$h_B = \frac{\bar{V}_1 t_{BP}}{\cos \alpha_c} = 3.59$ ft (1.09 m)

$h_p = \frac{\bar{V}_1}{2 \cos \alpha_c} [T_{AP} + T_{BP} + T_{AB}] =$

$\bar{T}_{AB} = 41.0$

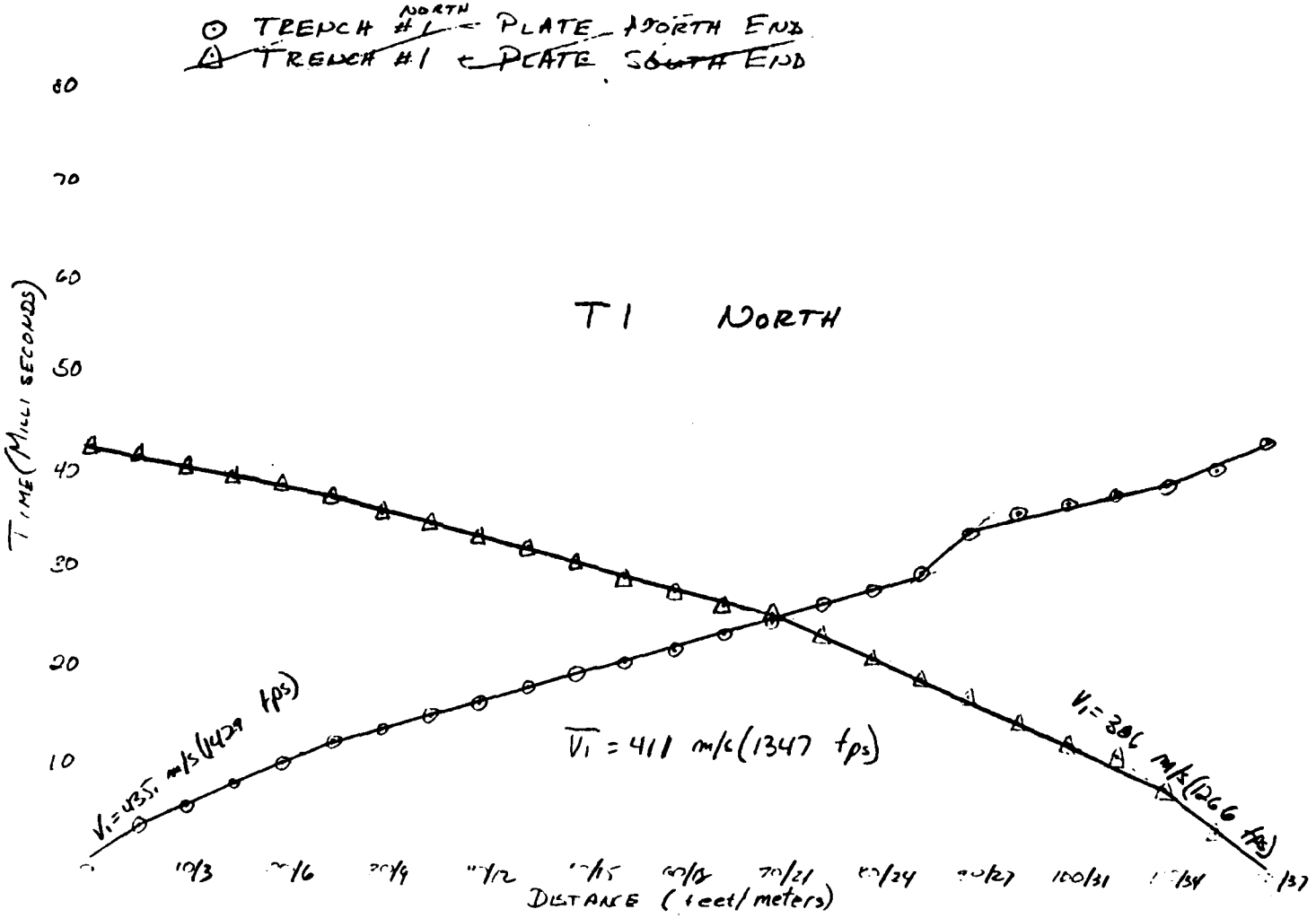

⊙ TRENCH #1 NORTH ← PLATE NORTH END
△ TRENCH #1 ← PLATE SOUTH END
T1 NORTH
TIME (MILLI SECONDS)
80
70
60
50
40
30
20
10
V_1 = 435 m/s (1429 fps)
$\overline{V_1}$ = 411 m/s (1347 fps)
V_1 = 386 m/s (1266 fps)
10/3
70/21
100/31
DISTANCE (feet/meters)

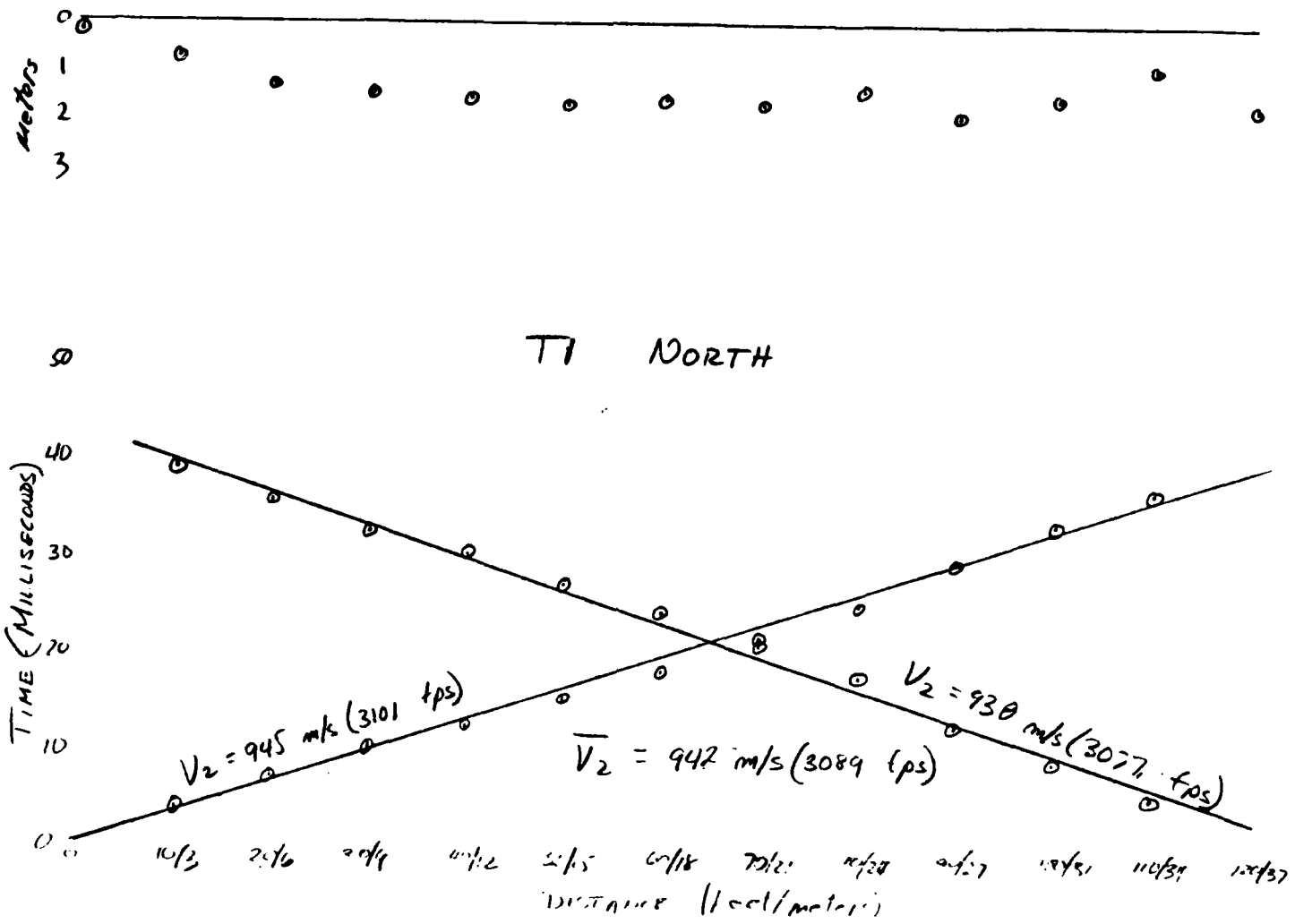
Meters
0
1
2
3
T1 NORTH
TIME (MILLISECONDS)
40
30
20
10
0
V_2 = 945 m/s (3101 fps)
$\overline{V}_2$ = 942 m/s (3089 fps)
V_2 = 938 m/s (3077 fps)
DISTANCE (Reel/meters)

T-1 [illegible]

	1	2	3	4	5	6	7	8	9	10	11	12	13
X → A	0	10	20	30	40	50	60	70	80	90	100	110	120
X ← B	120	110	100	90	80	70	60	50	40	30	20	10	0
T_{AP}	0	5.5	10.0	13.5	16.2	19.3	21.9	24.7	28.0	[illegible]	[illegible]	[illegible]	[illegible]
T_{BP}	42.5	40.5	38.5	35.7	33.5	32.9	[illegible]	[illegible]	[illegible]	[illegible]	[illegible]	[illegible]	[illegible]
$[T_{AP}+T_{BP}-T_{AB}]$		3.0	5.5	6.2	6.7	7.2	6.8	7.2	5.9	8.2	6.6	3.8	
T'_{AP}		4.0	7.25	10.4	12.9	15.7	18.5	21.1	25.1	29.9	33.7	37.0	
T'_{BP}		39.0	35.8	32.6	30.2	27.3	24.5	21.9	18.0	13.1	9.3	6.0	
h_P	ft / m	2.25 / .69	4.12 / 1.26	4.64 / 1.42	5.02 / 1.53	5.39 / 1.64	5.09 / 1.55	5.39 / 1.64	4.92 / 1.35	6.14 / 1.87	4.94 / 1.51	2.85 / .87	

$V_1 = \frac{5}{.0035} = 1428.6\,fps\,(435.4\,m/s)$

$V_1 = \frac{10}{.0079} = 1265.8\,fps\,(385.8\,m/s)$

$\bar{V}_1 = 1347.2\,fps\,(410.6\,m/s)$

$V_2 = \frac{50-10}{.0166-.0037} = 3100.8\,fps\,(945.1\,m/s)$

$V_2 = \frac{50-10}{.020-.007} = 3076.9\,fps\,(937.9\,m/s)$

$\bar{V}_2 = 3088.9\,fps\,(941.5\,m/s)$

$\sin\alpha_c = \frac{\bar{V}_1}{\bar{V}_2} = .4361$

$\alpha_c = 25.858°$

$t'_{AP} = .0003$

$t'_{BP} = .0036$

$h_A = \frac{\bar{V}_1\, t_{AP}}{\cos\alpha_c} = .50\,ft\ (.14\,m)$

$h_B = \frac{\bar{V}_1\, t_{BP}}{\cos\alpha_c} = 5.39\,ft\ (1.64\,m)$

$h_P = \frac{\bar{V}_1}{2\cos\alpha_c}\,[T_{AP}+T_{BP}-T_{AB}] =$

$\bar{T}_{AB} = 43.0$

⊙ TRENCH #1 SOUTH - PLATE NORTH END

~~⊙~~ TRENCH #1 SOUTH - PLATE SOUTH END

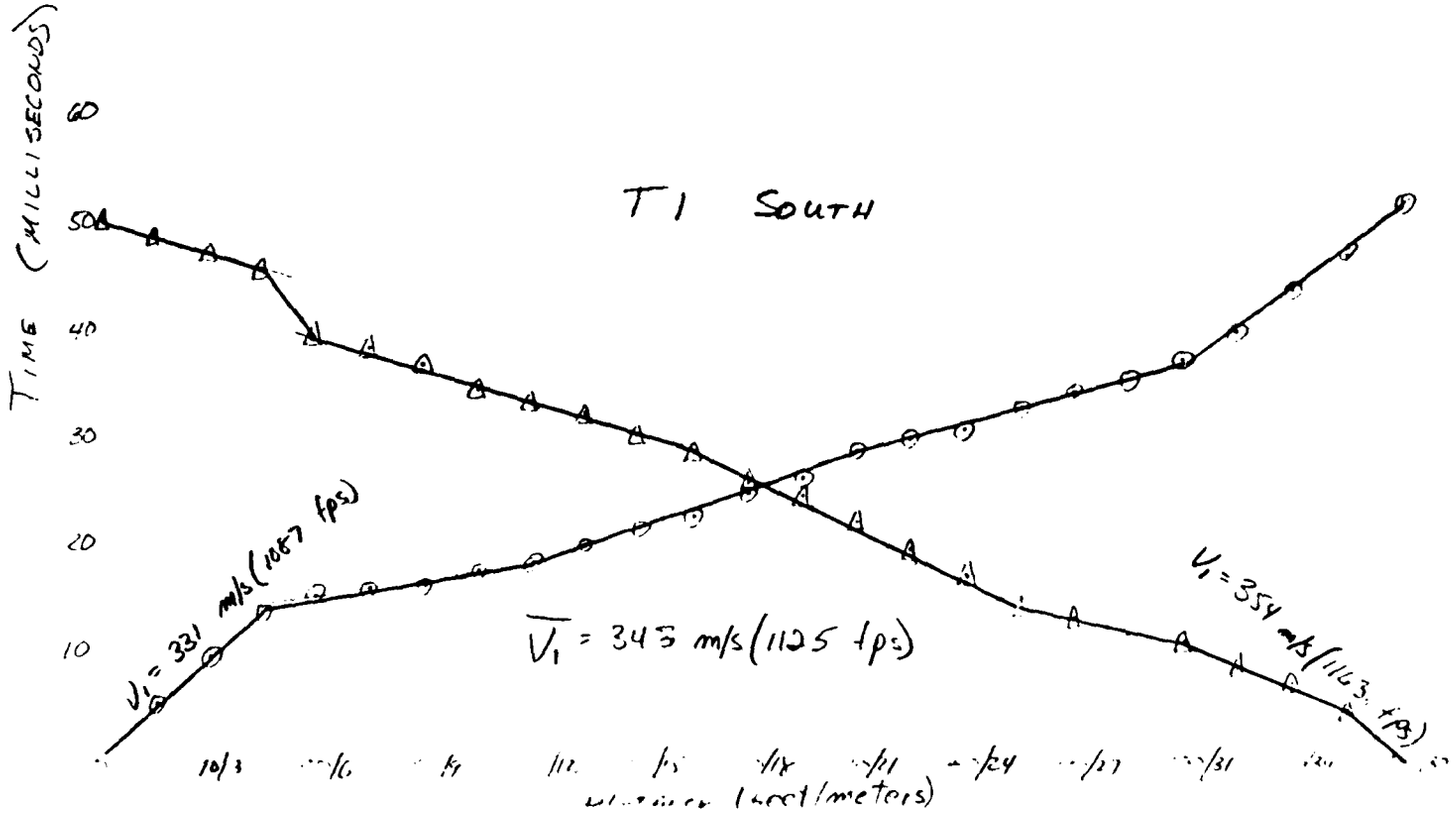

100

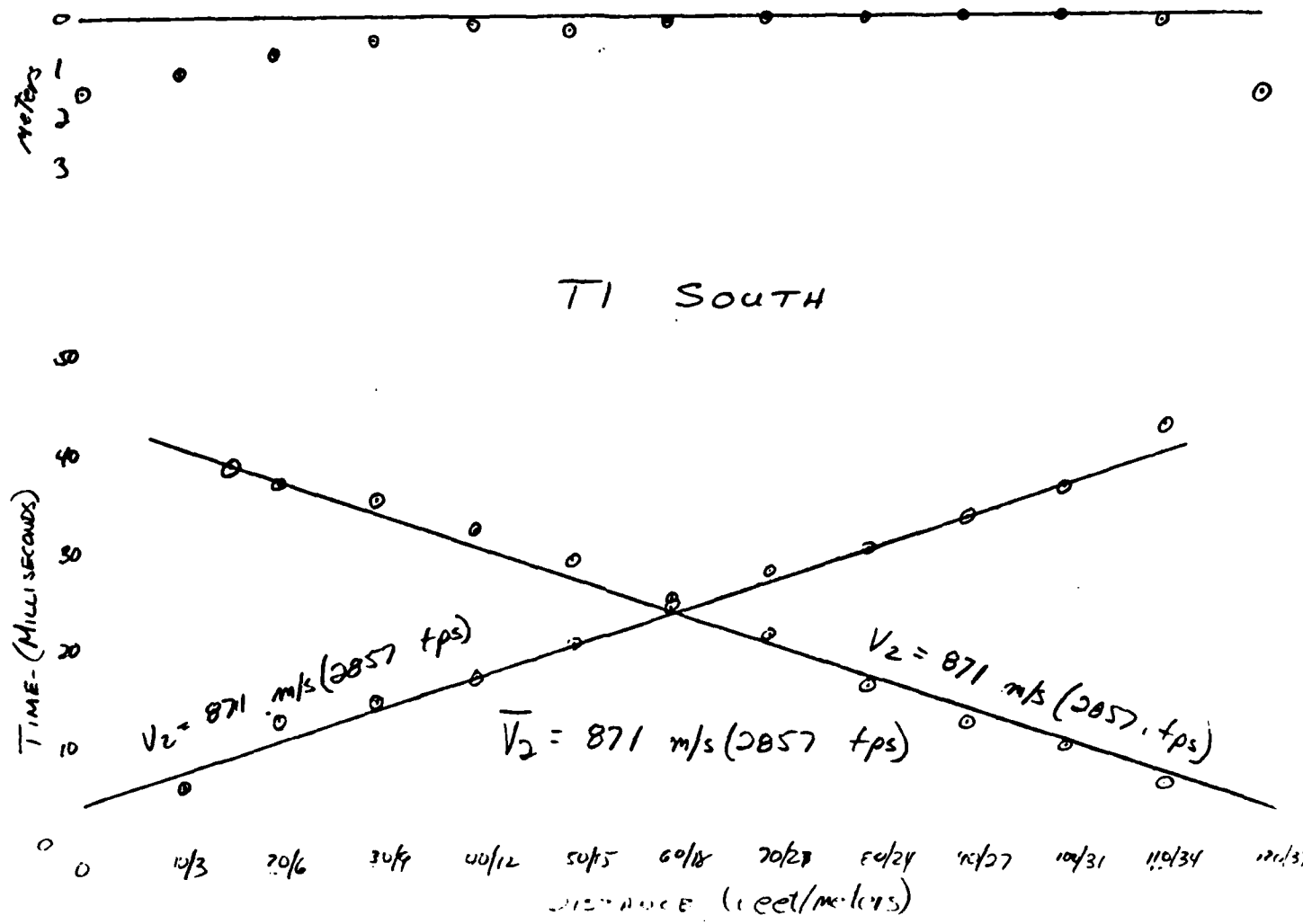
T1 SOUTH
TIME - (MILLISECONDS)
V_2 = 871 m/s (2857 fps)
$\overline{V_2}$ = 871 m/s (2857 fps)
V_2 = 871 m/s (2857 fps)

T-1 SOUTH

	1	2	3	4	5	6	7	8	9	10	11	12	13
X → A	0	10	20	30	40	50	60	70	80	90	100	110	120
X ← B	120	110	100	90	80	70	60	50	40	30	20	10	0
T_{AP}	0	9.1	15.0	16.0	19.0	21.5	24.6	28.3	32.9	37.2	41.1	44.5	47.5
T_{BP}	50.1	44.5	37.0	32.0	33.0	30.0	25.5	21.9	16.9	13.0	10.3	7.05	3.0
$[T_{AP}+T_{BP}-T_{AB}]$		6.2	4.0	2.5	1.0	1.5	.1	.20	–	–	–	.5	
T'_{AP}		6.1	13.0	14.8	17.5	20.8	24.5	28.2	30.3	33.8	36.9	43.3	
T'_{BP}		43.9	37.0	35.3	32.5	29.3	25.4	21.8	16.9	13.0	10.6	6.8	
h_p	ft / m	3.79 / 1.16	2.45 / .75	1.53 / .47	.62 / .19	.92 / .28	.06 / .02	.12 / .04	0 / 0	0 / 0	0 / 0	.31 / .09	

$V_1 = \frac{10}{.0092} = 1087.0$ fps (331.3 m/s)

$V_1 = \frac{5}{.0043} = 1162.8$ fps (354.4 m/s)

$\bar{V}_1 = 1124.9$ fps (342.9 m/s)

$V_2 = \frac{50-10}{.0215-.0075} = 2857.1$ fps (870.9 m/s)

$V_2 = \frac{50-10}{.0218-.0078} = 2857.1$ fps (870.9 m/s)

$\bar{V}_2 = 2857.1$ fps (870.9 m/s)

$\text{SIN}\ \alpha_c = \frac{\bar{V}_1}{\bar{V}_2} = .3937$

$\alpha_c = 23.186°$

$t'_{AP} = .0041$

$t'_{BP} = .0043$

$h_A = \frac{\bar{V}_1 t_{AP}}{\cos\alpha_c} = 5.02$ ft (1.53 m)

$h_B = \frac{\bar{V}_1 t_{BP}}{\cos\alpha_c} = 5.26$ ft (1.60 m)

$h_p = \frac{\bar{V}_1}{2\cos\alpha_c}[T_{AP}+T_{BP}+T_{AB}]$:

$\bar{T}_{AB} = 50.0$

NORTH — POINT A - NORTH 120 FEET — SOUTH

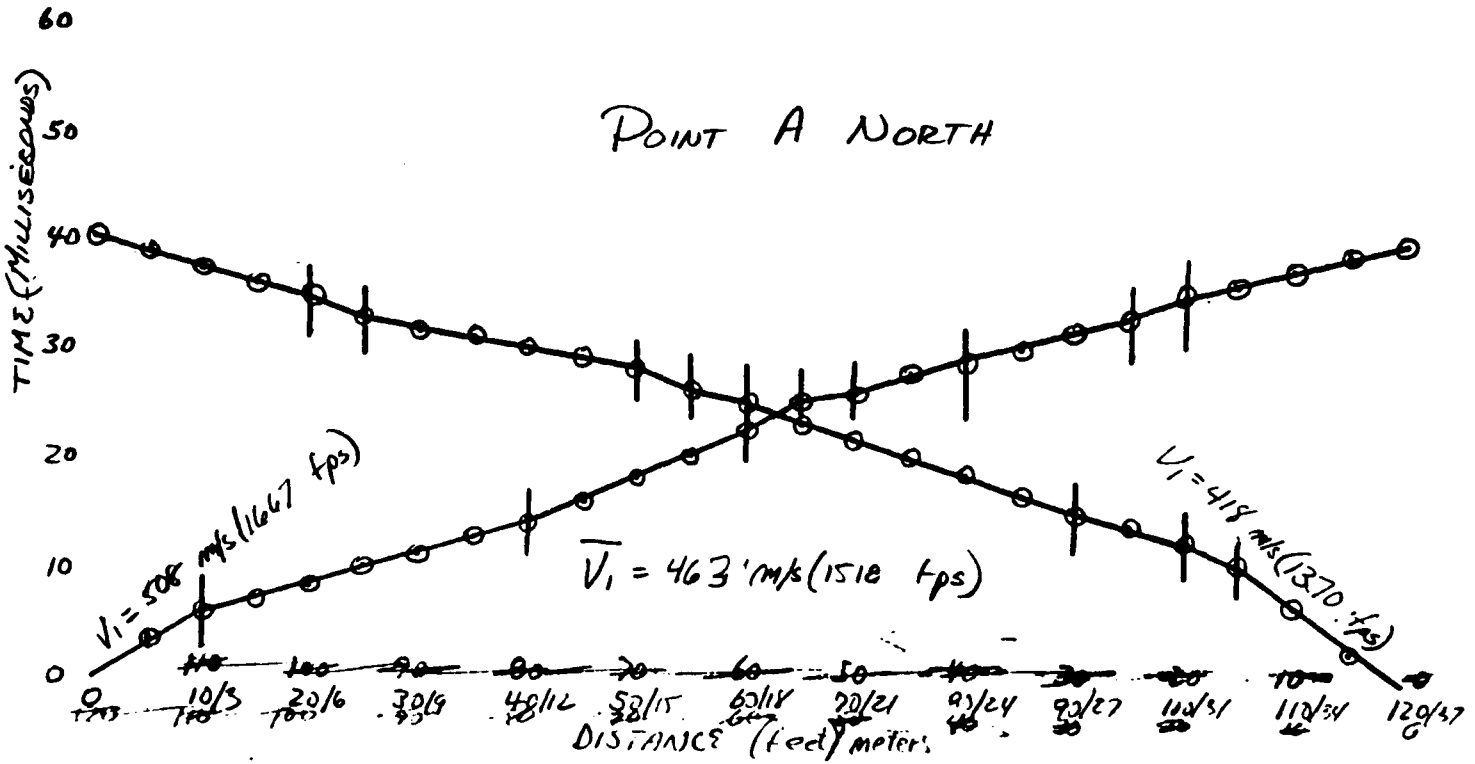

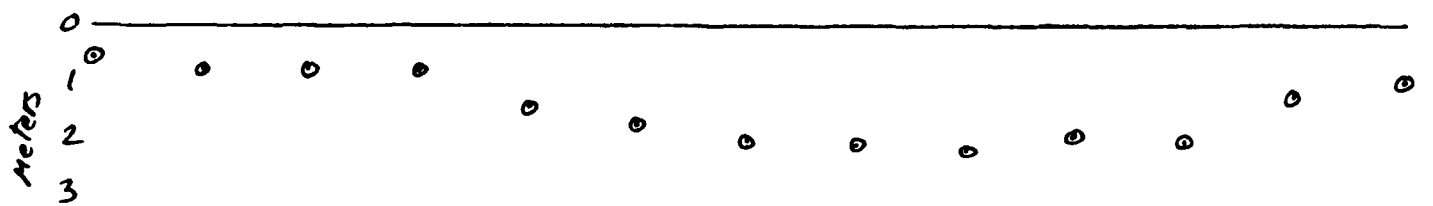
0
1
2
3
Meters

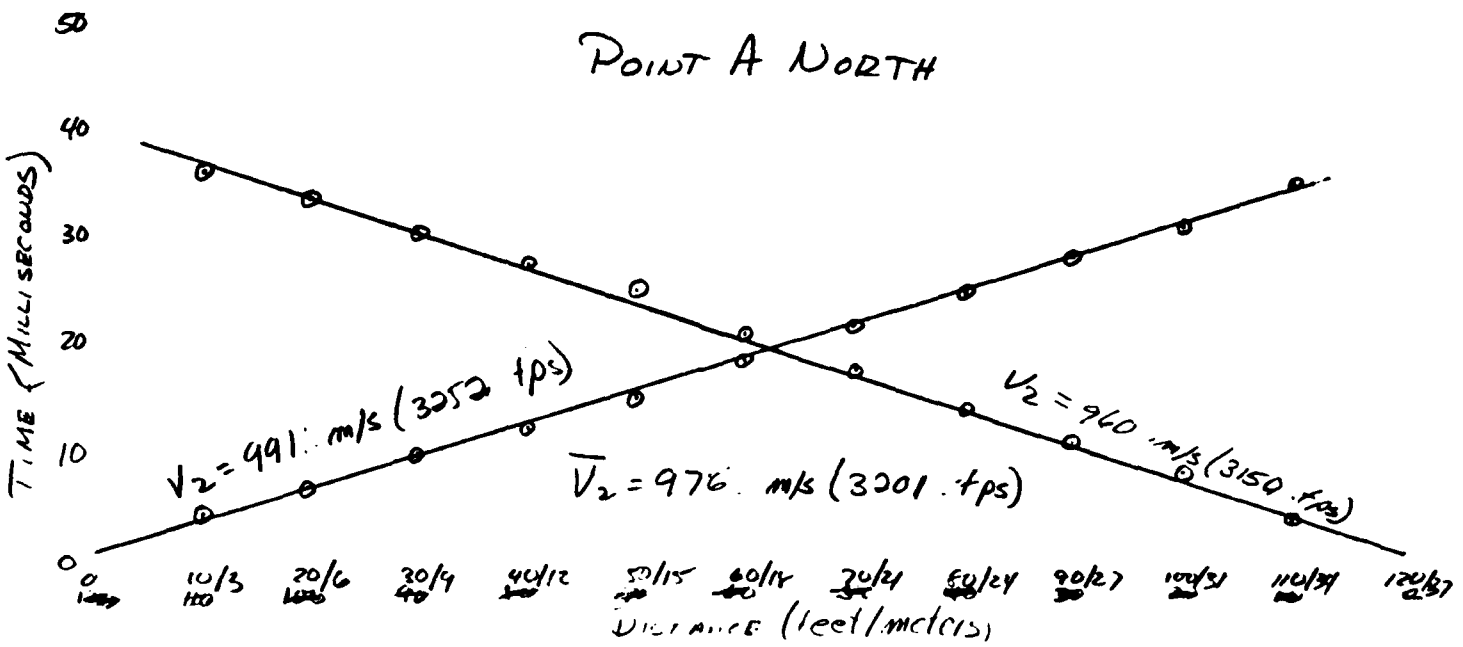
POINT A NORTH
50
40
30
20
10
0
TIME (MILLISECONDS)
V_2 = 991 m/s (3252 fps)
V_2 = 960 m/s (3150 fps)
$\overline{V}_2$ = 976 m/s (3201 fps)
0
10/3
20/6
30/9
40/12
50/15
60/18
70/21
80/24
90/27
100/31
110/34
120/37
DISTANCE (feet/meters)

Pt. A North

	1	2	3	4	5	6	7	8	9	10	11	12	13
X → A	0	10	20	30	40	50	60	70	80	90	100	110	120
X ← B	120	110	100	90	80	70	60	50	40	30	20	10	0
T_{AP}	0	6.0	[illegible]	11.6	[illegible]	18.7	[illegible]	[illegible]	7.6	[illegible]	[illegible]	[illegible]	[illegible]
T_{BP}	10.5	37.5	35.[illegible]	[illegible]	30.5	28.7	[illegible]	22.3	19.0	15.6	13.0	[illegible]	0
$[T_{AP}+T_{BP}-T_{AB}]$		3.0	3.0	3.1	5.5	6.9	8.0	8.3	8.6	7.6	8.0	4.8	
T'_{AP}		4.5	7.0	10.1	12.8	15.3	19.0	22.3	25.3	28.7	31.5	35.6	
T'_{BP}		36.0	33.5	30.5	27.8	25.3	21.5	18.1	14.7	11.8	9.0	4.9	
h_P	[illegible]	2.57/.79	2.59/.79	2.67/.82	4.74/1.45	5.95/1.81	6.90/2.10	7.16/2.18	7.42/2.26	6.55/2.00	6.90/2.10	4.14/1.26	

$V_1 = \frac{10}{.006} = 1666.7\,fps\ (508.0\,m/s)$

$V_1 = \frac{10}{.0073} = 1369.9\,fps\ (417.5\,m/s)$

$\bar{V}_1 = 1518.3\,fps\ (462.8\,m/s)$

$V_2 = \frac{50-10}{.0162-.004} = 3252.0\,fps\ (991.2\,m/s)$

$V_2 = \frac{50-10}{.0117-.0[illegible]} = 3149.6\,fps\ (960.0\,m/s)$

$\bar{V}_2 = 3200.8\,fps\ ([illegible]\,m/s)$

$\sin\alpha_c = \frac{\bar{V}_1}{\bar{V}_2} = .4744$

$\alpha_c = 28.317°$

$t'_{AP} = .001$

$t'_{BP} = .0019$

$h_A = \frac{\bar{V}_1 t_{AP}}{\cos\alpha_c} = 1.72\,ft\ (.53\,m)$

$h_B = \frac{\bar{V}_1 t_{BP}}{\cos\alpha_c} = 3.28\,ft\ 1.00\,m$

$h_P = \frac{\bar{V}_1}{2\cos\alpha_c}[T_{AP}+T_{BP}-T_{AB}]$:

$\bar{T}_{AB} = 40.5$

NORTH — POINT A - SOUTH 120 FEET — SOUTH

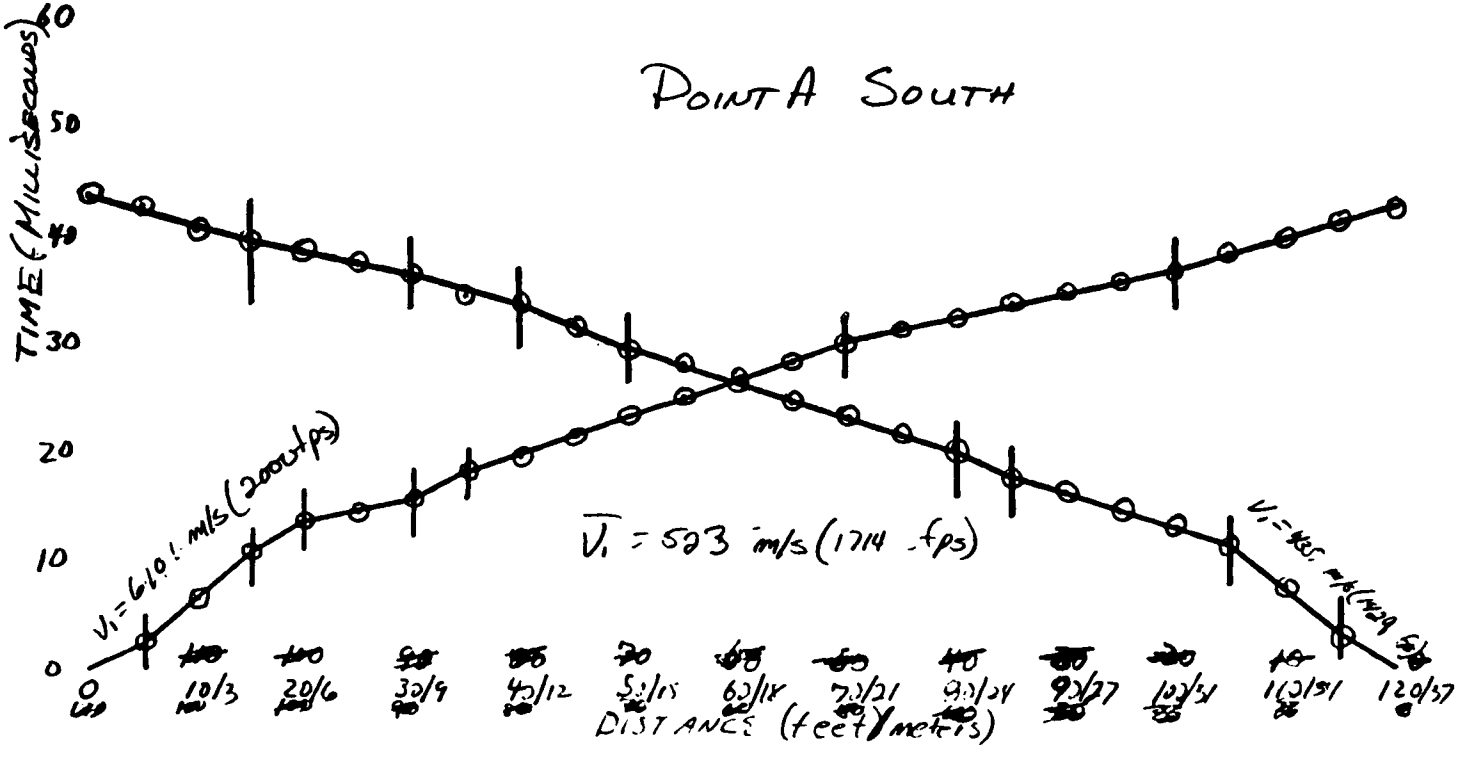

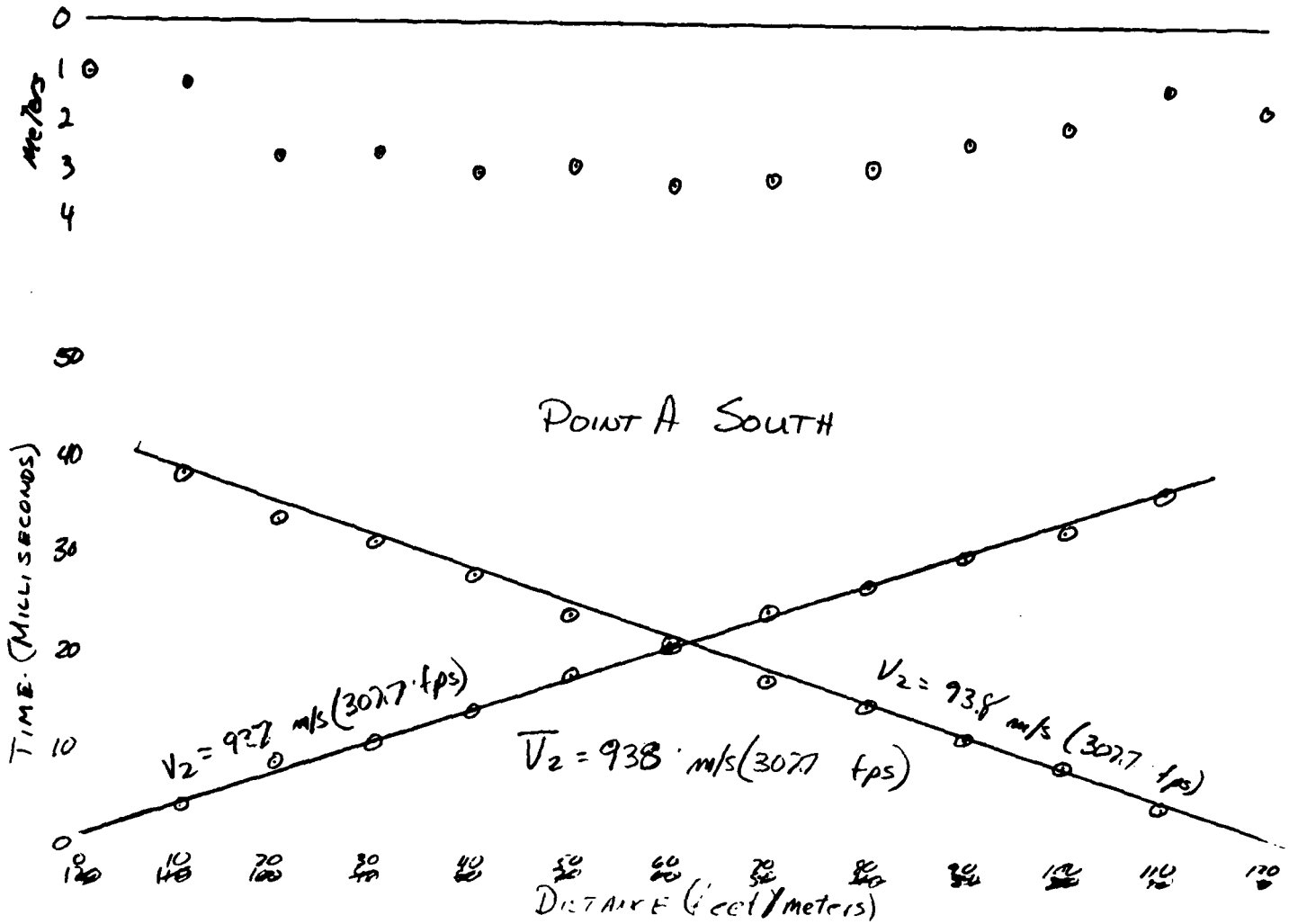
Meters
0
1
2
3
4
POINT A SOUTH
TIME (MILLISECONDS)
50
40
30
20
10
0
V_2 = 92.7 m/s (307.7 fps)
$\overline{V}_2$ = 93.8 m/s (307.7 fps)
V_2 = 93.8 m/s (307.7 fps)
0 10 20 30 40 50 60 70 80 90 100 110 120
0 10 20 30 40 50 60 70 80 90 100 110 120
DISTANCE (feet/meters)

Line A South

	1	2	3	4	5	6	7	8	9	10	11	12	13
X ← A	0	10	20	30	40	50	60	70	80	90	100	110	120
X ← B	120	110	100	90	80	70	60	50	40	30	20	10	0
T_{AP}	0	[illegible]	[illegible]	[illegible]	[illegible]	[illegible]	[illegible]	[illegible]	[illegible]	[illegible]	[illegible]	[illegible]	[illegible]
T_{BP}	[illegible]	[illegible]	[illegible]	[illegible]	[illegible]	[illegible]	[illegible]	[illegible]	[illegible]	[illegible]	[illegible]	[illegible]	[illegible]
$[T_{AP}+T_{BP}-T_{AB}]$		4,10	8,7	8,5	9,7	9,2	10,5	10,0	9,9	7,6	6,5	4,0	
T'_{AP}		4,5	9,2	11,3	14,7	18,4	21,8	25,0	27,6	30,7	33,3	37,5	
T'_{BP}		38,5	33,9	31,8	28,4	24,6	21,3	18,0	15,4	12,3	9,8	5,5	
h_p	ft / m	4,13 / 1,26	6,98 / 2,14	8,7 / 2,67	10,01 / 3,05	9,50 / 2,90	10,84 / 3,30	10,32 / 3,15	9,50 / 2,90	7,85 / 2,39	6,71 / 2,05	4,13 / 1,26	

$V_1 = \frac{5}{.0025} = 2000 fps\ (609.6 m/s)$

$V_1 = \frac{5}{.0035} = 1428.6 fps\ (435.4 m/s)$

$\bar{V}_1 = 1714.3 fps\ (522.5 m/s)$

$V_2 = \frac{50-10}{.010-.005} = 3076.9 fps\ (937.9 m/s)$

$V_2 = \frac{30-10}{.014-.006} = 3076.9 fps\ (937.9 m/s)$

$\bar{V}_2 = 3076.9 fps\ (937.9 m/s)$

$\sin \alpha_c = \frac{\bar{V}_1}{\bar{V}_2} = .5572$

$\alpha_c = 33.859°$

$t'_{AP} = .0016$

$t'_{BP} = .0026$

$h_A = \frac{\bar{V}_1 t_{AP}}{\cos \alpha_c} = \frac{3.3 ft}{(1.0 m)}$

$h_B = \frac{\bar{V}_1 t_{BP}}{\cos \alpha_c} = \frac{5.3 ft}{(1.64 m)}$

$h_p = \frac{\bar{V}_1}{2 \cos \alpha_c} [T_{AP} + T_{BP} - T_{AB}]$:

$\bar{T}_{AB} = 43.0$

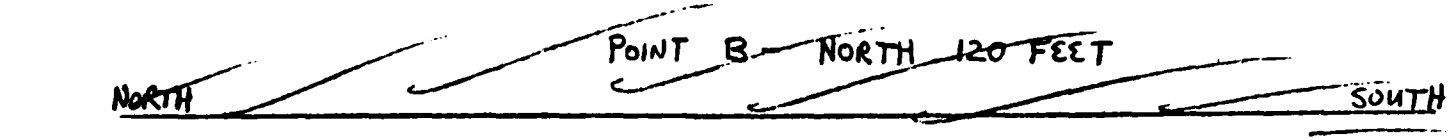
POINT B — NORTH 120 FEET
NORTH
SOUTH

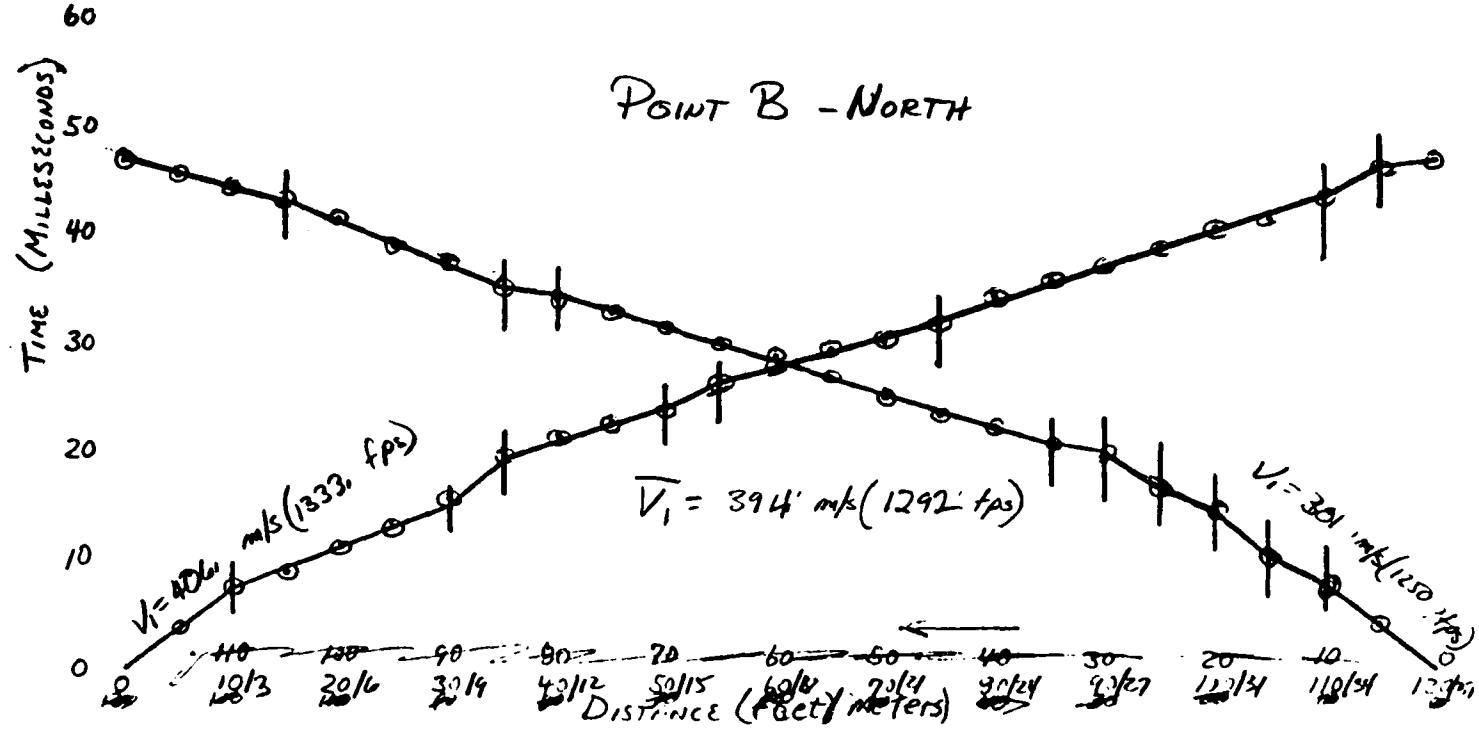
POINT B - NORTH
TIME (MILLISECONDS)
60
50
40
30
20
10
0
V_1 = 394 m/s (1292 fps)
V_1 = 406 m/s (1333 fps)
V_1 = 381 m/s (1250 fps)
DISTANCE (Feet/meters)

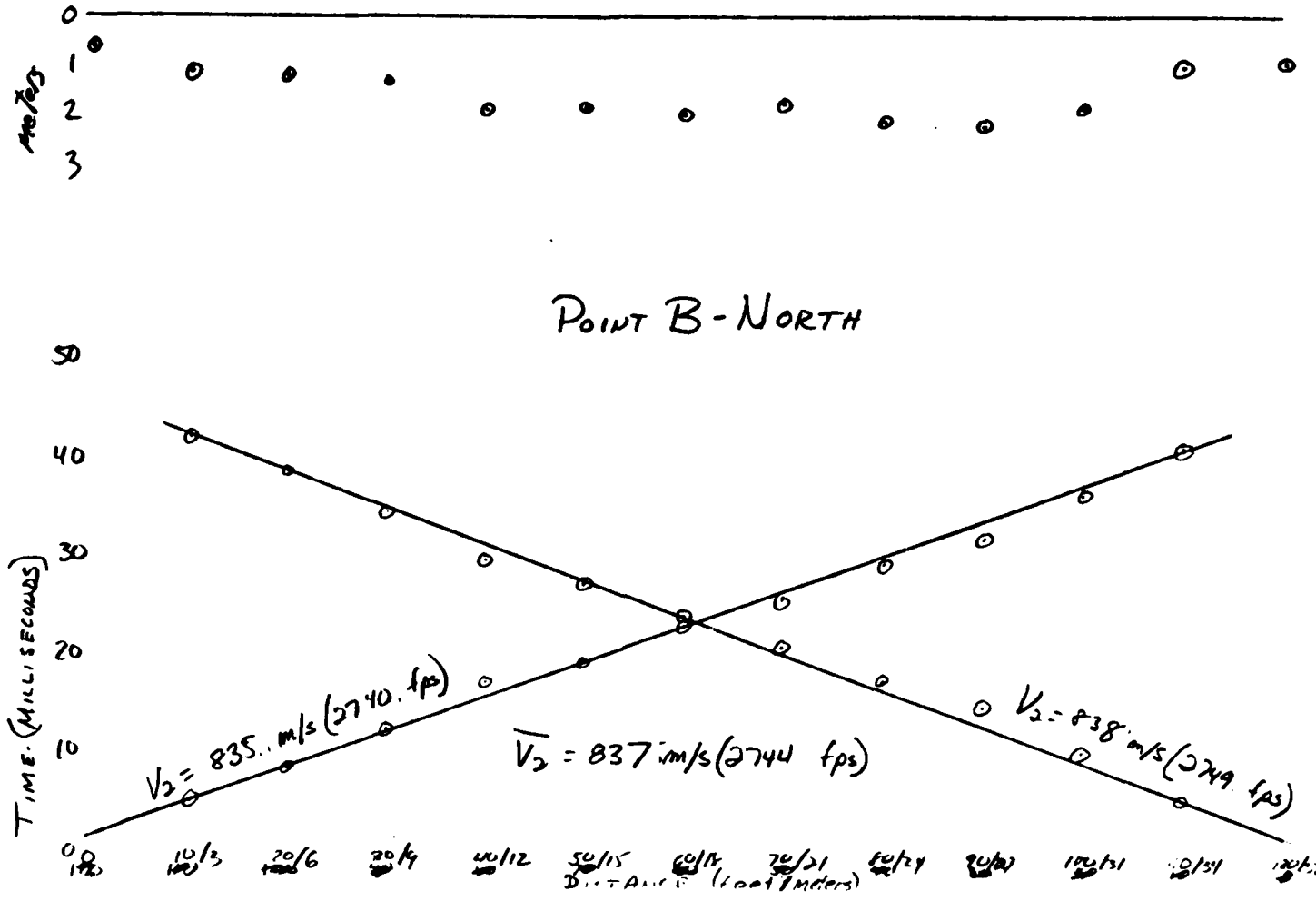
0
1
2
3
meters
POINT B - NORTH
50
40
30
20
10
0
TIME (MILLISECONDS)
V_2 = 835 m/s (2740 fps)
$\overline{V_2}$ = 837 m/s (2744 fps)
V_2 = 838 m/s (2749 fps)
10/3
20/6
30/9
40/12
50/15
60/18
70/21
80/24
90/27
100/31
110/34
120/37
DISTANCE (feet/meters)

PLOT DATA

	1	2	3	4	5	6	7	8	9	10	11	12	13
X → A	0	10	20	30	40	50	60	70	80	90	100	110	120
X → B	120	110	100	90	80	70	60	50	40	30	20	10	0
T_{AP}	0	7.5	11.0	15.T	21	23.7	27	30.0	33.0	37.0	40	43.0	47.0
T_{BP}	47.0	44.5	41.3	38.5	33.9	31.7	28.5	25.0	22.0	20.0	14.0	4.0	0
$[T_{AP}+T_{BP}-T_{AB}]$		5.0	5.3	6.0	5.4	8.2	9.0	8.0	9.5	10.0	8.0	4.5	
T'_{AP}		5.0	8.35	12.5	17.3	19.6	23.0	26.0	29.25	32.0	36.5	41.25	
T'_{BP}		42.0	38.65	34.5	29.7	27.4	24.0	21.0	17.75	15.0	10.5	5.75	
h_p	4T/m	3.66/1.12	3.88/1.18	4.39/1.34	6.13/1.87	6.00/1.83	6.59/2.01	5.86/1.79	6.95/2.12	7.32/2.23	5.86/1.79	3.29/1.00	

$V_1 = \frac{10}{.0075} = 1333.3 fps (406.4 m/s)$

$V_1 = \frac{10}{.0080} = 1250 fps (381.0 m/s)$

$\bar{V}_1 = 1291.7 fps (393.7 m/s)$

$V_2 = \frac{50-10}{.0196-.0050} = 2739.7 fps (835.1 m/s)$

$V_2 = \frac{50-10}{.0203-.0057} = 2749.1 fps (837.9 m/s)$

$\bar{V}_2 = 2744.4 fps (836.5 m/s)$

$\sin \alpha_c = \frac{\bar{V}_1}{\bar{V}_2} = .4707$

$\alpha_c = 28.078°$

$t'_{AP} = .0013$

$t'_{BP} = .0021$

$h_A = \frac{\bar{V}_1 t_{AP}}{\cos \alpha_c} = 1.90 ft \ (.58m)$

$h_B = \frac{\bar{V}_1 t_{BP}}{\cos \alpha_c} = 3.07 ft \ (.94m)$

$h_p = \frac{\bar{V}_1}{2 \cos \alpha_c} [T_{AP} + T_{BP} - T_{AB}] =$

$\bar{T}_{AB} = 47.0$

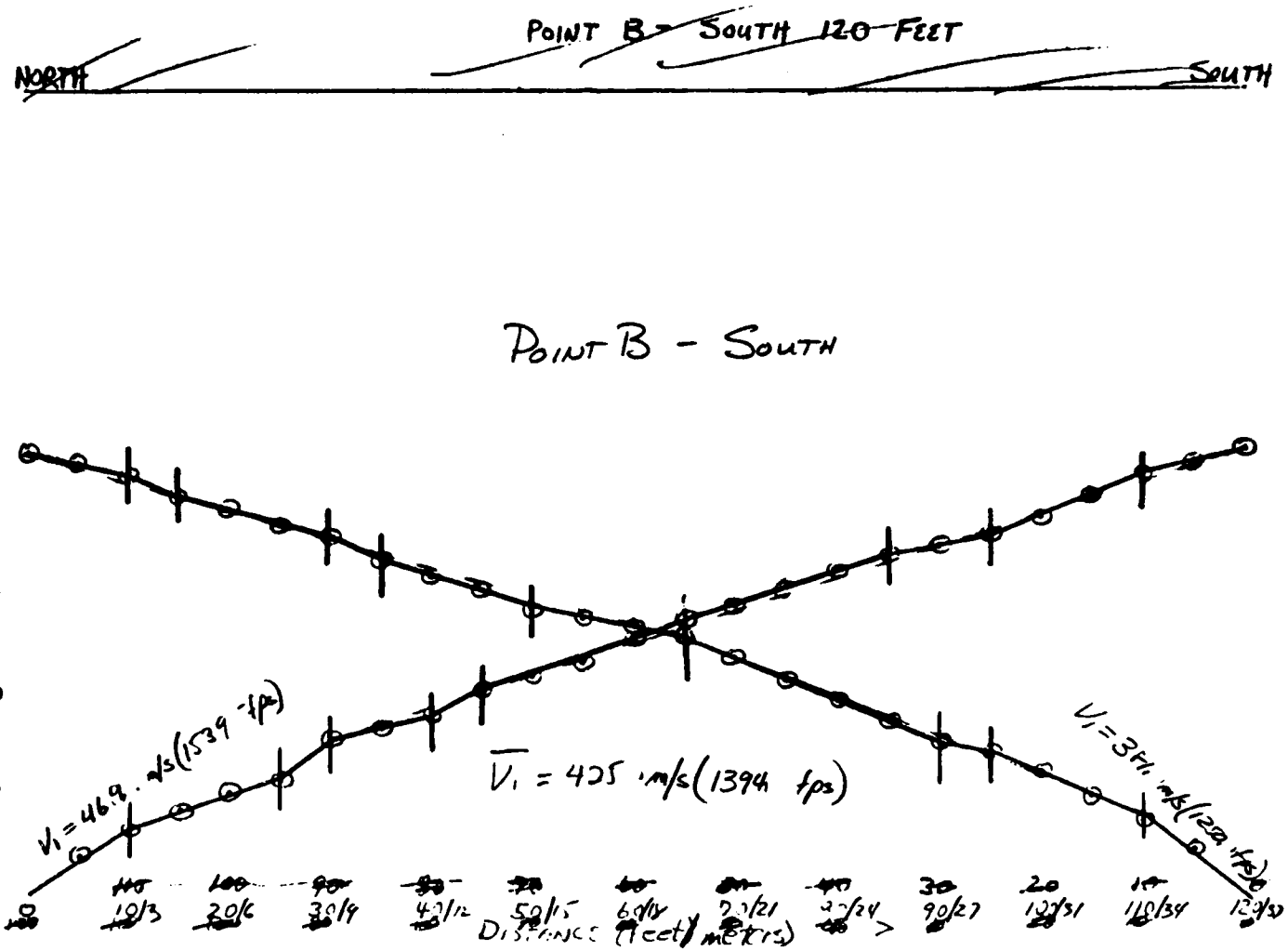
POINT B - SOUTH 120 FEET
NORTH
SOUTH
POINT B - SOUTH
TIME (MILLISECONDS)
60
50
40
30
20
10
0
V_1 = 469 m/s (1539 fps)
$\overline{V_1}$ = 425 m/s (1394 fps)
V_1 = 374 m/s (1228 fps)
10/3
20/6
30/9
40/12
50/15
60/18
70/21
80/24
90/27
100/31
110/34
120/37
DISTANCE (feet/meters)

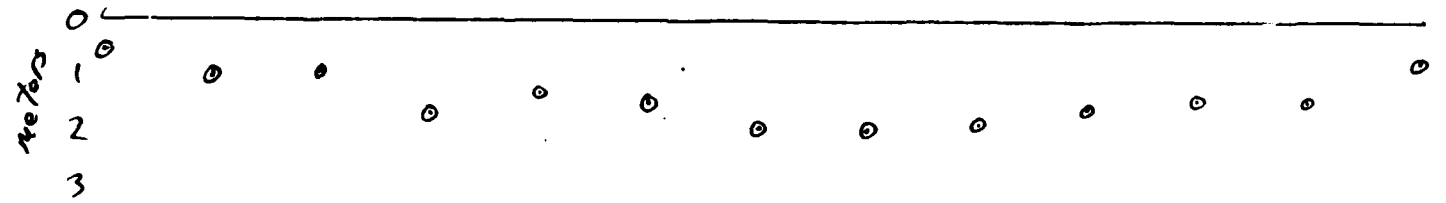

Point B - South

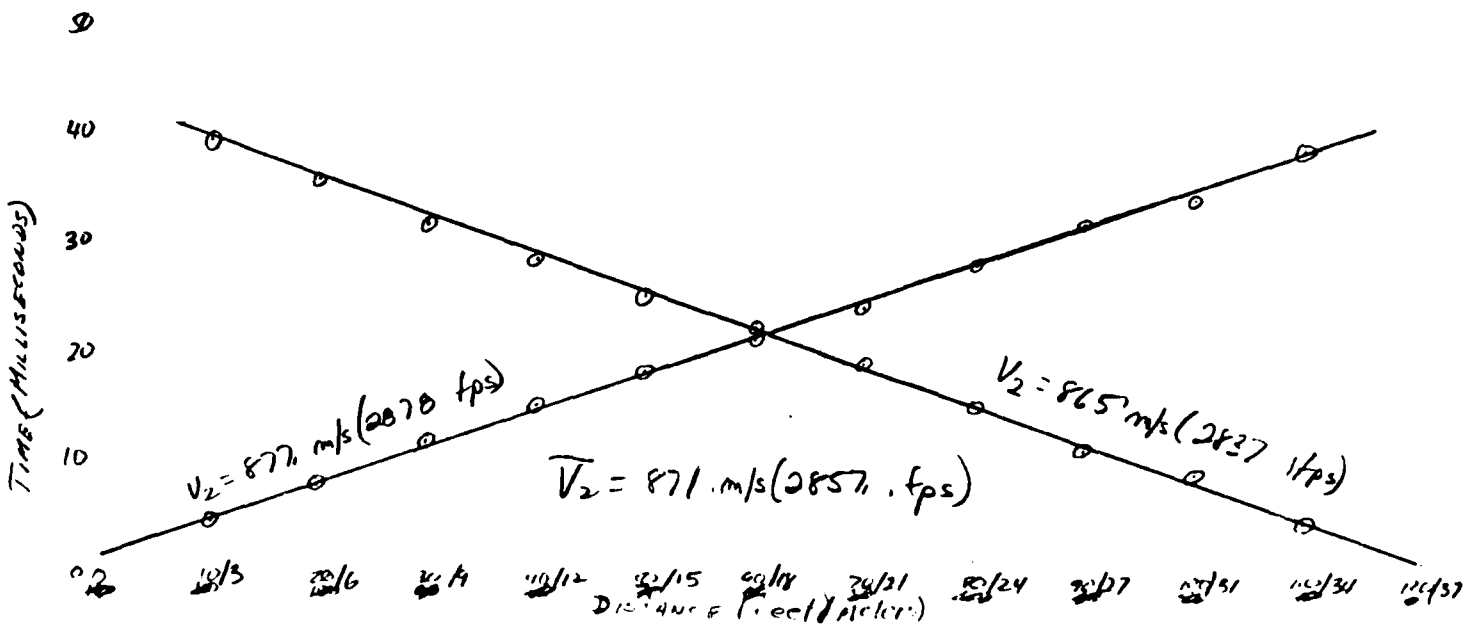

Pt B South

	0	10	20	30	40	50	60	70	80	90	100	110	120
	120	110	100	90	80	70	60	50	40	30	20	10	0
T_{AP}	0	6.5	10.0	15.5	18.0	21.7	25.5	28.7	32.3	35.5	37.5	40.0	44.0
T_{BP}	44.0	41.6	38.0	35.5	31.5	28.5	26.7	23.5	19.5	15.0	12.3	8.0	0
$[T_{AP}+T_{BP}-T_{AB}]$		4.1	4.0	7.0	5.5	6.3	8.2	8.2	7.8	6.5	5.8	6.0	
T'_{AP}		4.45	8.0	12.0	15.25	18.6	21.4	24.6	28.4	32.25	34.6	39.0	
T'_{BP}		39.55	36.0	32.0	28.75	25.4	22.6	19.4	15.6	11.75	9.4	5.0	
h_p ft/m		3.28/1.00	3.20/.97	5.59/1.70	4.39/1.34	4.95/1.51	6.55/2.00	6.55/2.00	6.23/1.90	5.19/1.58	4.63/1.41	4.79/1.46	

$V_1 = \frac{10}{.0065} = 1538.5$ fps (468.9 m/s)

$V_1 = \frac{10}{.0080} = 1250$ fps (381.0 m/s)

$\overline{V_1} = 1394.3$ fps (425.0 m/s)

$V_2 = \frac{50-10}{.0185-.0046} = 2877.7$ fps (877.1 m/s)

$V_2 = \frac{50-10}{.0192-.0051} = 2836.9$ fps (864.7 m/s)

$\overline{V_2}$ 2857.3 fps (870.9 m/s)

$\sin \alpha_c = \frac{\overline{V_1}}{\overline{V_2}} = .4880$

$\alpha_c = 29.208°$

$t'_{AP} = .0011$

$t'_{BP} = .0016$

$h_A = \frac{\overline{V_1}\, t'_{ap}}{\cos \alpha_c} = 1.76$ ft (.54 m)

$h_B = \frac{V_1\, t_{BP}}{\cos \alpha_c} = 2.56$ ft (.78 m)

h_p

$T_{AB} = 44.0$

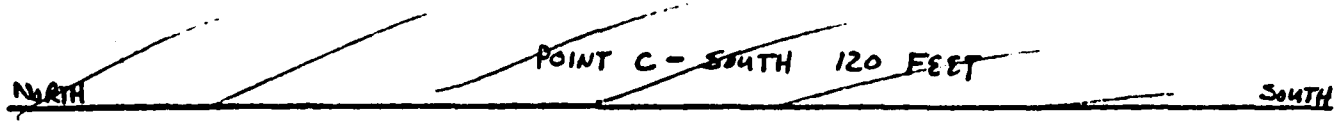
POINT C - SOUTH 120 FEET
NORTH
SOUTH

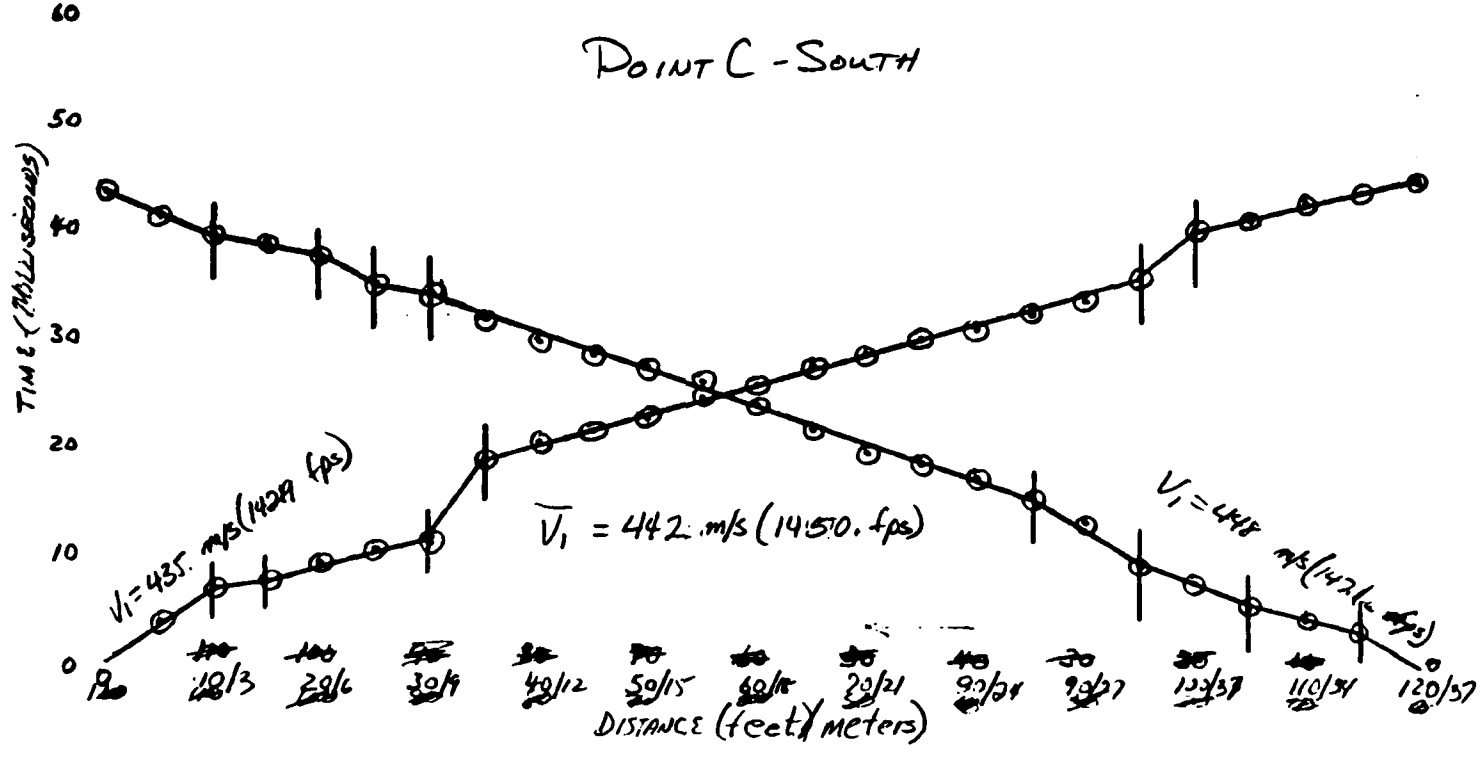
POINT C - SOUTH
TIME (MILLISECONDS)
60
50
40
30
20
10
0
V_1 = 435. m/s (1429 fps)
$\overline{V_1}$ = 442. m/s (1450. fps)
V_1 = 448 m/s (1471 fps)
10/3
20/6
30/9
40/12
50/15
60/18
70/21
80/24
90/27
100/30
110/34
120/37
DISTANCE (feet/meters)

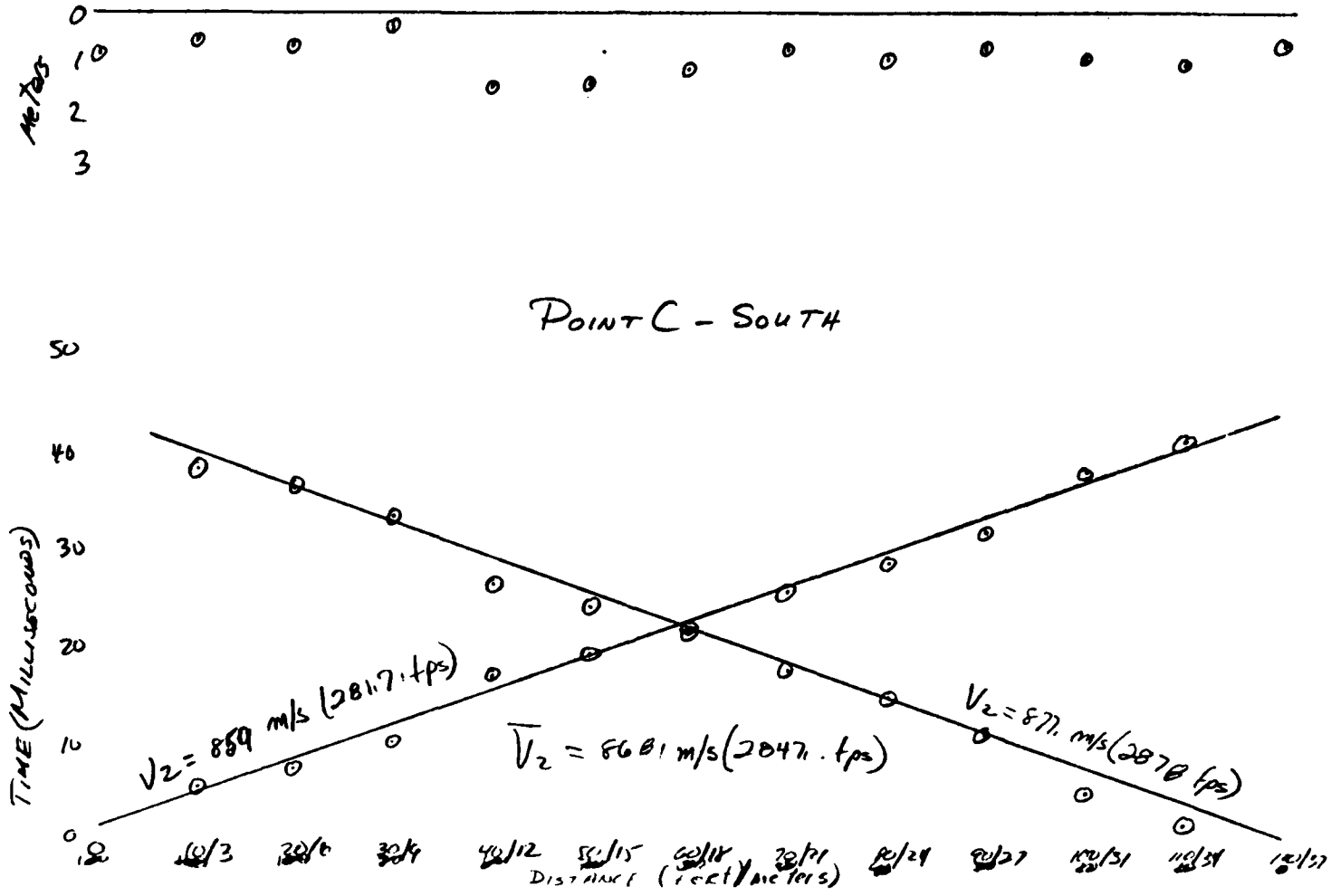
0
1
2
3
Meters
Point C - South
50
40
30
20
10
0
Time (Milliseconds)
V_2 = 889 m/s (2811.7 fps)
$\overline{V}_2$ = 8681 m/s (2847.1 fps)
V_2 = 877 m/s (2878 fps)
Distance (feet/meters)

H. C. [illegible]

	0	10	20	30	40	50	60	70	80	90	100	110	120
	120	110	100	90	80	70	60	50	40	30	20	10	0
T_{AP}	0	7.0	9.0	11.0	20.2	22.5	24.5	27.5	30.5	33.[illegible]	40.0	43.5	44.[illegible]
T_{BP}	45.5	39.2	37.[illegible]	34.0	29.2	[illegible]	[illegible]	[illegible]	[illegible]	[illegible]	[illegible]	[illegible]	[illegible]
$[T_{AP}+T_{BP}-T_{AB}]$		2.2	2.5	1.0	5.8	5.5	4.5	3.0	3.8	2.7	3.7	4.0	
T'_{AP}		5.9	7.75	10.5	17.3	19.75	22.25	26.0	28.9	32.15	38.15	41.5	
T'_{BP}		38.1	36.25	33.5	26.7	24.25	21.75	18.0	15.1	11.85	5.85	2.5	
h_p ft/m		1.85/.57	2.11/.64	.84/.26	4.88/1.49	4.63/1.41	3.79/1.16	2.53/.77	3.20/.98	2.27/.69	3.12/.95	3.37/1.03	

$V_1 = \frac{10}{.007} = 1428.6$ fps (435.4 m/s)

$\underline{V}_1 = \frac{5}{.0034} = 1470.6$ fps (448.2 m/s)

$\bar{V}_1 = 1449.6$ fps (441.8 m/s)

$V_2 = \frac{50-10}{.0145-.0053} = 2816.9$ fps (858.6 m/s)

$\underline{V}_2 = \frac{50-10}{.0189-.005} = 2877.7$ fps (877.1 m/s)

$\bar{V}_2 = 2847.3$ fps (867.9 m/s)

$\sin\alpha_c = .5091$

$\alpha_c = 30.605°$

$t'_{AP} = .0016$

$t'_{BP} = .0012$

$h_A = 2.70$ ft (.82 m)

$h_B = 2.02$ ft (.62 m)

$\bar{T}_{AB}$ 44.0

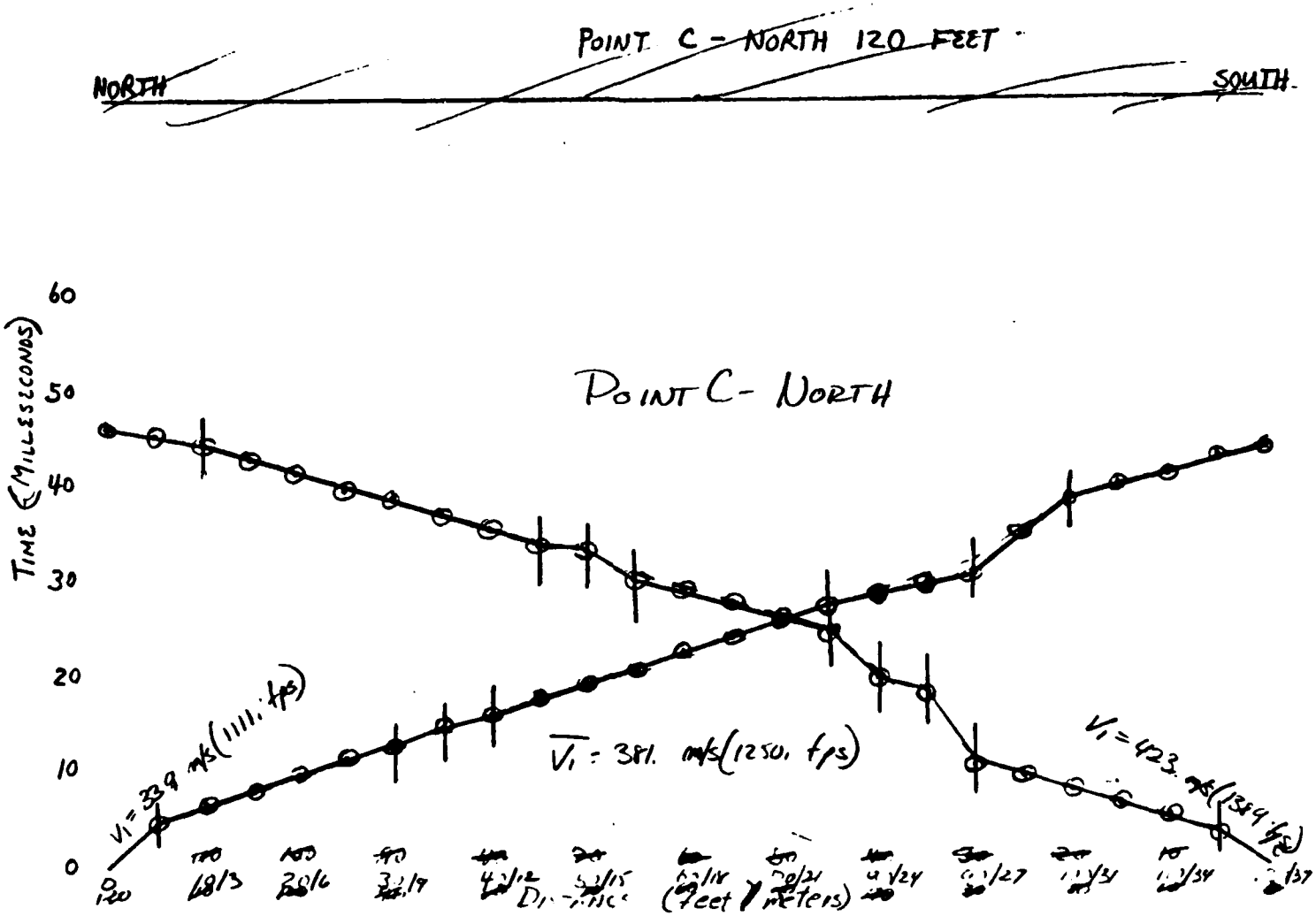
POINT C - NORTH 120 FEET
NORTH
SOUTH
POINT C - NORTH
TIME (MILLISECONDS)
60
50
40
30
20
10
0
V_1 = 339 m/s (1111. f/s)
$\overline{V_1}$ = 381. m/s (1250. f/s)
V_1 = 423. m/s (1389. f/s)
(Feet / meters)

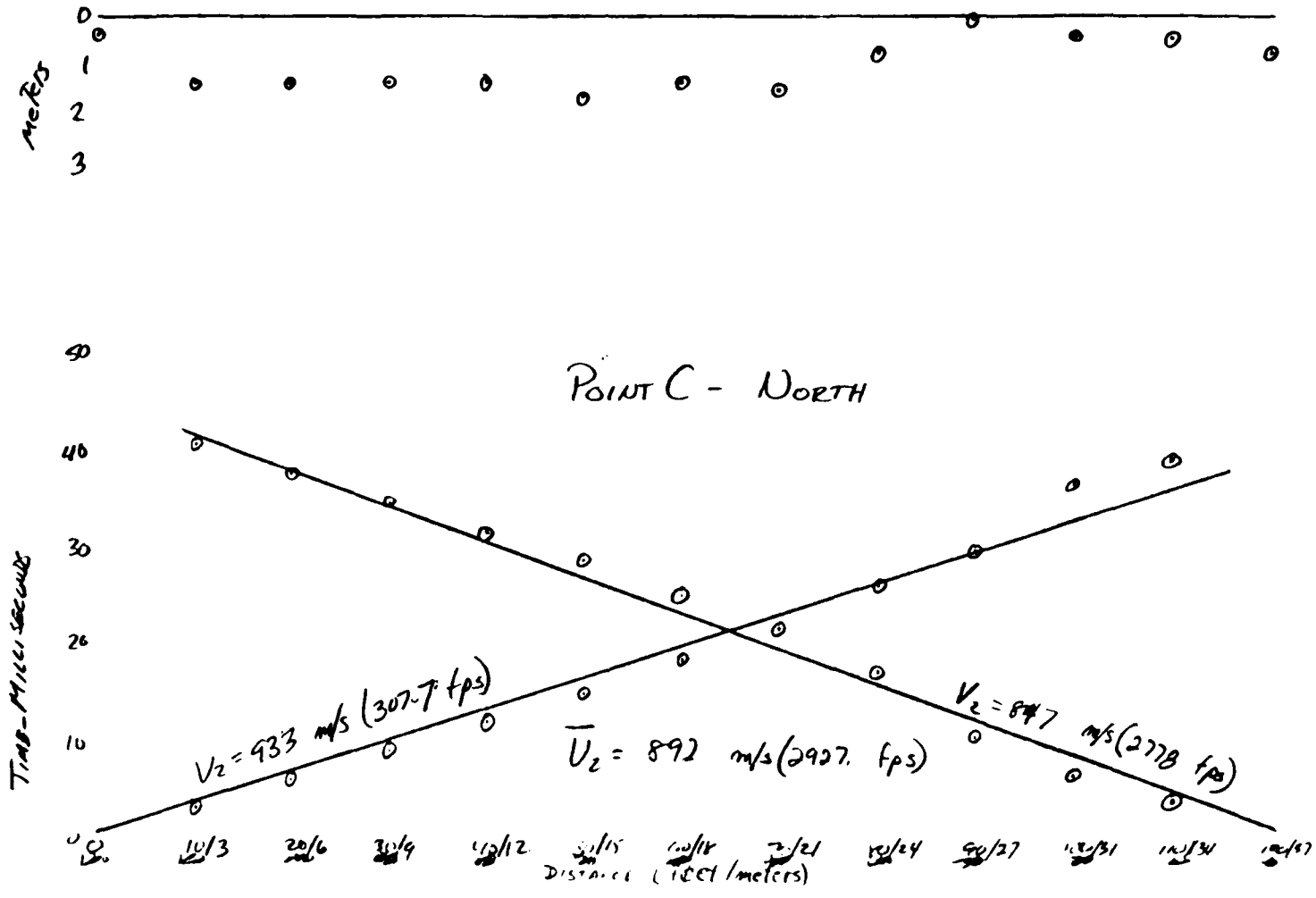

Point C - North
Meters
0
1
2
3
Time-Milliseconds
50
40
30
20
10
0
V_2 = 933 m/s (307.7 fps)
$\overline{V}_2$ = 892 m/s (2927. fps)
V_2 = 847 m/s (2778 fps)
10/3
20/6
30/9
40/12
50/15
60/18
70/21
80/24
90/27
100/31
110/34
120/37
Distance (feet/meters)

	0	10	20	30	40	50	60	70	80	90	100	110	120
	120	110	100	90	80	70	60	50	40	30	20	10	0
T_{AP}	0	6.5	9.5	12.5	17.6	13.9	22.0	[illegible]	28.0	33.0	38.0	42.6	47.5
T_{BD}	45.5	41.0	41.0	33.0	35.0	32.3	23.5	[illegible]	12.5	11.0	6.0	[illegible]	0
$[T_{AP}+T_{BP}-T_{AB}]$		6.5	6.5	6.5	6.6	7.7	6.5	7.0	3.5	–	2.0	2.1	
T'_{AP}		3.25	6.25	9.25	12.3	15.05	18.75	22.0	26.25	30.0	37.0	39.55	
T'_{BP}		40.75	37.75	34.75	31.7	28.95	25.25	22.0	17.75	11.0	7.0	4.45	
h_p ft/m		4.44/1.37	4.44/1.37	4.49/1.37	4.56/1.39	5.32/1.62	4.49/1.37	4.84/1.48	2.42/.74	0/0	1.38/.42	1.45/.44	

$V_1 = \frac{5}{.0045} = 1111.1 fps (338.7 m/s)$ $\quad \sin \alpha_c = .4270$

$V_1 = \frac{5}{.0036} = 1388.9 fps (423.3 m/s)$ $\quad \alpha_c = 25.277°$

$\bar{V}_1 = 1250 fps$ (381 m/s) $\quad t'_{ap} = .0008$

$V_2 = \frac{50-10}{.017-.004} = 3076.9 fps (937.9 m/s)$ $\quad t'_{Bp} = .0010$

$V_2 = \frac{50-10}{.0144-.0054} = 2777.8 fps (846.7 m/s)$ $\quad h_A = 1.11 ft (.34 m)$

$\bar{V}_2 = 2927.4 fps (892.3 m/s)$ $\quad h_B = 2.44 ft (.76 m)$

$\bar{T}_{AB}$ 44.0

⊙ D NORTH - PLATE NORTH END
△ D NORTH - PLATE SOUTH END

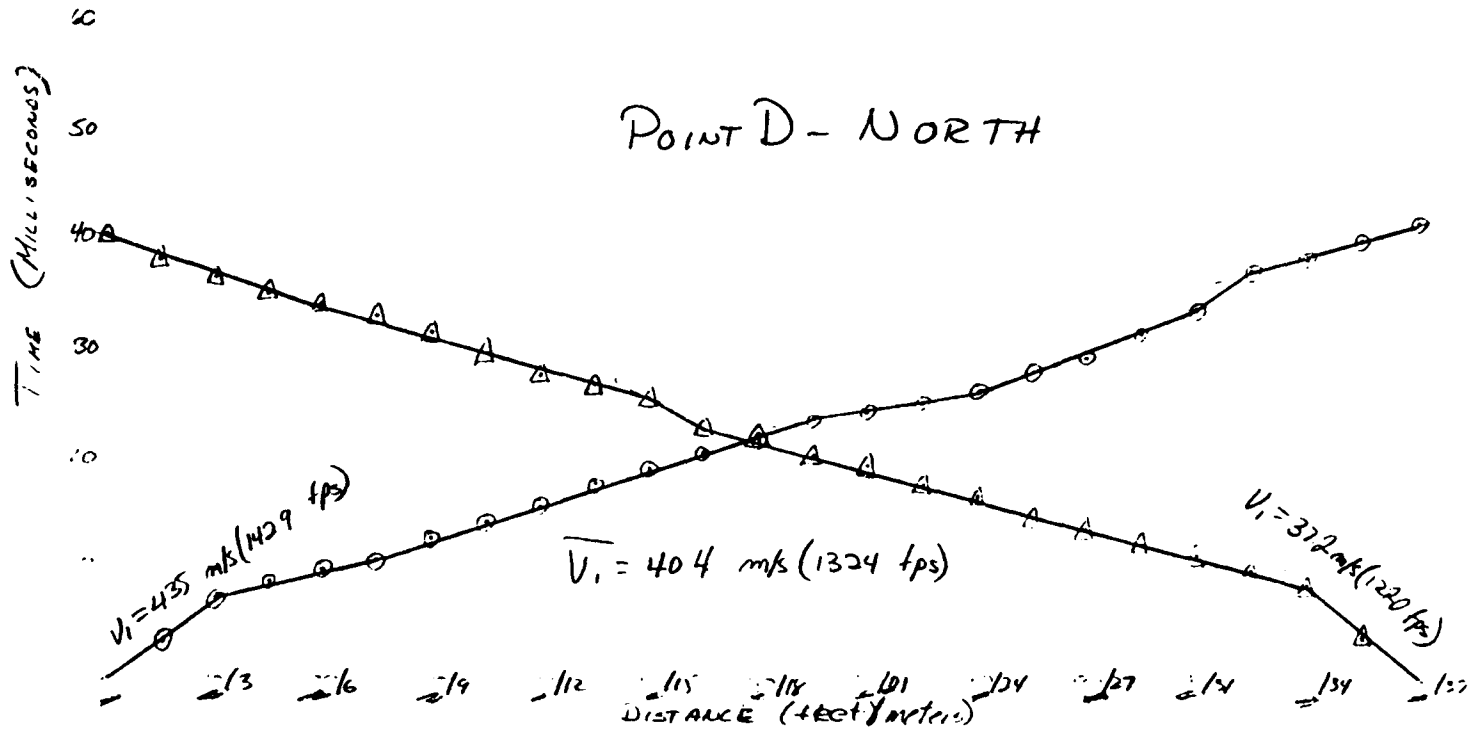

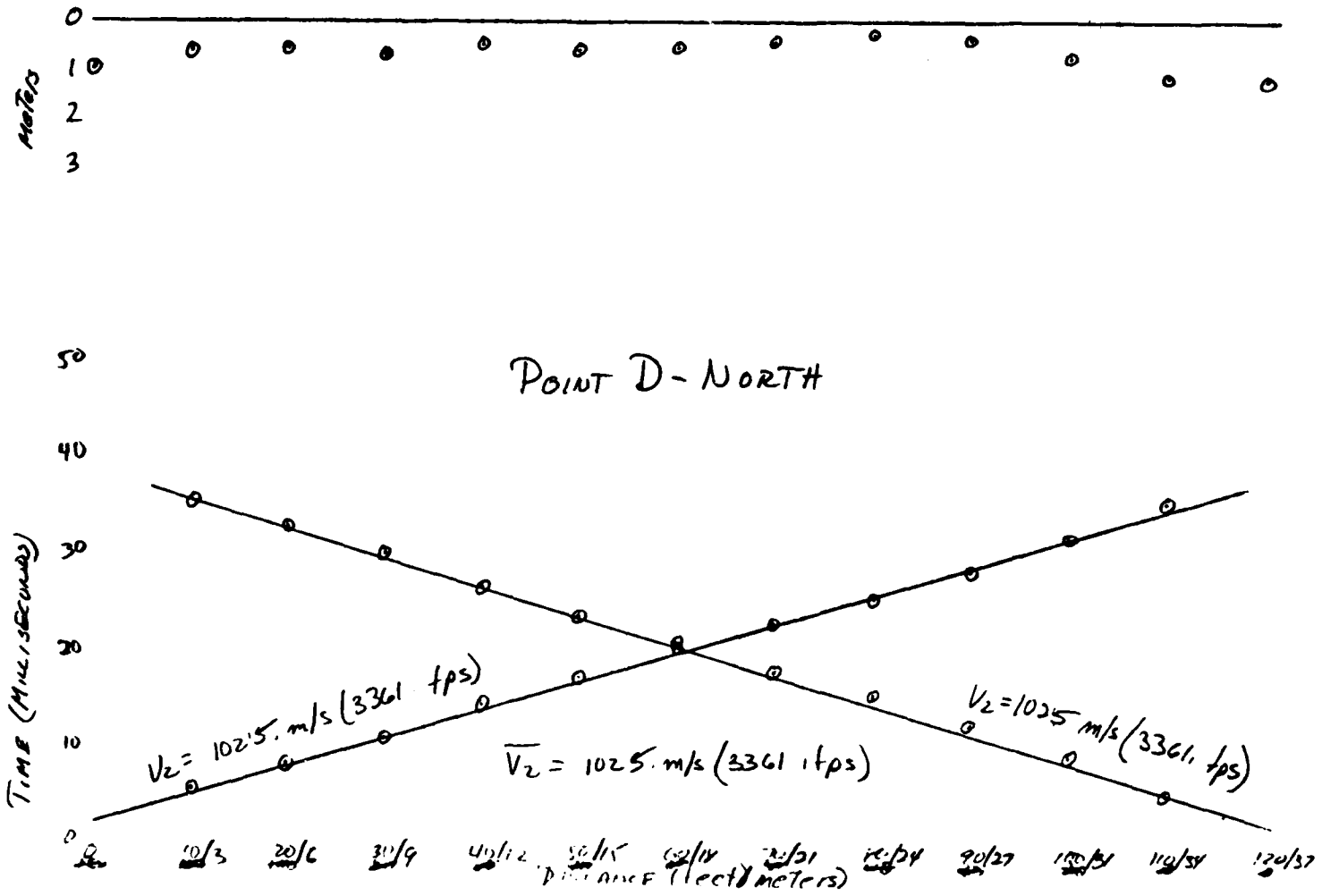
Meters
0
1
2
3
POINT D - NORTH
TIME (MILLISECONDS)
50
40
30
20
10
0
V_2 = 1025. m/s (3361 fps)
$\overline{V_2}$ = 1025. m/s (3361. fps)
V_2 = 1025 m/s (3361. fps)
10/3
20/6
30/9
40/12
50/15
60/18
70/21
80/24
90/27
100/30
110/34
120/37
DISTANCE (Feet/Meters)

	0	10	20										
	120												
T_{AP}	0	7.0	9.5		15.5	18.1	21.5	24.0	26.0	28.0	33.5	38.0	41.0
T_{BD}	42.5	36.5	33.1										0
$[T_{AP}+T_{BD}-T_{AB}]$		2.5	2.4	3.0	2.0	2.7	2.5	2.0	1.2	1.5	3.5	5.2	
T'_{AP}		5.75	8.3	11.0	14.5	17.35	20.25	23.0	25.4	28.25	31.75	35.4	
T'_{BD}		35.25	32.7	30.0	26.5	23.65	20.75	18.0	15.6	12.75	9.25	5.6	
Δp ft/in		1.80/1.55	1.73/1.53	2.16/1.66	1.44/1.44	1.45/1.59	1.80/1.55	1.41/1.41	.86/.26	1.08/1.33	2.52/1.77	3.75/1.14	

$V_1 = \frac{10}{.007} = 1428.6$ fps (435.4 m/s)

$V_2 = \frac{10}{.00862} = 1219.5$ fps (371.7 m/s)

$\bar{V}_1 = 1324.1$ fps (403.6 m/s)

$V_2 = \frac{50-10}{.0117-.0051} = 3361.4$ fps (1024.5 m/s)

$V_2 = \frac{50-10}{.0118-.0056} = 3361.4$ fps (1024.5 m/s)

$\bar{V}_2 = 3361.4$ fps (1024.5 m/s)

$\sin \alpha_c = .3939$

$\alpha_c = 23.198°$

$t'_{AP} = .0021$

$t'_{BD} = .0025$

$l_A = 3.031$ ft (.92 m)

$l_B = 3.604$ ft (1.10 m)

$\bar{T}_{AB}$ 41.0

⊙ D SOUTH - PLATE NORTH END
△ D SOUTH - PLATE SOUTH END

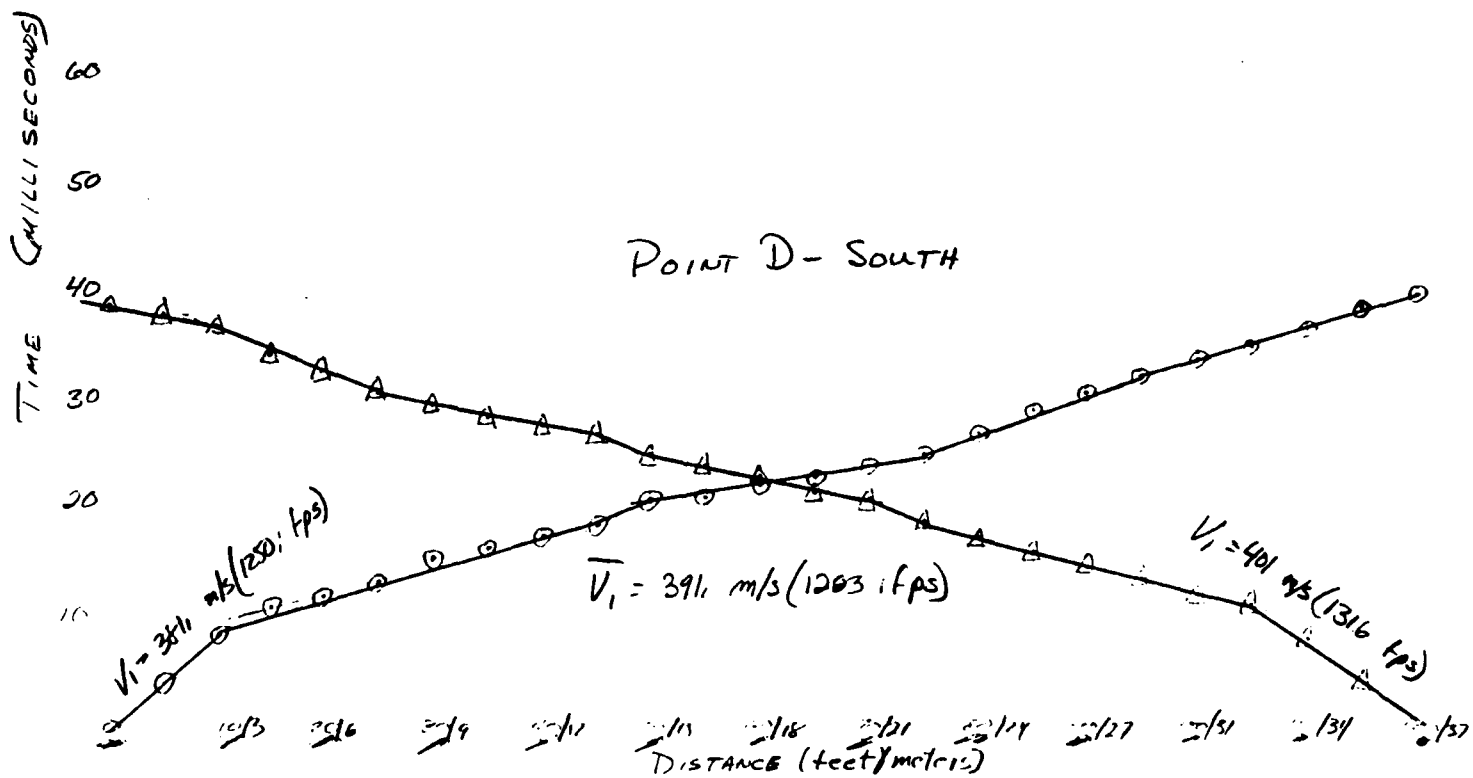

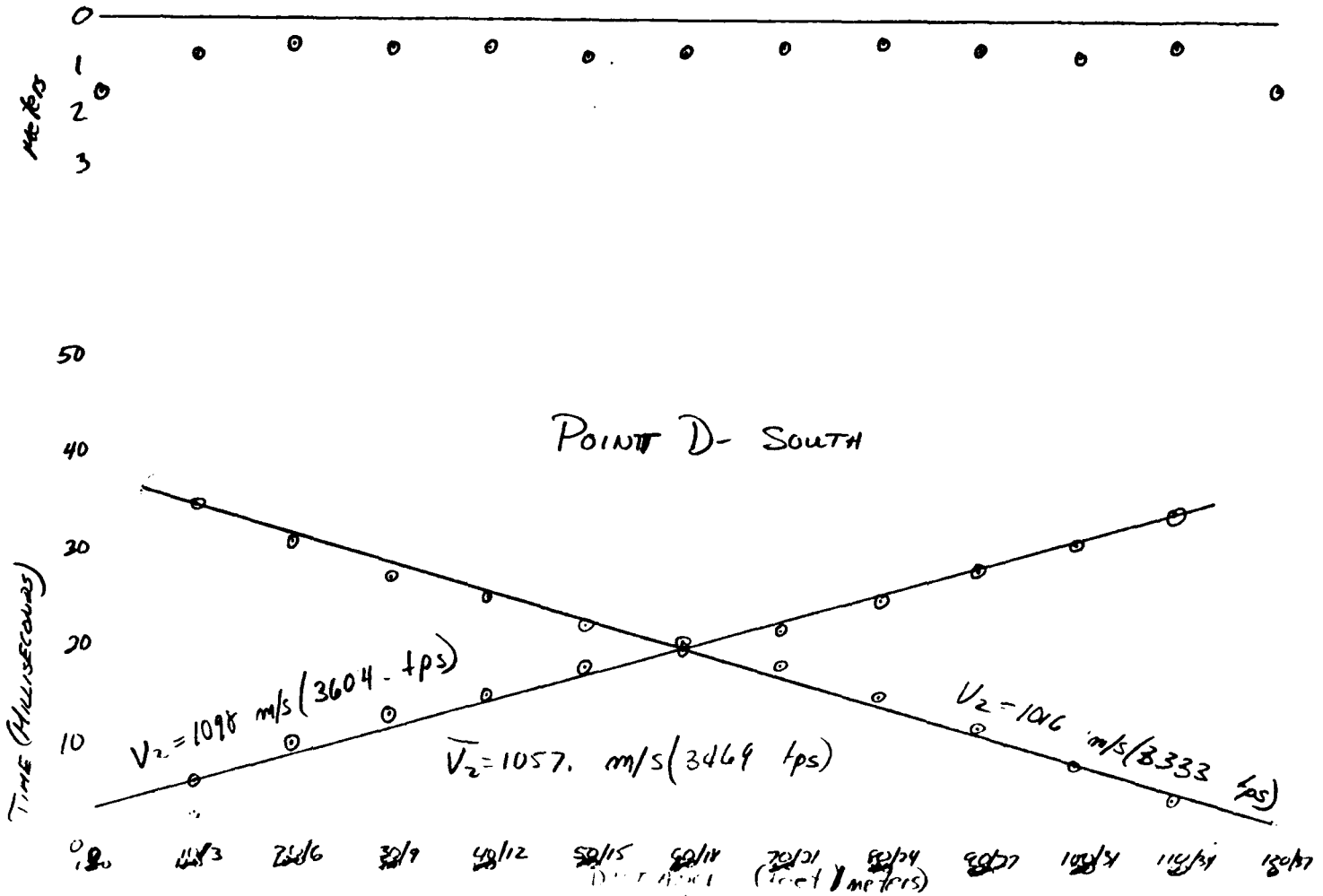
0
1
2
3
50
40
30
20
10
TIME (MILLISECONDS)
POINT D- SOUTH
$V_2 = 1098$ m/s (3604 fps)
$\bar{V}_2 = 1057.$ m/s (3469 fps)
$V_2 = 1016$ m/s (8333 fps)

Pt 2 Source

	0 / 120	10 / 110	20 / 100	30 / [illegible]	[illegible] / [illegible]	[illegible] / [illegible]	60 / 60	70 / [illegible]	80 / [illegible]	90 / 30	100 / 20	110 / 10	120 / 0
T_{AP}	0	8.0	11.5	15.0	17.0	20.2	21.7	[illegible]	[illegible]	30.0	[illegible]	[illegible]	[illegible]
T_{BP}	43.5	36.5	32.3	29.0	[illegible]	[illegible]	22.5	20.2	[illegible]	14.0	[illegible]	[illegible]	0
$[T_{AP}+T_{BP}-T_{AB}]$		3.25	2.55	2.75	2.75	3.45	2.95	2.45	1.95	2.75	3.25	2.15	
T'_{AP}		6.38	10.23	13.63	15.63	18.48	20.23	22.28	25.53	28.63	31.38	34.83	
T'_{BP}		34.88	31.03	27.63	25.63	22.78	21.03	18.98	15.73	12.63	9.88	6.43	
h_p ft/m		2.24 / .68	1.76 / .54	1.90 / .58	1.90 / .58	2.38 / .73	2.04 / .62	1.69 / .52	1.35 / .41	1.90 / .58	2.24 / .68	1.48 / .45	

$V_1 = \frac{10}{.008} = 1250$ fps (381.0 m/s)

$V_1 = \frac{10}{.0076} = 1315.8$ fps (401.1 m/s)

$\bar{V}_1 = 1282.9$ fps (391.0 m/s)

$V_2 = \frac{50-10}{.0076-.0056} = 3603.6$ fps (1098.4 m/s)

$V_2 = \frac{50-10}{.0076-.0056} = 3333.3$ fps (1016.0 m/s)

$\bar{V}_2 = 3468.5$ fps (1057.2 m/s)

$\sin \alpha_c = .3699$

$\alpha_c = 21.708°$

$t'_{AP} = .0035$

$t'_{BP} = .0033$

$h_A = 4.83$ ft (1.47 m)

$h_B = 4.56$ ft (1.39 m)

$\bar{T}_{AB} = 41.25$

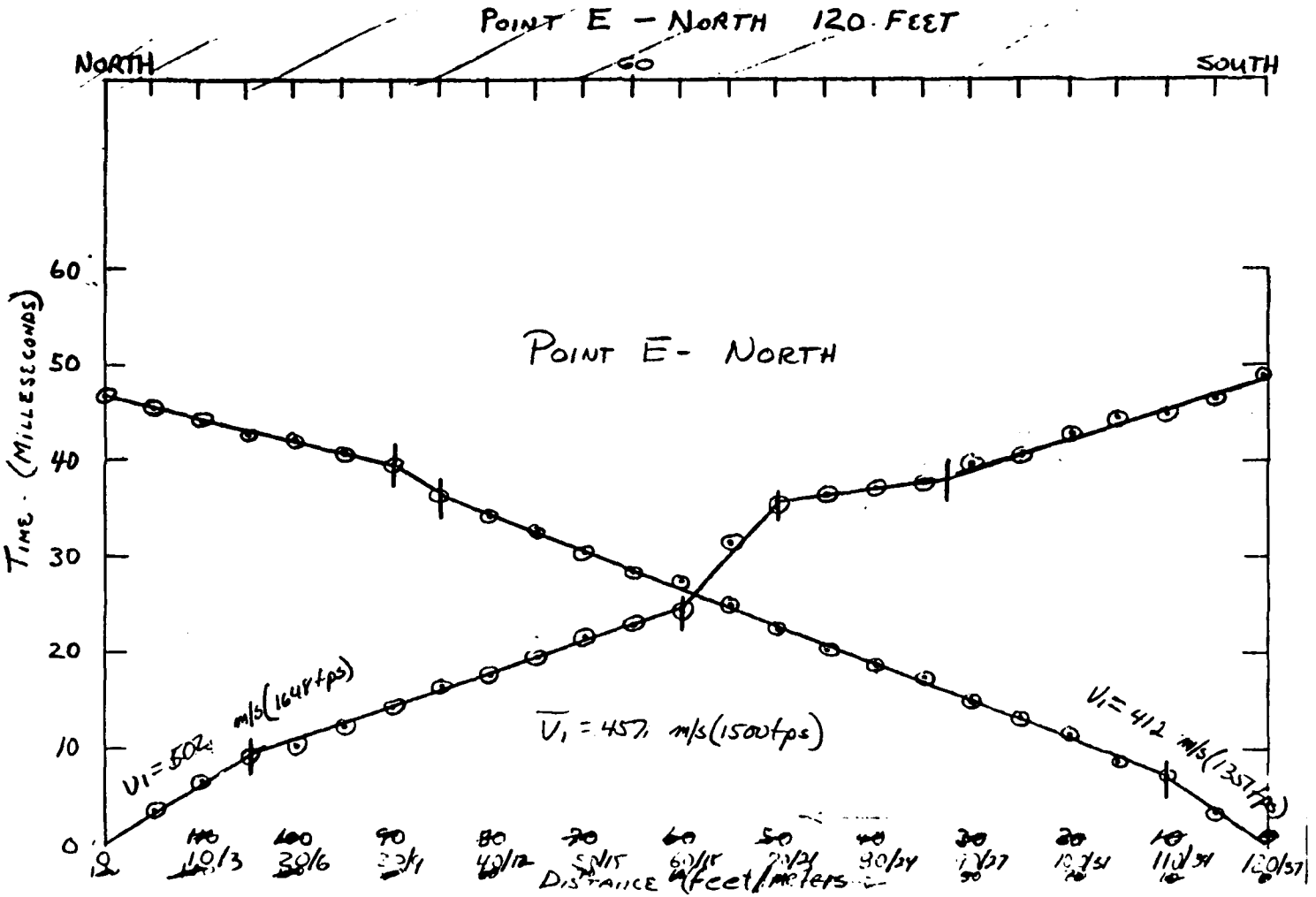
POINT E - NORTH 120 FEET
NORTH
60
SOUTH
POINT E- NORTH
TIME - (MILLISECONDS)
60
50
40
30
20
10
0
V1= 502 m/s(1648 fps)
$\overline{V_1}$ = 457 m/s(1500 fps)
V1= 412 m/s(1357 fps)
DISTANCE (feet/meters)

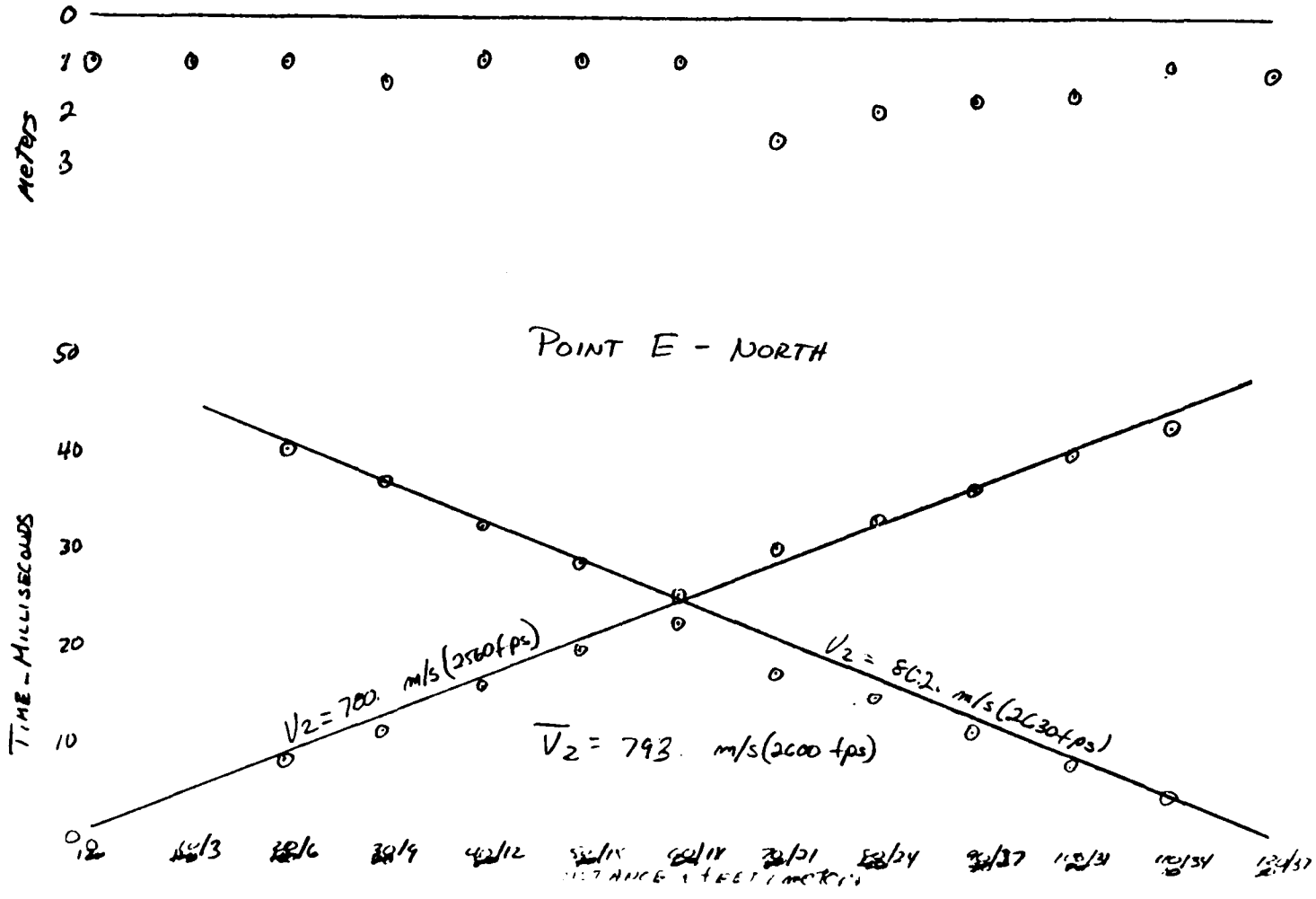
POINT E - NORTH
METERS
0
1
2
3
TIME - MILLISECONDS
50
40
30
20
10
0
V_2 = 700. m/s (2560 fps)
V_2 = 802. m/s (2630 fps)
$\overline{V}_2$ = 793. m/s (2600 fps)

POINT E - NORTH 120 FEET

$X_A \rightarrow$	0	5	10	15	20	25	30	35	40	45	50	55	60
$\leftarrow X_B$	120	115	110	105	100	95	90	85	80	75	70	65	60
T_{AP}	0	3.5	6.7	9.1	10.3	12.5	14.2	16.5	17.8	19.1	21.5	23.0	24.5
T_{BP}	47.0	45.5	44.2	42.8	42.0	40.6	39.5	36.5	34.2	32.5	30.5	28.5	27.5
(49) T'_{AP}				7.65	8.65	10.45	11.85	14.5	16.3	17.8	20.0	21.75	23.0
(47) T'_{AP}				6.65	7.65	9.45	10.85	13.5	15.3	16.8	19.0	20.75	22.0
(49) T'_{BP}				41.35	40.35	38.55	37.15	34.5	32.7	31.2	29.0	27.25	26.0
(49) h_p ft				2.7	3.0	3.8	4.3	3.7	2.8	2.4	2.8	2.3	2.8
(47) m				.82	.91	1.16	1.31	1.13	.85	.73	.85	.70	.85

$V_1 = \frac{15}{.0091} = 1648$ fps (502.31 m/s)

$V_1 = \frac{10}{.0074} = 1351$ (411.8 m/s)

$\overline{V_1} = 1,500$ fps (457.2 m/s)

$V_2 = 2560$ fps (780.3 m/s)

$V_2 = 2630$ fps (

$\sin \alpha_c = \frac{1,500}{2,000}$

$\alpha_c = 35.234°$

$h_p = \frac{V_1}{2 \cos \alpha_c} [T_{AP} + T_{BP} - T_{AB}]$

$h_p = \frac{1,500}{2 \cos 35.234} [T_{AP} + T_{BP} - T_{AB}]$ (913.21)

$h_A = \frac{1,500 (.0015)}{\cos 35.234} = 2.8$ (.85 m)

$h_B = \frac{1,500 (.0016)}{\cos 35.234} = 3.5$ (1.07 m)

POINT E - NORTH 120 FEET

XA →	65	70	75	80	85	90	95	100	105	110	115	120
← XB	55	50	45	40	35	30	25	20	15	10	5	0
T_{AP}	31.4	35.6	36.0	37.0	37.8	39.9	40.5	43.0	44.0	45.0	46.6	49.0
T_{BP}	25.0	22.5	20.5	18.5	17.5	15.0	13.2	11.5	8.9	7.4	3.8	0
(49) T'_{AP}	27.7	31.0	32.35	33.0	34.65	36.95	38.15	40.25	42.35	43.3		
(47) T'_{AO}	26.7	30.0	31.35	32.6	33.85	35.95	37.15	39.35	41.35	42.3		
(49) T'_{BP}	21.3	18.0	16.65	15.4	14.95	12.05	10.35	8.75	6.65	5.7		
(49) h_A (ft)	6.8	6.3	6.7	6.2	5.8	5.4	4.3	5.1	4.1	3.1		
(m)	2.07	2.53	2.04	1.89	1.77	1.65	1.31	1.55	1.25	.95		

POINT E - SOUTH 120 FEET

NORTH SOUTH

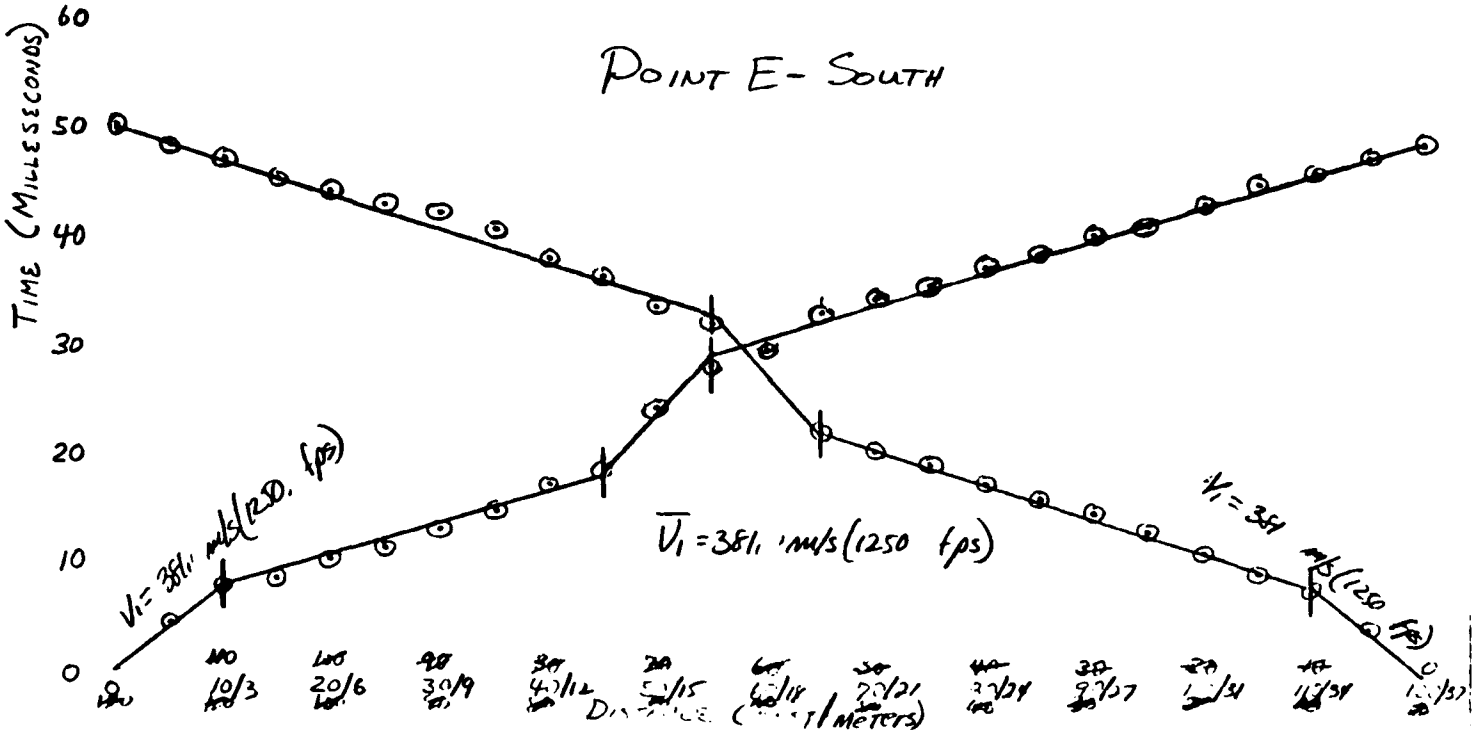

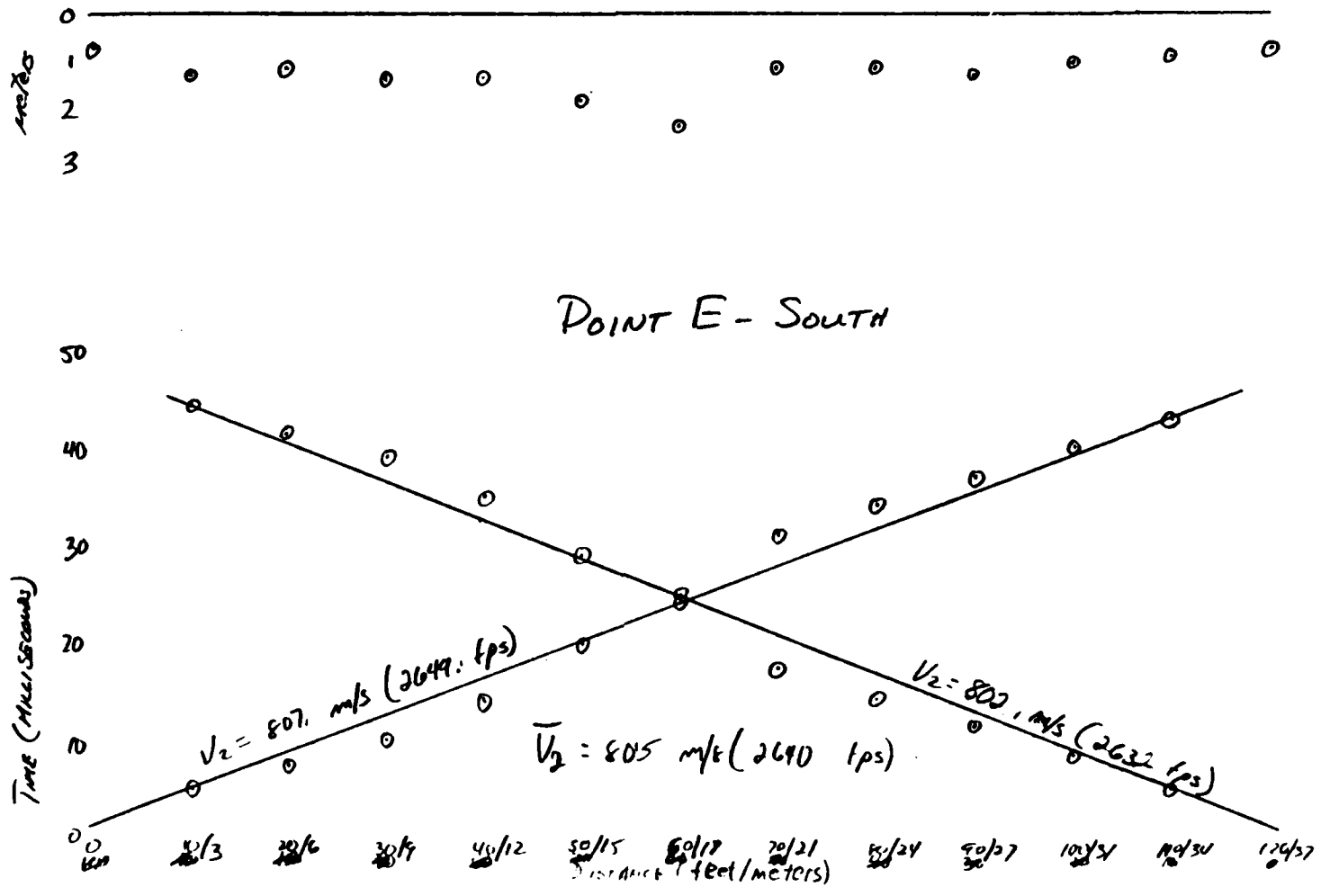
0
1
2
3
meters
POINT E - SOUTH
50
40
30
20
10
0
TIME (MILLISECONDS)
V_2 = 807 m/s (2649 fps)
V_2 = 802 m/s (2632 fps)
$\bar{V}_2$ = 805 m/s (2640 fps)
0 km
10/3
20/6
30/9
40/12
50/15
60/18
70/21
80/24
90/27
100/30
110/33
120/37
DISTANCE (feet/meters)

Pt. 1 Section II

	0 / 170	10 / 110	20 / 100	30 / 90	40 / 80	50 / 70	60 / 60	70 / 50	80 / 40	90 / 30	100 / 20	110 / 10	120 / 0
T_{AP}	0	8.0	10.5	12.3	17.5	24.5	30.0	28.1	34.5	40.5	44.5	42.5	40.5
T_{BP}	50.5	47.5	44.5	42.5	33.2	33.6	30.5	30.5	19.5	17.1	11.0	8.0	4.0
$[T_{AP}+T_{BP}-T_{AB}]$		5.7	5.2	6.2	5.9	8.3	10.7	5.2	5.2	5.7	4.7	4.2	
T'_{AP}		5.2	7.9	10.4	14.6	20.3	24.6	31.9	39.9	37.6	40.6	43.9	
T'_{BP}		44.7	41.9	39.4	35.3	29.4	25.1	17.9	14.9	12.1	9.1	3.9	
h_P ft/mm	4.04/1.23	3.69/1.12	4.40/1.34	4.19/1.28	5.89/1.80	7.59/2.31	3.69/1.12	3.69/1.12	4.04/1.23	3.34/1.02	2.48/.91		

$V_1 = \frac{10}{.008} = 1250.0 \text{ fps } (381.0 \text{ m/s})$

$V_1 = \frac{10}{.008} = 1250.0 \text{ fps } (381.0 \text{ m/s})$

$\bar{V}_1 = 1250.0 \text{ fps } (381.0 \text{ m/s})$

$V_2 = \frac{30-10}{.0076-.0055} = 2649.0 \text{ fps } (807.4 \text{ m/s})$

$V_2 = \frac{30-10}{.0211-.0059} = 2631.6 \text{ fps } (802.1 \text{ m/s})$

$\bar{V}_2 = 2640.3 \text{ fps } (804.8 \text{ m/s})$

$\sin \alpha_c = .4934$

$\alpha_c = 28.257°$

$t'_{AP} = .0015$

$t'_{BP} = .00165$

$h_A = 2.13 \text{ ft } (.65 \text{ m})$

$h_P = 2.34 \text{ ft } (.71 \text{ m})$

$\bar{T}_{AB} = 49.8$

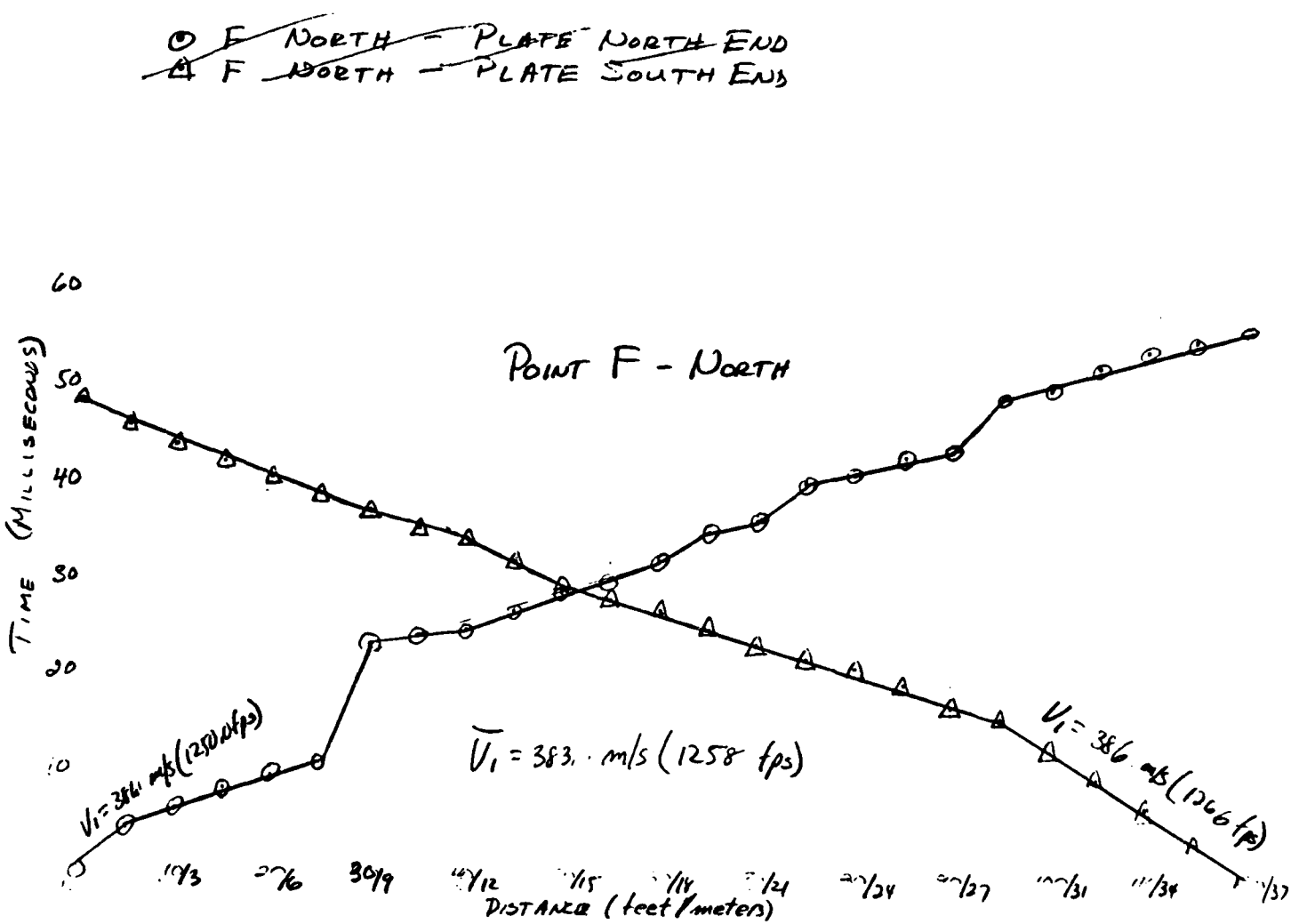
F North - Plate North End
F North - Plate South End
Point F - North
Time (Milliseconds)
60
50
40
30
20
10
0
V_1 = 384 mps (1260 fps)
$\bar{V}_1$ = 383. m/s (1258 fps)
V_1 = 386 mps (1266 fps)
10/3
20/6
30/9
40/12
50/15
60/18
70/21
80/24
90/27
100/31
110/34
120/37
Distance (feet/meters)

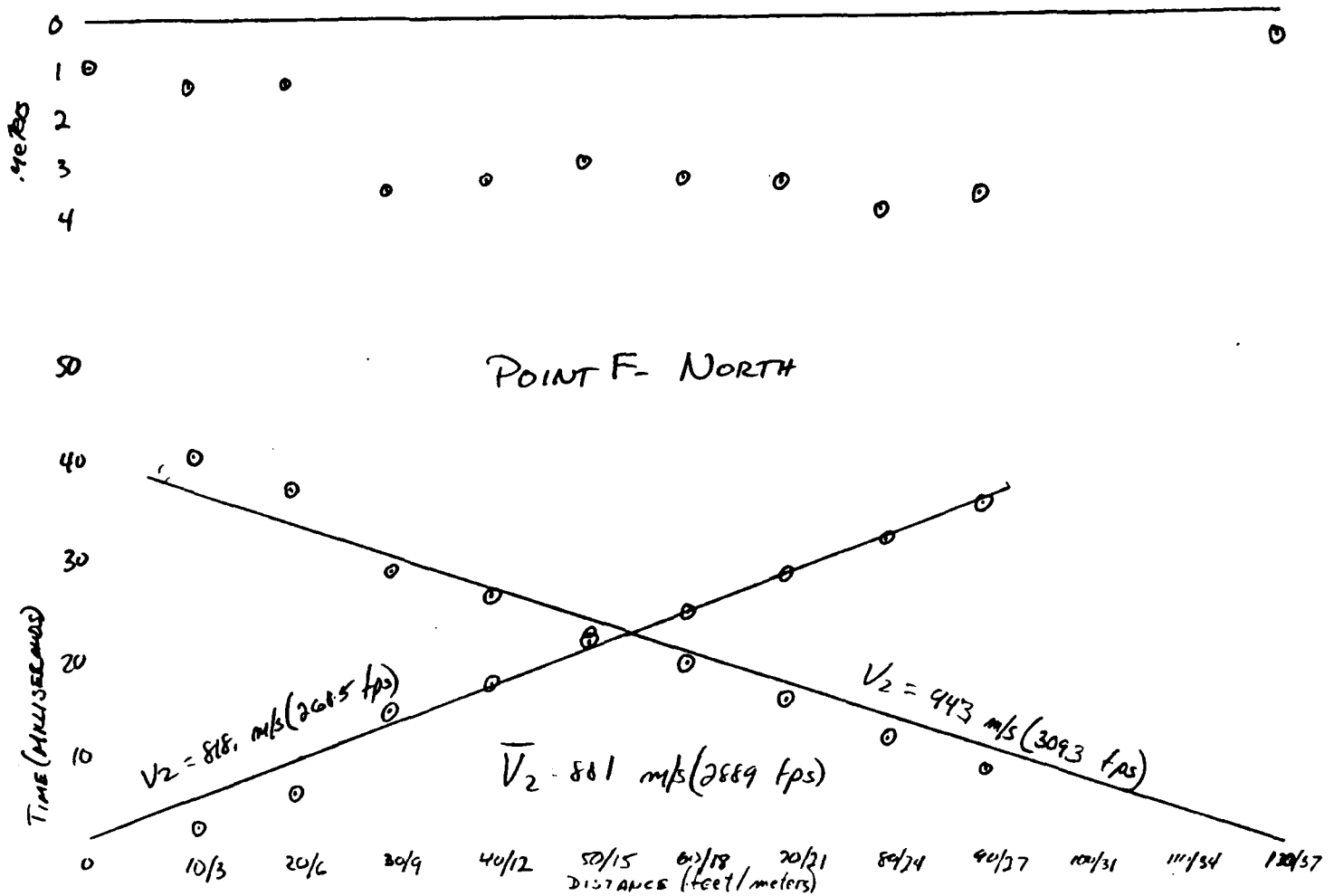
POINT F- NORTH
TIME (MILLISECONDS)
DISTANCE (feet/meters)
V_2 = 818 m/s (2685 fps)
V_2 = 943 m/s (3093 fps)
$\overline{V}_2$ = 881 m/s (2889 fps)

PH. F NORTH

	0	10	20	30	40	50	60	70	80	90	100	110	120
	120	110	100	90	80	70	60	50	40	30	20	10	0
T_{AP}	0	6.0	9.3	23.0	25.0	28.5	32.0	36.0	41.0	43.1	V_1	V_1	V_1
T_{BP}		43.9	40.3	37.0	34.0	29.0	26.9	23.1	21.0	17.0	V_1	V_1	V_1
$[T_{AP}+T_{BP}-T_{AB}]$		6.2	5.9	16.3	15.3	13.8	15.2	15.8	18.3	16.8			
T'_{AP}		2.9	6.3	14.8	17.3	21.6	24.4	28.1	31.8	35.1			
T'_{BP}		40.8	37.3	28.8	26.3	22.1	19.3	15.6	11.8	8.6			
hp ft/m		4.92/1.52	4.12/1.26	11.4/3.47	10.69/3.26	9.69/2.83	10.62/3.24	11.03/3.37	12.88/3.80	11.74/3.58			

$V_1 = \frac{5}{.004} = 1250.0 fps (381.0 m/s)$

$V_1' = \frac{10}{.0079} = 1265.8 fps (385.8 m/s)$

$\overline{V_1} = 1257.9 fps (383.4 m/s)$

$V_2 = \frac{50-10}{.0209-.006} = 2684.6 fps (818.3 m/s)$

$V_2 = \frac{60-30}{.0305-.0108} = 3092.8 fps (942.7 m/s)$

$\overline{V_2} = 2888.7 fps (880.5 m/s)$

$\sin \alpha_c = .4355$

$\alpha_c = 25.814°$

$t'_{AP} = .002$

$t'_{BP} = .001$

h_A 2.80 ft. (.85 m)

$h_B = 1.40 ft (.43 m)$

$\overline{T_{AB}} = 43.7$

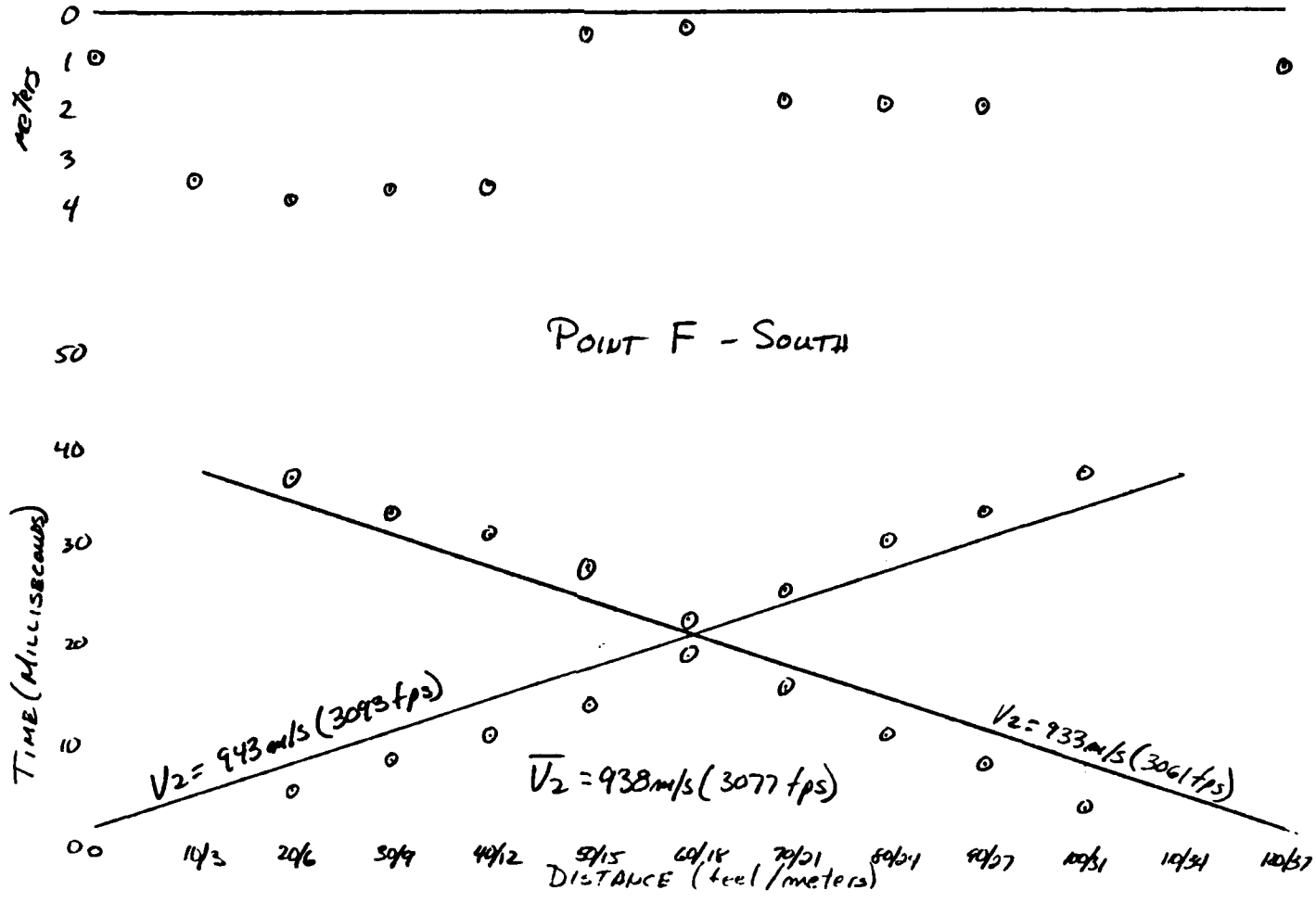
0
1
2
3
4
METERS
50
40
30
20
10
0
TIME (MILLISECONDS)
POINT F - SOUTH
V_2 = 943 m/s (3093 fps)
V_2 = 933 m/s (3061 fps)
$\overline{V_2}$ = 938 m/s (3077 fps)
10/3
20/6
30/9
40/12
50/15
60/18
70/21
80/24
90/27
100/31
110/34
120/37
DISTANCE (feet/meters)

⊙ F SOUTH – PLATE NORTH END
△ F SOUTH – PLATE SOUTH END

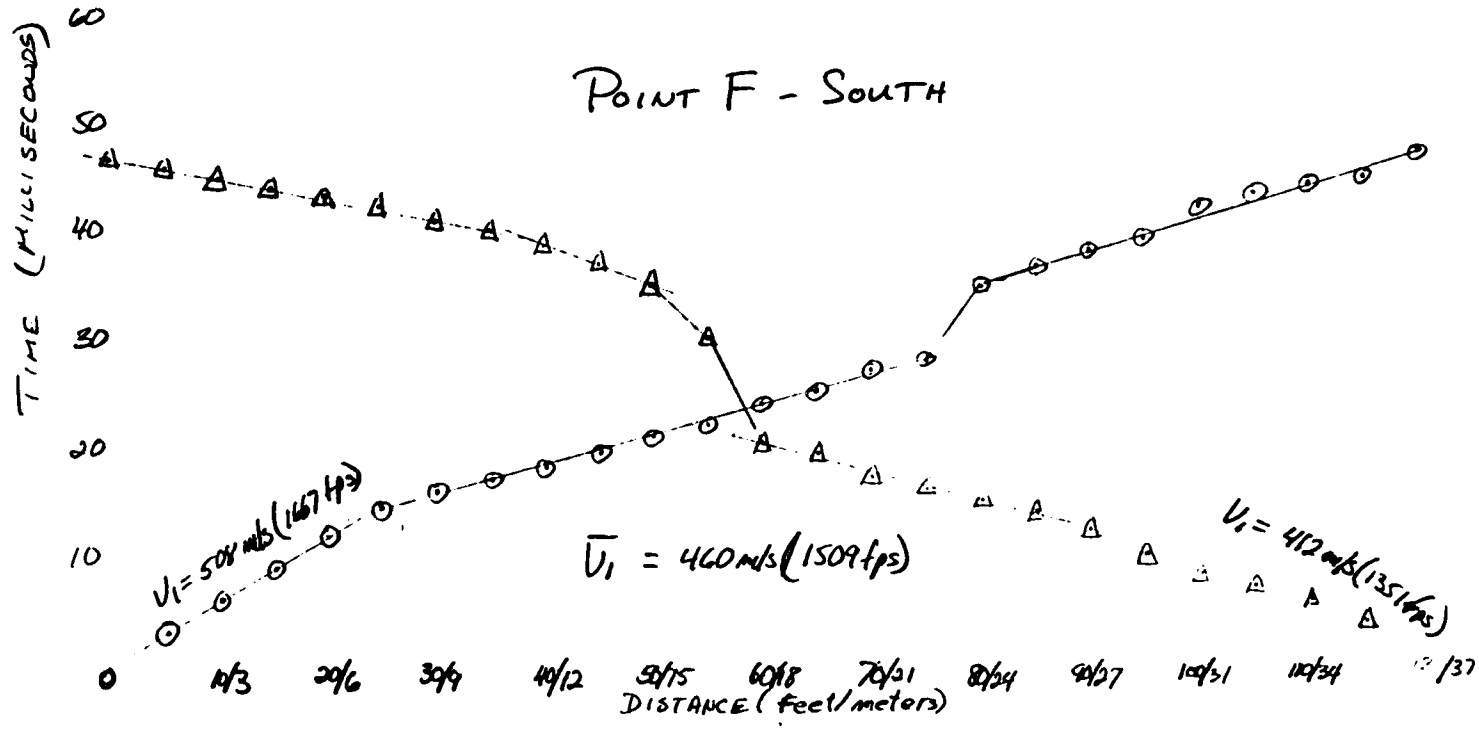

H. F SOUTH

	0 / 120	10 / 110	20 / 100	30 / 90	40 / 80	50 / 70	60 / 60	70 / 50	80 / 40	90 / 30	100 / 20	110 / 10	120 / 0
T_{AP}	–	–	12.0	16.0	18.0	20.7	23.9	27.0	34.5	37.5	41.9	44.0	45.9
T_{BP}			43.5	41.0	39.1	35.0	29.2	24.0	15.0	12.7	8.0		
$[T_{AP}+T_{BP}-T_{AB}]$			12.8	14.3	13.8	13.2	11.4	11.3	6.8	7.0	7.2	–	–
T'_{AP}			5.6	8.8	11.1	14.3	23.2	26.3	31.1	34.0	38.3		
T'_{BP}			37.1	33.8	31.6	28.4	19.5	16.3	11.6	8.7	4.4		
h_p ft/m			11.1 / 3.4	12.9 / 3.8	12.0 / 3.6	11.4 / 3.5	1.2 / .4	1.1 / .3	5.9 / 1.8	6.1 / 1.9	6.2 / 1.9		

$V_1 = \frac{15}{.009} = 1667 \text{ fps} (508 \text{ m/s})$

$V_1 = \frac{5}{.0037} = 1351 \text{ fps} (412 \text{ m/s})$

$\bar{V}_1 = 1509 \text{ fps} (460 \text{ m/s})$

$V_2 = \frac{50-20}{.010-.0083} = 3093 \text{ fps} (943 \text{ m/s})$

$V_2 = \frac{50-20}{.0085-.0087} = 3061 \text{ fps} (933 \text{ m/s})$

$\bar{V}_2 = 3077 \text{ fps} (938 \text{ m/s})$

$\sin \alpha_c = .4904$

$\alpha_c = 29.36°$

$t'_{AP} = .0018$

$t'_{BP} = .0091$

$l_A = 3.1 \text{ ft} (.9 \text{ m})$

$l_B = 3.6 \text{ ft} (1.1 \text{ m})$

$\bar{T}_{AB} = 42.7$

APPENDIX A

GRAIN-SIZE DISTRIBUTION CURVES

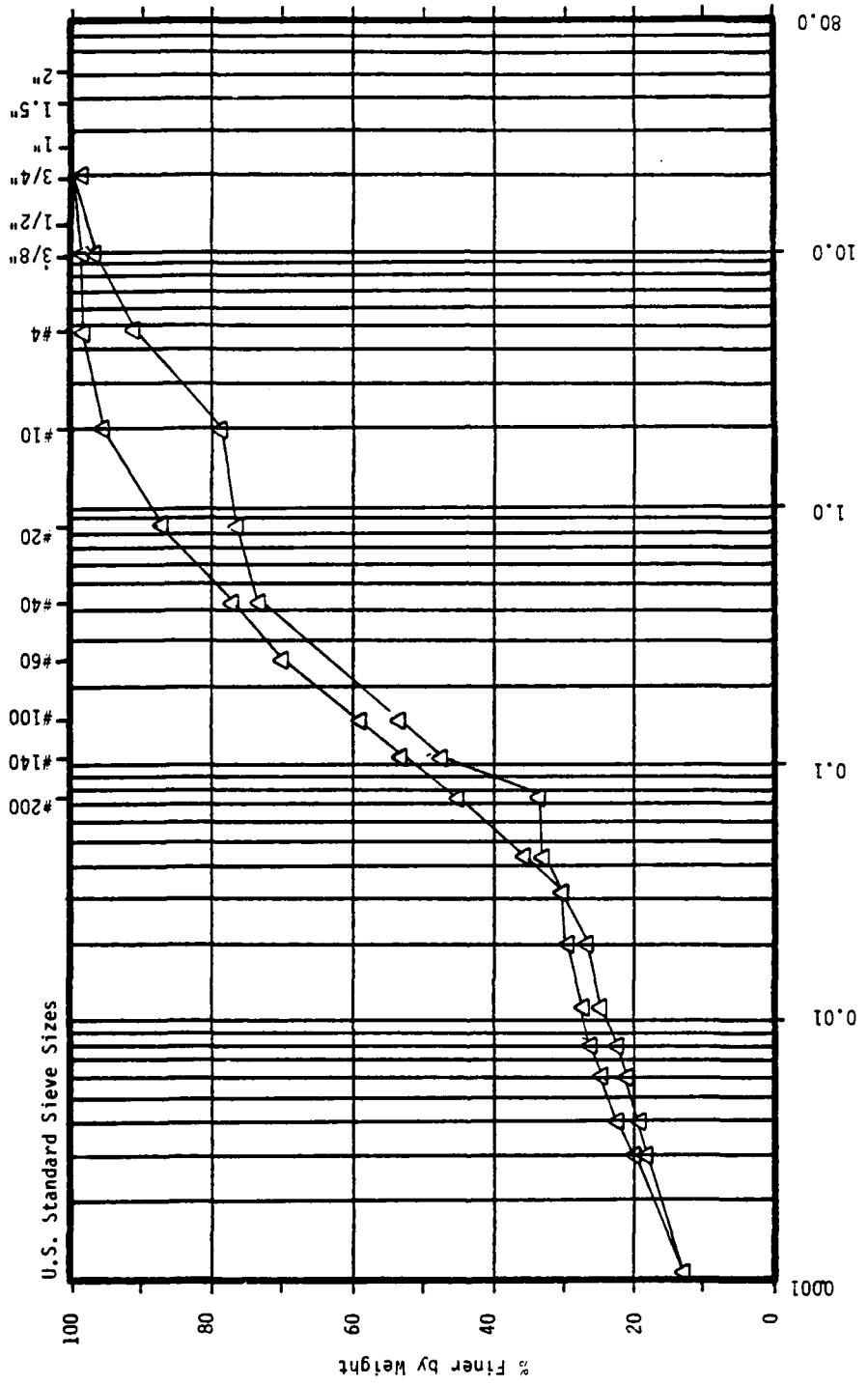
U.S. Standard Sieve Sizes
2"
1.5"
1"
3/4"
1/2"
3/8"
#4
#10
#20
#40
#60
#100
#140
#200
80.0
10.0
1.0
0.1
0.01
.001
100
80
60
40
20
0
% Finer by Weight
Grain Size in Millimeters
B1 0.31-1.37 m

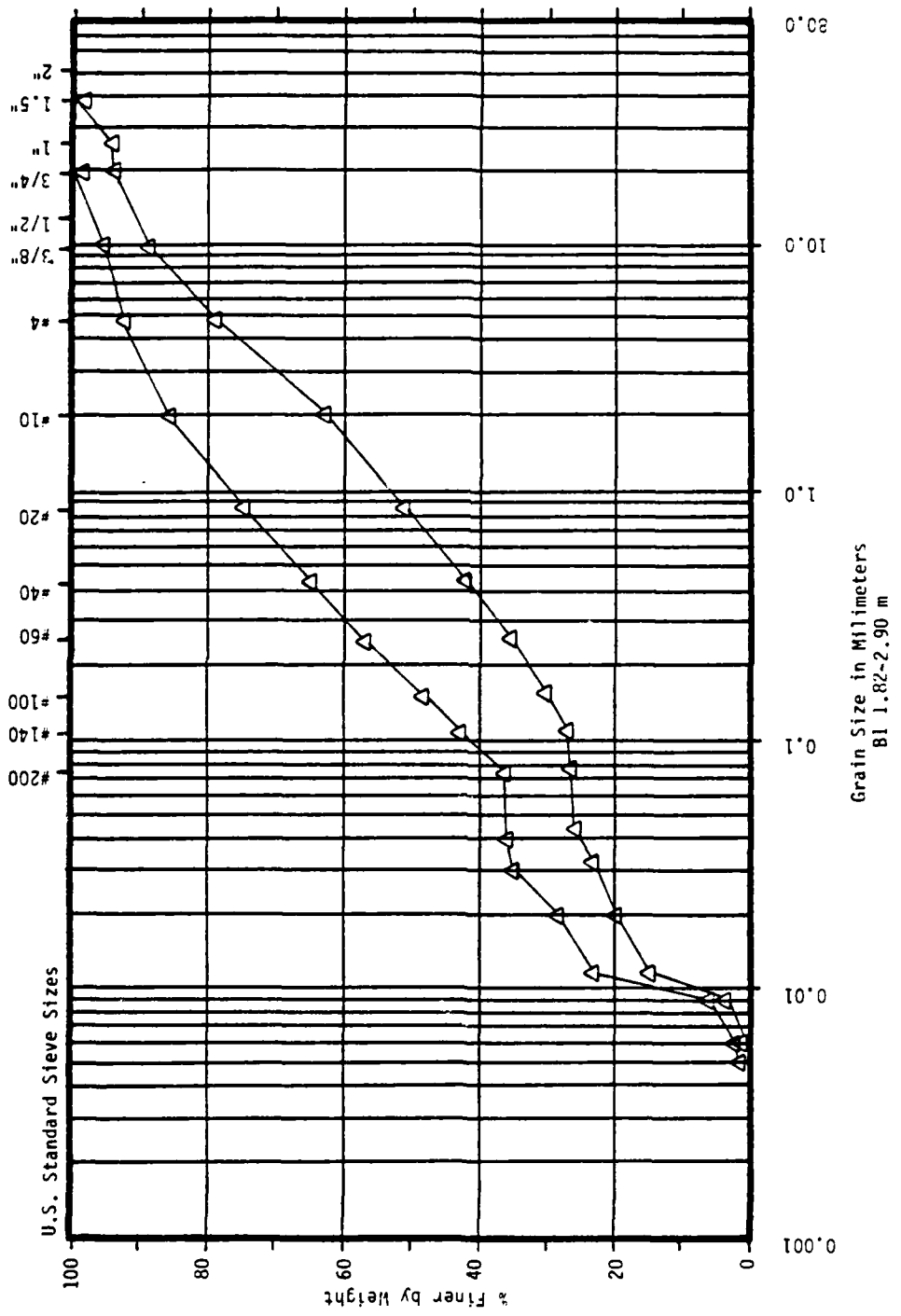
U.S. Standard Sieve Sizes
2"
1.5"
1"
3/4"
1/2"
3/8"
#4
#10
#20
#40
#60
#100
#140
#200
% Finer by Weight
100
80
60
40
20
0
Grain Size in Millimeters
B1 1.82-2.90 m
80.0
10.0
1.0
0.1
0.01
0.001

U.S. Standard Sieve Sizes
2"
1.5"
1"
3/4"
1/2"
3/8"
#4
#10
#20
#40
#60
#100
#140
#200
% Finer by Weight
100
80
60
40
20
0
80.0
10.0
1.0
0.1
0.01
0.001
Grain Size in Millimeters
BI 3.35-5.94 m

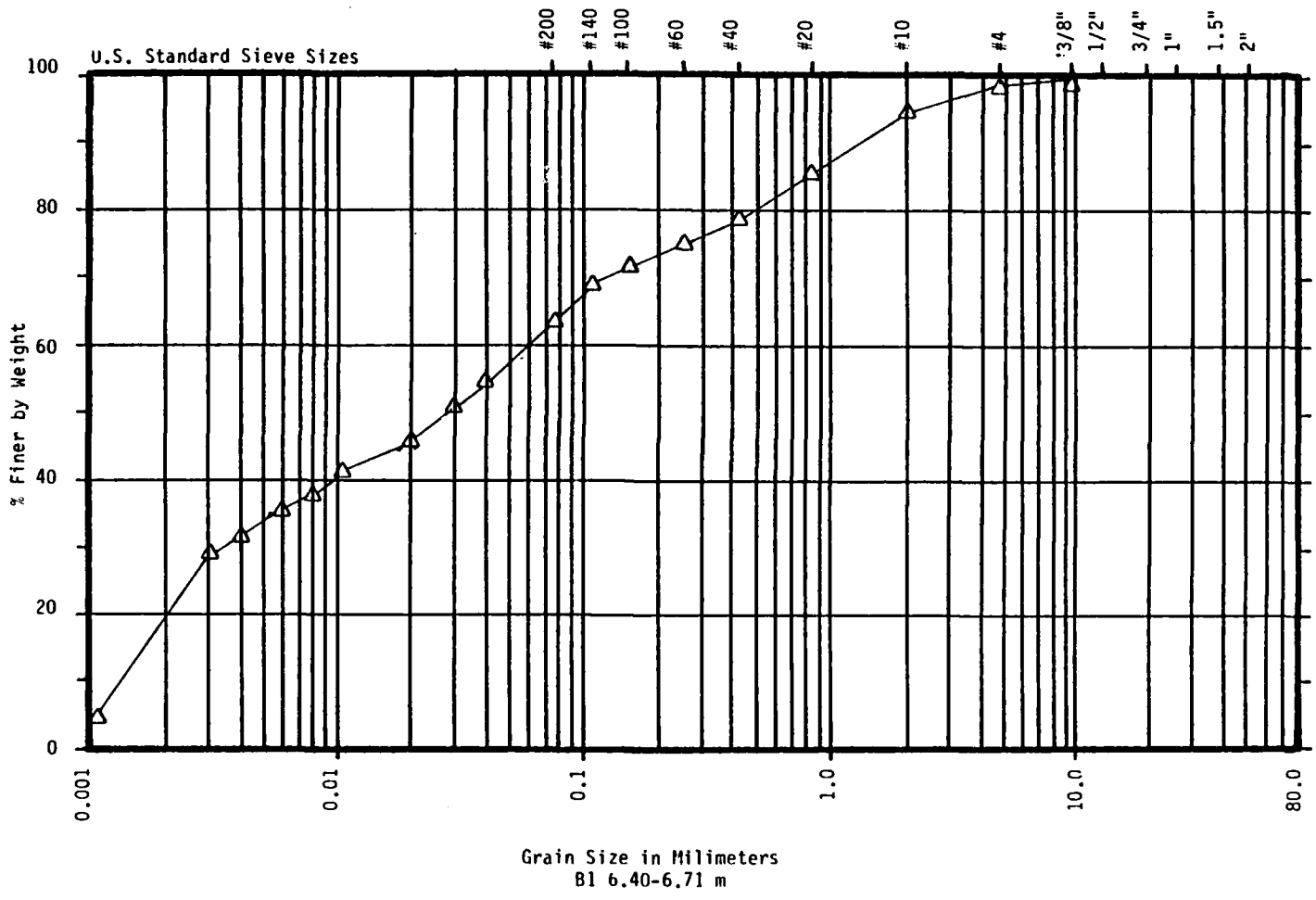
U.S. Standard Sieve Sizes
#200
#140
#100
#60
#40
#20
#10
#4
3/8"
1/2"
3/4"
1"
1.5"
2"
100
80
60
40
20
0
% Finer by Weight
0.001
0.01
0.1
1.0
10.0
80.0
Grain Size in Milimeters
B1 6.40-6.71 m

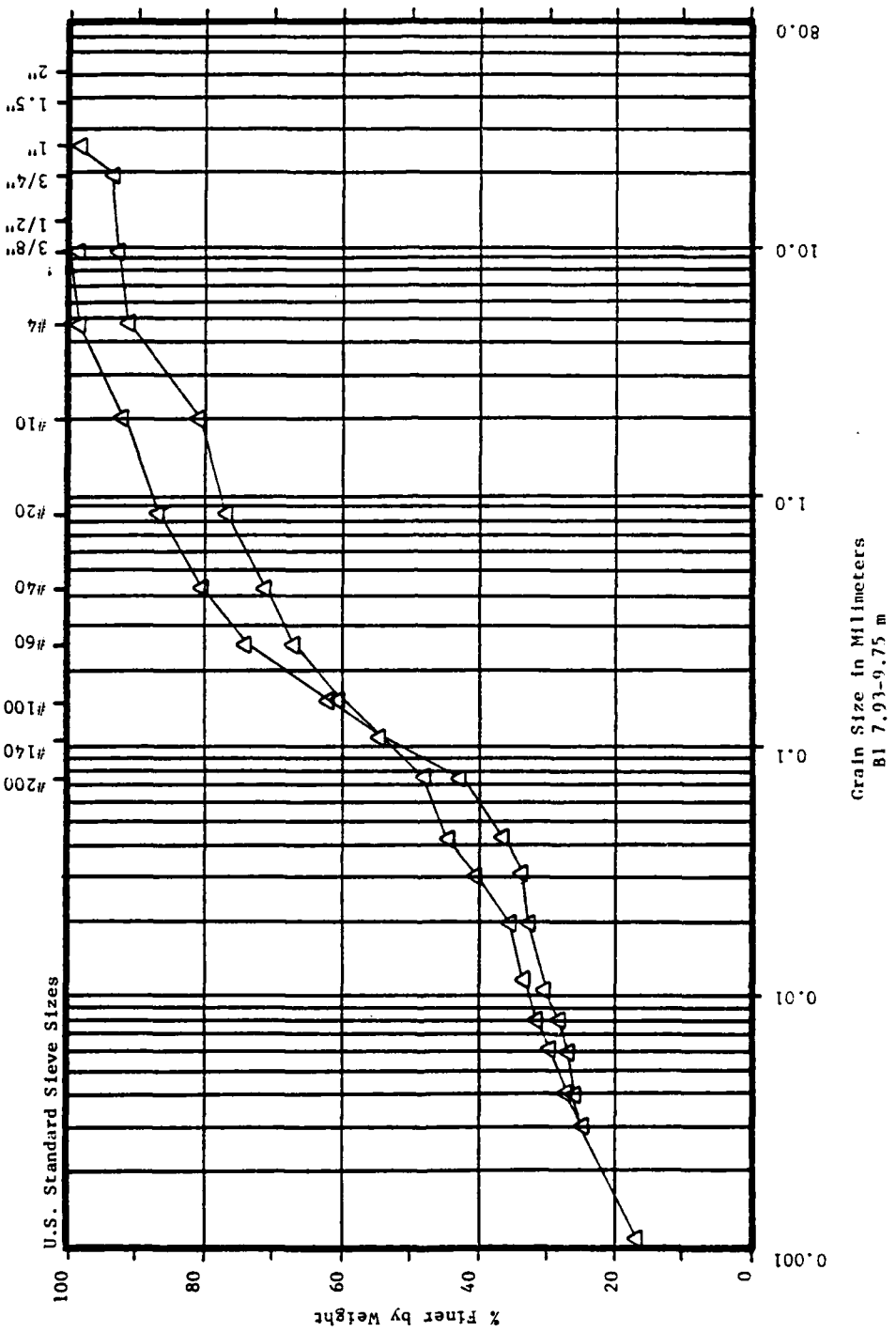
U.S. Standard Sieve Sizes
2"
1.5"
1"
3/4"
1/2"
3/8"
#4
#10
#20
#40
#60
#100
#140
#200
% Finer by Weight
100
80
60
40
20
0
Grain Size in Millimeters
80.0
10.0
1.0
0.1
0.01
0.001
B1 7.93-9.75 m

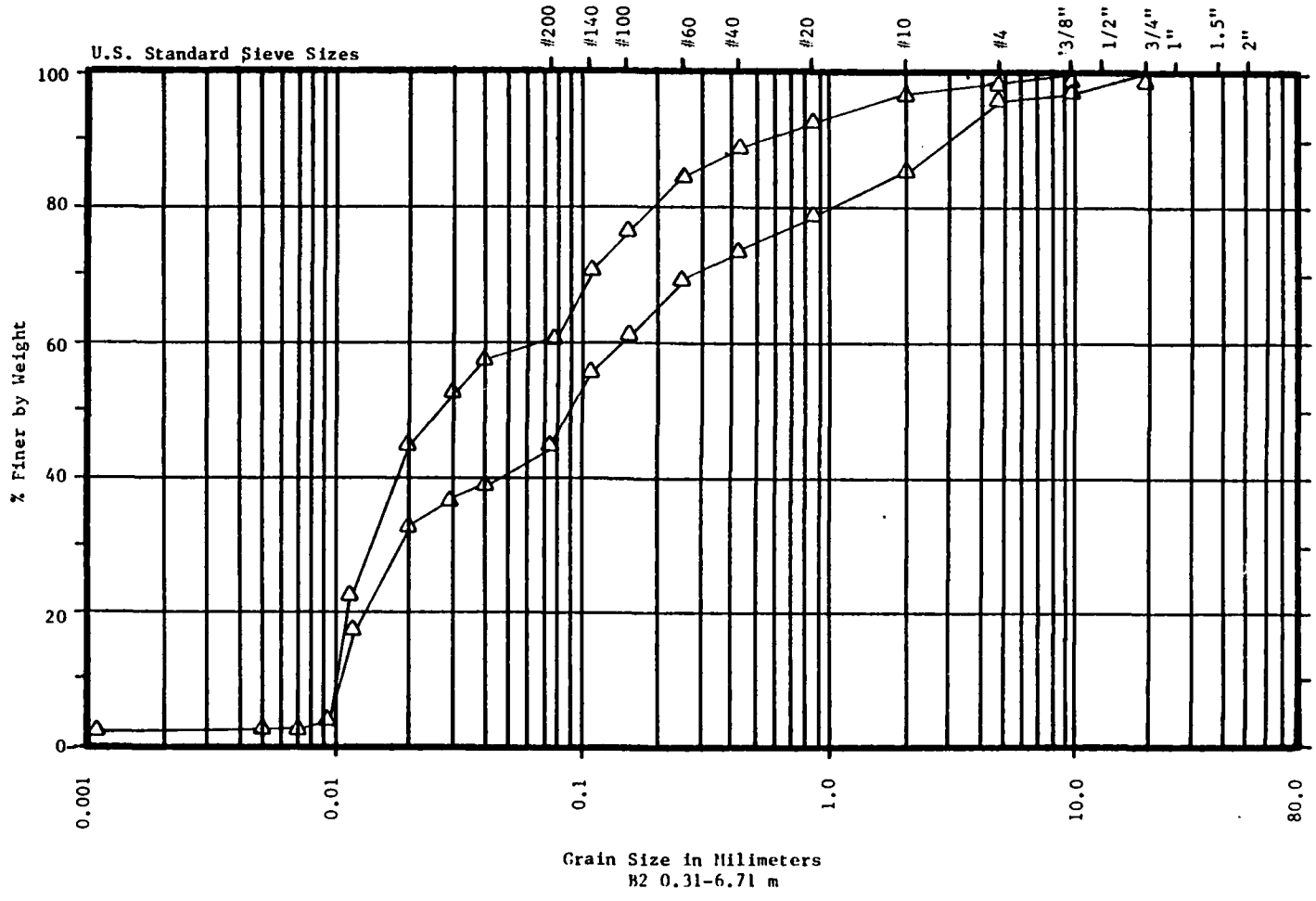
U.S. Standard Sieve Sizes
#200
#140
#100
#60
#40
#20
#10
#4
3/8"
1/2"
3/4"
1"
1.5"
2"
100
80
60
40
20
0
% Finer by Weight
0.001
0.01
0.1
1.0
10.0
80.0
Grain Size in Milimeters
B2 0.31-6.71 m

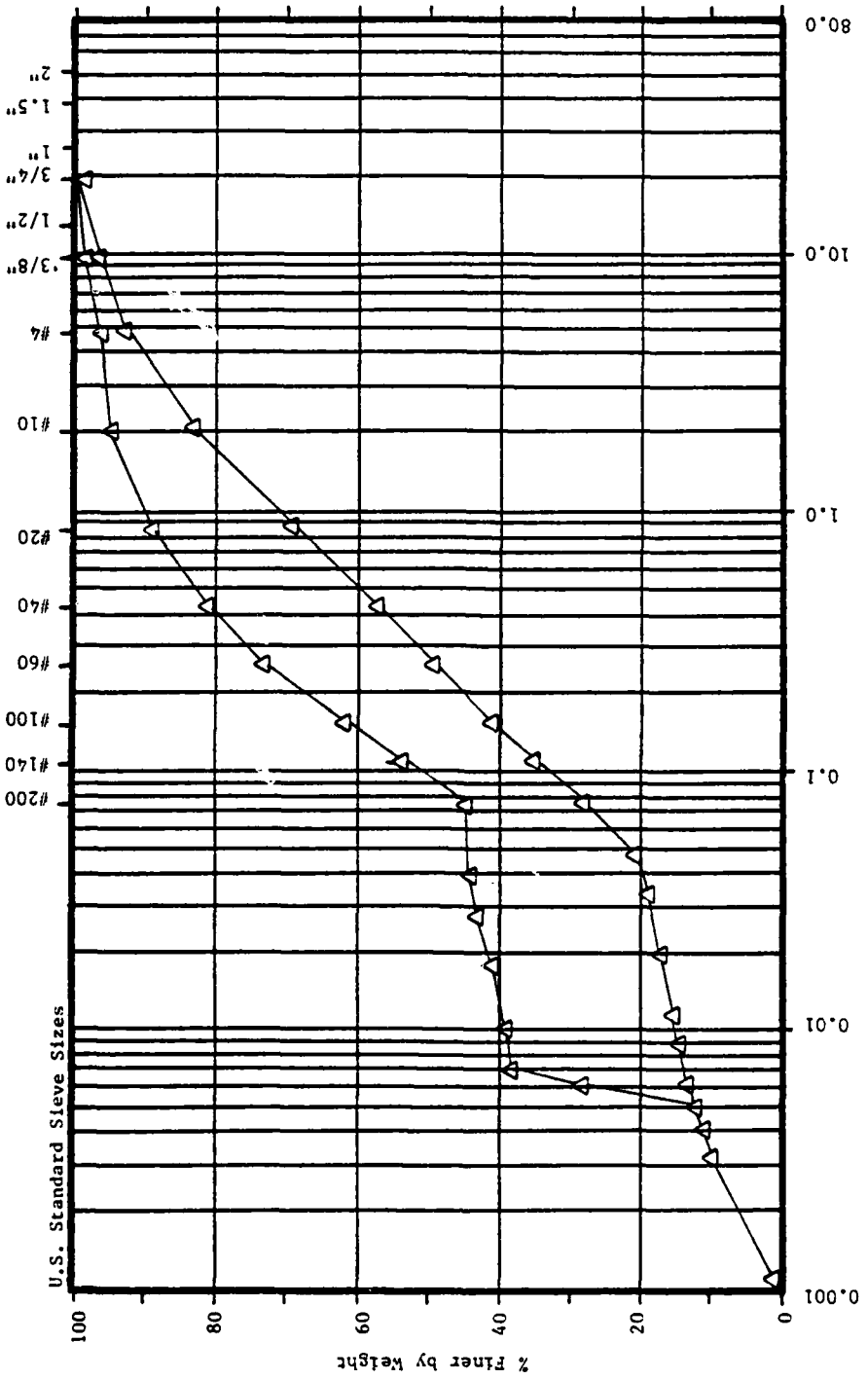
U.S. Standard Sieve Sizes
2"
1.5"
1"
3/4"
1/2"
3/8"
#4
#10
#20
#40
#60
#100
#140
#200
% Finer by Weight
100
80
60
40
20
0
80.0
10.0
1.0
0.1
0.01
0.001
Grain Size in Millimeters
B2 7.62-9.75 m

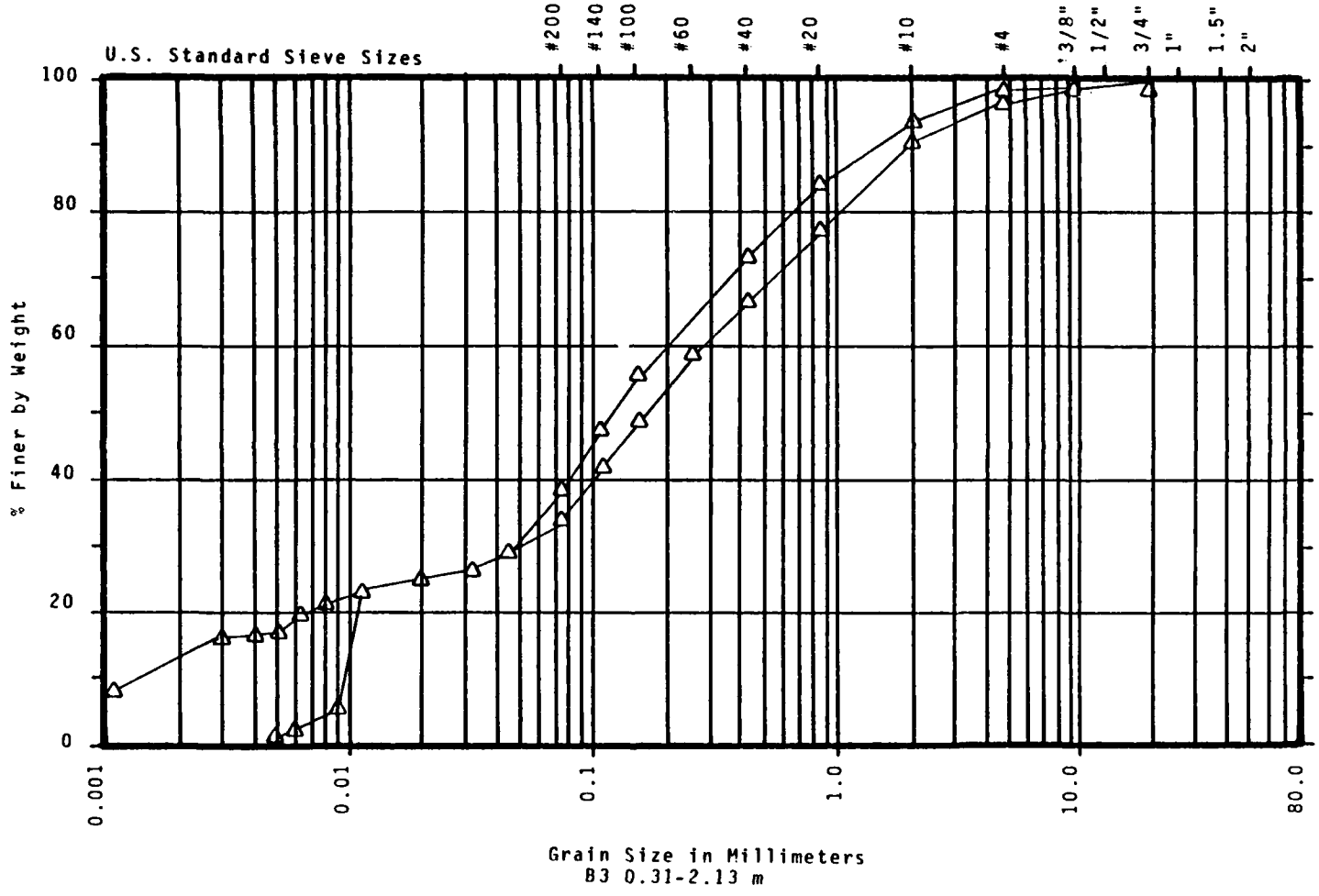
U.S. Standard Sieve Sizes
#200
#140
#100
#60
#40
#20
#10
#4
3/8"
1/2"
3/4"
1"
1.5"
2"
100
80
60
40
20
0
% Finer by Weight
0.001
0.01
0.1
1.0
10.0
80.0
Grain Size in Millimeters
B3 0.31-2.13 m

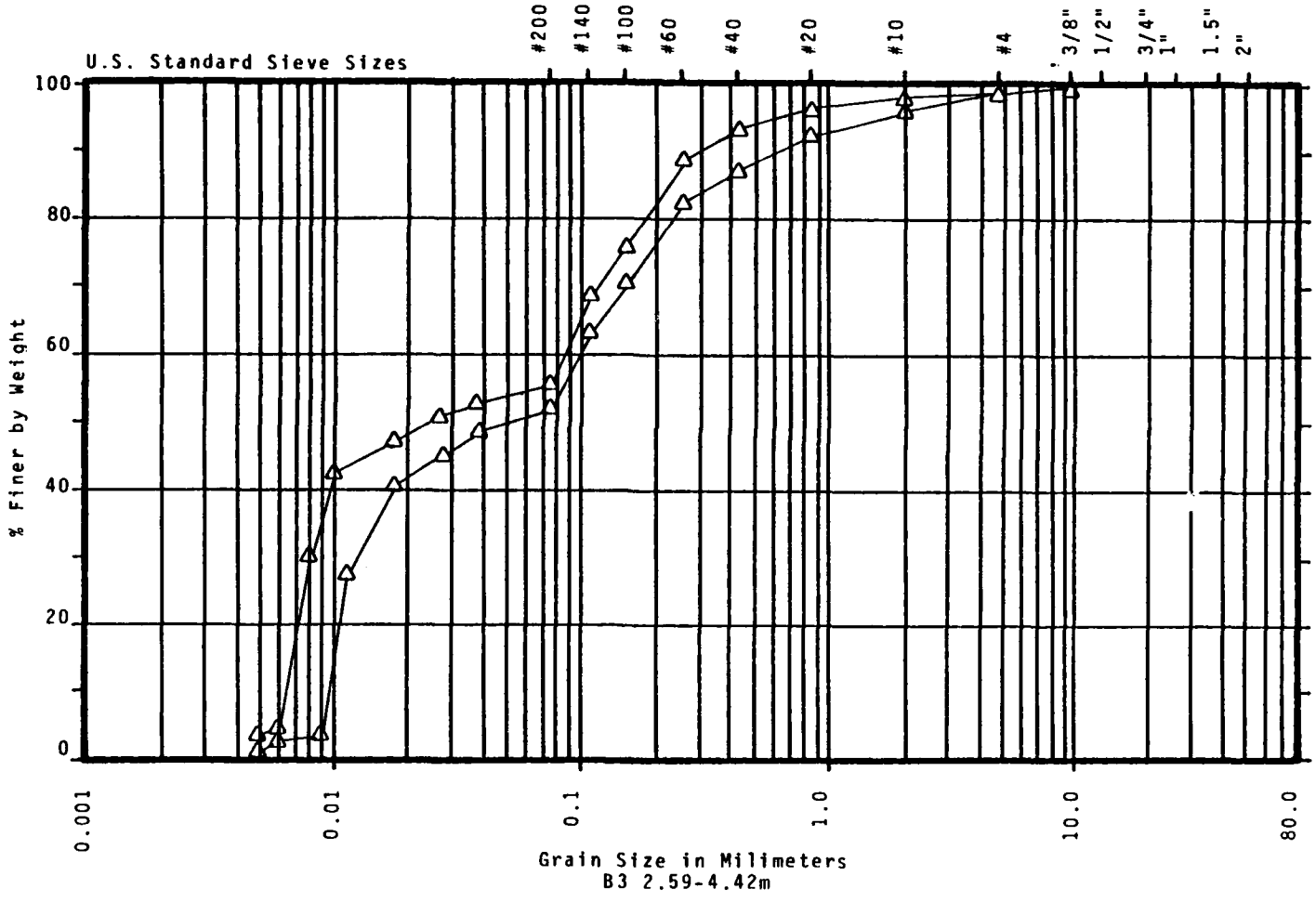
U.S. Standard Sieve Sizes
#200
#140
#100
#60
#40
#20
#10
#4
3/8"
1/2"
3/4"
1"
1.5"
2"
100
80
60
40
20
0
% Finer by Weight
0.001
0.01
0.1
1.0
10.0
80.0
Grain Size in Milimeters
B3 2.59-4.42m

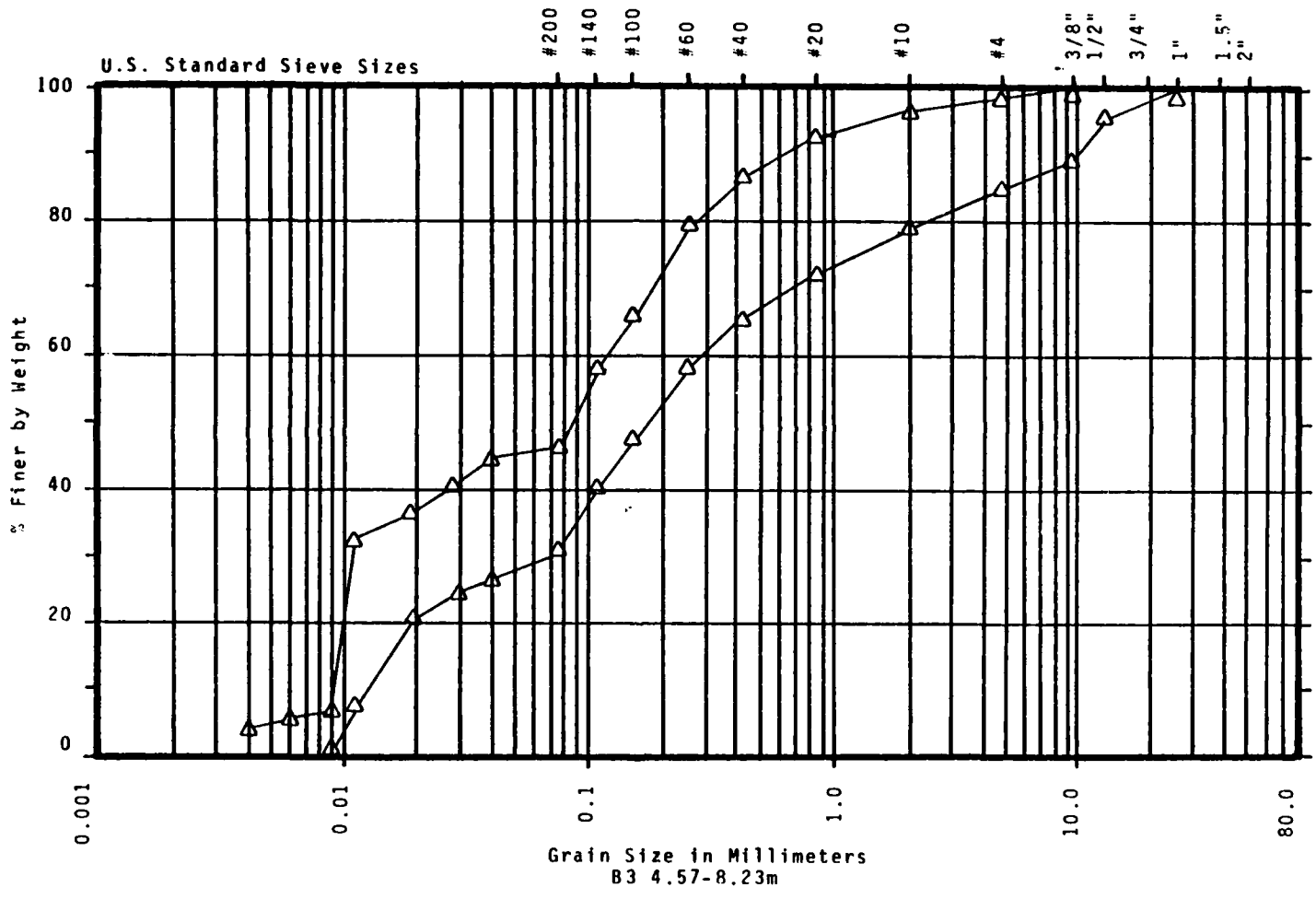
U.S. Standard Sieve Sizes
#200
#140
#100
#60
#40
#20
#10
#4
3/8"
1/2"
3/4"
1"
1.5"
2"
100
80
60
40
20
0
% Finer by Weight
0.001
0.01
0.1
1.0
10.0
80.0
Grain Size in Millimeters
B3 4.57-8.23m

% finer by weight
100
80
60
40
20
0
U.S. Standard Seive Sizes
2"
1.5"
1"
3/4"
1/2"
3/8"
#4
#10
#20
#40
#60
#100
#140
#200
80.0
10.0
1.0
0.1
0.01
0.001
Grain Size in Millimeters
B3 9.45-9.75m

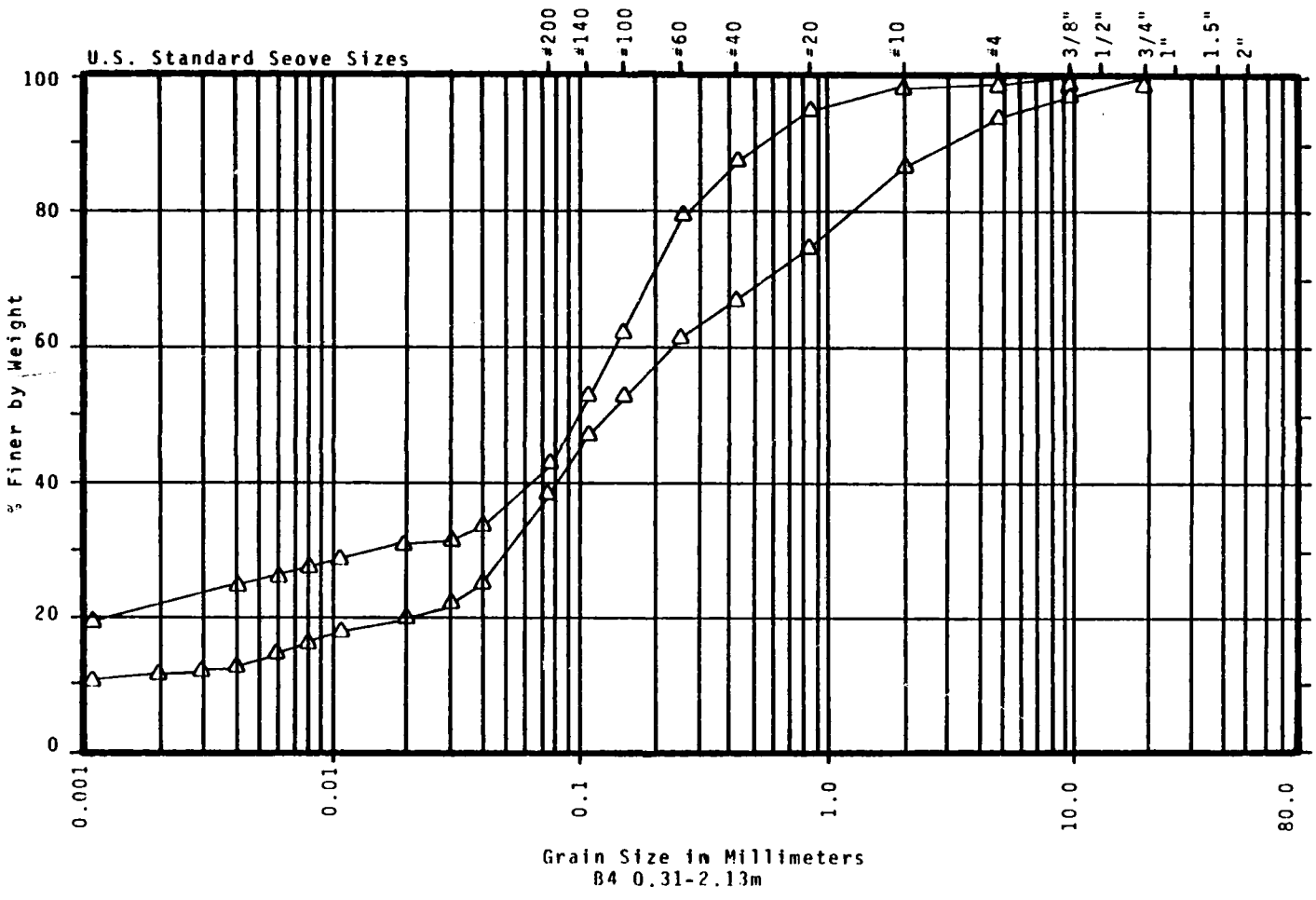
U.S. Standard Seove Sizes
#200
#140
#100
#60
#40
#20
#10
#4
3/8"
1/2"
3/4"
1"
1.5"
2"
100
80
60
40
20
0
% Finer by Weight
0.001
0.01
0.1
1.0
10.0
80.0
Grain Size in Millimeters
B4 0.31-2.13m

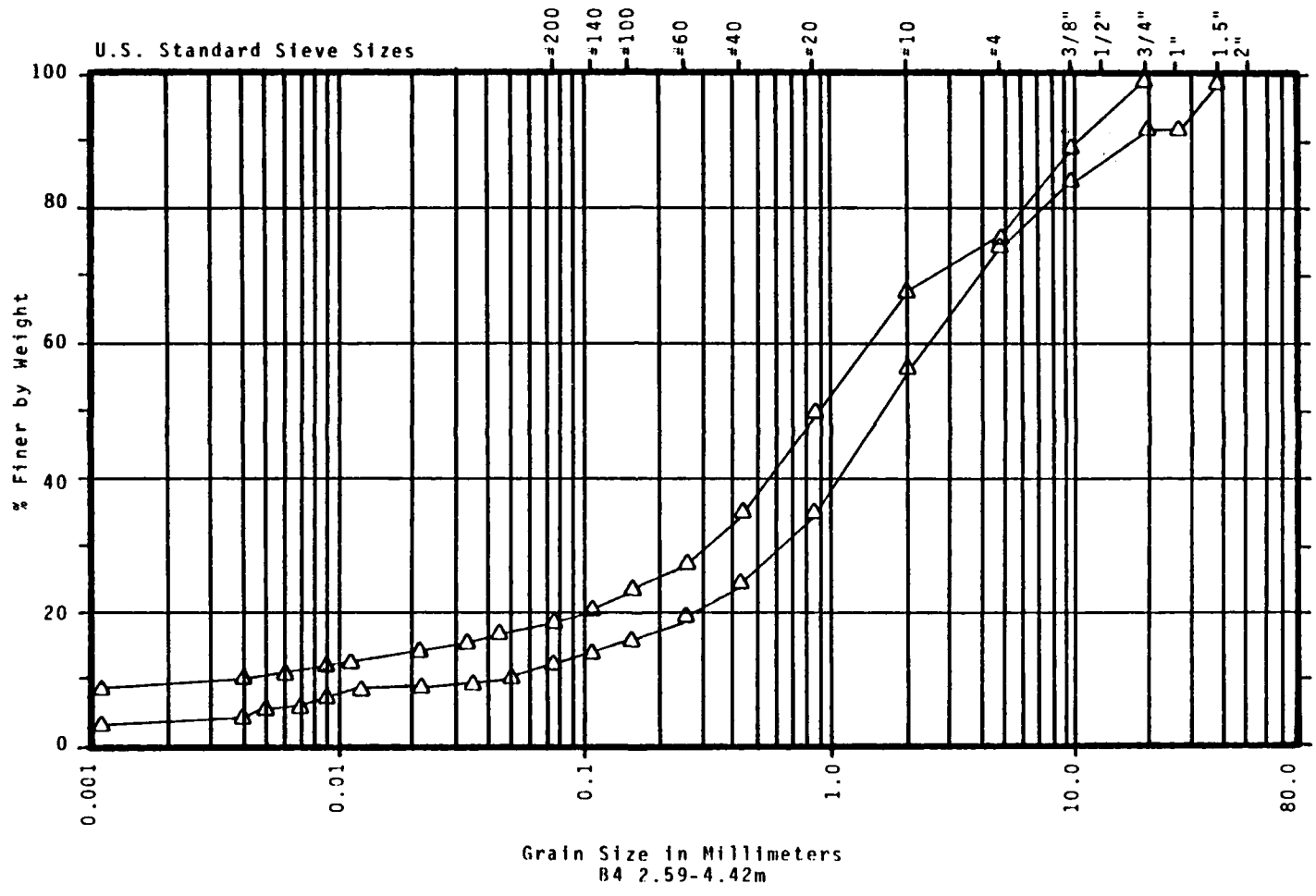
U.S. Standard Sieve Sizes
#200
#140
#100
#60
#40
#20
#10
#4
3/8"
1/2"
3/4"
1"
1.5"
2"
100
80
60
40
20
0
% Finer by Weight
0.001
0.01
0.1
1.0
10.0
80.0
Grain Size in Millimeters
B4 2.59-4.42m

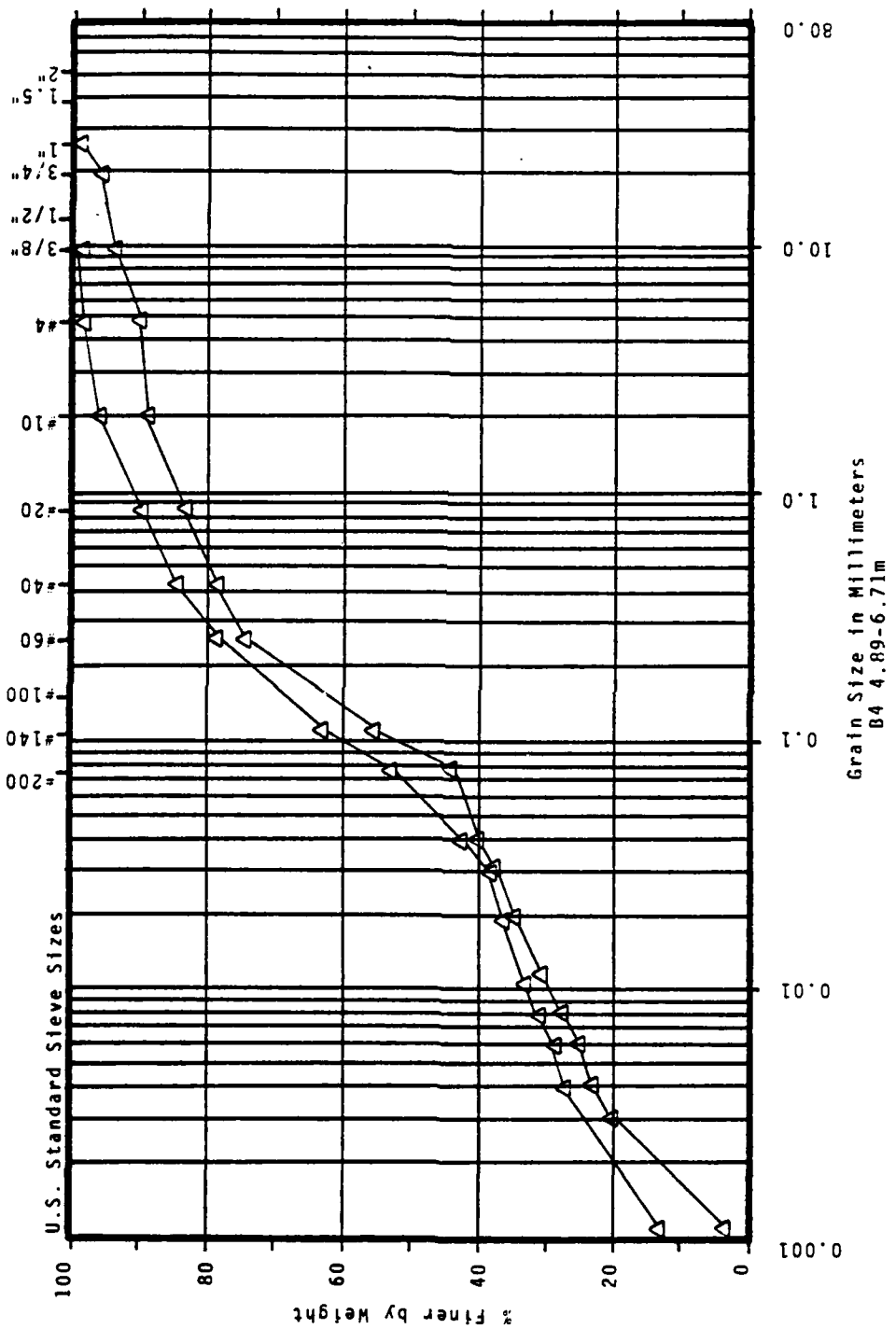
U.S. Standard Sieve Sizes
2"
1.5"
1"
3/4"
1/2"
3/8"
#4
#10
#20
#40
#60
#100
#140
#200
% Finer by Weight
100
80
60
40
20
0
Grain Size in Millimeters
80.0
10.0
1.0
0.1
0.01
0.001
B4 4.89-6.71m

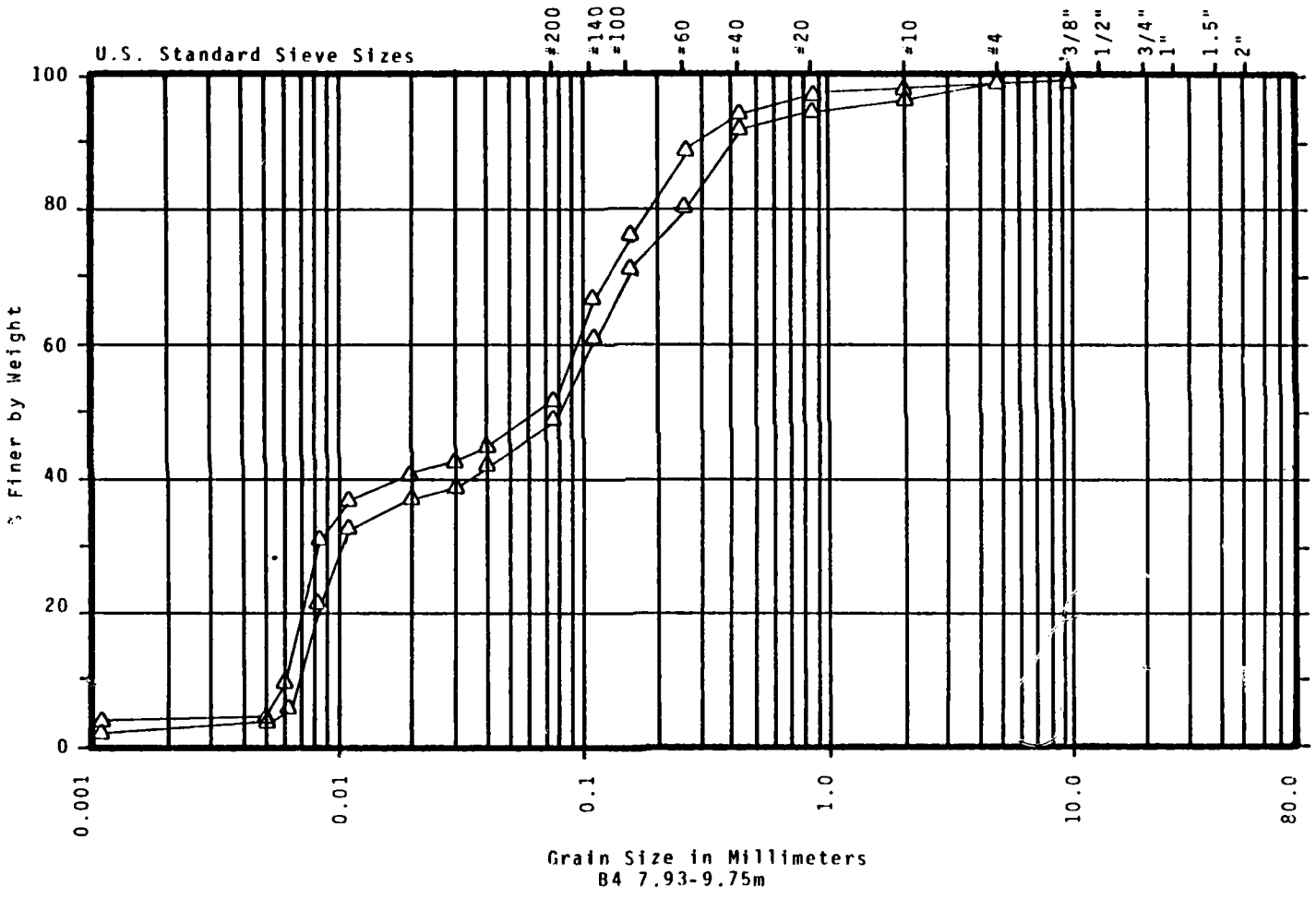
U.S. Standard Sieve Sizes
#200
#140
#100
#60
#40
#20
#10
#4
3/8"
1/2"
3/4"
1"
1.5"
2"
100
80
60
40
20
0
% Finer by Weight
0.001
0.01
0.1
1.0
10.0
80.0
Grain Size in Millimeters
B4 7.93-9.75m

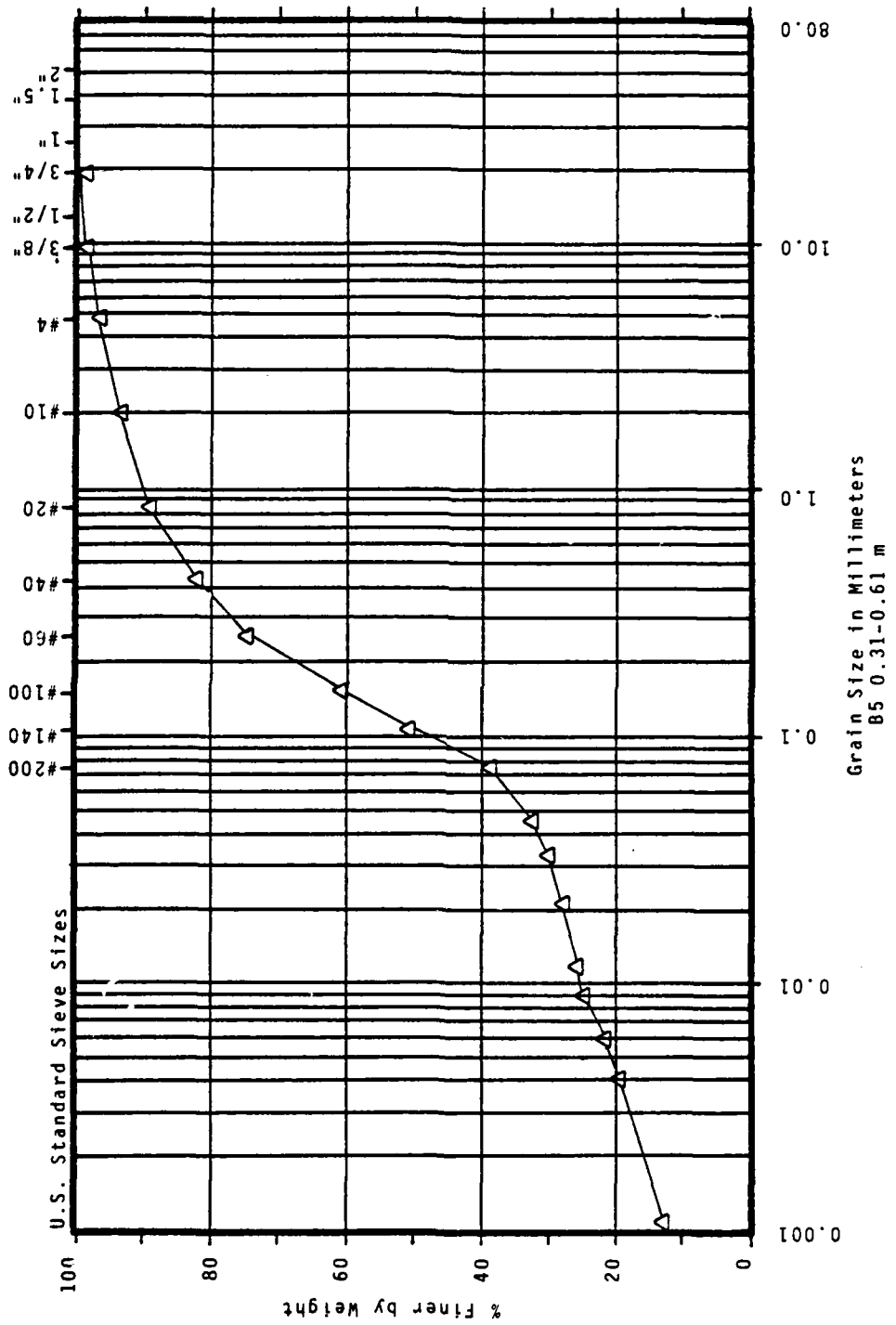
U.S. Standard Sieve Sizes
2"
1.5"
1"
3/4"
1/2"
3/8"
#4
#10
#20
#40
#60
#100
#140
#200
% finer by weight
100
80
60
40
20
0
Grain Size in Millimeters
80.0
10.0
1.0
0.1
0.01
0.001

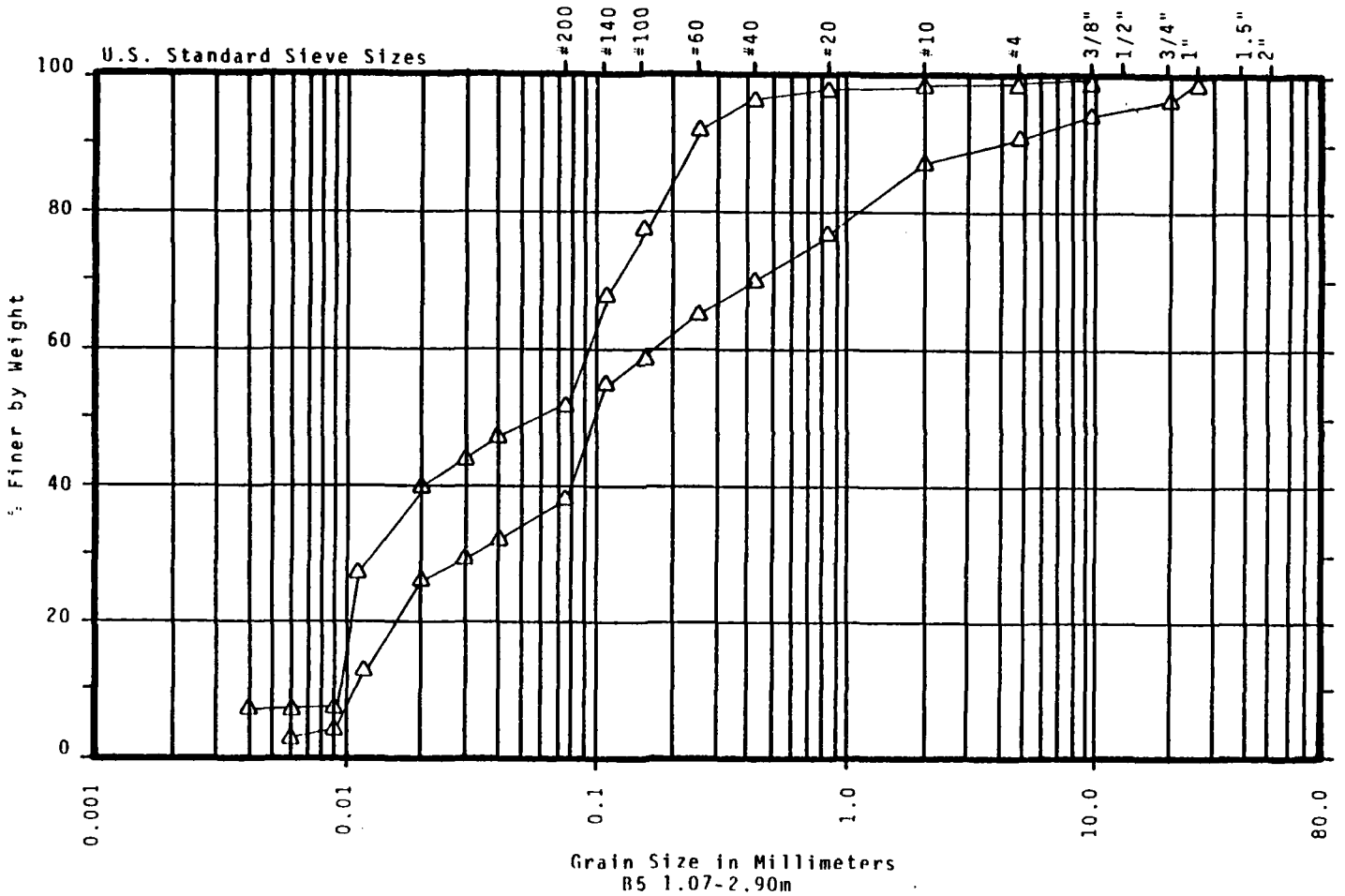
U.S. Standard Sieve Sizes
#200
#140
#100
#60
#40
#20
#10
#4
3/8"
1/2"
3/4"
1"
1.5"
2"
100
80
60
40
20
0
% Finer by Weight
0.001
0.01
0.1
1.0
10.0
80.0
Grain Size in Millimeters
B5 1.07-2.90m

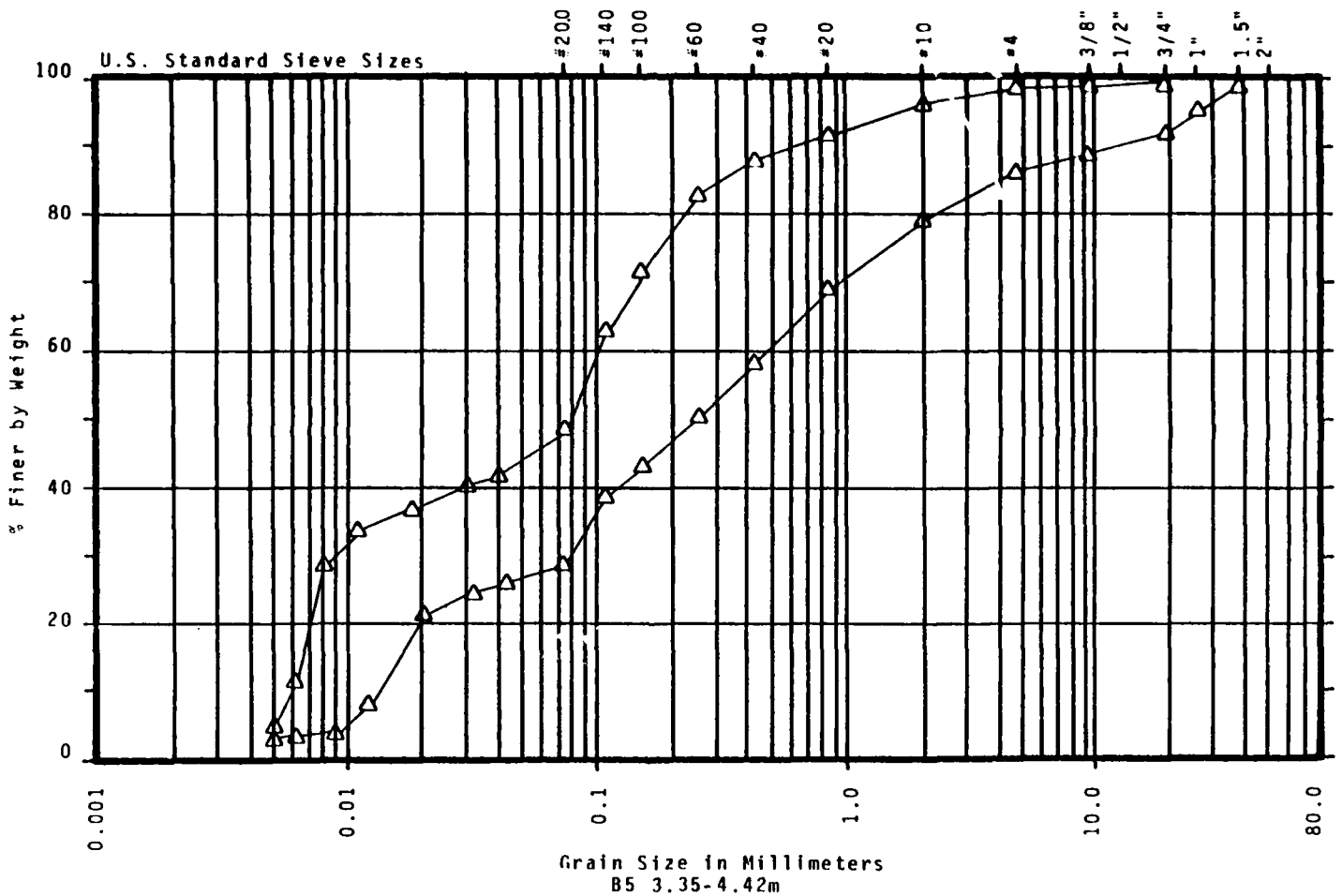
U.S. Standard Sieve Sizes
#200
#140
#100
#60
#40
#20
#10
#4
3/8"
1/2"
3/4"
1"
1.5"
2"
100
80
60
40
20
0
% Finer by Weight
0.001
0.01
0.1
1.0
10.0
80.0
Grain Size in Millimeters
B5 3.35-4.42m

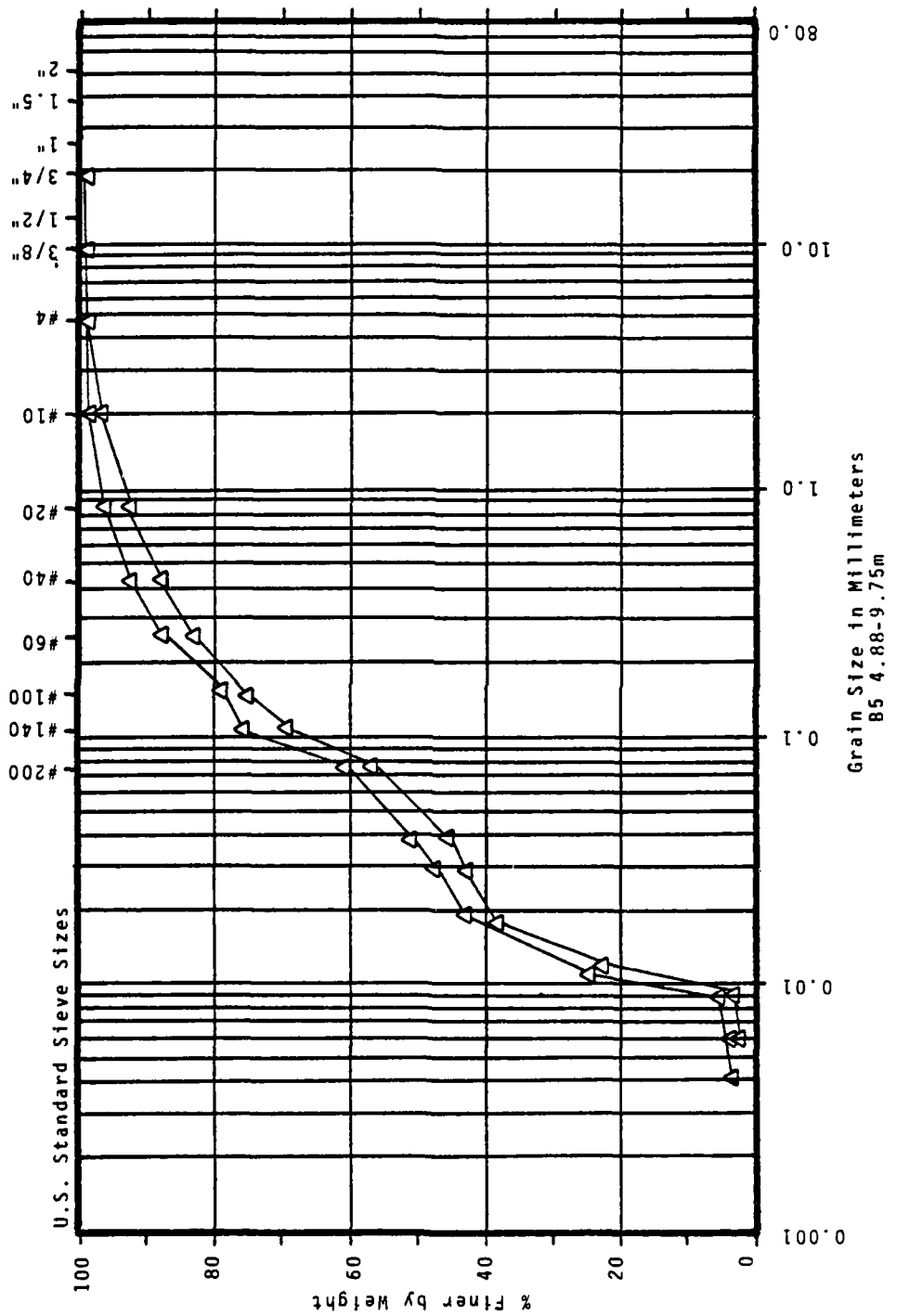
U.S. Standard Sieve Sizes
2"
1.5"
1"
3/4"
1/2"
3/8"
#4
#10
#20
#40
#60
#100
#140
#200
% Finer by Weight
100
80
60
40
20
0
Grain Size in Millimeters
BS 4.88-9.75m
80.0
10.0
1.0
0.1
0.01
0.001

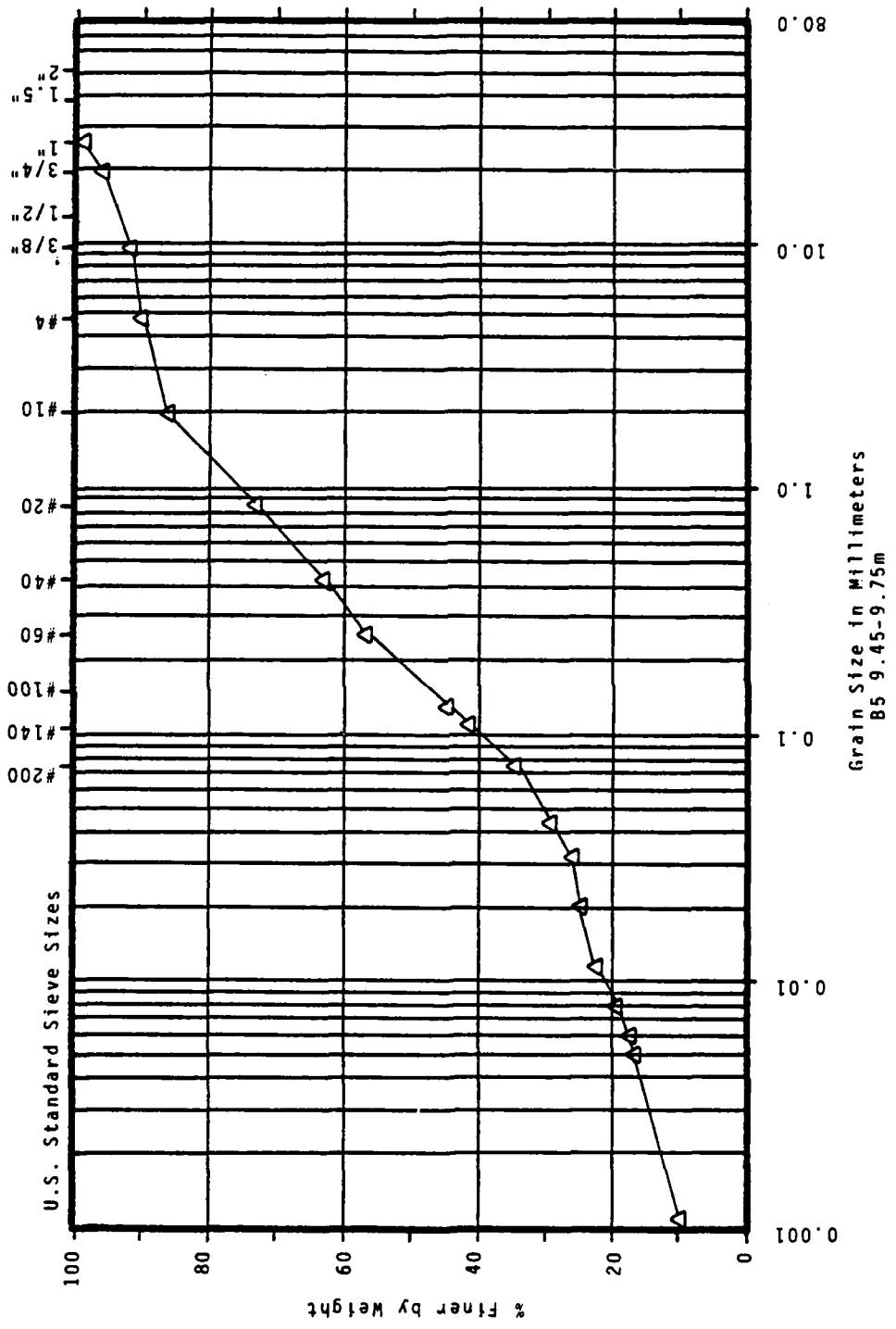
U.S. Standard Sieve Sizes
2"
1.5"
1"
3/4"
1/2"
3/8"
#4
#10
#20
#40
#60
#100
#140
#200
100
80
60
40
20
0
% finer by weight
80.0
10.0
1.0
0.1
0.01
0.001
Grain Size in Millimeters
BS 9.45-9.75m

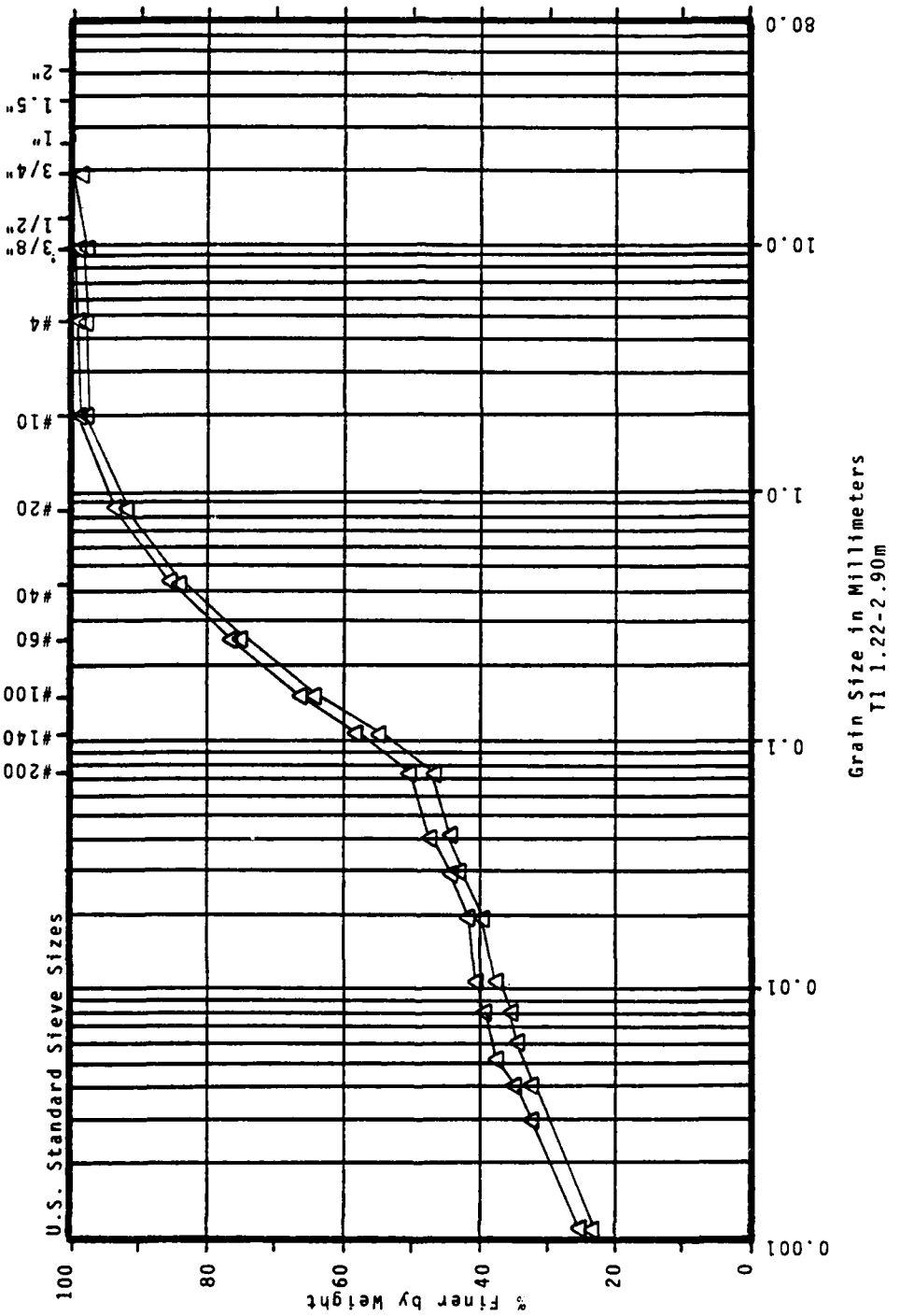
U.S. Standard Sieve Sizes
2"
1.5"
1"
3/4"
1/2"
3/8"
#4
#10
#20
#40
#60
#100
#140
#200
% Finer by Weight
100
80
60
40
20
0
80.0
10.0
1.0
0.1
0.01
0.001
Grain Size in Millimeters
T1 1.22-2.90m

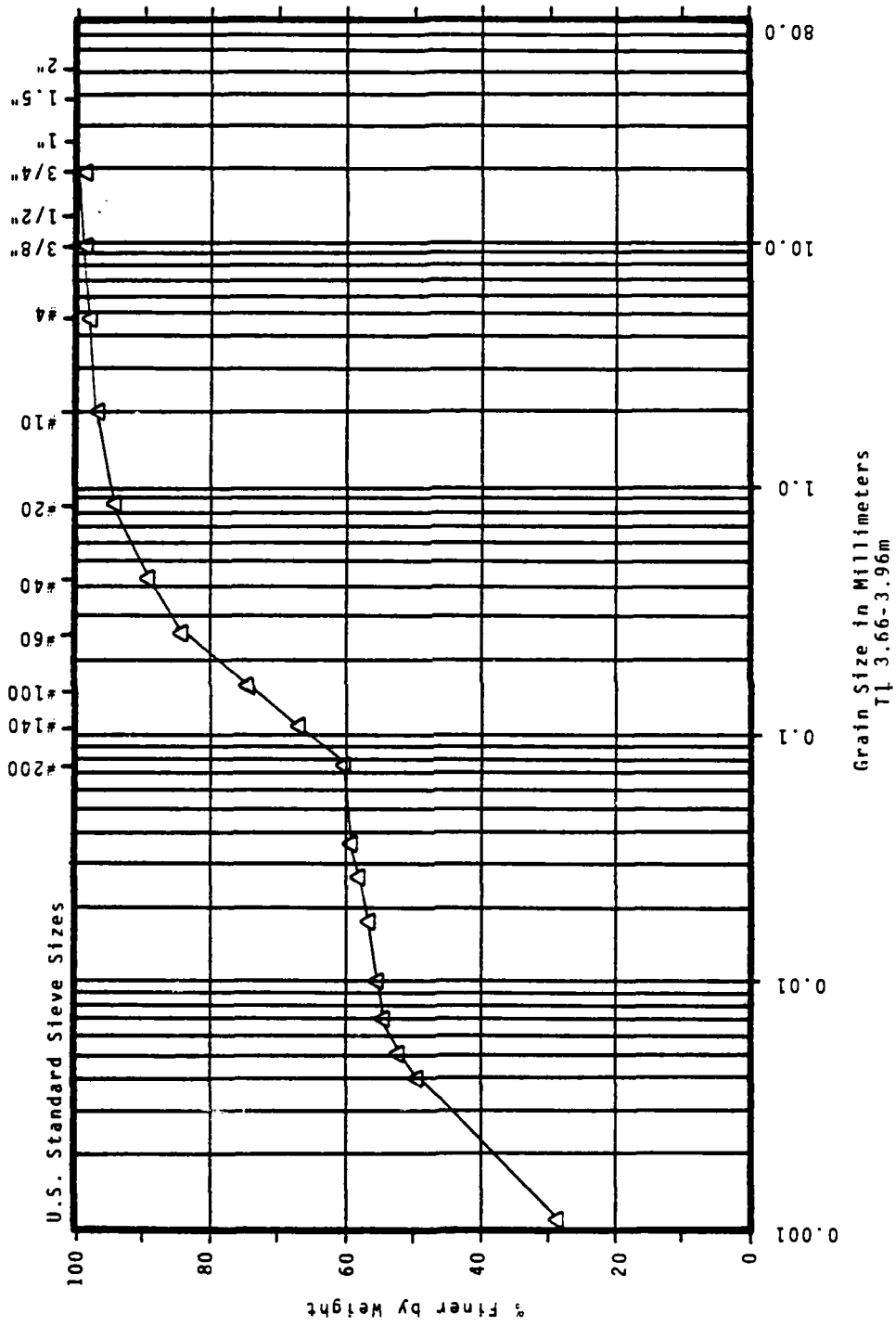
U.S. Standard Sieve Sizes
2"
1.5"
1"
3/4"
1/2"
3/8"
#4
#10
#20
#40
#60
#100
#140
#200
% Finer by Weight
100
80
60
40
20
0
Grain Size in Millimeters
T1 3.66-3.96m
80.0
10.0
1.0
0.1
0.01
0.001

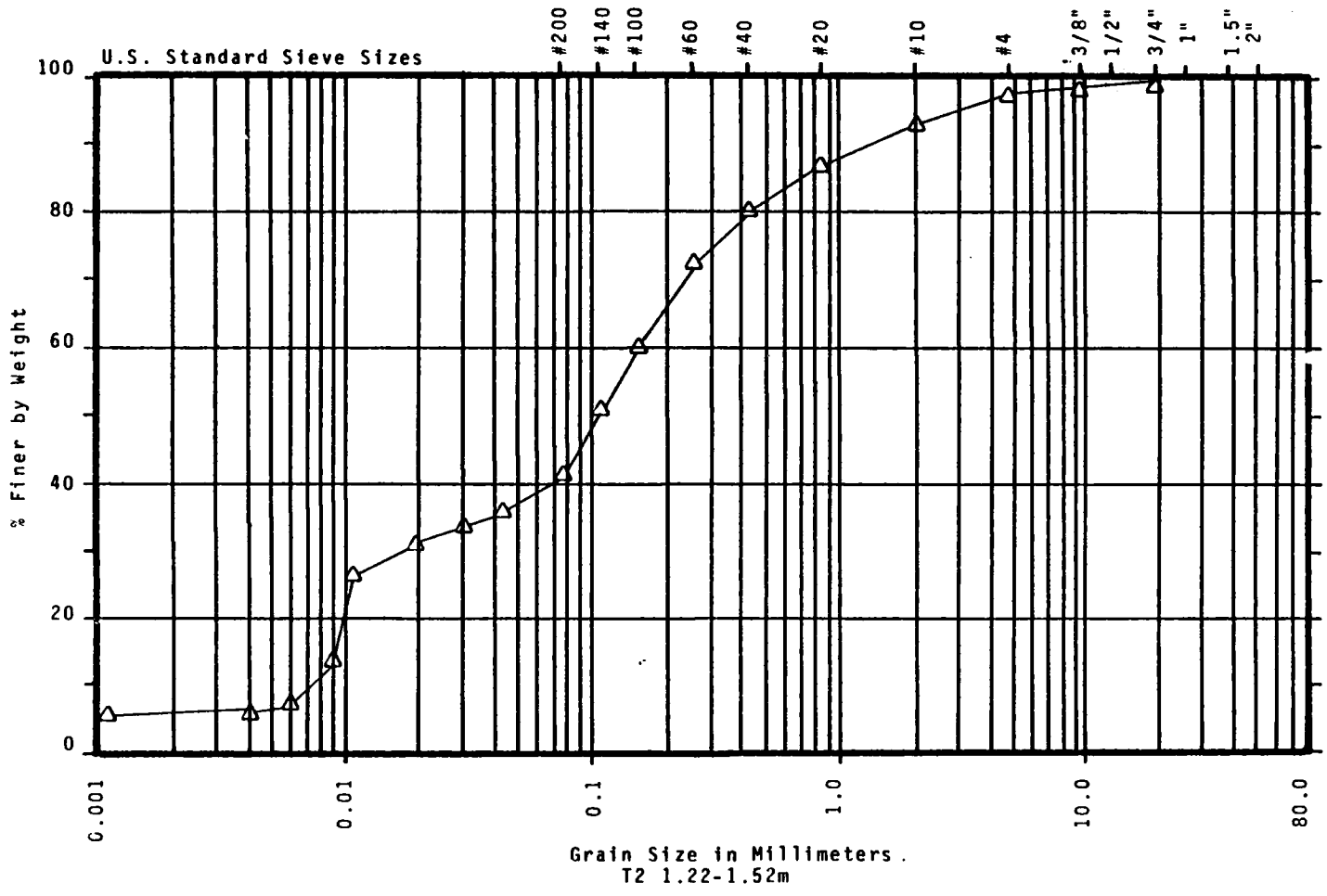
U.S. Standard Sieve Sizes
#200
#140
#100
#60
#40
#20
#10
#4
3/8"
1/2"
3/4"
1"
1.5"
2"
100
80
60
40
20
0
% Finer by Weight
0.001
0.01
0.1
1.0
10.0
80.0
Grain Size in Millimeters.
T2 1.22-1.52m

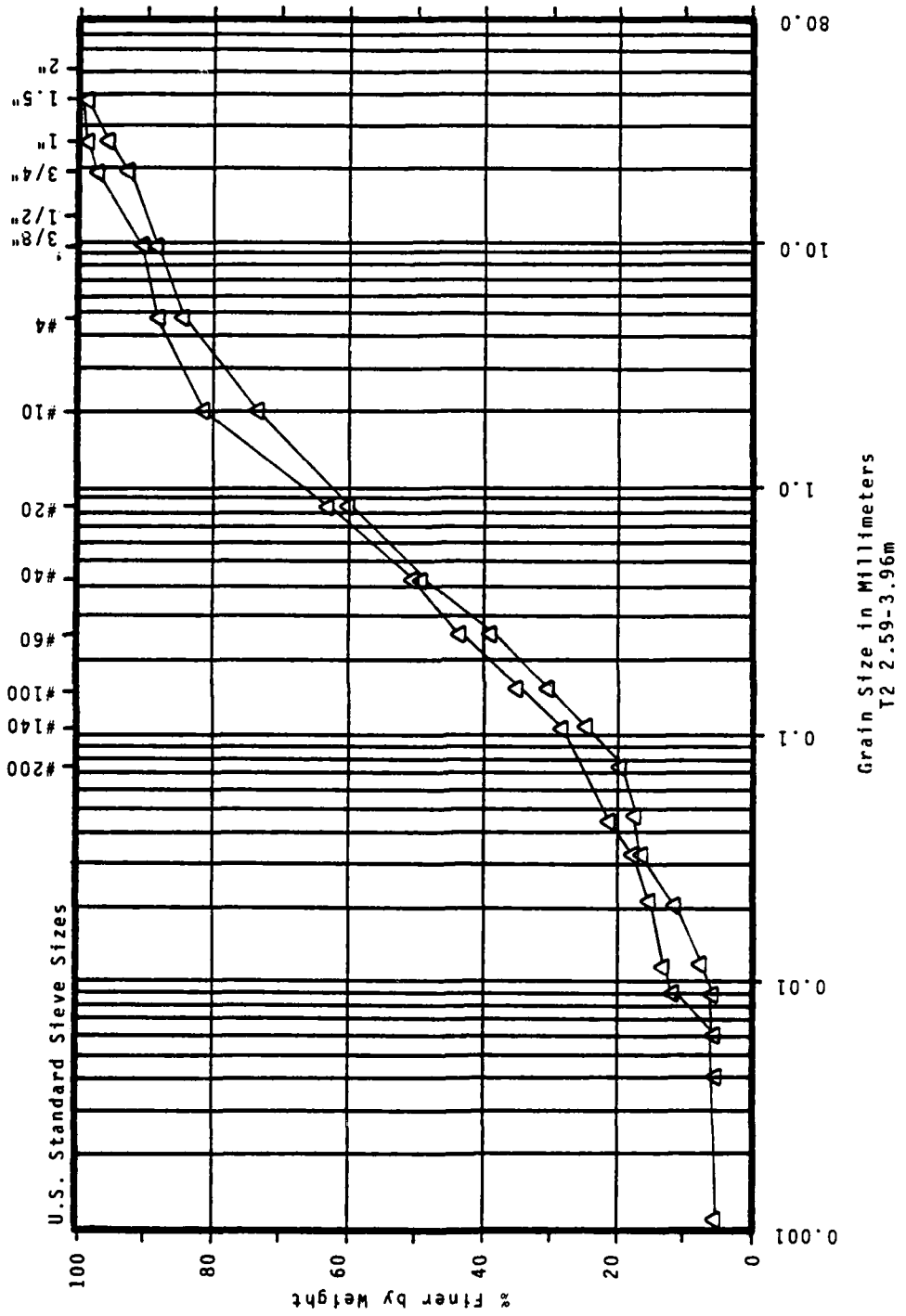
U.S. Standard Sieve Sizes
2"
1.5"
1"
3/4"
1/2"
3/8"
#4
#10
#20
#40
#60
#100
#140
#200
% Finer by Weight
100
80
60
40
20
0
Grain Size in Millimeters
T2 2.59-3.96m
80.0
10.0
1.0
0.1
0.01
0.001

APPENDIX B

UNCONFINED COMPRESSION TESTS ON SOIL

SAMPLES AIR-DRIED FROM VARIOUS INITIAL WATER CONTENTS

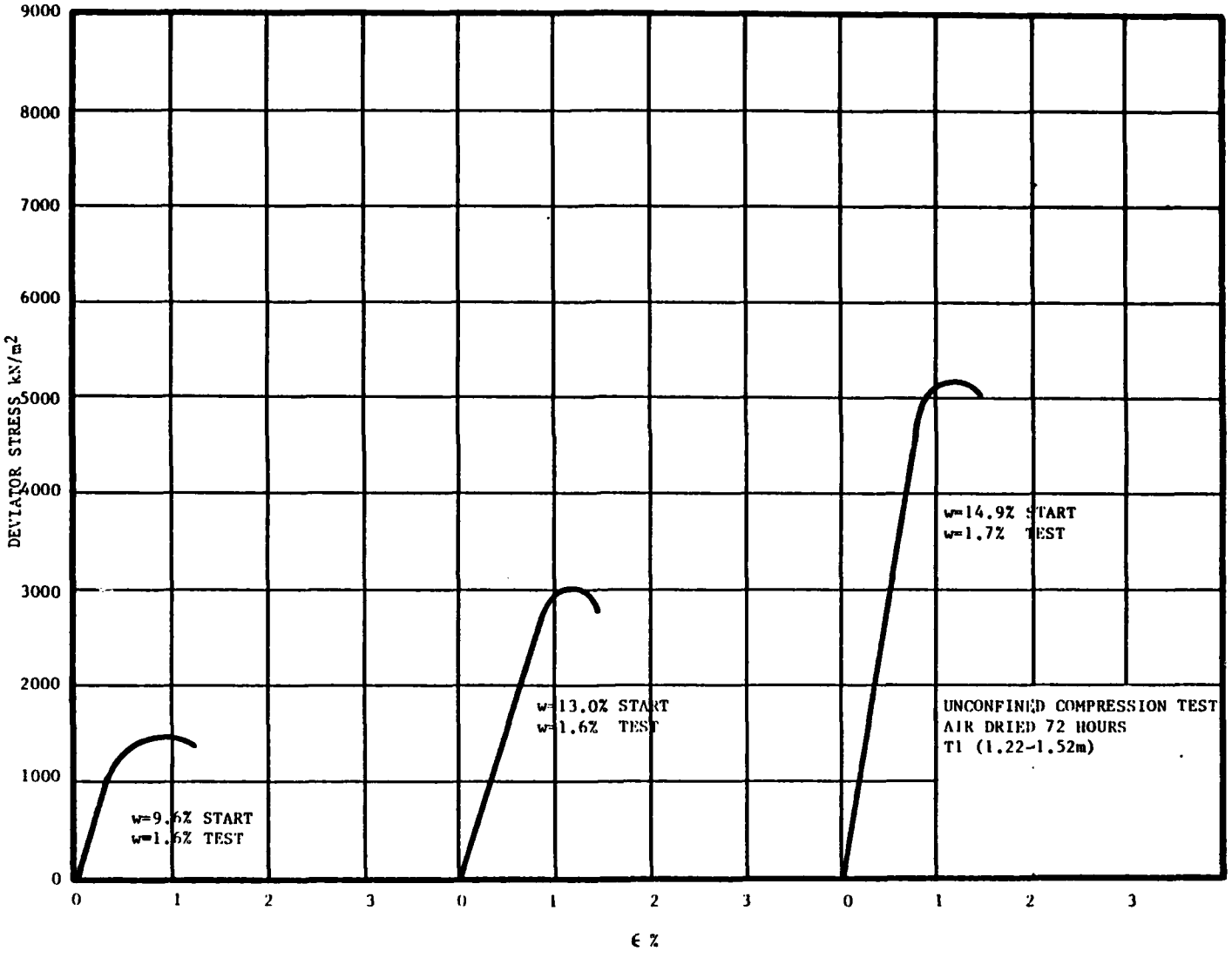
DEVIATOR STRESS kN/m²
9000
8000
7000
6000
5000
4000
3000
2000
1000
0
0
1
2
3
0
1
2
3
0
1
2
3
ε %
w=9.6% START
w=1.6% TEST
w=13.0% START
w=1.6% TEST
w=14.9% START
w=1.7% TEST
UNCONFINED COMPRESSION TEST
AIR DRIED 72 HOURS
T1 (1.22-1.52m)

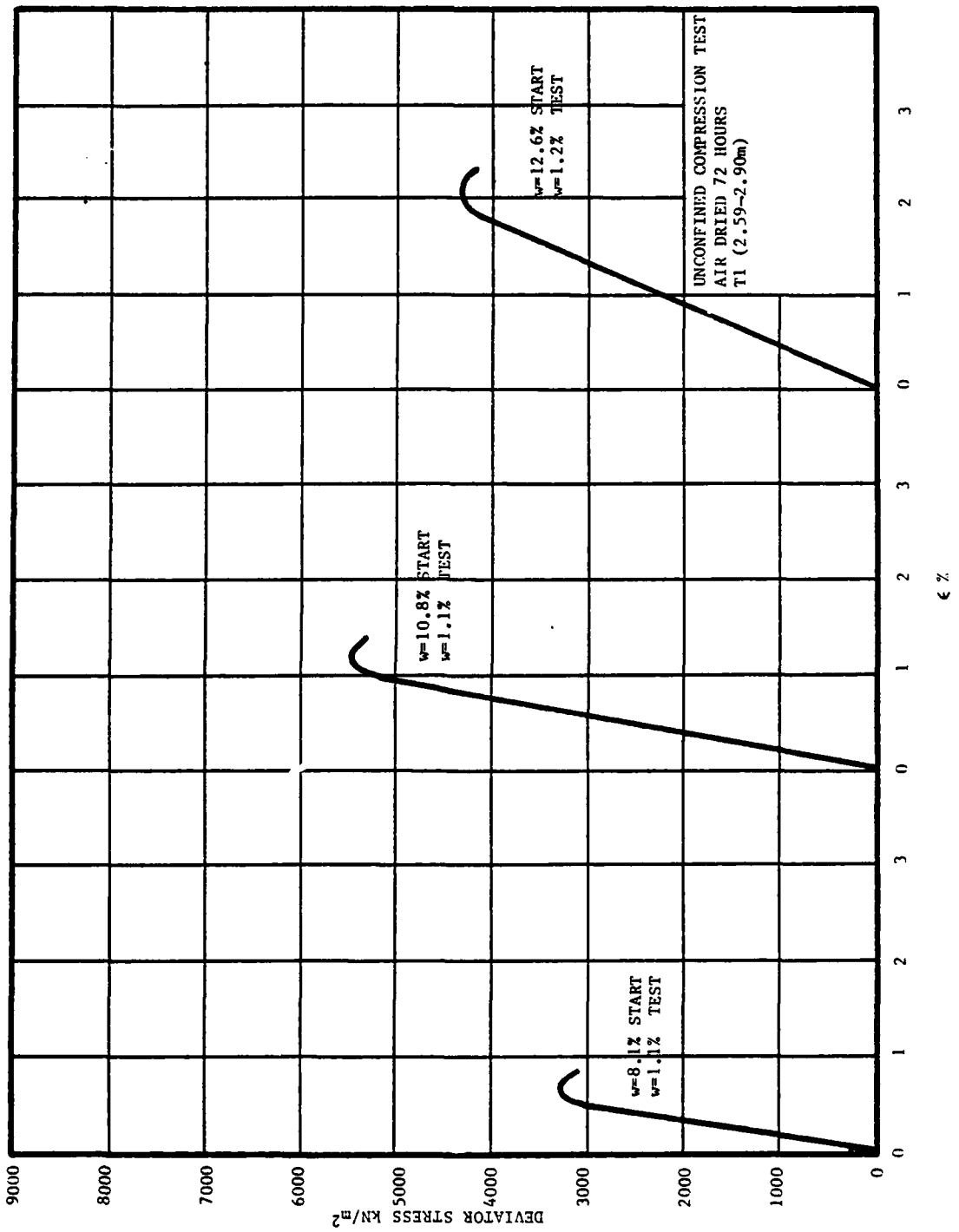
UNCONFINED COMPRESSION TEST
AIR DRIED 72 HOURS
T1 (2.59~2.90m)
w=12.6% START
w=1.2% TEST
w=10.8% START
w=1.1% TEST
w=8.1% START
w=1.1% TEST
DEVIATOR STRESS kN/m²
9000
8000
7000
6000
5000
4000
3000
2000
1000
0
0
1
2
3
0
1
2
3
0
1
2
3
ε %

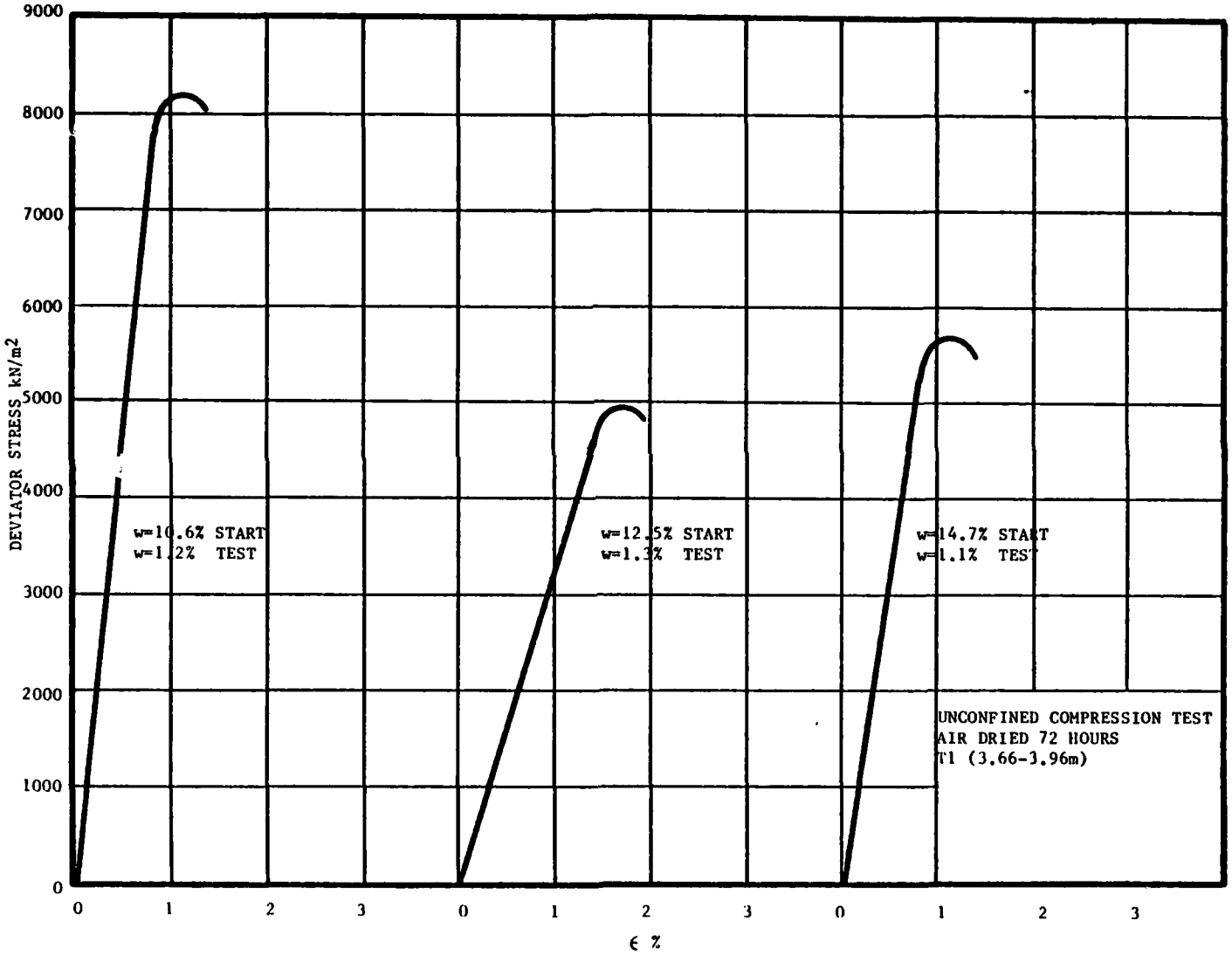
9000
8000
7000
6000
5000
4000
3000
2000
1000
0
DEVIATOR STRESS kN/m2
w=10.6% START
w=1.2% TEST
w=12.5% START
w=1.3% TEST
w=14.7% START
w=1.1% TEST
UNCONFINED COMPRESSION TEST
AIR DRIED 72 HOURS
T1 (3.66-3.96m)
0
1
2
3
0
1
2
3
0
1
2
3
ϵ %

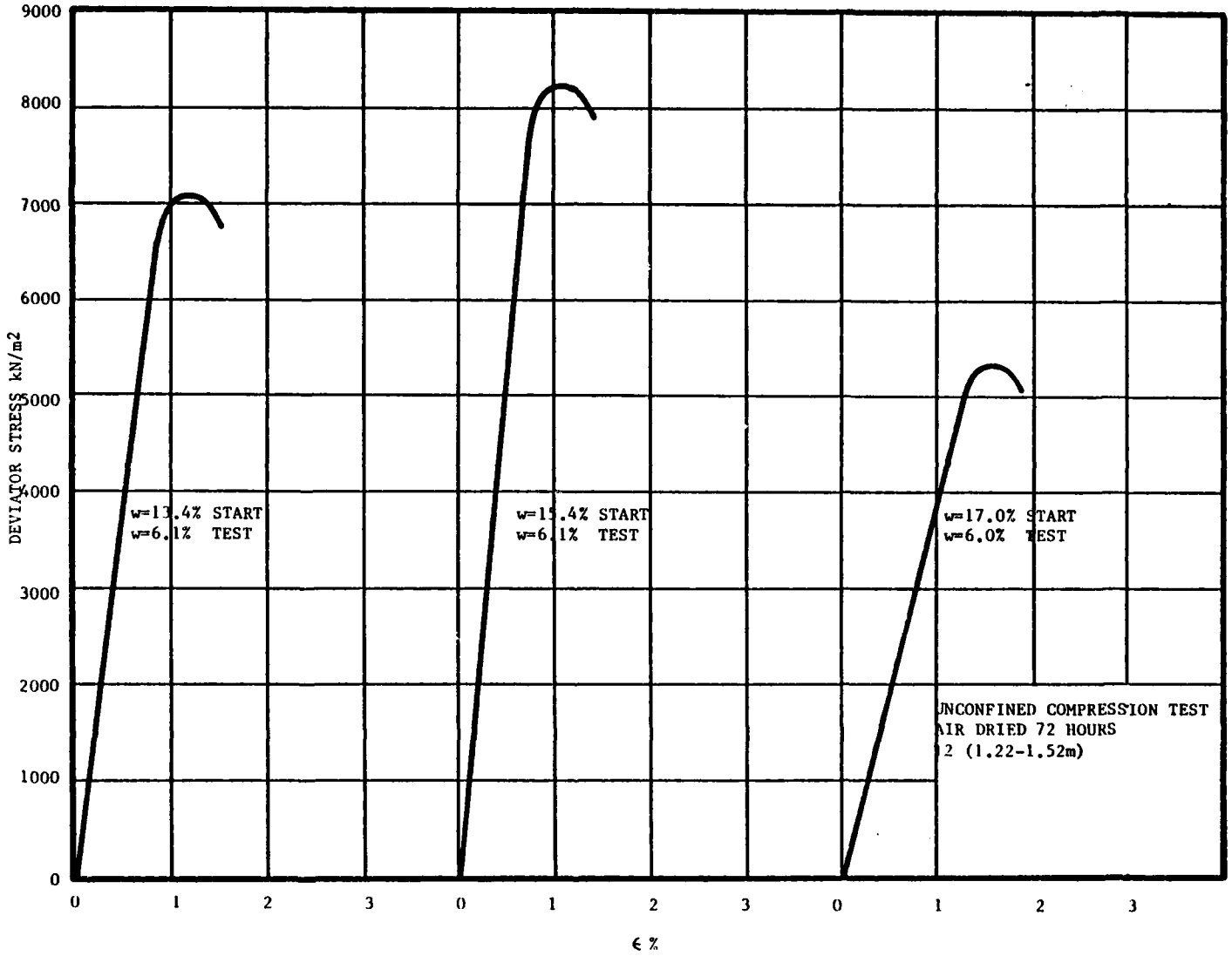
9000
8000
7000
6000
5000
4000
3000
2000
1000
0
DEVIATOR STRESS kN/m2
w=13.4% START
w=6.1% TEST
w=13.4% START
w=6.1% TEST
w=17.0% START
w=6.0% TEST
UNCONFINED COMPRESSION TEST
AIR DRIED 72 HOURS
2 (1.22-1.52m)
0
1
2
3
0
1
2
3
0
1
2
3
ε %

APPENDIX C

UNCONFINED COMPRESSION TESTS ON SOIL SAMPLES AT VARIOUS WATER CONTENTS

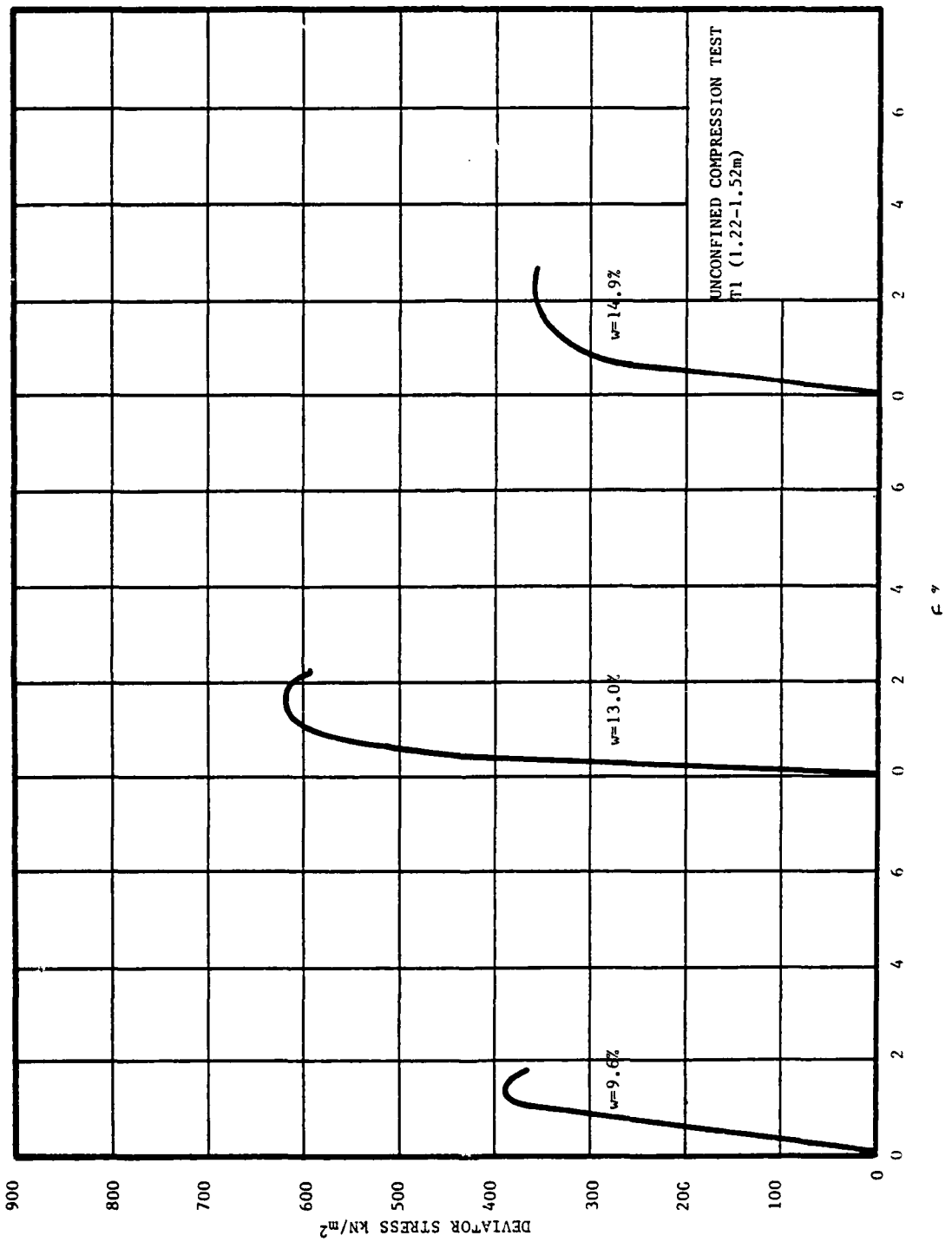
UNCONFINED COMPRESSION TEST
T1 (1.22-1.52m)
w=14.9%
w=13.0%
w=9.6%
DEVIATOR STRESS kN/m²
0
100
200
300
400
500
600
700
800
900
0
2
4
6
0
2
4
6
0
2
4
6
ε %

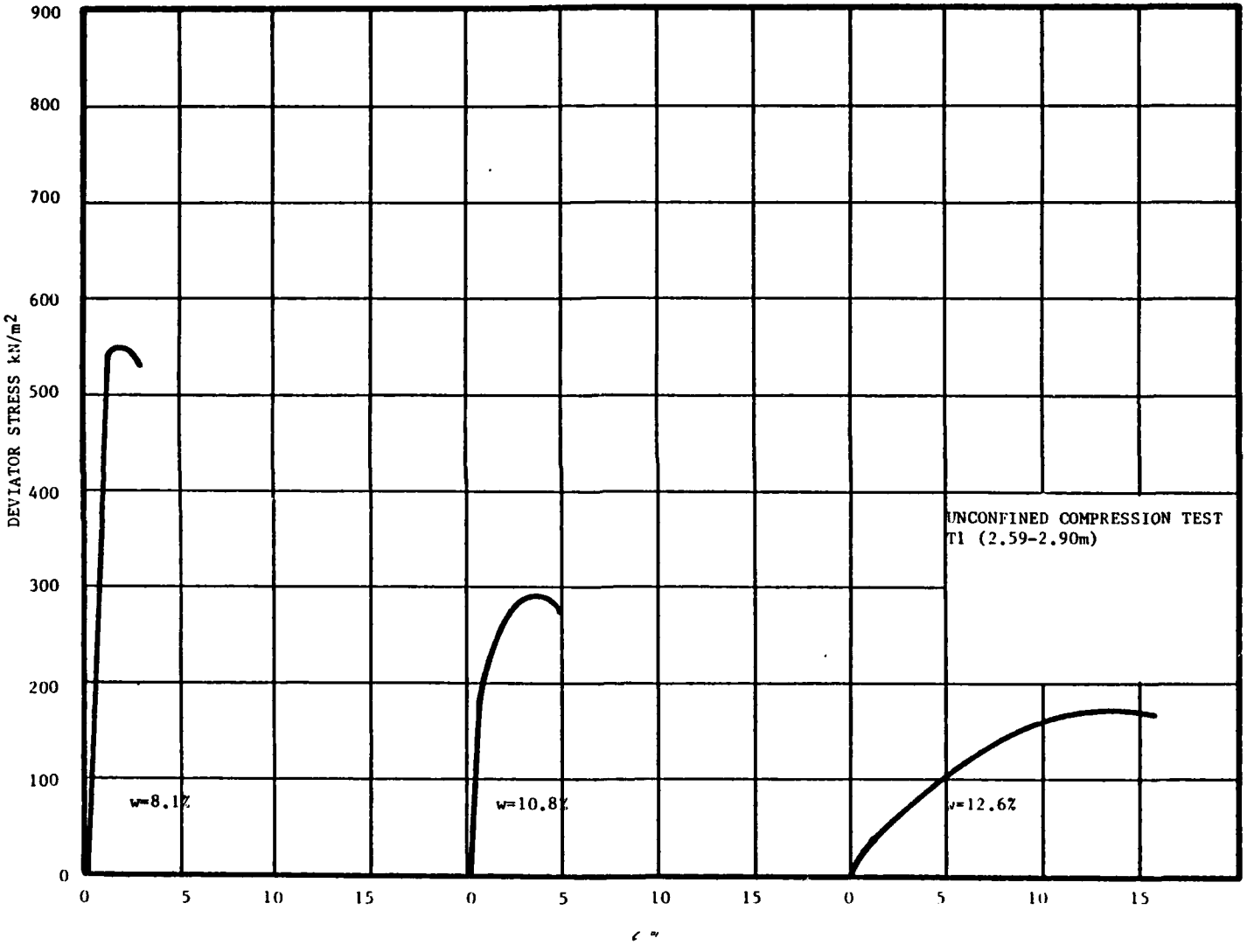
DEVIATOR STRESS kN/m²
900
800
700
600
500
400
300
200
100
0
0
5
10
15
0
5
10
15
0
5
10
15
UNCONFINED COMPRESSION TEST
T1 (2.59-2.90m)
w=8.1%
w=10.8%
w=12.6%

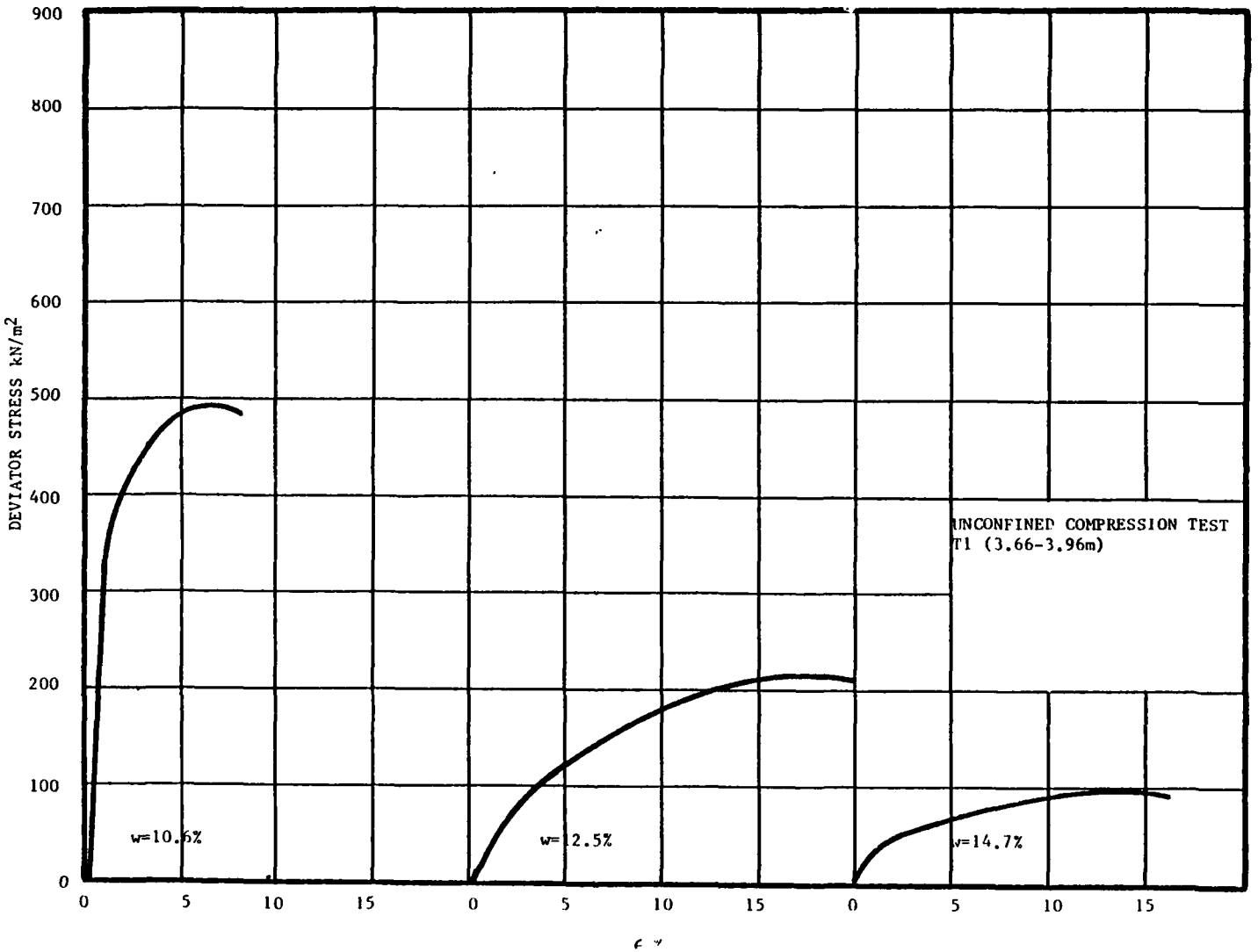
900
800
700
600
500
400
300
200
100
0
DEVIATOR STRESS kN/m2
0
5
10
15
0
5
10
15
0
5
10
15
ε %
w=10.6%
w=12.5%
w=14.7%
UNCONFINED COMPRESSION TEST
T1 (3.66-3.96m)

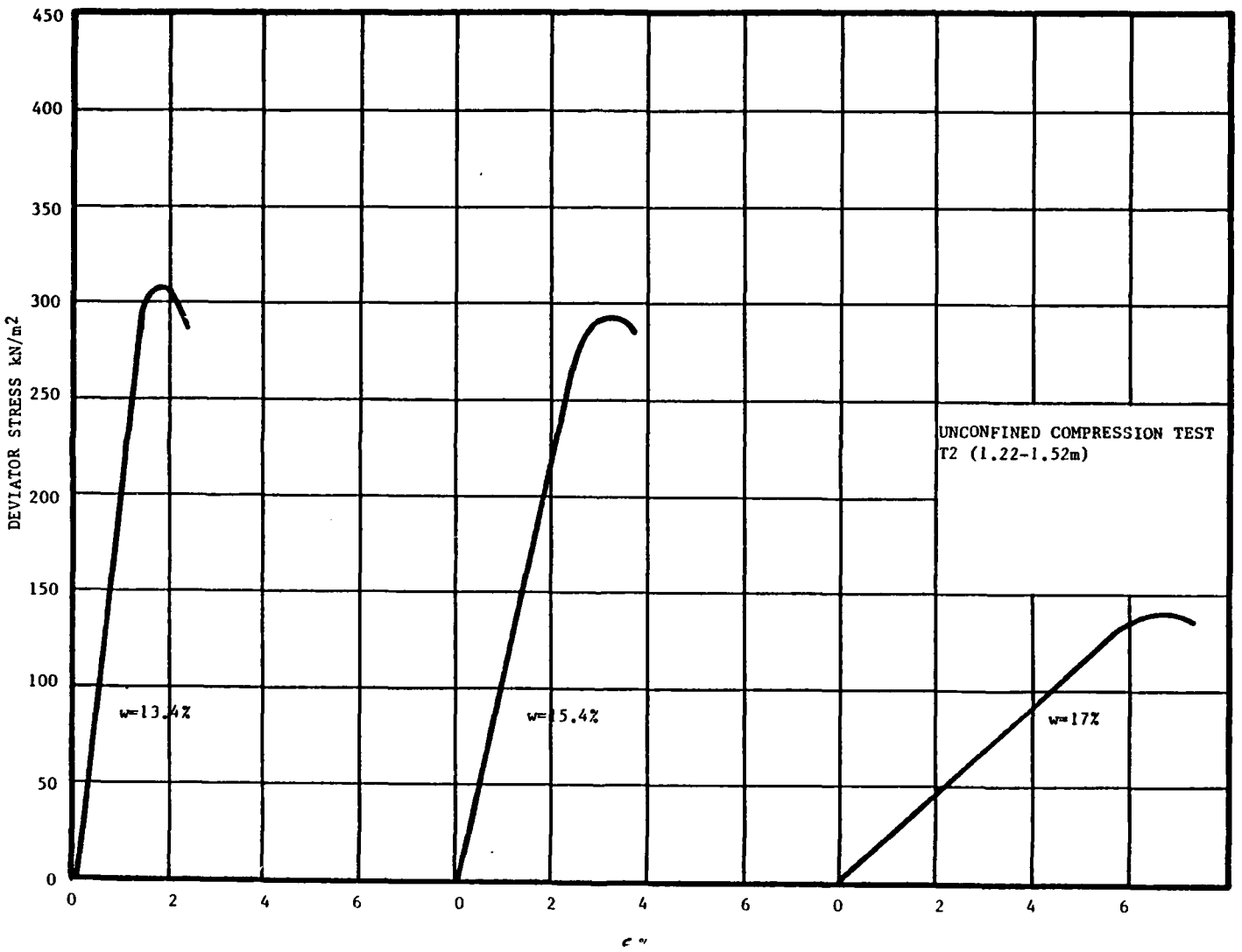
DEVIATOR STRESS kN/m2
450
400
350
300
250
200
150
100
50
0
0
2
4
6
UNCONFINED COMPRESSION TEST
T2 (1.22-1.52m)
w=13.4%
w=15.4%
w=17%

APPENDIX D

TRIAXIAL COMPRESSION TESTS ON AIR-DRIED SOIL SAMPLES

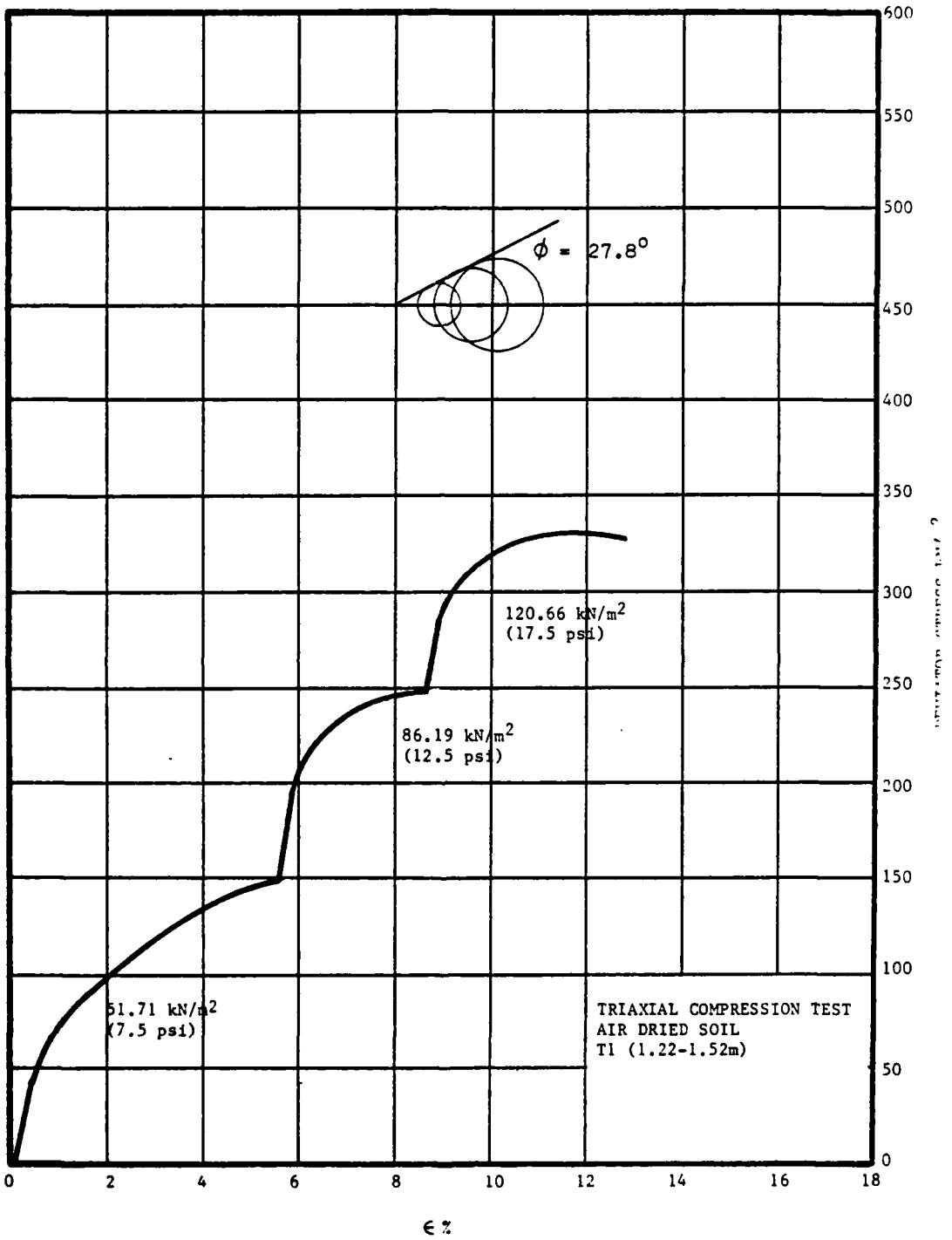
600
550
500
450
400
350
300
250
200
150
100
50
0
ϕ = 27.8°
120.66 kN/m^2
(17.5 psi)
86.19 kN/m^2
(12.5 psi)
51.71 kN/m^2
(7.5 psi)
TRIAXIAL COMPRESSION TEST
AIR DRIED SOIL
T1 (1.22-1.52m)
0
2
4
6
8
10
12
14
16
18
ϵ %

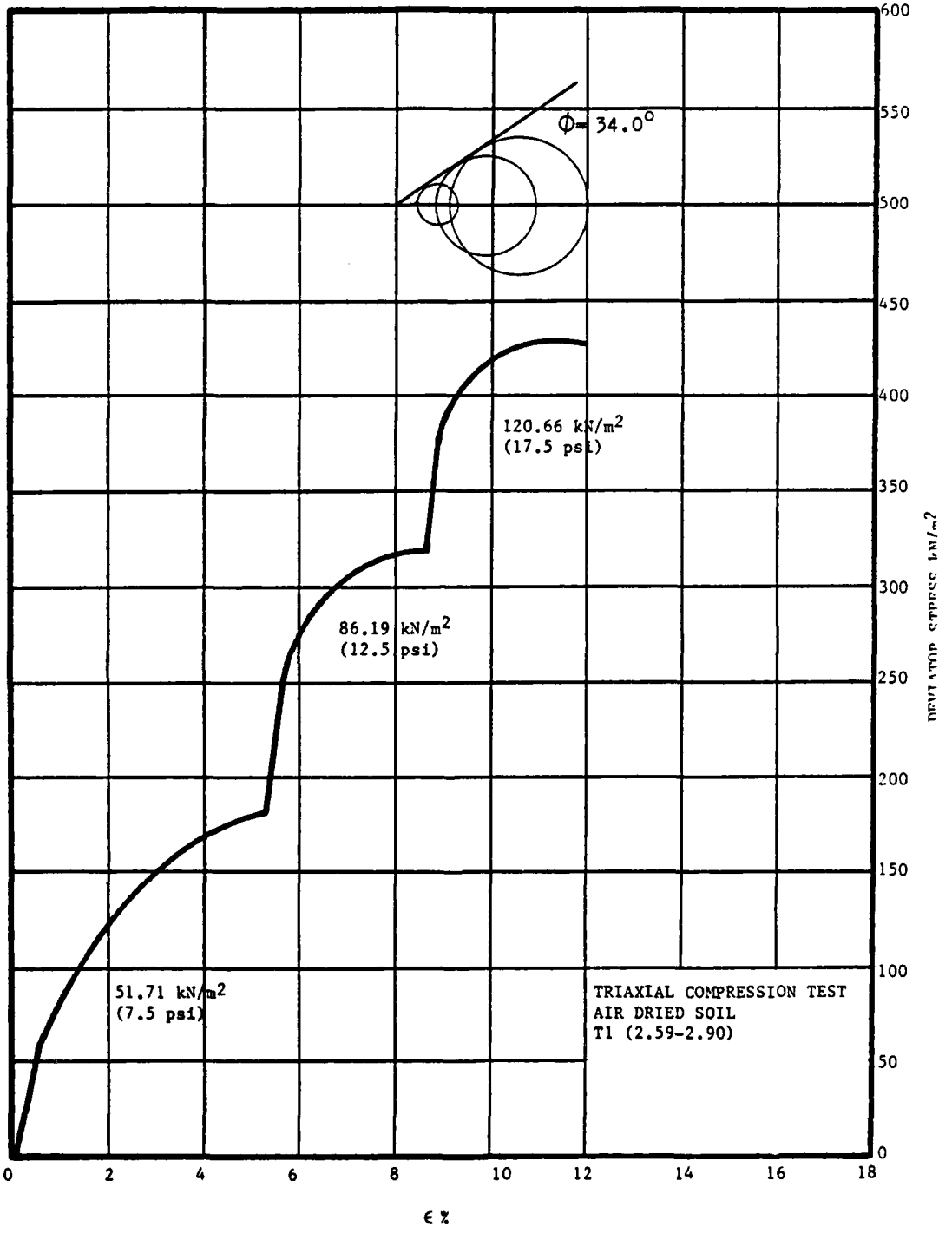
ϕ= 34.0°
120.66 kN/m^2
(17.5 psi)
86.19 kN/m^2
(12.5 psi)
51.71 kN/m^2
(7.5 psi)
TRIAXIAL COMPRESSION TEST
AIR DRIED SOIL
T1 (2.59-2.90)
0
50
100
150
200
250
300
350
400
450
500
550
600
0
2
4
6
8
10
12
14
16
18
ϵ %

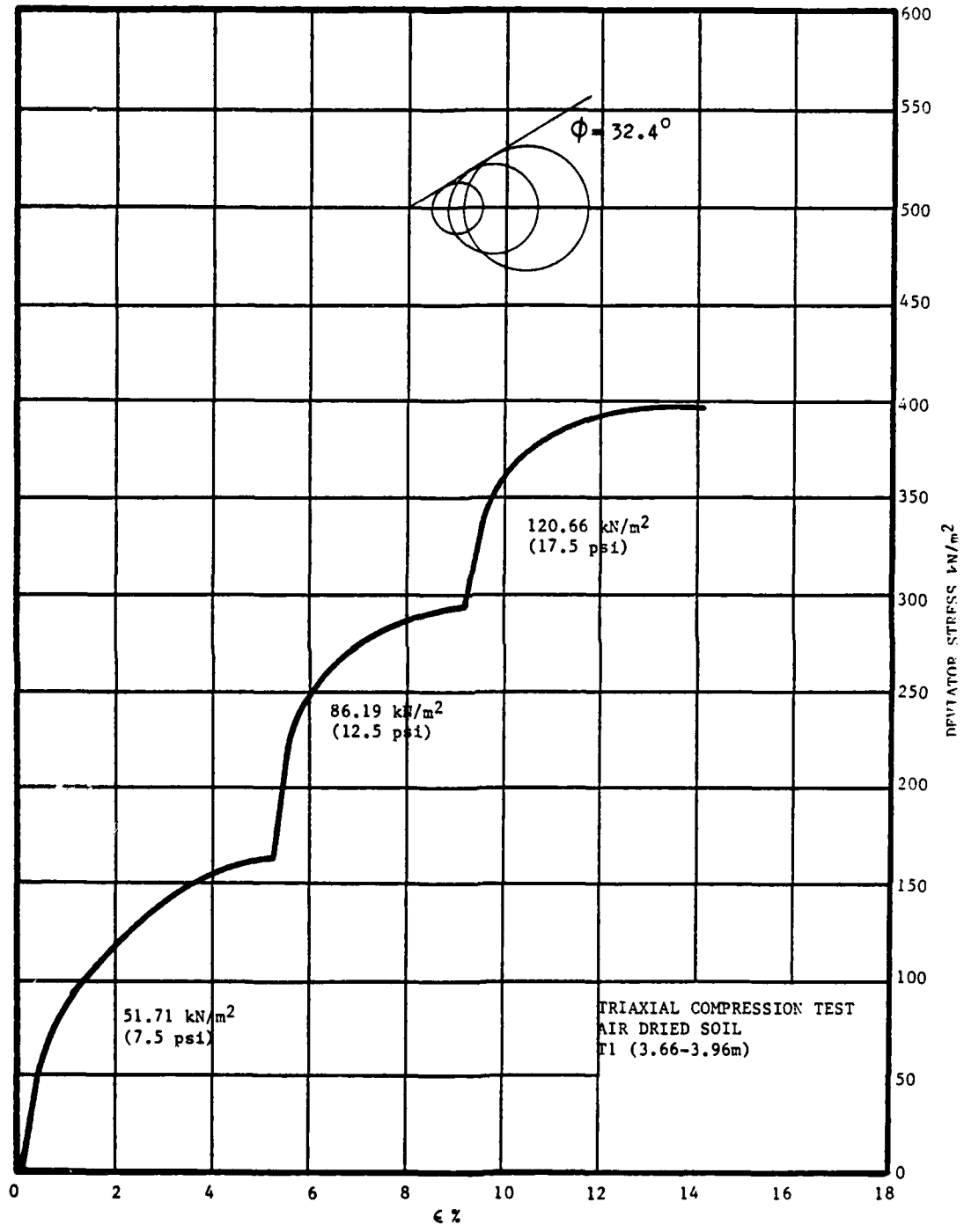
Φ = 32.4°
120.66 kN/m2
(17.5 psi)
86.19 kN/m2
(12.5 psi)
51.71 kN/m2
(7.5 psi)
TRIAXIAL COMPRESSION TEST
AIR DRIED SOIL
T1 (3.66-3.96m)
DEVIATOR STRESS kN/m2
600
550
500
450
400
350
300
250
200
150
100
50
0
0
2
4
6
8
10
12
14
16
18
ε %

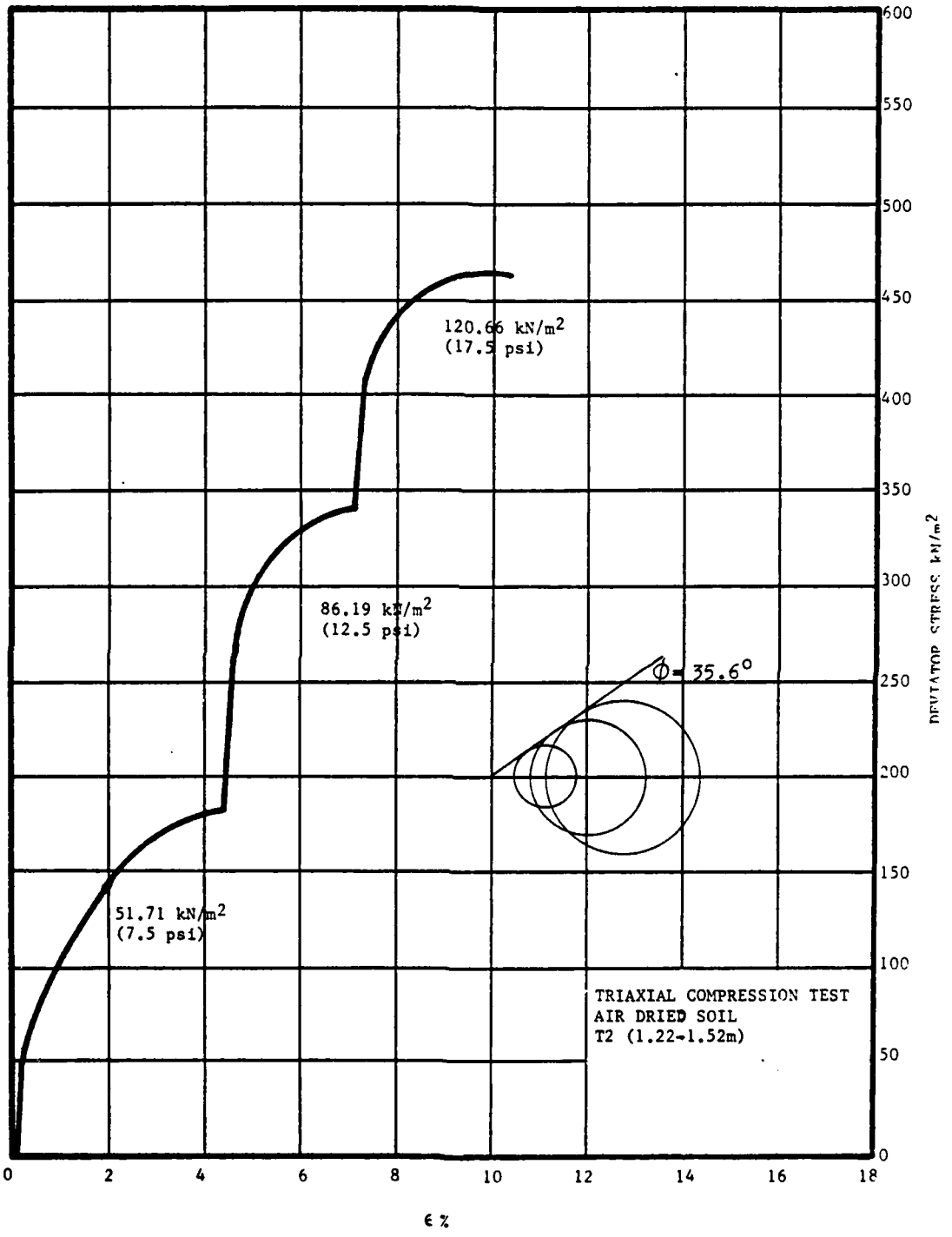
120.66 kN/m2
(17.5 psi)
86.19 kN/m2
(12.5 psi)
51.71 kN/m2
(7.5 psi)
Φ = 35.6°
TRIAXIAL COMPRESSION TEST
AIR DRIED SOIL
T2 (1.22-1.52m)
DEVIATOR STRESS kN/m2
600
550
500
450
400
350
300
250
200
150
100
50
0
0
2
4
6
8
10
12
14
16
18
ε %

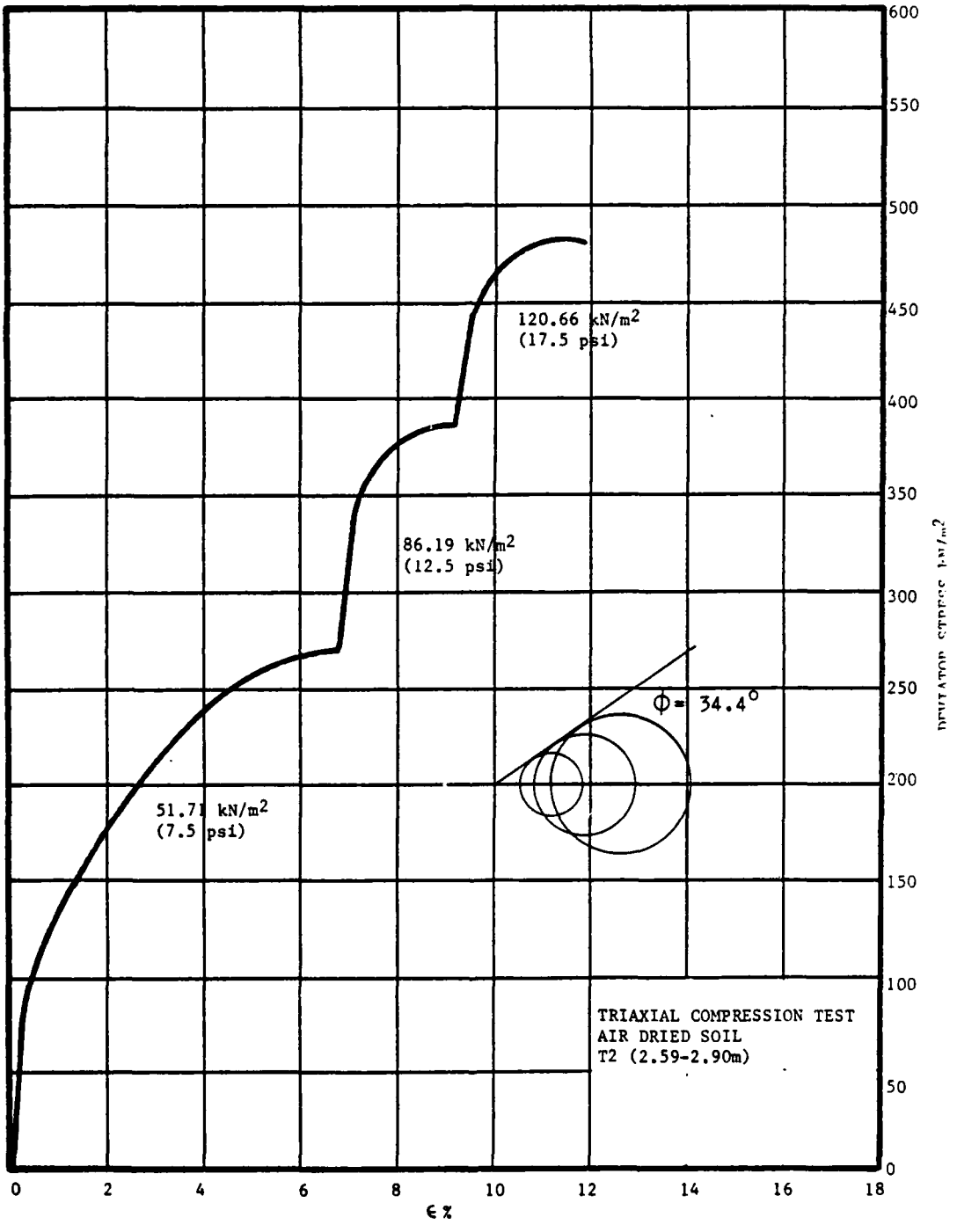
120.66 kN/m2
(17.5 psi)
86.19 kN/m2
(12.5 psi)
51.71 kN/m2
(7.5 psi)
Φ = 34.4°
TRIAXIAL COMPRESSION TEST
AIR DRIED SOIL
T2 (2.59-2.90m)
0
50
100
150
200
250
300
350
400
450
500
550
600
0
2
4
6
8
10
12
14
16
18
ε %

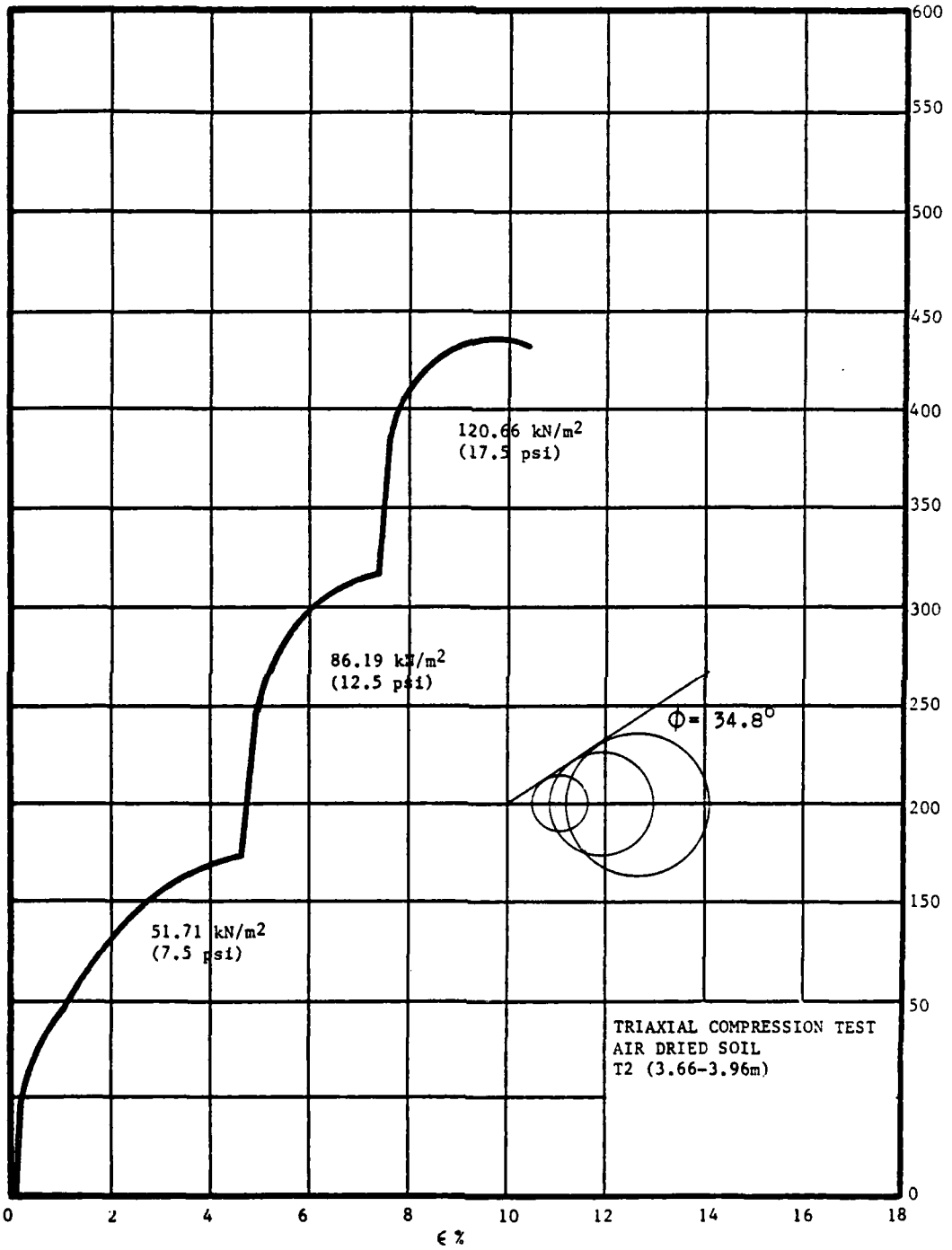
600
550
500
450
400
350
300
250
200
150
50
0
120.66 kN/m2
(17.5 psi)
86.19 kN/m2
(12.5 psi)
51.71 kN/m2
(7.5 psi)
Φ= 34.8°
TRIAXIAL COMPRESSION TEST
AIR DRIED SOIL
T2 (3.66-3.96m)
0
2
4
6
8
10
12
14
16
18
ε %

APPENDIX E

TRIAXIAL COMPRESSION TESTS ON SOIL SAMPLES AT VARIOUS WATER CONTENTS

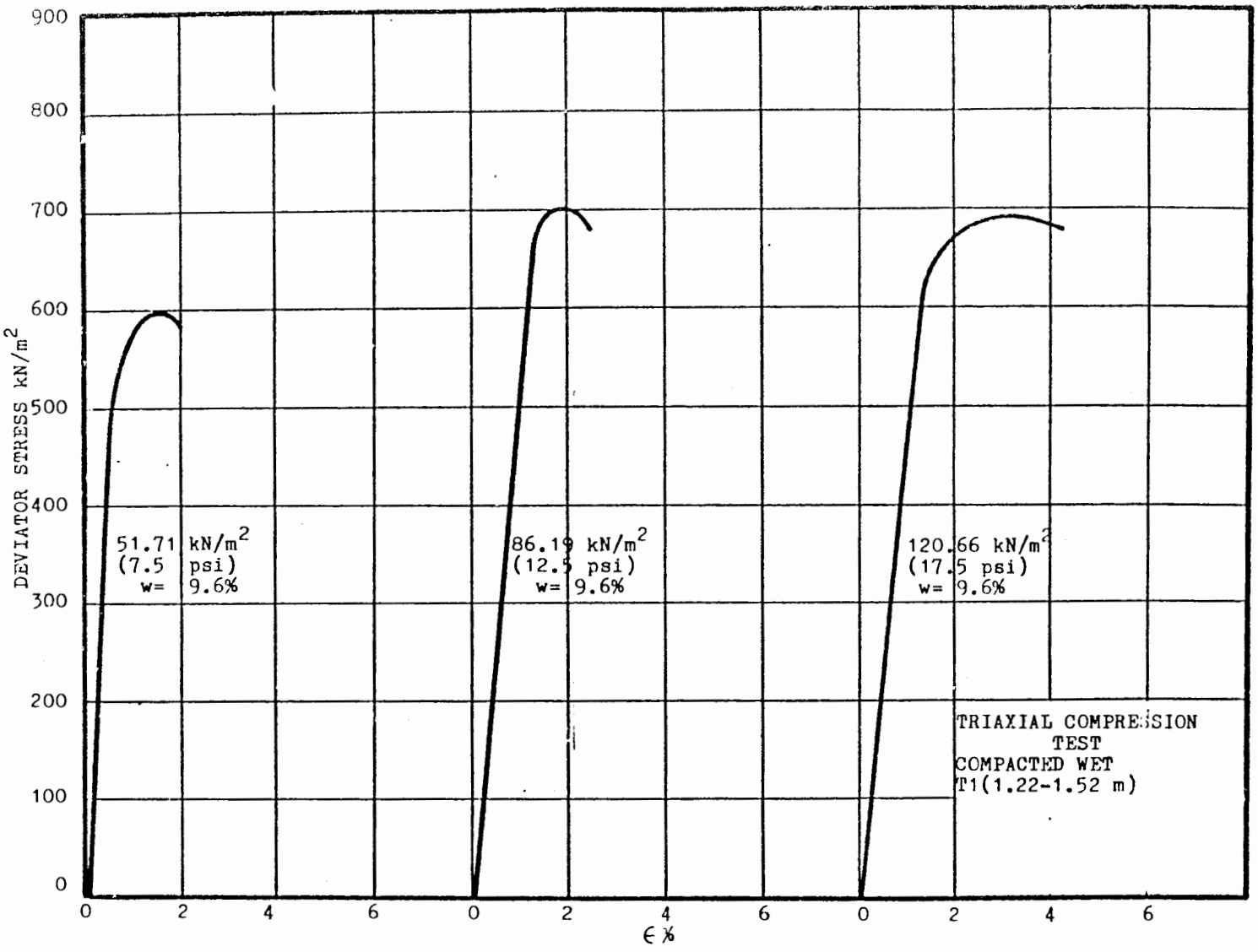
DEVIATOR STRESS kN/m2
900
800
700
600
500
400
300
200
100
0
0
2
4
6
0
2
4
6
0
2
4
6
ϵ %
51.71 kN/m2
(7.5 psi)
w= 9.6%
86.19 kN/m2
(12.5 psi)
w= 9.6%
120.66 kN/m2
(17.5 psi)
w= 9.6%
TRIAXIAL COMPRESSION
TEST
COMPACTED WET
T1(1.22-1.52 m)

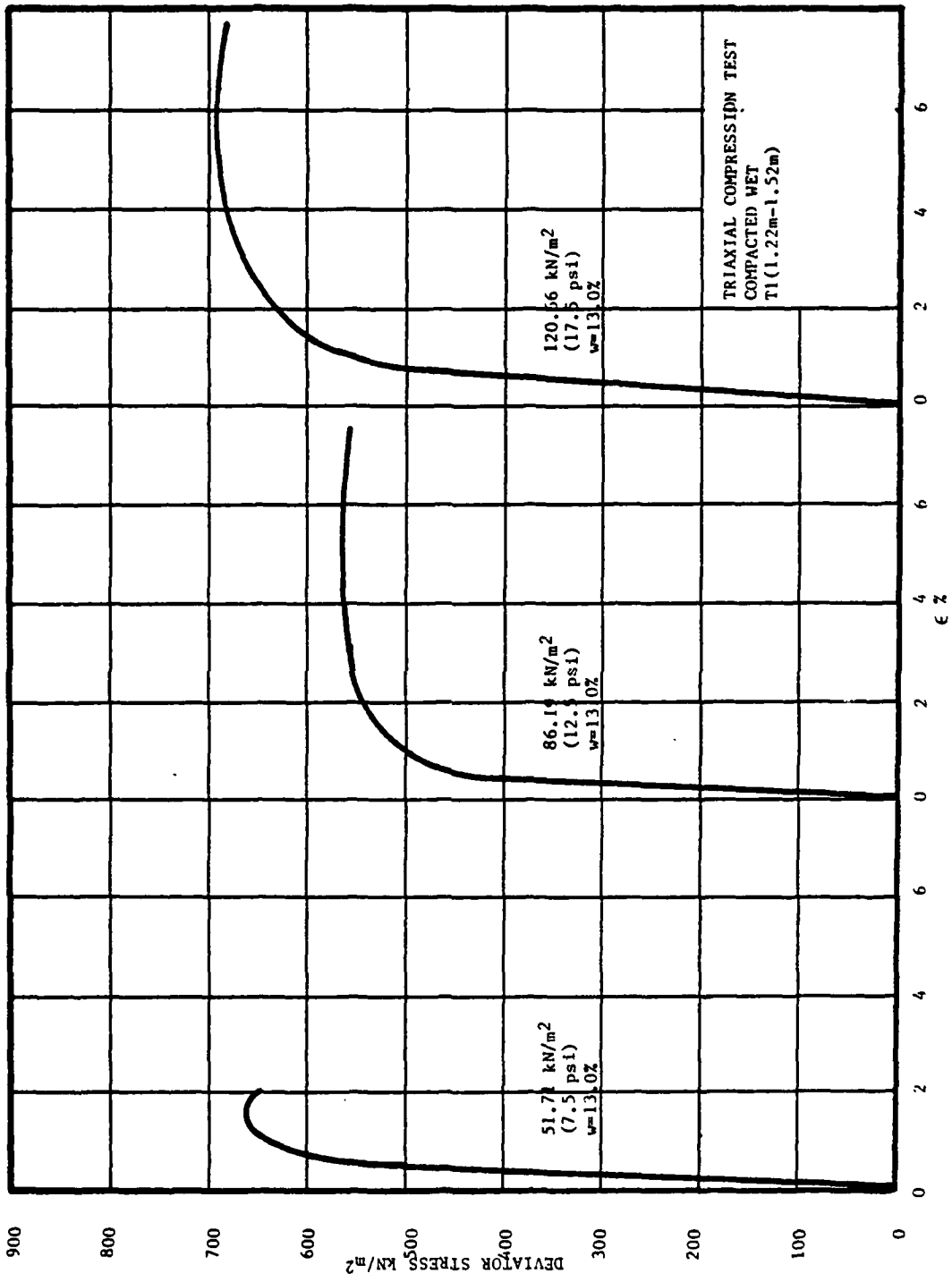
TRIAXIAL COMPRESSION TEST
COMPACTED WET
T1(1.22m-1.52m)
120.66 kN/m2
(17.5 psi)
w=13.0%
86.19 kN/m2
(12.5 psi)
w=13.0%
51.71 kN/m2
(7.5 psi)
w=13.0%
DEVIATOR STRESS kN/m2
0
100
200
300
400
500
600
700
800
900
ε %
0
2
4
6
0
2
4
6
0
2
4
6

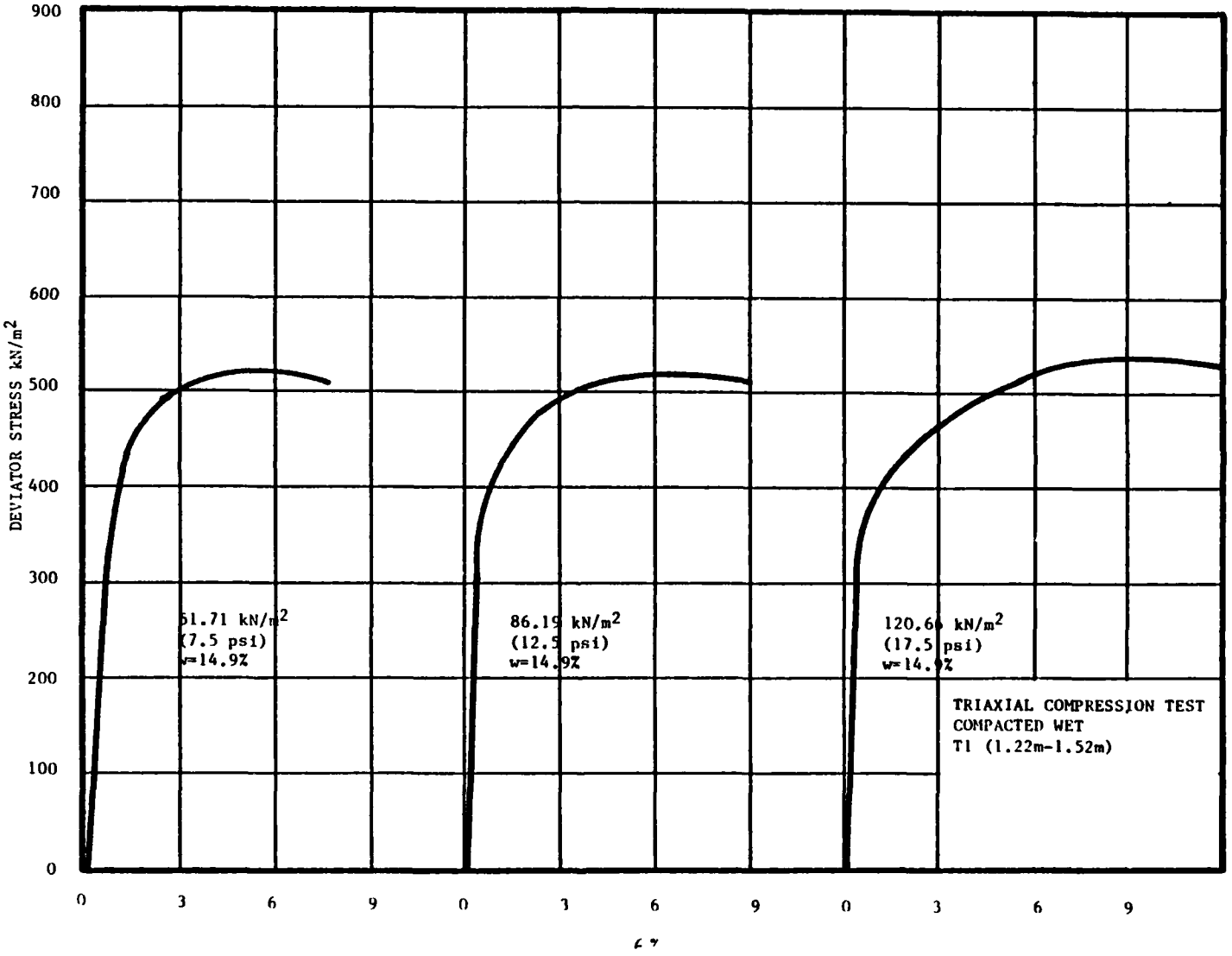
DEVIATOR STRESS kN/m2
900
800
700
600
500
400
300
200
100
0
0
3
6
9
0
3
6
9
0
3
6
9
51.71 kN/m2
(7.5 psi)
w=14.9%
86.19 kN/m2
(12.5 psi)
w=14.9%
120.66 kN/m2
(17.5 psi)
w=14.9%
TRIAXIAL COMPRESSION TEST
COMPACTED WET
T1 (1.22m-1.52m)

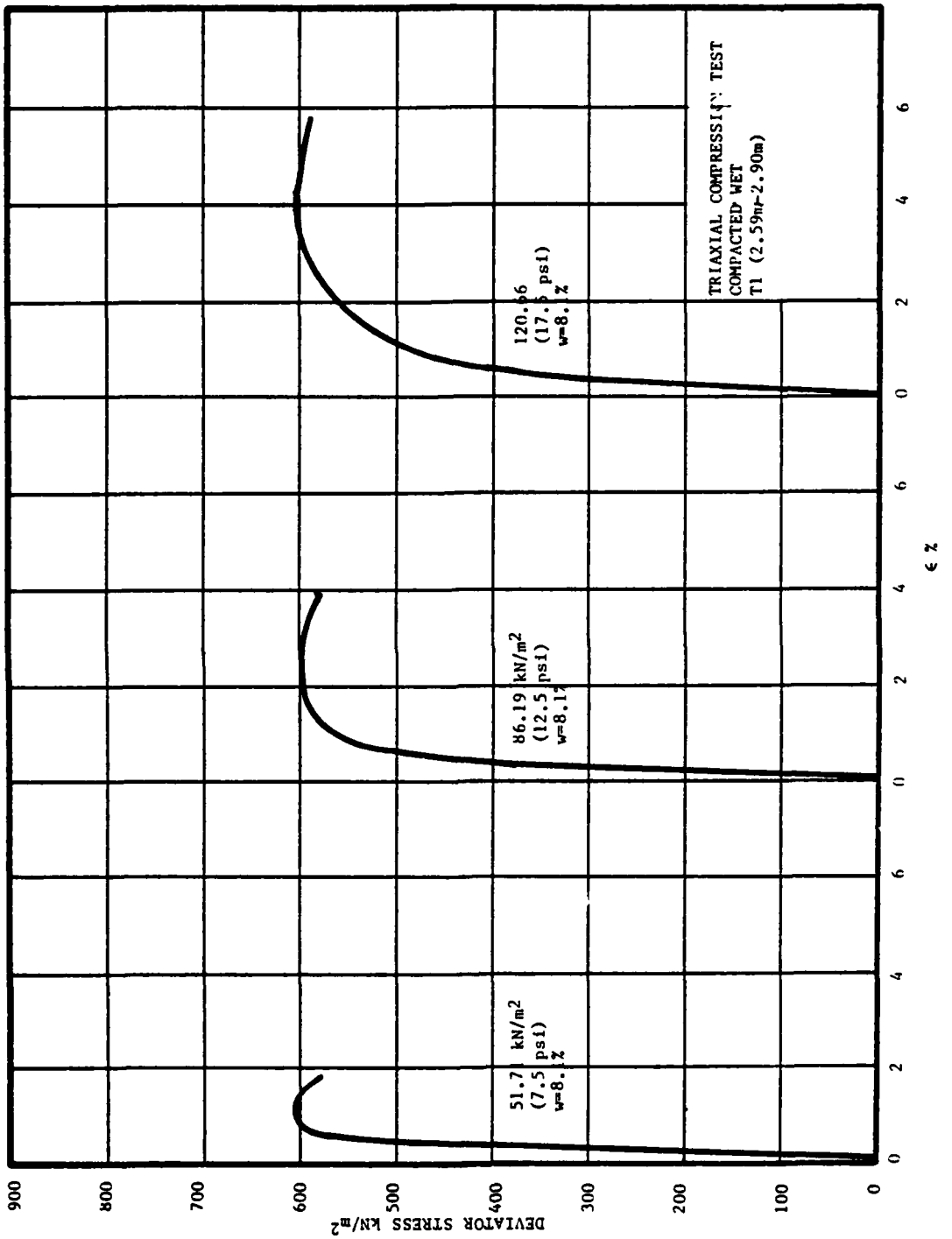
TRIAXIAL COMPRESSION TEST
COMPACTED WET
T1 (2.59m-2.90m)
120.66
(17.5 psi)
w=8.1%
86.19 kN/m²
(12.5 psi)
w=8.1%
51.7 kN/m²
(7.5 psi)
w=8.1%
DEVIATOR STRESS kN/m²
ε %
0
100
200
300
400
500
600
700
800
900
2
4
6

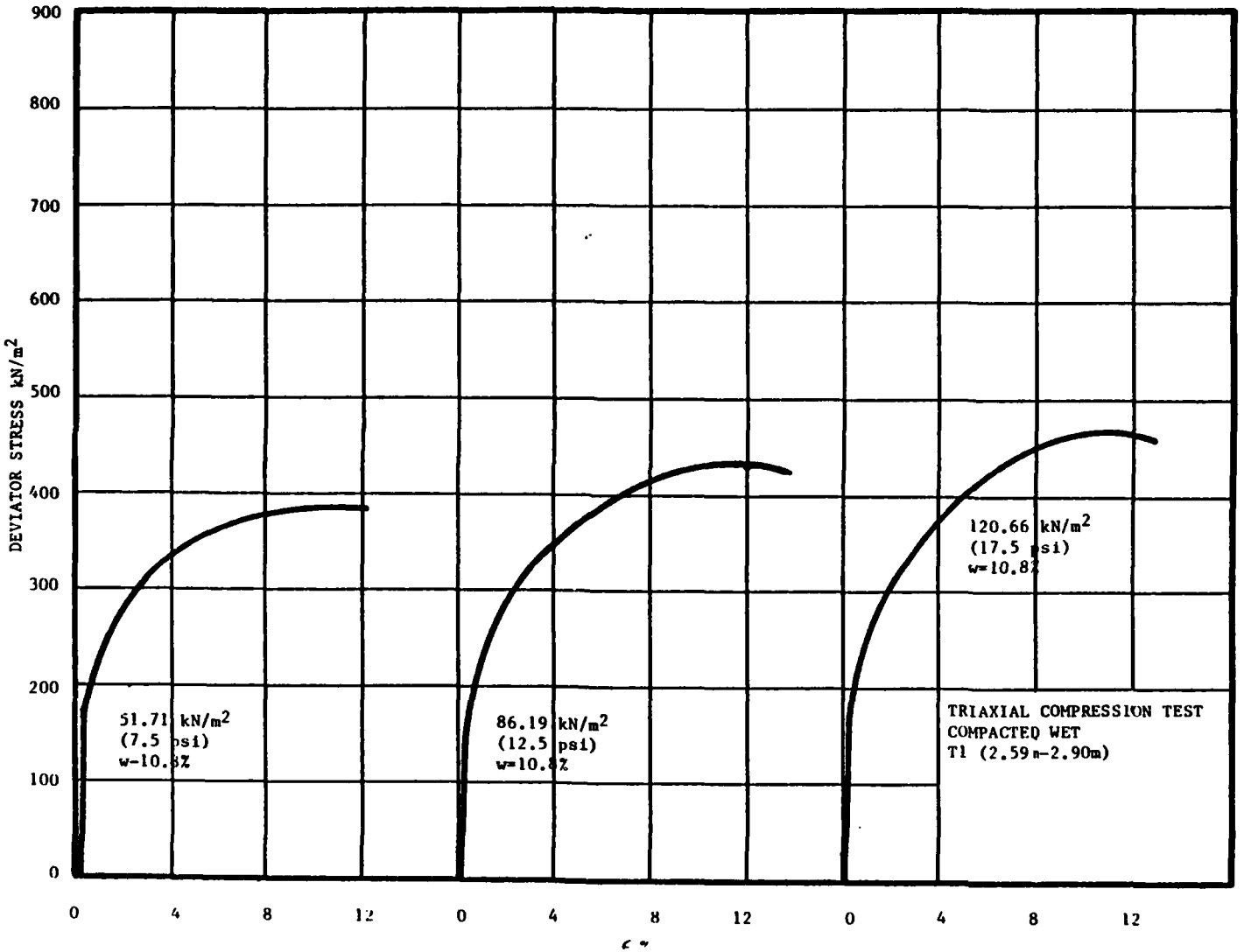
DEVIATOR STRESS kN/m²
900
800
700
600
500
400
300
200
100
0
0
4
8
12
51.71 kN/m²
(7.5 psi)
w=10.8%
86.19 kN/m²
(12.5 psi)
w=10.8%
120.66 kN/m²
(17.5 psi)
w=10.8%
TRIAXIAL COMPRESSION TEST
COMPACTED WET
T1 (2.59m-2.90m)

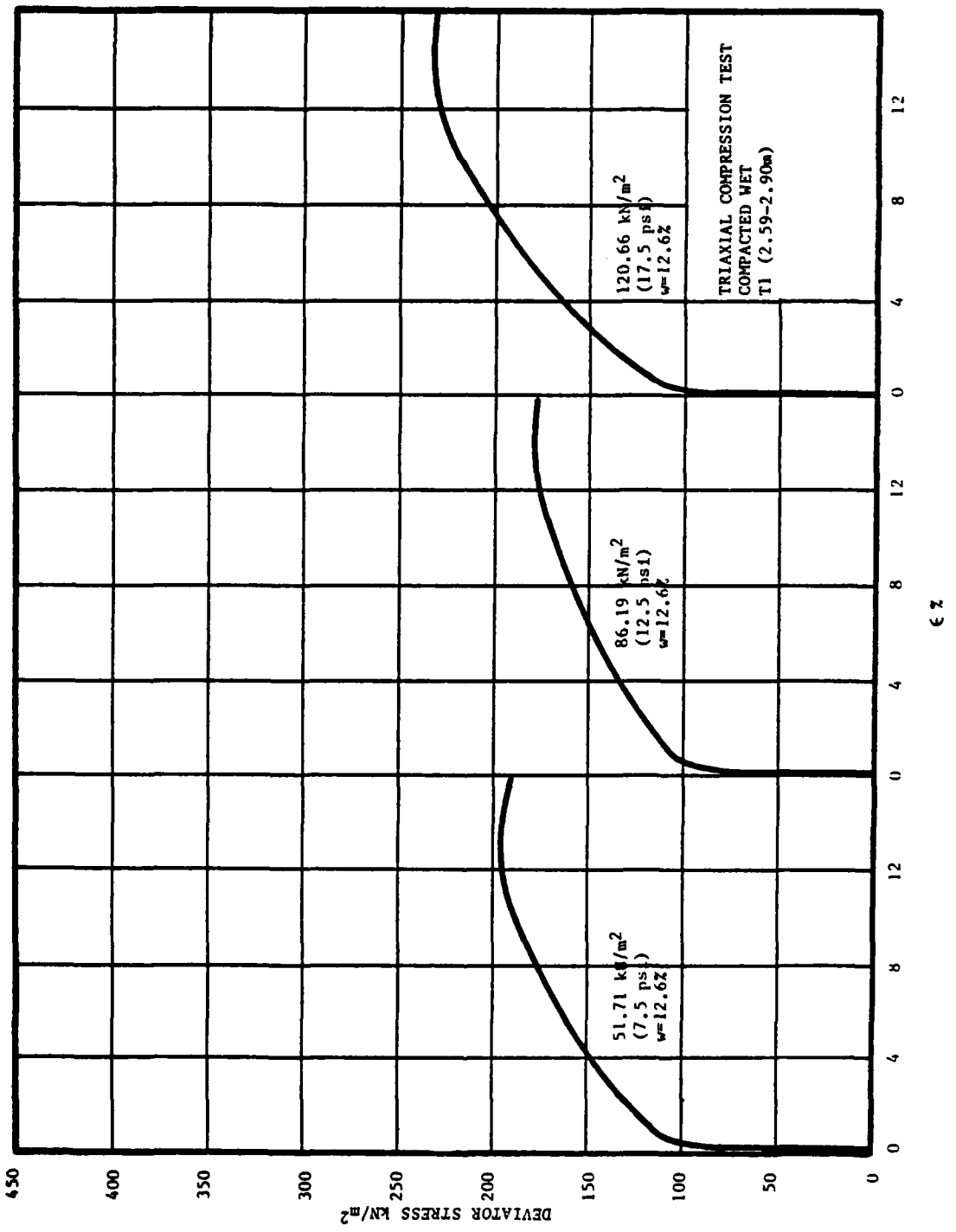
TRIAXIAL COMPRESSION TEST
COMPACTED WET
T1 (2.59-2.90m)
120.66 kN/m2
(17.5 psi)
w=12.6%
86.19 kN/m2
(12.5 psi)
w=12.6%
51.71 kN/m2
(7.5 psi)
w=12.6%
DEVIATOR STRESS kN/m2
450
400
350
300
250
200
150
100
50
0
0
4
8
12
ε %

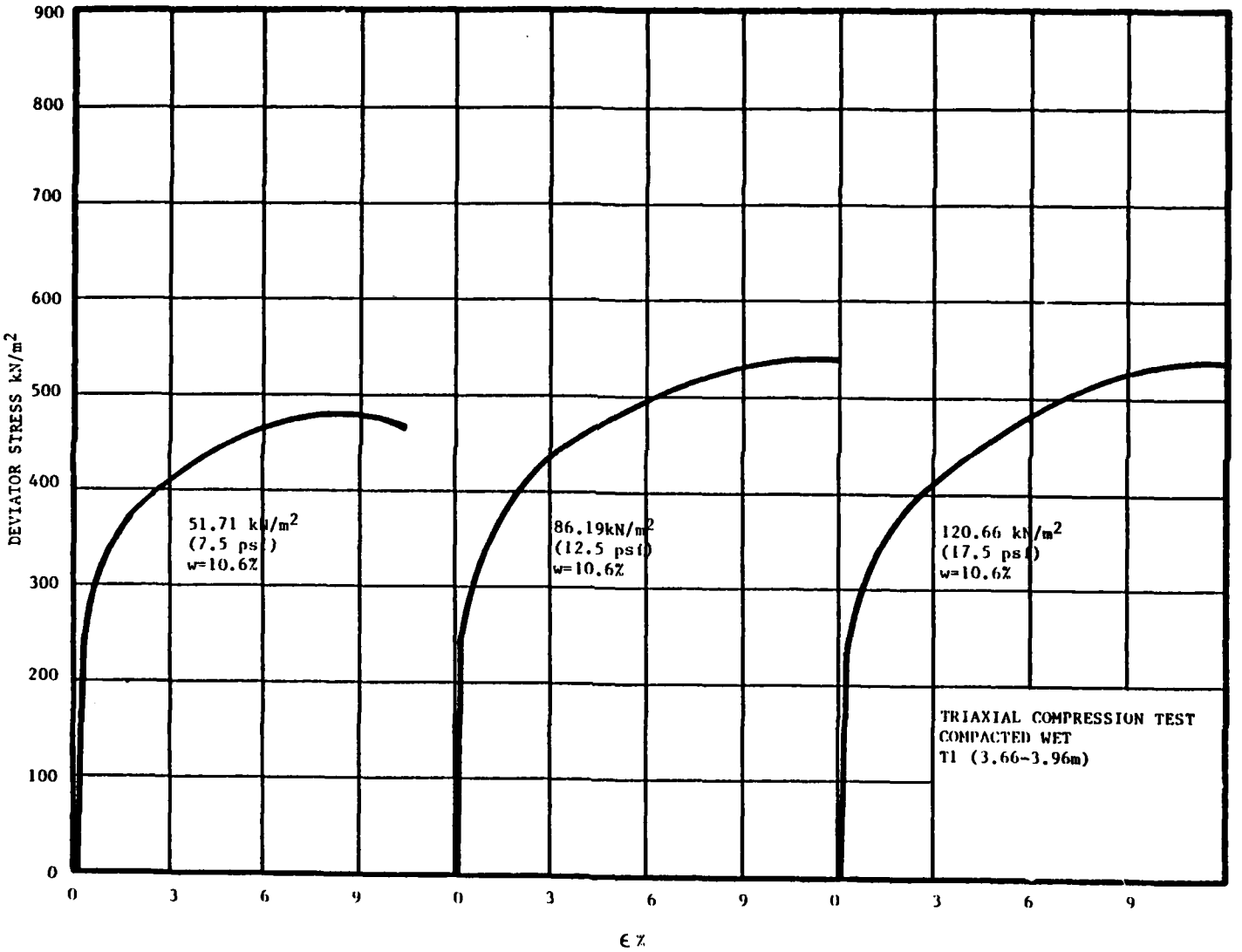
DEVIATOR STRESS kN/m²
900
800
700
600
500
400
300
200
100
0
0
3
6
9
0
3
6
9
0
3
6
9
ε %
51.71 kN/m²
(7.5 psi)
w=10.6%
86.19kN/m²
(12.5 psi)
w=10.6%
120.66 kN/m²
(17.5 psi)
w=10.6%
TRIAXIAL COMPRESSION TEST
COMPACTED WET
T1 (3.66-3.96m)

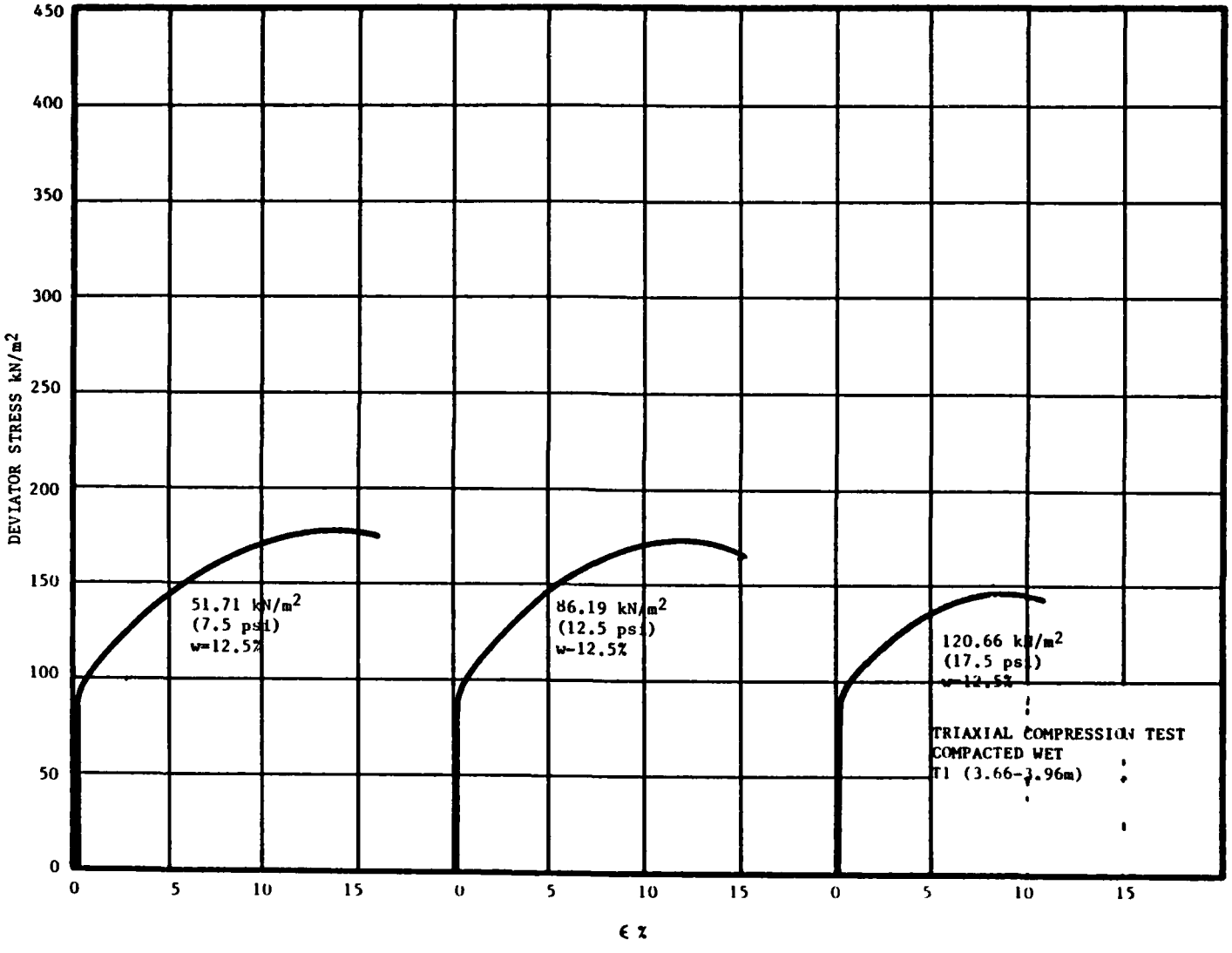
DEVIATOR STRESS kN/m²
450
400
350
300
250
200
150
100
50
0
0
5
10
15
ε %
51.71 kN/m² (7.5 psi) w=12.5%
86.19 kN/m² (12.5 psi) w=12.5%
120.66 kN/m² (17.5 psi) w=12.5%
TRIAXIAL COMPRESSION TEST
COMPACTED WET
T1 (3.66-3.96m)

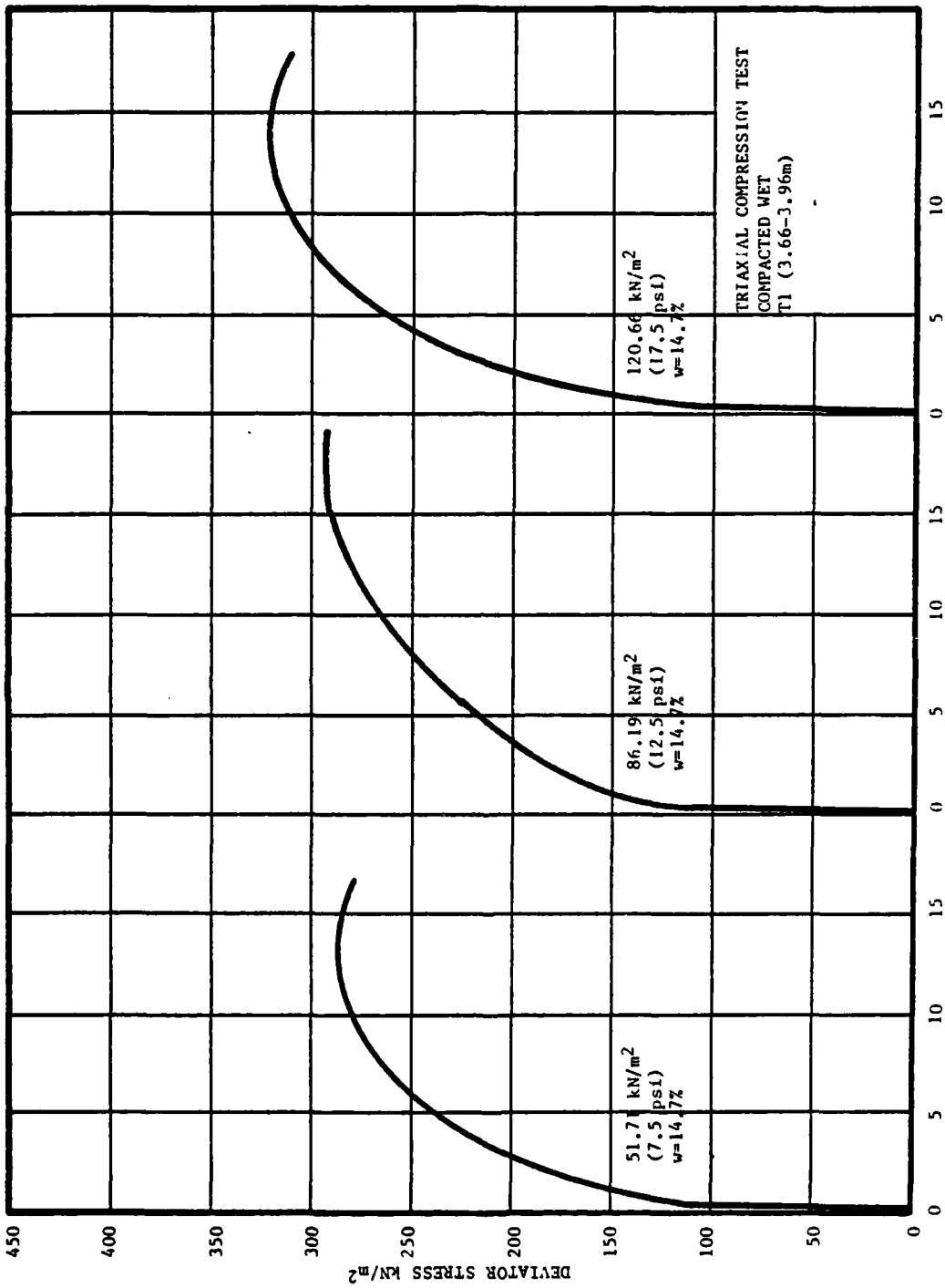
TRIAXIAL COMPRESSION TEST
COMPACTED WET
T1 (3.66-3.96m)
120.66 kN/m2
(17.5 psi)
w=14.7%
86.19 kN/m2
(12.5 psi)
w=14.7%
51.71 kN/m2
(7.5 psi)
w=14.7%
DEVIATOR STRESS kN/m2
0
50
100
150
200
250
300
350
400
450
0
5
10
15
0
5
10
15
0
5
10
15

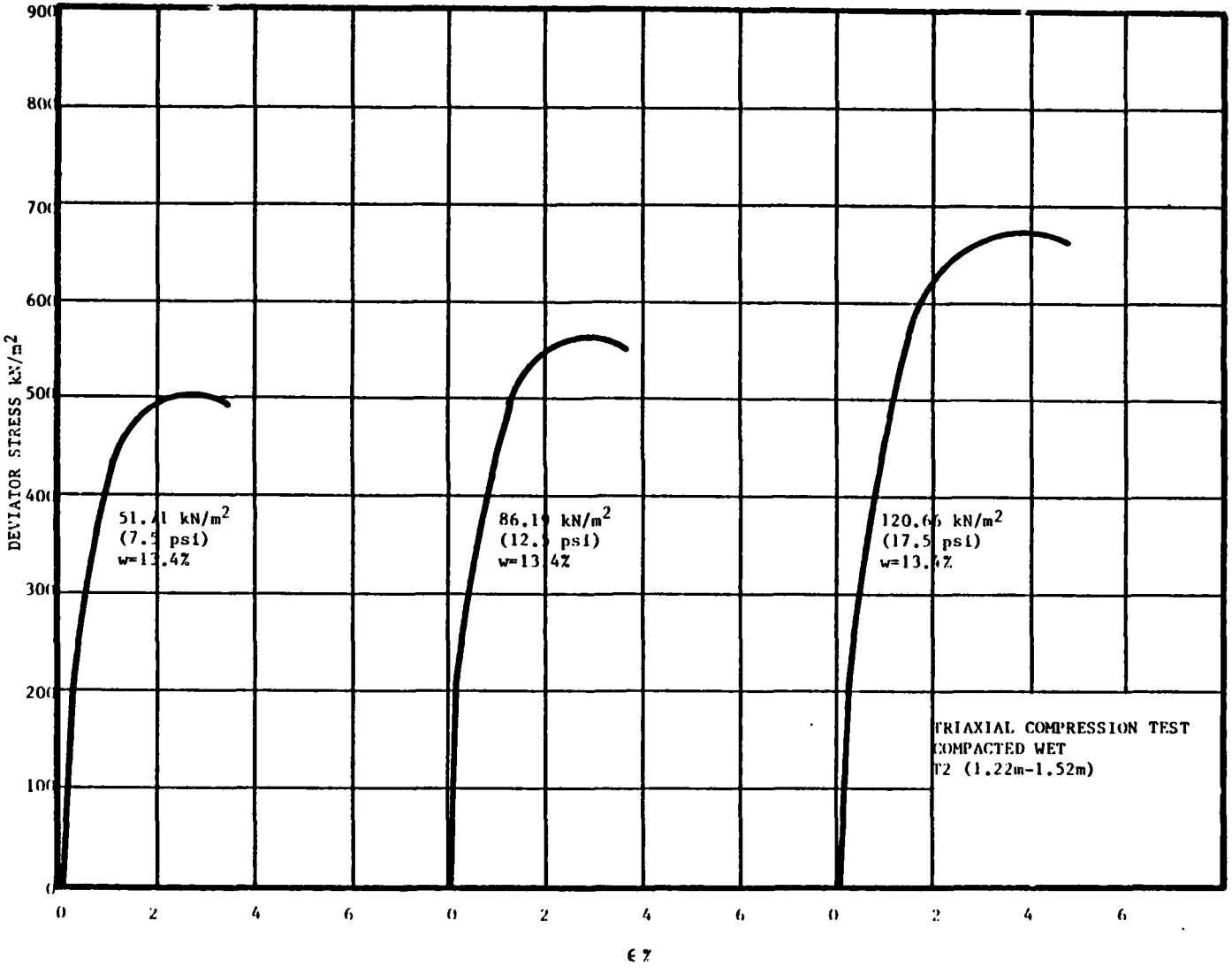
DEVIATOR STRESS kN/m2
900
800
700
600
500
400
300
200
100
0
51.71 kN/m2
(7.5 psi)
w=13.4%
86.19 kN/m2
(12.5 psi)
w=13.4%
120.66 kN/m2
(17.5 psi)
w=13.4%
TRIAXIAL COMPRESSION TEST
COMPACTED WET
T2 (1.22m-1.52m)
0
2
4
6
0
2
4
6
0
2
4
6
ε %

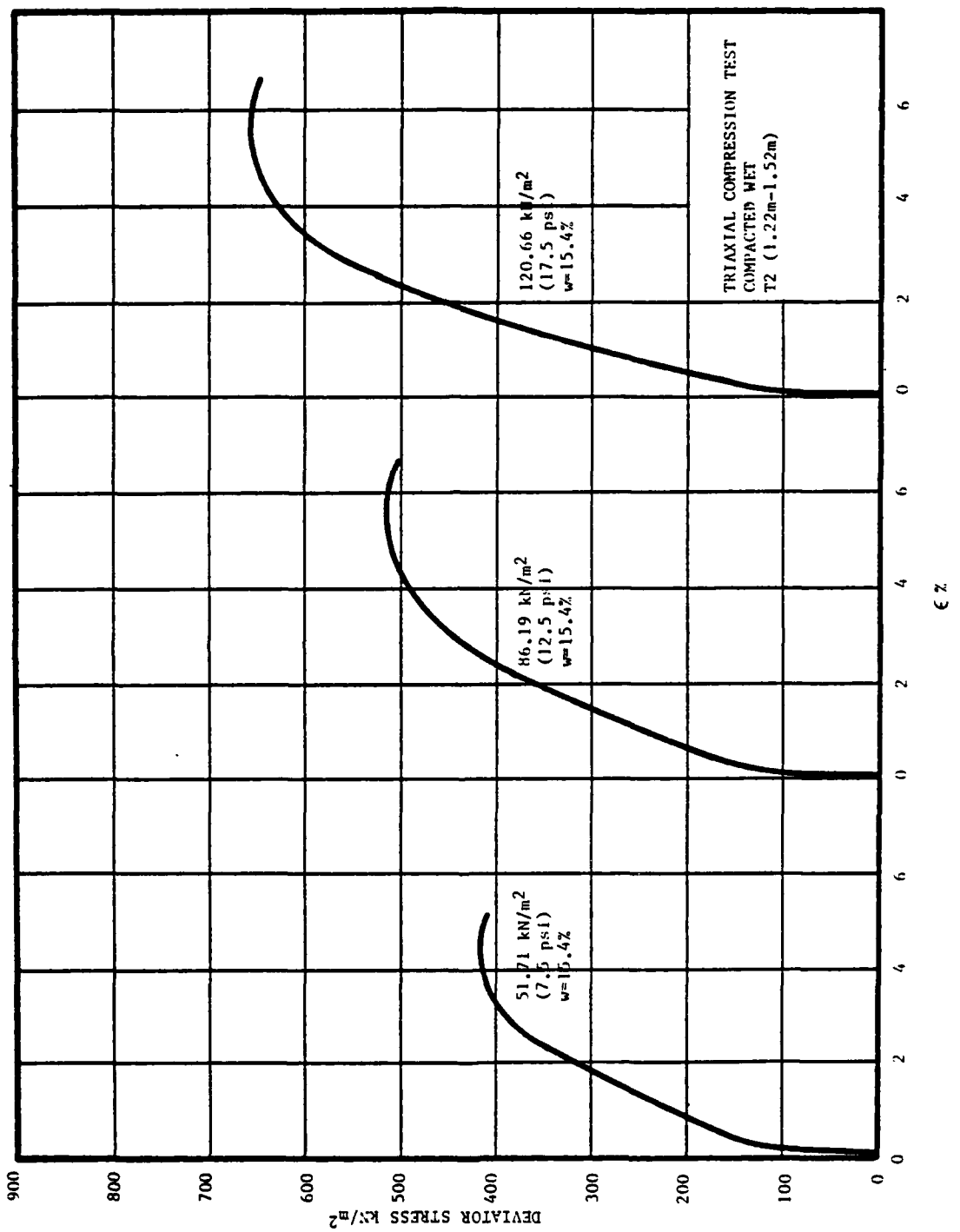
TRIAXIAL COMPRESSION TEST
COMPACTED WET
T2 (1.22m-1.52m)
120.66 kN/m²
(17.5 psi)
w=15.4%
86.19 kN/m²
(12.5 psi)
w=15.4%
51.71 kN/m²
(7.5 psi)
w=15.4%
DEVIATOR STRESS kN/m²
900
800
700
600
500
400
300
200
100
0
0
2
4
6
0
2
4
6
0
2
4
6
ε %

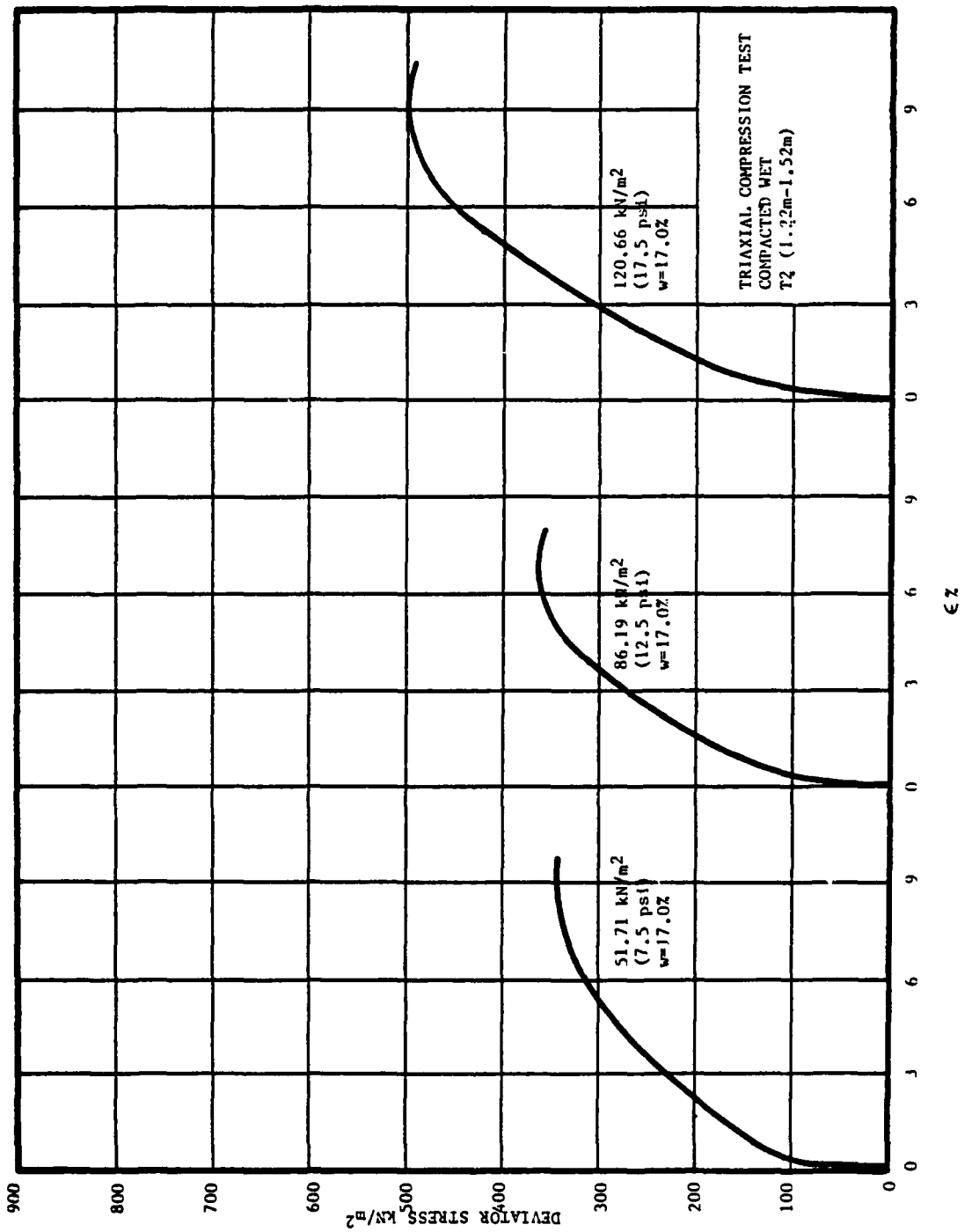
TRIAXIAL COMPRESSION TEST
COMPACTED WET
T2 (1.22m-1.52m)
120.66 kN/m2
(17.5 psi)
w=17.0%
86.19 kN/m2
(12.5 psi)
w=17.0%
51.71 kN/m2
(7.5 psi)
w=17.0%
DEVIATOR STRESS, kN/m2
900
800
700
600
500
400
300
200
100
0
0
3
6
9
0
3
6
9
0
3
6
9
ε z

APPENDIX F

SITE PLAN, WHITE SANDS MISSILE

RANGE SURVEY AREA

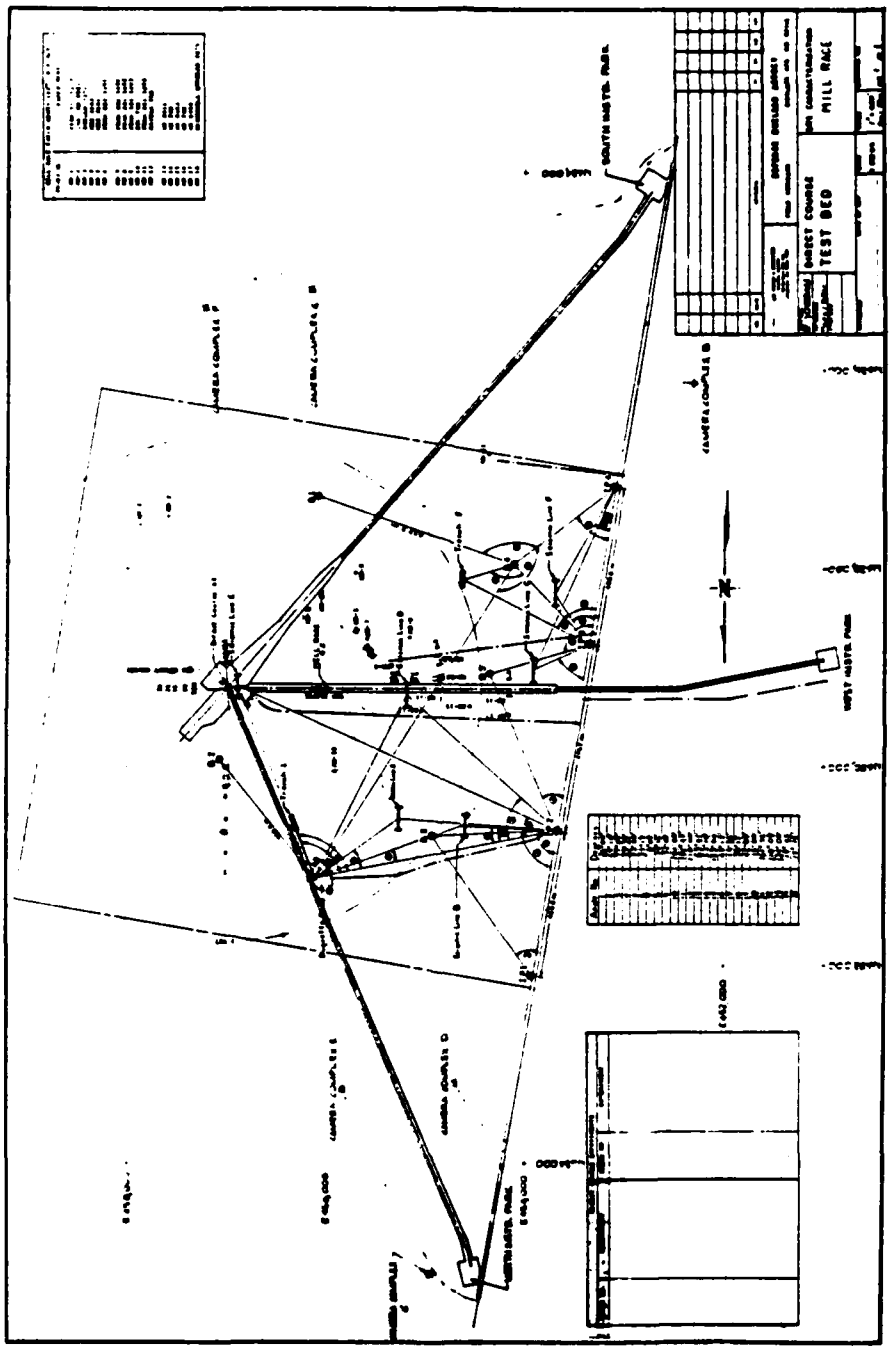
TEST BED
MILL RACE

REFERENCES

1. AMEND, ULLRICH and THOMAS, Have Host Cylindrical In-situ Test (CIST) Data Analysis and Material Model Report, (AFWL) DE-TN-77-005, Kirtland Air Force Base, New Mexico, March 1977.

2. BEDSUN, DAVID A., A Summary of the Geologic Characterization of the MILL RACE Site, WSMR, Air force Weapons Laboratory, Kirtland Air Force Base, New Mexico, June 1981.

3. BEDSUN, DAVID A., Soil Sampling and Downhole Seismic Surveys at the Pre-Direct Course and Direct Course Sites, WSMR, Air Force Weapons Laboratory, Kirtland Air Force Base, New Mexico, May 1982.

4. CALHOUN, D.E. and TRIANDAFILIDIS, G.E., 7th Proceedings of the International Conference of soil Mechanics and Foundation Engineering, Dynamic Oedometer Study of Lateral Yield Effects, 1969.

5. EM 110-2-1906, Engineering and Design Laboratory Soils Testing, Headquarters, Department of the Army, Office of the Chief of Engineers, 30 November 1970.

6. HESSE, P.R., A Textbook of Soil Chemical Analysis, Chemical Publishing Company, Inc., New York, 1972.

7. LAMBE, T.W., Soil Testing for Engineers, Massachusetts Institute of Technology, John Wiley and Sons, Inc., New York, London, Sydney, 1967.

8. LAMBE, T.W. and WHITEMAN, R.V., Soil Mechanics, Massachusetts Institute of Technology, John Wiley and Sons, New York, London, Sydney, Toronto, 1969.

9. MECHTLY, E.A., The International System of Units, Physical Contants and' Conversion Factors, NASA SP-7012, National Aeronautics and Space Administration, Washington D.C., 1973.

10. MELZER, SCHENKER, HULCHER and RINEHART, Geological Influences on Nuclear Weapon Effects in Western Alluvial Valleys, AFWL-TR-78-155, Kirtland Air Force Base, New Mexico, June 1979.

11. MIL-STD-619A, Unified Soil Classification System For Roads, Airfields, Embankments and Foundations, 20 March 1962.

12. PERKIN-ELMER CORP, Analytical Methods for Atomic Absorbtion Spectrophotomethry, Norwalk, Connecticut, January 1982.

13. PERKIN-ELMER CORP, Instructions Model 560 Atomic Absorbtion Spectrophotometer, Norwalk, Connecticut, April 1979.

14. POR 7072, MISTY CASTILE Series, MILL RACE EVENT, Test Execution Report, WSMR, Defense Nuclear Agency, Washington D.C., 18 December 1981.

(References Continued)

15. SANGLERAT, G., The Penetrometer and Soil Exploration, Interpretation of penetration diagrams-theory and practice, Elsevier Publishing Company, Amsterdam, London, New York, 1972.

16. TERZAGHI, K. and PECK, R.B., Soil Mechanics in Engineering Practice, John Wiley and Sons, New York, Chichester, Brisbane, Toronto, 1967.

17. WELLS and SCHULTZ, Properties and Prediction of Caliche in Alluvial Basins of the Southwestern United States, AFOSR-78-3572, Air Force Systems Command, USAF, Bolling Air Force Base, Washington D.C., July 1980.